

# Synthesis of an alkaloid inspired compound collection

**Yao, Ruwei**

*Publication date:*
2022

*Document Version*
Publisher's PDF, also known as Version of record

DTU Chemistry
Department of Chemistry

Technical University of Denmark


# Synthesis of an alkaloid inspired compound collection

PhD thesis

Author: Ruwei Yao

Supervisor: Associate Professor Luca Laraia

December 2022

PROJECT TITLE: Synthesis of an alkaloid inspired compound collection

SUBMISSION DATE: 2022.12.21

AUTHOR: Ruwei Yao

ruweiy@kemi.dtu.dk

SUPERVISOR:
Associate Professor Luca Laraia
luclar@kemi.dtu.dk

DEPARTMENT:
Department of Chemistry
Technical University of Denmark
Kemitorvet, building 207
2800 Kongens Lyngby
Denmark

---

Ruwei Yao
2022.12.21, Kongens Lyngby

## Preface

The work presented in this PhD thesis is the result of experimental research under the supervision of Associate Professor Luca Laraia at the Department of Chemistry, Technical University of Denmark (DTU). This project is the combination of organic synthesis performed at DTU, and biological screening mainly carried out by our collaborators Professor Anders A. Jensen and Trond Ulven at Copenhagen University (KU).

## Acknowledgements

From the bottom of my heart, I´m so grateful for my supervisor Associated Professor Luca Laraia. Thank you for offering me a great chance being a member of your fantastic group! Thank you for founding such an amazing research group focus on chemical biology, organic chemistry, and medicinal chemistry that I thus have the opportunity to touch and learn new knowledge from all of our group members I met! Thank you for supporting and helping me address all the questions I had throughout my PhD study until today!

I would like to thank our main collaborators Professor Anders A. Jensen and Trond Ulven, who both come from the Department of Pharmacy, Copenhagen University. Thank you for being so generous that provided the cellular assays and screened our compound library. In addition, your postdoc Libin Zhou, and PhD student Katrine Schultz-Knudsen assisted me a lot in the pharmacological screening for my project, respectively.

I would like to thank our former master students Nicklas Peter Hovendal and Annika Garcia Eriksen, who both involved in the synthesis of my PhD project. I would like to thank Henrik Pedersen (Lundbeck A/S) that helped me resolute the racemate of my active compound. I would like to thank technicians Marius Kubus for solving X-ray crystal structures data for my several compounds, Kasper Enamark-Rasmussen performing the high resolution NMR for my several compounds.

I would like to thank our former and current colleagues Mikkel, Thomas, Cecilia, Nianzhe, Frederik, Joseph, Laura, Nienke, Hogen, Yajun for your company during my whole PhD study.

I would like to thank Dr. Vsevolod Peshkov, many thanks for your recommendation and encouragement that I thus can come to Denmark for my PhD education. I also would like to thank my friend Ming Zhang for helping me a lot during my moving to DTU.

Lastly, many thanks for China Scholarship Council, SC Van Fonden, and DTU chemistry funding. Thank you for your generosity that sponsored my education and research at DTU.

## Abstract

Pseudo-natural products, defined as the non-biogenic fusion of natural product fragments, have emerged as an inspiration for rapidly identifying novel biologically active molecules. We synthesized a library of 64 pseudo-natural products, which contain ten structurally diverse spirocycles based on tropane and quinuclidine alkaloid scaffolds. The library has a high $Fsp^3$ content and Lipinski's *rule-of-five* compliance, making it highly drug-like. Through targeted screening we discover unnatural quinoxaline-fused tropanes targeting the 5-HT2A serotonin receptor. Additionally, we identify and further optimize a lead 5HT2B/C antagonist derived from chromanone-fused quinuclidines with a surprising selectivity profile against a panel of aminergic G-protein coupled receptors (GPCRs), alongside α4β2 and α3β4 nicotinic acetylcholine receptors (nAChRs).

We extended this strategy to identify other aminergic G-protein coupled receptors (GPCRs) modulators in the central nervous system (CNS). Herein, we reported the synthesis of a library containing 22 analogues based on quinolizidine alkaloid scaffolds. Biological screening against dopamine receptors revealed that the unnatural quinoline-fused quinolizidines are new chemotype ligands at the dopamine 2 receptor (D2R), which does not often exist in naturally occurring quinolizidines. We further identified our lead compounds can exhibit high selectivity over α4β2 and α3β4 nAChRs.

## Resume

Pseudo-naturprodukter, defineret som den ikke-biogene fusion af naturlige produktfragmenter, har vist sig som inspiration til hurtigt at identificere nye biologisk aktive molekyler. Vi syntetiserede et bibliotek med 64 pseudo-natur produkter, som indeholder ti strukturelt forskellige spirocykler baseret på tropan og quinuclidin alkaloid-strukturerne. Biblioteket har et højt $Fsp^3$-indhold og god overholdelse af Lipinskis *rule-of-five*, hvilket gør det meget medicinlignende. Gennem målrettet screening opdagede vi unaturlige quinoxalin-fusionerede tropaner, som var målrettet mod 5-HT2A serotoninreceptoren. Derudover identificerede og optimerede vi yderligere en *lead* 5HT2B/C-antagonist afledt af kromanon-fusionerede quinuclidiner med en overraskende selektivitetsprofil mod et panel af aminergisk G-protein-koblede receptorer (GPCRs) sammen med α4β2- og α3β4-nikotinacetylacetyl-receptorer (nAChRs).

Vi udvidede denne strategi til at identificere andre modulatorer af aminergisk G-protein-koblede receptorer (GPCRs)i centralnervesystemet (CNS). Heri rapporterede vi syntesen af et bibliotek indeholdende 22 analoger baseret på quinolizidin alkaloid-strukturen. Biologisk screening mod dopaminreceptorer afslørede, at de unaturlige quinolin-fusionerede quinolizidiner er nye kemotype-ligander for dopamin 2-receptoren (D2R), som ofte ikke findes i naturligt forekommende quinolizidiner. Vi identificerede yderligere, at vores *lead*-molekyle kan udvise høj selektivitet over α4β2 og α3β4 nAChRs.

## Abbreviations

| | |
|---|---|
| 5-MeO-DMT | 5-methoxy-N, N-dimethyltryptamine |
| 5-HTR | Serotonin receptors |
| BIOS | Biology-oriented synthesis |
| cAMP | Cyclic adenosine monophosphate |
| Cbz | Carbobenzyloxy |
| CNS | Central nervous system |
| COPD | Chronic obstructive pulmonary disease |
| CtD | Complexity-to-diversity |
| D1R | Dopamine 1 receptor |
| D2R | Dopamine 2 receptor |
| DABCO | 1,4-diazabicyclo[2.2.2]octane |
| DCC | N,N′-Dicyclohexylcarbodiimide |
| DMAP | 4-Dimethylaminopyridine |
| DMU | 1,3-dimethylurea |
| DOS | Diversity-oriented synthesis |
| FOS | Function-oriented synthesis |
| Fsp3 | *sp*3-hybridized carbons |
| GPCRs | G-protein coupled receptors |
| HCV | Hepatitis C virus |
| HPLC | High-performance liquid chromatography |
| LAH | Lithium aluminium hydride |
| LC–MS | Liquid chromatography–mass spectrometry |
| LLAMA | Lead-Likeness and Molecular Analysis |
| LSD | Lysergic acid diethylamide |
| M | Muscarinic acetylcholine |
| MCAP | Multicomponent assembly process |
| MsOH | Methanesulfonic acid |
| nAChRs | Nicotinic acetylcholine receptors |
| NBS | N-bromosuccinimide |
| NOESY | Nuclear Overhauser Effect Spectroscopy |
| NPs | Natural products |
| Oxone | KHSO5-1/2KHSO4-1/2K2SO4 |
| PNP | Pseudo Natural Products |
| SAR | Structure-activity relationships |
| SCQ1 | Spiro-chromanoquinuclidines |
| SCONP | The structural classification of NPs |
| SFC | Supercritical fluid chromatography |
| TfOH | Triflic acid |
| THPs | Tedrahydropyridines |
| THβC | Tetrahydro-β-carboline |
| TLC | Thin layer chromatography |
| TMSCl | Trimethylsilyl chloride |
| TMSI | Trimethylsilyl iodide |
| TsOH·H2O | Toluenesulfonic acid monohydrate |

# Table of Contents

# 1 Introduction

## 1.1 Natural products as an inspiration for drug discovery

Traditionally, large compound collections prepared by combinatorial chemistry using simple cross coupling and condensation reactions have been characterized by a low fraction of *sp*3-hybridized carbons ($Fsp^3$), ample rotatable bonds, and biased functional groups, which might limit the ability of these compounds to effectively explore chemical and biological space.[1]

Natural products (NPs) derive from animals, plants, and microorganisms, and are an important class of therapeutics. They have historically been used to treat human diseases, and possess immense structural diversity and widespread biological activities. NPs have evolved over millions of years, to exhibit biologically relevant functions, determined by their complex structures. For example, Taxol was first isolated from the *Pacific yew,* obtained FDA approval in 1993, and is currently employed to treat a range of cancers.[2]Another well-known NP therapeutic initiated by Tu *et al.* was a novel therapy for malaria *via Artemisia annua L.* extracts inspired by Chinese traditional medicine.[3] A retrospective analysis based on the evaluation of the dataset of all published microbial and marine-derived NPs from the period 1941 to 2015, found that 76.8 % have been structurally similar to previous compounds, continued increase of the exploration of new NPs have few scaffold precedents .[4] As such, NPs together with the structurally privileged scaffolds should be both considered as an inspiration for drug discovery and developmnet. (**Figure 1.1**).[5] Not surprisingly, it was recently demonstrated that 13% of all FDA approved first-in-class drugs are either NPs, or NP-derived respectively.[6] Due to their wider coverage of chemical and biological space, NPs and their derivatives deliver higher hit rates compared to purely synthetic compounds, giving them a crucial role in drug discovery.

A generalized approach to deliver sufficient quantities of NPs for investigation in a variety of biological assays remains challenging. Therefore, the focus has at least partially shifted from reported NP entities towards NP-like libraries. The prevailing strategies for accessing NP-inspired compounds are Biology-oriented synthesis (BIOS), Ring Distortion Strategy (complexity-to-diversity, CtD), diversity-oriented synthesis (DOS), and the synthesis of Pseudo Natural Products (PNP).

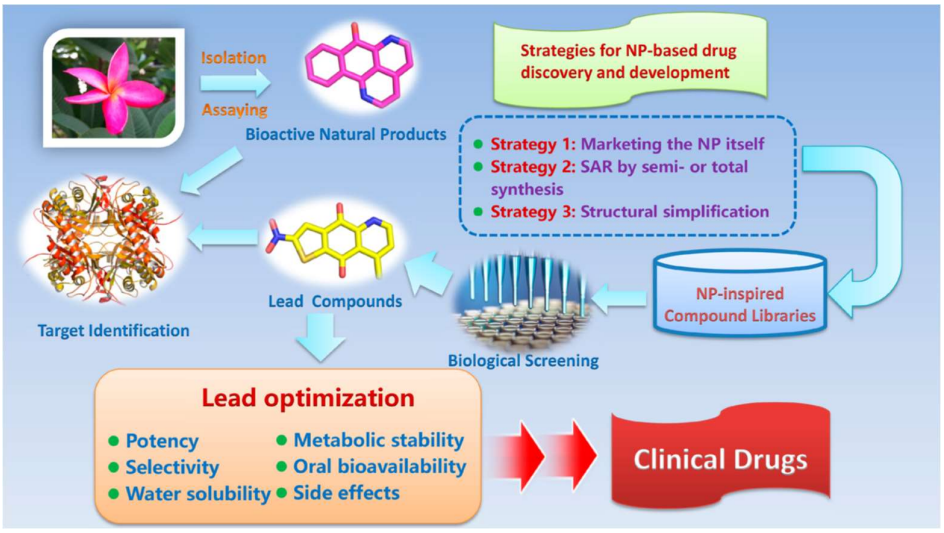


**Figure 1.1 Strategies for NP-based drug discovery and development. Reproduced from Wang *et al.*[5]**

### 1.1.1. Biology-Oriented Synthesis

The structural classification of NPs (SCONP) defines removing the complexities of the parental NPs in a stepwise way, the essential biological activities retain when the core scaffold remains referred to the guiding NPs.[7] BIOS was initially pioneered by the Waldmann lab, who embraced the concept of the existence of biologically privileged scaffolds in medicinal chemistry and chemical biology.[8] They applied this strategy to synthesise and screen an average library size of 200 – 500 compounds, with 0.2–1.5% hit rates.[9]

An example of the synthesis of a BIOS compound collection relied on the NP yohimbine. Yohimbine, derived from the bark of the *Pausinystalia yohimbe tree*, is part of a family of indole alkaloids, which displays a broad range of biological activities, and has been identified as an inhibitor of phosphatase Cdc25A.[5] Following the principle of SCONP, the pentacyclic scaffold of yohimbine was truncated into simpler compounds. The simplified tetracyclic scaffolds displayed wide-ranging biological activities, with distinct binding targets (**Figure 1.2**).[5]

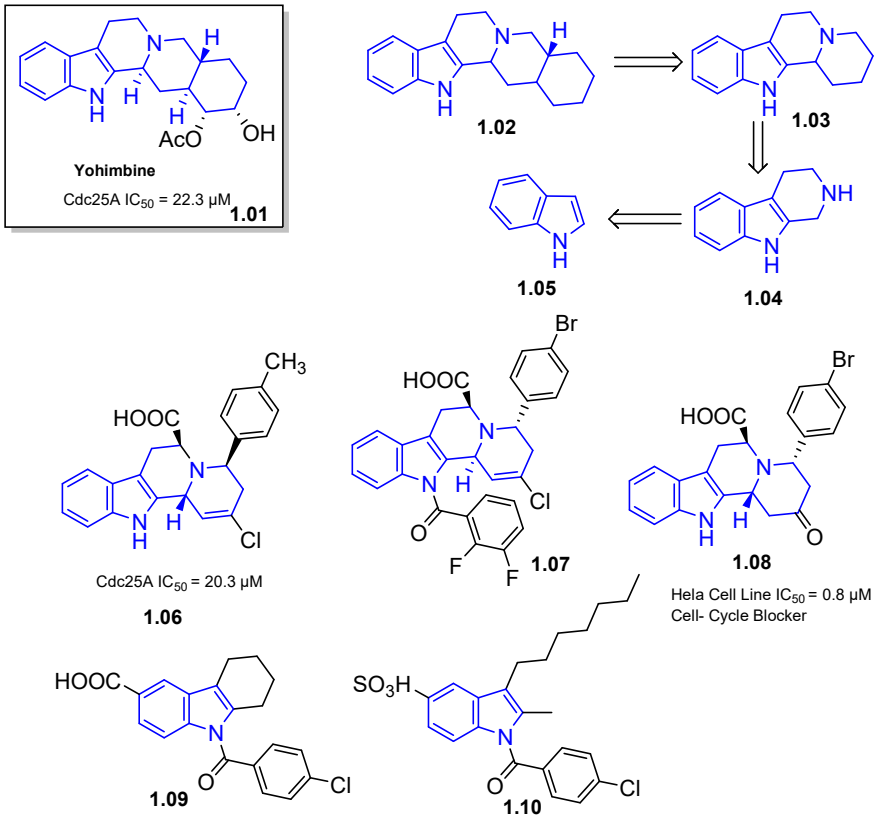


**Figure 1.2 Structural simplification of yohimbine using the SCONP** [5]

### 1.1.2. Ring Distortion Strategy

NPs offer a wide coverage of chemical space, and have a fraction of *sp3*-hybridized carbons (0.68 on average), which is much higher than common commercially available compound collections. As such, it is potentially worthwhile to take them as starting materials to manipulate for the design and synthesis of screening libraries. Most NPs engage a broad range of biological activities, and almost half of the approved small molecule anticancer drugs from 1940s to 2014 are associated with NPs.[10] To make the most of scaffold diversity and bioactivity, leveraging the power of synthetic chemistry, Hergenrother proposed a strategy termed complexity-to-diversity (CtD), which enables ring system distortion usually involved in ring fusion, ring expansion, ring cleavage, rapidly creating diverse compound collections.[11]

Isolated mainly from plants, or synthesized by organic chemists, alkaloids offer the initial source of therapeutics to treat cancer, malaria, and have been well documented. However, the use of parental NPs as chemical starting points for diversification and modification, to enrich the number of chemical entities for screening and increase potency in biological studies, to facilitate drug discovery, remains rare. Approaches to rapidly and efficiently synthesize alkaloid derivatives have been reported recently. Quinine **1.11**, is a low cost antimalarial therapeutic, contains two discrete ring frames, and has multiple stereocenters and functional handles. It has been used in the design of organocatalysts, potentially facilitate ring distortion (**Figure 1.3**). Hergenrother disclosed quinine **1.11** treated with thionochloroformate result in tandem ring cleavage/ring fusion compound **1.13**. The treatment with isoamylmagnesium bromide of quinine **1.11** results in nucleophilic addition to the quinoline ring followed by hemiaminal ether formation compound **1.16**.[11] It will be interesting to see whether these compounds possess bioactivity profiles.

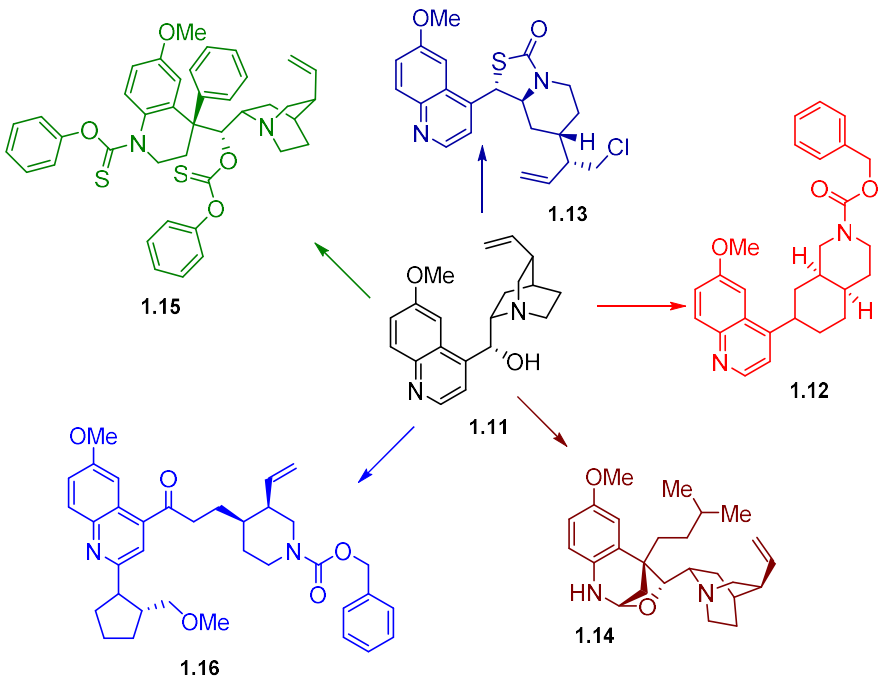


**Figure 1.3 Application of ring-distortion reactions with quinine** [11]

In 2018, Hergenrother *et al.* also reported the synthesis of a 52-membered compound collection from the commercially available NP lycorine (**Figure 1.4**). Cross couplings, substitutions, ring expansions and rearrangements were all possible.[12] Lycorine **1.17** was reduced with $H_2$, and the resulting diol could be oxidized to a dialdehyde, which after a double reductive amination with amines enabled the formation of compound **1.21**. Lycorine **1.17** was transformed into diacetyl lycorine in order to improve the solubility in organic solvent, and subsequent treatment with a benzyne precursor offered the expanded product **1.18**. A proposed plausible mechanism was suggested in which the nucleophilic tertiary amine attacks the triple bond of benzyne, yielding an unstable reactive intermediate, followed by 1,5-H shift, and the sequential 1, 2-alkyl shift to enable the expansion and subsequent aromatization. This similar philosophy has been extended to access commercially available NPs including abietic acid [13], sinomenine[14] and pleuromutilin[15].

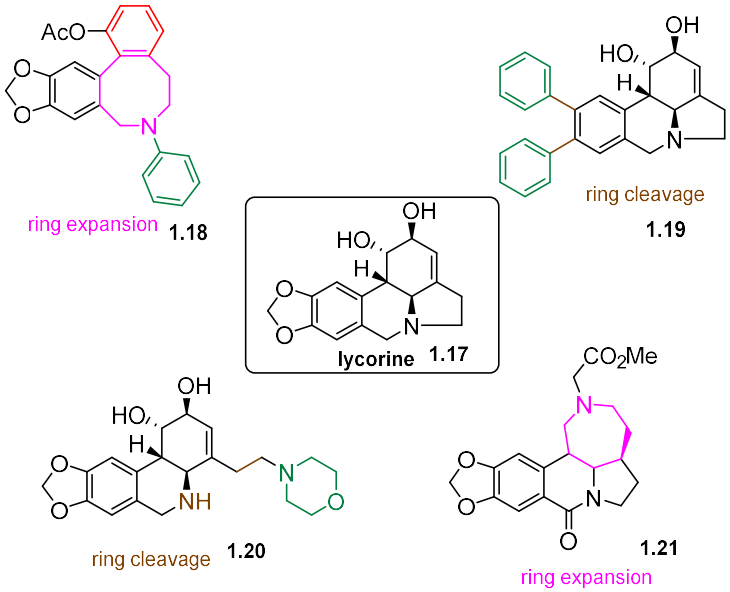


**Figure 1.4 Application of ring-distortion reactions with lycorine** [12]

### 1.1.3. Diversity-Oriented Synthesis

The aim of diversity-oriented synthesis (DOS) is to create structurally diverse and thus functionally diverse collections.[16] Spring *et al.* summarized that building block diversity, functional group diversity, stereochemical diversity as well as scaffold diversity are crucial to design a structurally diverse collection.[17] The general strategies for the synthesis of diverse compounds using DOS can be referred to as either reagent-based or substrate-based (**Figure 1.5**). Additionally, Schreiber *et al.* proposed a sequential build/couple/pair (B/C/P) strategy (**Figure 1.6**) to assemble the structurally diverse collections from the relatively simple starting materials.[18] The build stage and coupling stage are mainly responsible for the stereochemical diversity. Once the coupling stage is completed, the resulting coupling intermediate containing multiple active function moieties can selectively undergo intramolecular cyclizations and contribute to increasing scaffold diversity.

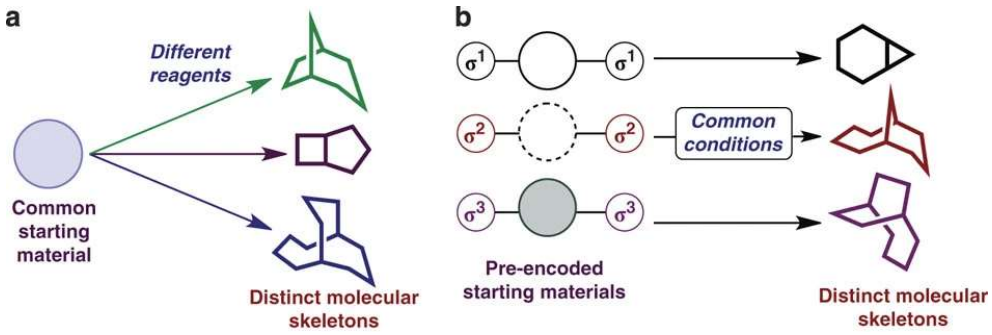


**Figure 1.5 DOS approaches to scaffold diversity. Reproduced from Spring *et al.*** [17]

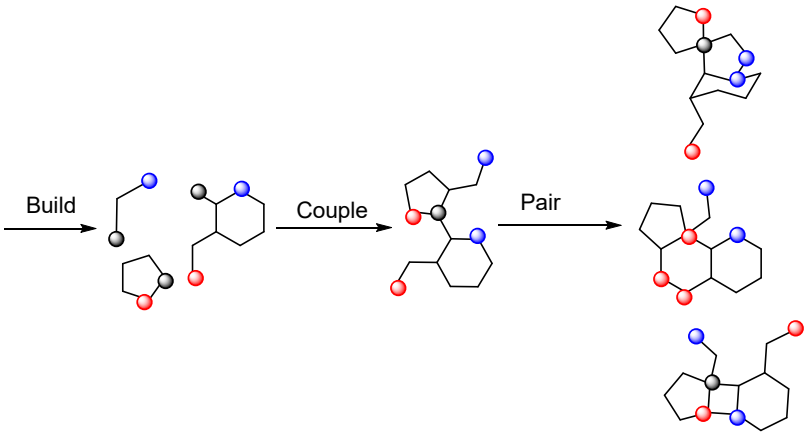


**Figure 1.6 Example of diversity with a build/ couple/ pair strategy**[18]

The tactics to address alkaloid diversity concerns by increasing the population of complex small molecules for screening libraries have been delivered. These strategies are associated with constructing building blocks with simple small molecule, building structural complexity in subsequent synthetic reactions. The most established approaches are DOS and BIOS, which have been previously presented and were pioneered by Schreiber and Waldmann, respectively. These have recently unveiled a series of biological discoveries of therapeutic relevance. Lei *et al.* proposed lycopodium alkaloid contains multiple stereo chemical centers and rigid ring systems can be synthesized *via* a DOS approach.[19] In contrast to other accessible total synthesis, the reported Build/Couple/Pair/ strategy has successfully introduced four lycopodium alkaloids, it also allows the paring intermediate to synthesize unnatural paralleled skeletons (**Figure 1.7**). As such, I believe the chemical space of unexpected compounds can be further explored and an array of biological assays could be envisaged.

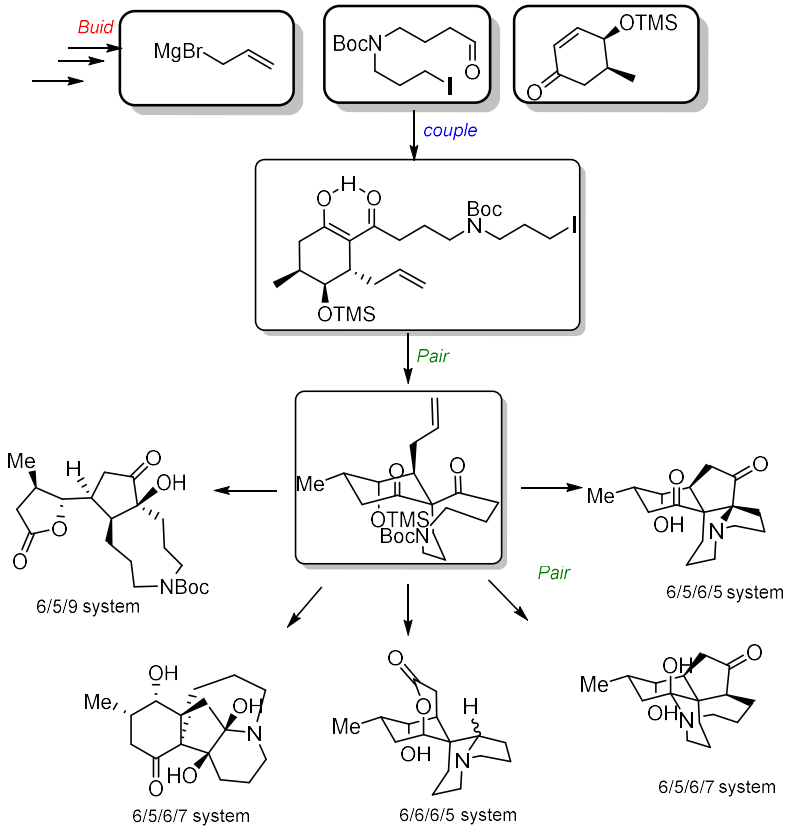


**Figure 1.7 Examples of alkaloid diversity with a build/ couple/ pair strategy**[19]

### 1.1.4. The Synthesis of Pseudo Natural Products

The combinatorial-type libraries from the period between 1980 and 1990 were typically created by combining a number of common scaffolds with variation of substituents, using the same synthetic methodology. As such, the obvious drawback of these libraries is that they possess low levels of scaffold diversity, which restricts the further exploration of chemical space. To address the lack of structural and biological diversity of compound collections, researchers sought to use pre-validated and biologically relevant scaffolds found in NPs, in strategies such as BIOS. However, BIOS is still unable to answer the question of unknown chemical space and the generalized simplified structure is often biologically inactive compared to the NP starting point.

Waldmann *et al.* define Pseudo Natural products (PNP) as small-molecule compound collections composed of unprecedented combinations of NP fragments.[20] The proposed plausible five assembling patterns have been illustrated to connect distinct NPs fragments, which are comprised of monopodal connections, edge fusions, spiro fusions, bridged fusions, as well as bridged bipodal connections (**Table 1.1**). Overall, it consists of ring fusion and ring connection. The guidelines for the design of promising PNP candidates have recently been systematically summarized. The NPs fragments from NPs undoubtedly might be preferred to assemble because they involve a series of relevant beneficial biological activities**.**

Following the original design principles, Karageorgis *et al.* devised a one-pot modified Biginelli multicomponent reaction for the synthesis of chromopynone libraries (**Figure 1.8**).[21] This mechanism was proposed to be the condensation of benzaldehydes with a substituted urea and methylacetoacetate, resulting in a dihydropyrimidinone intermediate. The intermediate goes through an intramolecular cyclization similar to a Michael addition, followed by the decarboxylation under the acidic conditions. The chromopynones were screened in a phenotypic assay and identified as novel glucose uptake inhibitors targeting glucose transporters GLUT-1 and GLUT-3. Interestingly, NPs containing chromane or tetrahydropyrimidine did not share the similar biological effects.

**Table 1.1 Possible NPs fragments connections to guide design of PNP[20]**

| Connection Type | PNP | NPs |
|---|---|---|
| 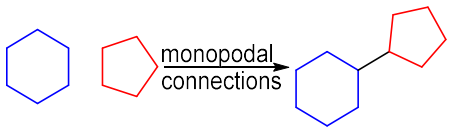 | 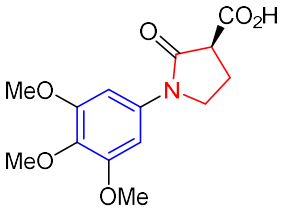 | 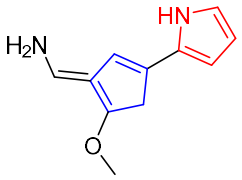 |
| 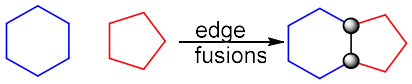 | 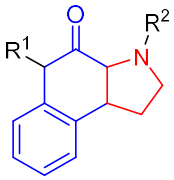 | 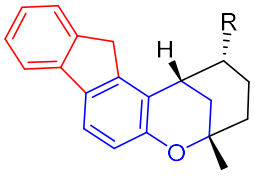 |
| 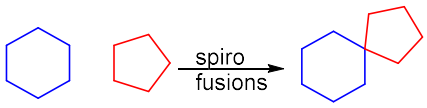 | 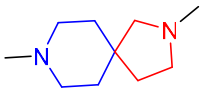 | 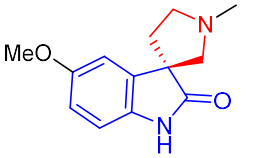 |
| 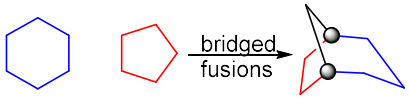 | 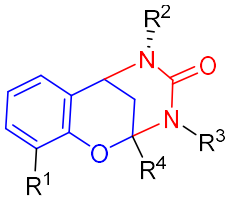 | 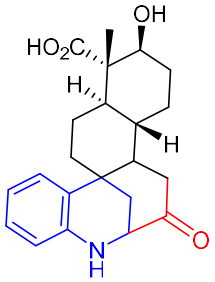 |
| 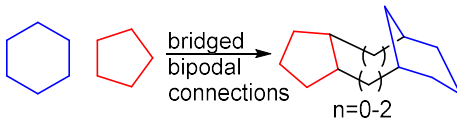 | 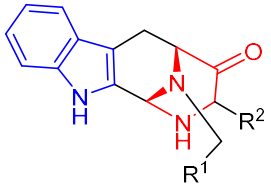 | 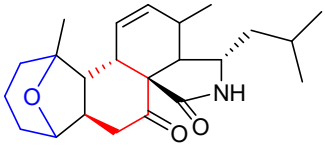 |

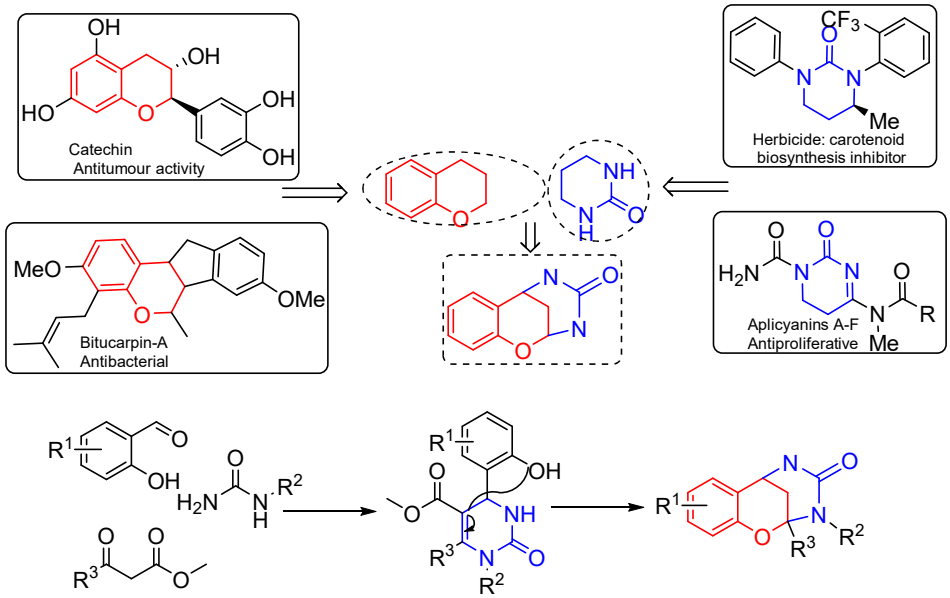


**Figure 1.8 Fusion of fragments chromane and tetrahydropyrimidinone using a multicomponent reaction**[21]

Palladium catalyzed α-arylation of imines derived from ketone has become an efficient method to yield indoles and derivatives. Foley *et al.* have recently invesed this protocol for the synthesis of an indole alkaloid inspired PNP library containing over 46 analogues (Figure **1.9**).[22] The resulting compound collection was profiled with the cell painting assays. The hit compound **1.23** was found to selectively inhibit both starvation and rapamycin-induced autophagy by targeting the lipid kinase VPS34.

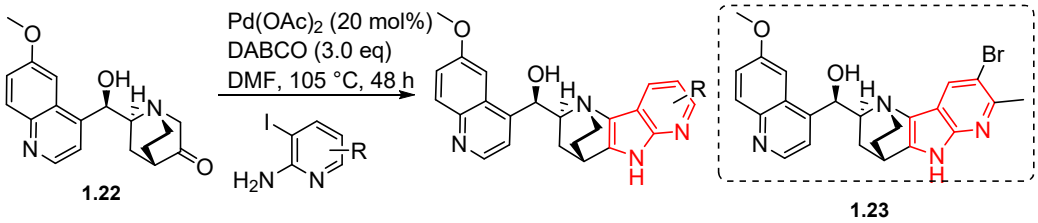


**Figure 1.9 Library synthesis from the Pd catalyzed annulation**[22]

The synthetic strategies of pseudo natural products also comprise the natural product fragment combination with spirocyclic fusions. For example, Burhop *et al*. employed the oxa Pictet-Spengler reaction to fuse α-hydroxyethyl indoles from griseofulvin-derived ketone **1.24** (**Figure 1.10**).[23] The polycyclic compound collections were subsequently screened in target unbiased biological assays, where the most potent compound **1.26** was found to inhibit starvation-induced autophagy. Notably, such biological function did not shared with the parental fragments including the NP griseofulvin **1.24** and compound **1.25**.

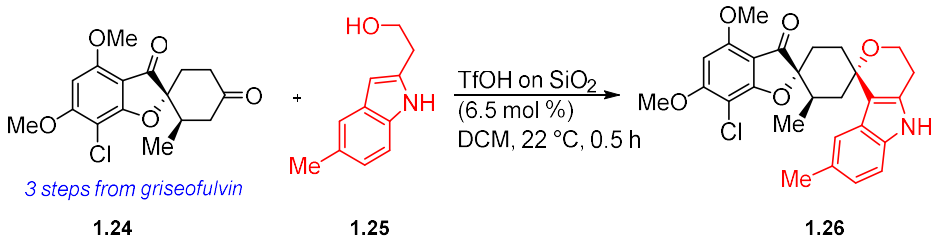


**Figure 1.10 Example of indofulvin PNP as a new autophagy inhibitor *via* oxa Pictet-Spengler reaction**[23]

Aster family (Aster-A, Aster B, Asters C) belong to the cholesterol transport proteins that mediate sterol transport in mammalian cells.[24] So far, there are a limited number of chemical tools to selectively inhibit Aster family. The synthesis of entities with structural relevance to cholesterol has contributed to discover the selective Asters C inhibitor.[25] However, this strategy only covered a large number of analogues derived from existing cholesterol scaffolds. To address the lack of structural and biological diversity, increasing the chance of identification of new sterol transport modulators, our group employed the synthesis of diverse set of PNP from one primary scaffold fused to different secondary scaffolds. As such, it currently enabled us to identify the novel selectively potent Asters C inhibitor (-)-Astercin featuring fused pyrazoles, which was prepared from ketone **1.30** in three steps (**Figure 1.11**).[26] This strategy could be also applied to identify selective modulators against other sterol transporter family by using diverse secondary fragments.

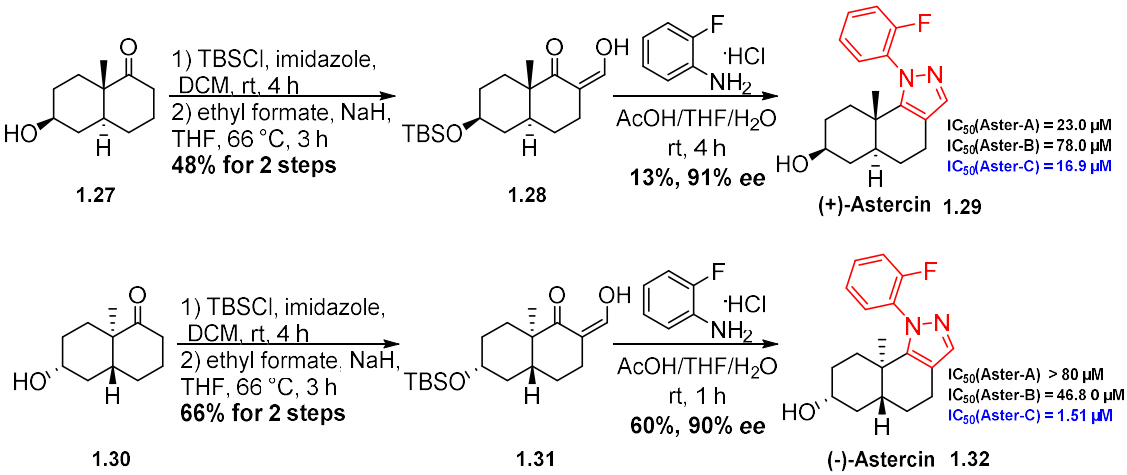


**Figure 1.11 Example of sterol inspired compound as a new Asters C inhibitor**[26]

## 1.2 Naturally occurring alkaloids and their applications

So far, there is no unified definition of alkaloids due to the similarities with other secondary metabolites. Chemists define alkaloids as biogenic, nitrogen-containing and mostly N-heterocyclic compounds and often possess a strong physiological activity.

Alkaloids are secondary metabolites, extensively distribute in plants, animals, fungus and marine organism. Alkaloids frequently occurs in the plant kingdom, and they are found in ~20% of vascular plants. It´s estimated that among over 4,000 plant species, more than 3,000 different types of alkaloids have been identified.[27] Therapeutic potentials of naturally occurring alkaloids constitute anticancer and antimalarial among many others (**Figure 1.12)**. For example, Homoharringtonine is a plant alkaloid derived from *Cephalotaxus fortune,* which has been approved by FDA as a treatment of chronic myeloid leukemia. Vincristine is a vinca alkaloid isolated from *Catharanthus roseus*, the medical treatments include an array of cancers.

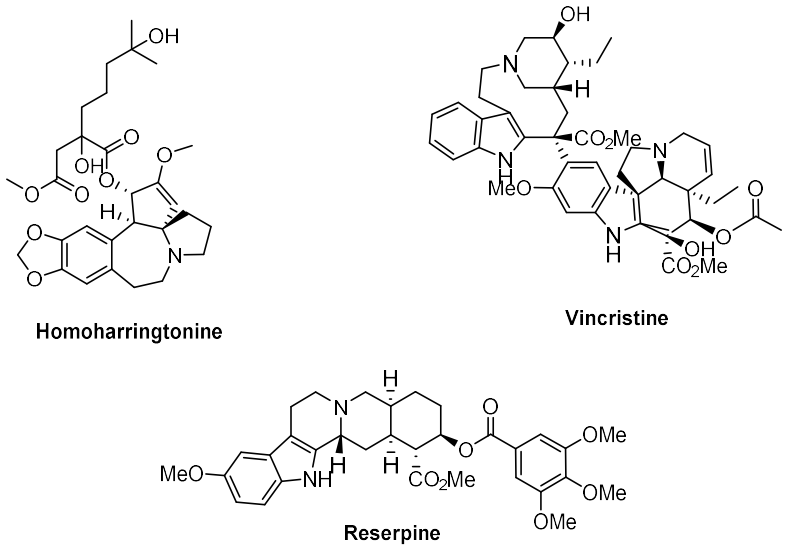


**Figure 1.12 Examples of naturally occurring alkaloids as drugs**

Naturally occurring alkaloids can also act as depressants or stimulants in the central nervous system (CNS) (**Figure 1.13)**. Morphine was first isolated in 1805 by Friedrich Sertürner[28]. It used to serve as a painkiller to treat who have suffered acute and chronic severe pain. Cocaine is a well-known addictive stimulant drug primarily extracted from the leaves of two coca species indigenous to South America.


Morphine Cocaine

**Figure 1.13 Examples of naturally occurring alkaloids as depressants or stimulants**

The naturally occurring alkaloids such as ergometrine belongs to ergot alkaloids, structurally similar to the psychedelic drug Lysergic acid diethylamide (LSD) (**Figure 1.14)**. In the computational mode, ergometrine was predicted to possess high affinities at serotonin receptors (5-HTR), dopamine receptors, as well as androgenic receptors.[29]As such, it might need additional pharmacological experiments to study. In fact, it used to be a mediation to inhibit excessive bleeding resulting from abortion or childbirth. The popular neurological active alkaloids also include apomorphine (**Figure 1.14)**, which is a type of aporphine alkaloids used to treat Parkinson´s disease.[30] Due to the structural similarities, it can be produced from morphine in acidic conditions. Pharmacological findings suggests apomorphine is a nonselective agonist at D2-like receptors because it shows decent antagonism affinities at 5-HTR and androgenic receptors.[31]

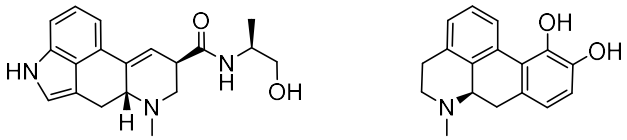


Ergometrine Apomorphine

**Figure 1.14 Examples of naturally occurring alkaloids as drugs targeting 5-HTR and dopamine receptors**

## 1.3 Alkaloid inspired collections for CNS drug discovery

Alkaloid-derived compound collections can only be synthesized from alkaloid starting materials, if they are readily available in sufficient quantities. The application of naturally occurring alkaloids as starting materials to afford sufficient diverse and complex transformations remains challenging, and only a few case studies were reported in the last decade. Instead of investing considerable efforts to produce alkaloid-derived collections, alkaloid inspired compounds possess simplified structures containing core scaffolds that might be more accessible.

To develop structurally simplified and safer psychedelic candidates, Olson *et al.* employed function-oriented synthesis (FOS) inspired by naturally occurring alkaloids of ibogaine family.[32] Olson reasoned two different pathways could disconnect the complex structure of ibogaine and noribogaine **(Figure 1.15)**. Compound **1.35** and compound **1.36** are composed of an indole and an isoquinuclidine, but lack tetrahydroazepine. Removing the isoquinuclidine ring led to the formation of azepinoindole such as **1.37** (IBG) and **1.38** (TBG), which were prepared by Fisher indole cyclization in a single step. Psychoplastogenic studies evaluated by the images of rat embryonic cortical neurons (DIV6) indicated that IBG was efficacious to promote neuronal growth compared to a vehicle control. Profiling revealed that IBG and TBG both demonstrated a potent agonist activity at 5-HT2A receptor. Compared to the hallucinogenic 5-HT2A agonist 5-methoxy-N, N-dimethyltryptamine (5-MeO-DMT), using the head-twitch response assay IBG exhibited significantly reduced hallucinogenic response and TBG was tested inactive, respectively.

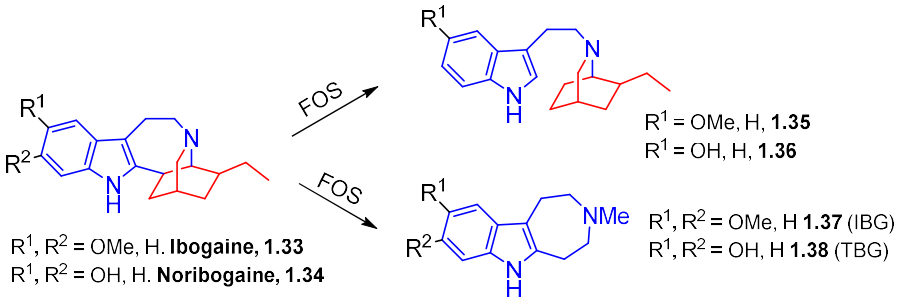


**Figure 1.15 Examples of synthesis of azepinoindoles via Function-oriented synthesis**

To explore selective and potent 5-HT2A agonists for developing the new generation antidepressant drugs, the alkaloid inspired library has been recently extended to a bespoke virtual library of tedrahydropyridines (THPs) using the structure-based docking.[33] The sequential condensation, [4+2] cycloaddition, and hydrogenation allow the rapid construction of the THPs bearing various substitutions (**Figure 1.16**).

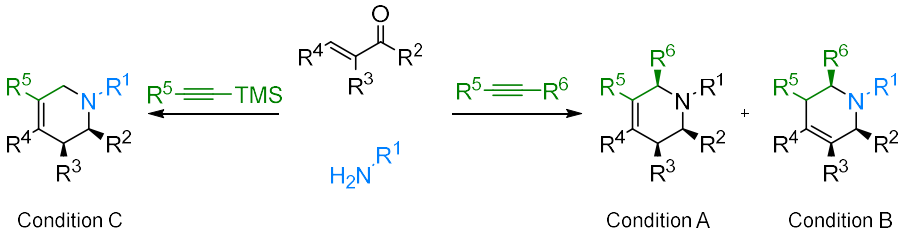


**Figure 1.16 THPs from commercially available alkynes, amines and α, β-unsaturated carbonyl compounds**

Ellman *et al.* docked this virtual library of 75 million analogues against a model of 5-HT2A receptor (**Figure 1.17**). As a result, four selected hit compounds displayed the micromolar potency at either 5-HT2A receptor or 5-HT2B receptor. The subsequent structure-activity relationship (SAR) study led to the validation of two selective 5-HT2A agonists with $EC_{50}$ of 41 nM and 110 nM, respectively. These two ligands were determined the selectivity over 5-HT2B and 5-HT2C. Interestingly, they both demonstrated rather selective versus 5-HT2C than 5-HT2B. Ellman further investigated the selectivity over a panel of 318 other G protein-coupled receptors (GPCRs), unexpectedly, the two ligands both showed negligible pharmacological response at 10 μM against the majority of the chosen receptors.

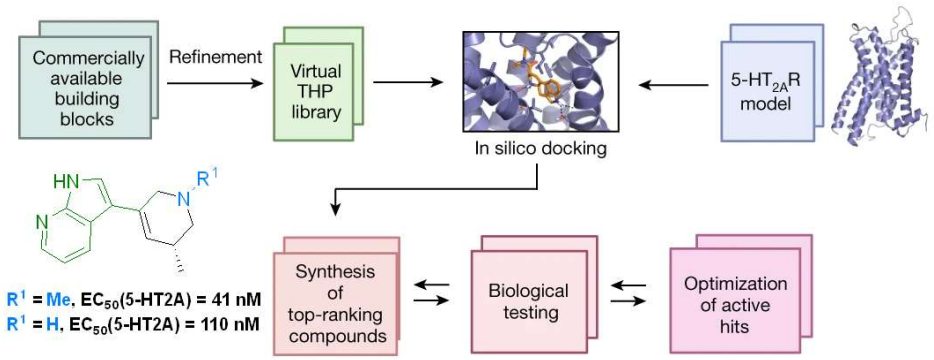


**Figure 1.17 High throughput virtual screening for docking THPs using a homology model of 5-HT2A. Adapted from Ellman *et al.*[33]**

To extend the chemical space of alkaloid mimics, Martin *et al.* introduced a well-established multicomponent assembly process (MCAP).[34,35] This approach featured that the combination of an aldehyde, an acylating agent, and an amine lead to generate a reactive N-acyl iminium ion that can react to a nucleophile in one pot reaction (**Figure 1.18**). This protocol well accommodated various nucleophiles, such as allylzinc bromide. As such, the resulting intermediates **1.40** undergo an intramolecular metathesis followed by the Heck cross coupling, which can be further reduced by $Et_3SiH$ in an acidic condition. As a result, the new two entities **1.41** are promising handles for late-stage diversification. For example, the sequential Buchwald–Hartvig amination followed by treating TMSI and aqueous $NaHCO_3$ enabled the generation of norbenzomophan **1.44**. Martin in cooperation with Roth further identified this alkaloid mimics as a potent and selective Sigma-1 ligand which demonstrates 82 fold selectivity versus Sigma-2. Synthesis of homonorbenzomophan **1.46** was achieved by the Suzuki coupling, the removal of Cbz, and subsequent Michael addition. Interestingly, homonorbenzomophan was characterized as a selective ligand at Sigma-2 showing 52 folds versus Sigma-1.

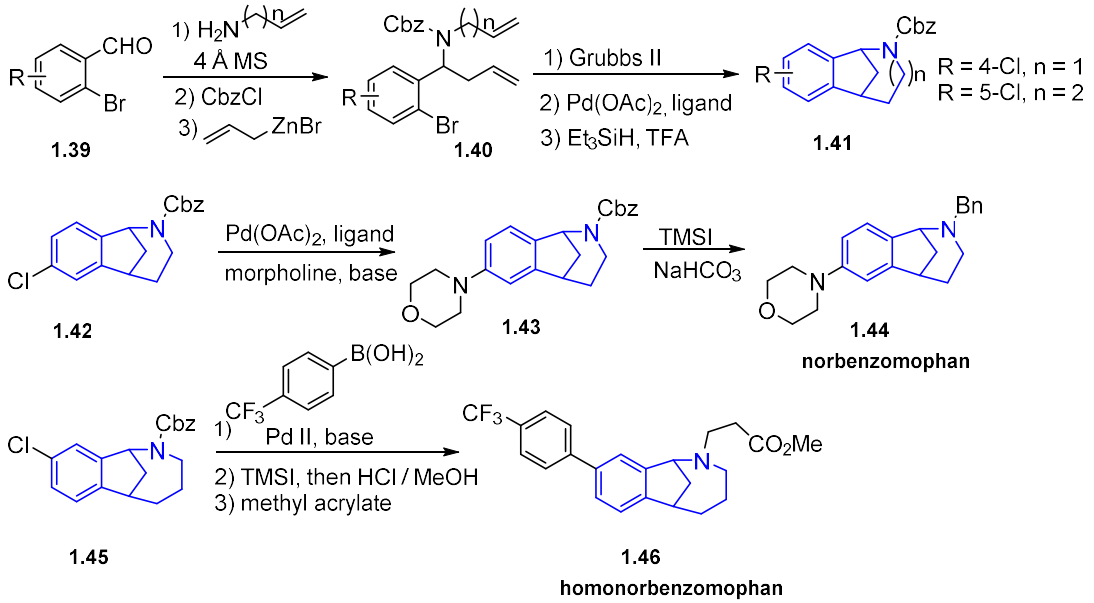


**Figure 1.18 Examples of synthesis of alkaloid mimics norbenzomophan and homonorbenzomophan *via* MCAP**

Aube initially analyzed that the selected families of alkaloids with privileged structures cover versatile biological properties. The privileged scaffold attached to diverse modifications may yield unexpected bioactive molecules at distinct targets. This idea shares the similar philosophy of PNP, was subsequently concepted by Klein.[36] A library of Stemonaceae alkaloids analogues were synthesized and tested with Sigma-1 receptors (Figure **1.19**), surprisingly several appeared to novel biological activities not denoted by natural alkaloid containing the similar scaffold.[37] Inspired by his previous outstanding research outcome, Aube continued to identify the prioritised skeletons of other family alkaloids whether can be incorporated into more fragments for library screening.

This puzzle has been answered since structurally diverse alkaloids mimics of the cylindricine, amaryllidaceae and lupin families (over 600 compounds) were rapidly synthesized.[38] It is important to note that chemistry to enable scaffold fusion plays a crucial role in incorporating the diverse heterocycles into the parent scaffolds efficiently. Ring fusion strategies indeed provide further diversification by connecting disparate structural elements in the pre-existing alkaloid ring system. Although impressive work has been introduced into generating alkaloids following the strategy of PNP, there is still an unmet need for efficient and versatile design of diverse, alkaloid-inspired structures, particularly for tropane, quinuclidine, and quinolizidine alkaloids.

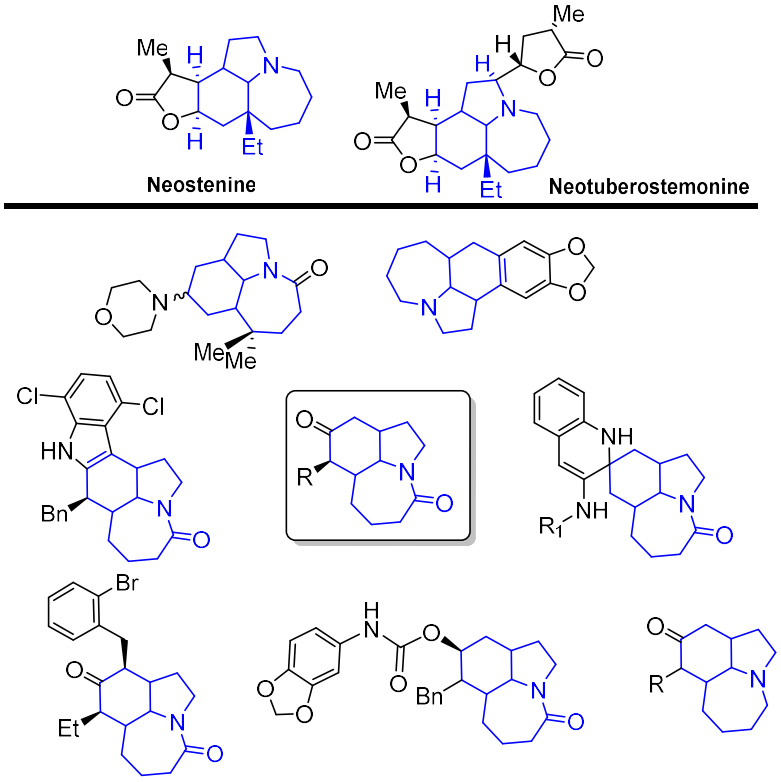


**Figure 1.19 Examples of synthesis of Stemona inspired analogues**[37]

# 2 Aims and objectives

The aim of this thesis is to synthesize heterocyclic derivatives of tropane and quinuclidine, together with quinolizidine alkaloid mimics, to identify new biologically active and selective molecules against aminergic G-protein coupled receptors (GPCRs), particularly biased towards serotonin 5-HT2 receptors or dopamine 2 receptor (D2R).

5-HT2 and D2R have been identified as the main targets to treat a series of psychiatric diseases including depression, anxiety and schizophrenia. Despite the availability of a significant amount of ligands demonstrating high affinity at 5-HT2 or D2R, they usually possess additional high potency at other aminergic GPCRs. As such, they may cause unnecessary side effects in the clinic trials, which exert extra risks on drug developments. A further introduction to the relevant aminergic GPCRs will be presented in the relevant results chapters.

Diverse alkaloid inspired collections provide a promising strategy to identify novel ligands against the chosen aminergic GPCRs, which we exemplified the impressive findings in the last decades. Compared to the aforementioned tactics, we focus on the synthesis of alkaloid mimics featuring diverse spirocyclic fusions. Here, we choose ketones as the key functional handles since they have been documented to be particularly useful in the construction of PNP.[39]

Tropane alkaloids, an important class of alkaloids, have displayed remarkable medical applications, such as the treatment of neurological and psychiatric impairments. For project I, We propose to synthesize a library of tropanes, starting from commercially available tropinone or *N*-Boc-4-nortropinone, a divergent synthetic strategy will enable the construction of spiro- or edge- fused heterocycles. In addition, we propose to synthesize a library of quinuclidine alkaloid mimics with spirocyclic fusions. We aim to identify the selective modulators through screening the combined tropane and quinuclidine alkaloid inspired collections against 5HT2 receptors.

Quinolizidine alkaloids are natural products known for their diverse biological activities including antimalarial, anti-cancer, antivirus and neurological functions. Owing to their significant therapeutic potentials, quinolizidine as an inspiration to identify structurally unknown D2R ligands through a focused synthetic library are particularly less explored. For this project, starting from described ketone intermediate, a range of different spirocyclic heterocycles will be appended to the quinolizidine scaffold to produce a large number of quinolizidine analogues.

# 3 Project aim and outline

The recombination of natural product fragments in unprecedented ways to deliver so-called pseudo-natural products has emerged as an important strategy for bioactive compound discovery. In this context, we propose that privileged primary fragments tropanes and quinuclidines predicted to be enriched in activity against a specific target class, can be coupled to diverse secondary fragments to engineer selectivity among closely related targets (**Figure 3.1**).

Tropanes and quinuclidines are found in many approved drugs, and they particularly constitute privileged scaffolds for muscarinic acetylcholine (M) GPCRs and nicotinic acetylcholine receptors (nAChRs). The current synthetic strategies for the synthesis of targeted libraries focus on a specific scaffold with a large number of analogues, which may hamper the development of new ligands.

Commercially available tropinone or *N*-Boc nortropinone and quinuclidinone, alongside related α-bromoketone and β-keto ester derivatives can serve as essential building blocks to fuse diverse aromatic heterocycles *via* a series of classic reactions. This will enable us to access high levels of scaffold diversity. In general, each scaffold in the whole library will be represented by several analogues, which are will provide preliminary structure-activity relationship (SAR) information.

With the resulting compound collections in hand, we tested both antagonist and agonist activities at the receptors 5-HT2A and 5-HT2C in a functional assay. To study the selectivity over other related receptors, the collections were also tested against D1R (D1-like) using a cAMP assay and D2R (D2-like) using a β-arrestin recruitment assay, respectively. The selectivity was further determined by screening α4β2 and α3β4 nAChRs.

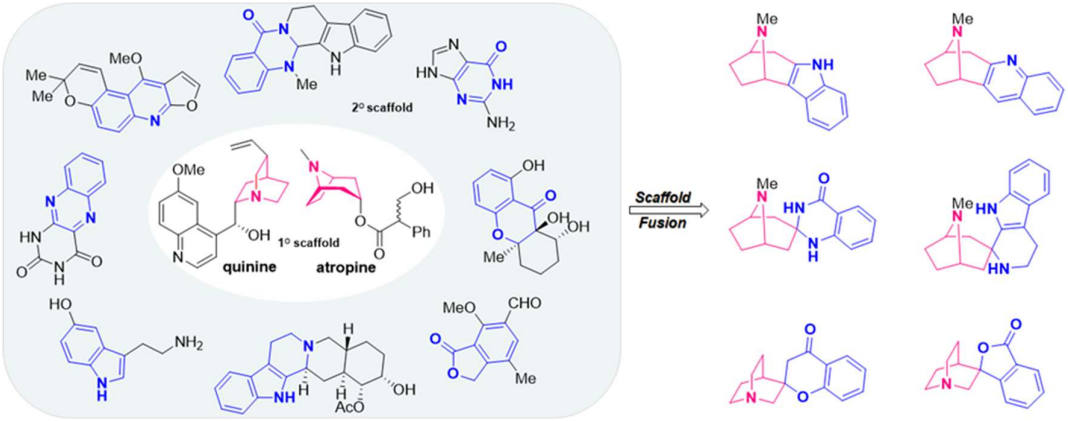


**Figure 3.1 Design strategy for a diverse, 3-dimensional alkaloid-inspired compound collection**

## 3.1 Drugs contain tropanes and quinuclidines against GPCRs or ion channels

Naturally occurring alkaloids provide a rich source of modulators of ligand-gated ion channels and G-protein coupled receptors (GPCRs).[40–42] In particular, alkaloids with basic amines such as those found in tropanes and quinuclidines have historically been found to constitute privileged scaffolds for monoaminergic and muscarinic acetylcholine (M) GPCRs (**Figure 3.2**). So far, there are more than 20 drugs containing tropanes in the core framework.[43] Among them, tropane alkaloids including atropine, hyoscyamine, and scopolamine act as anticholinergic drugs against M receptors.[44] Tropane analogues also play an indispensable role in developing the novel chemotherapy due to the competitive potency against aminergic GPCRs or ligand-gated ion channels such as tiotropium, varenicaline, and tropisetron. In particular, tiotropium and varenicaline are competitive marketed small molecule drugs to treat chronic obstructive pulmonary disease (COPD) and smoking cessation, respectively. In parallel, quinuclidines exist in many approved drugs such as cevimeline, mequitzine, and palonosetron. Pharmacological findings reveal that cevimeline is an agonist for M1 and M3 receptors, while mequitazine is an antagonist against histamine H1 receptor, respectively. In contrast, palonosetron is a selective antagonist at serotonin 5-HT3 receptor, which belongs to ligand-gated ion channels.

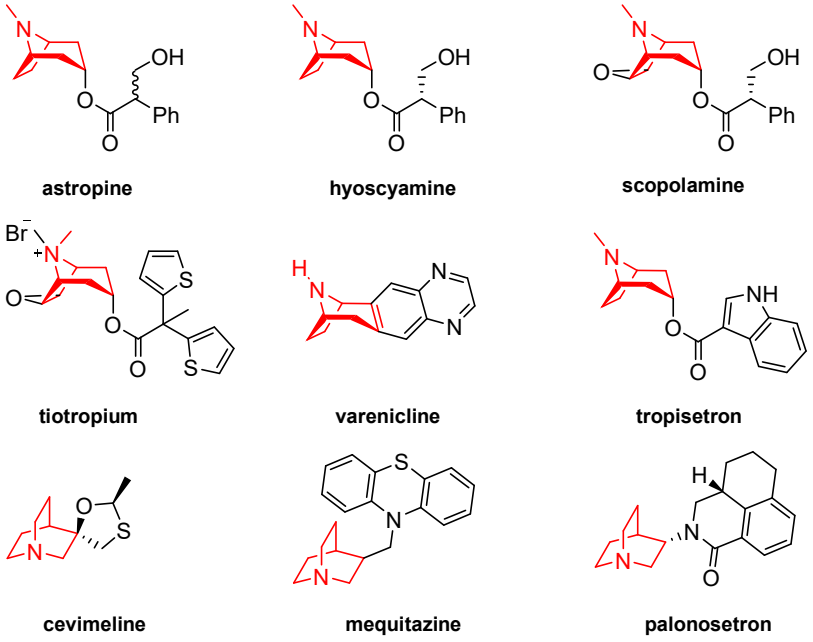


**Figure 3.2 Examples of drugs containing tropanes and quinuclidines against GPCRs or ion channels**

## 3.2 The reported library synthesis of tropane and quinuclidine

Although significant literature on the synthesis of tropane- and quinuclidine-containing compounds exists, there is little diversity in the structures accessed so far. Only within the more general field of alkaloid-inspired compound synthesis a few notable exceptions exist, where a significant number of scaffolds, have been prepared. In 2013, Waldmann reported the enantioselective synthesis of a library of tropanes between cyclic azomethine ylide precursor **3.01** and nitroalkenes **3.02** *via* an asymmetric Cu(I)-catalyzed [3+2] cycloaddition (**Figure 3.3A**).[45] Further biological screening revealed that the new class of tropanes **3.03** can modulate Hedgehog signalling. More recently, Marsden in collaboration with Nelson reported the synthesis of diverse tropane inspired library from the building blocks **3.04** and **3.05**.[46] The synthetic collections featured monopodal connections and edged fusions. The subsequent phenotypic screening suggested that compound **3.07** is an inhibitor of Hedgehog signalling, and compound **3.06** is an inhibitor of *P. falciparum* survival (**Figure 3.3B**). Furthermore, the identification of a dual ligand at 5-HT3 and α7 was achieved from the monopodal connections between quinuclidines and triazoles *via* an established click reaction (**Figure 3.3C**).[47]

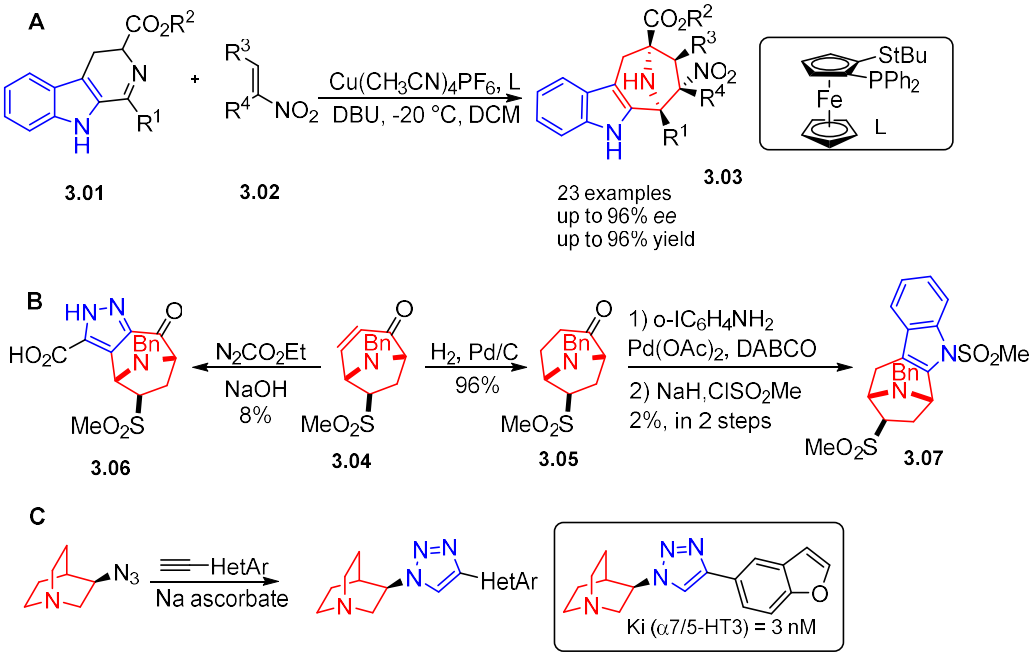


**Figure 3.3 Selected examples of the synthesis of biological active tropanes and quinuclidines**

## 3.3 G protein-coupled receptors (GPCRs)

G protein-coupled receptors (GPCRs), also called seven transmembrane receptors, represent the largest family of membrane receptors in eukaryotes. To date, approximately 800 GPCRs are encoded in the human genome.[48] They engage a series of cascade physiological processes when bound to a ligand such as neurotransmitter, hormone *etc.* As such, GPCRs are often targeted to treat a broad spectrum of human diseases. Not surprisingly, it has recently been calculated that roughly 34 % of all FDA approved drugs target this family.[49]

### 3.3.1 The classification of serotonin receptors (5-HTR)

Serotonin receptors (5-HTR**)** are divided into the GPCR family and ligand-gated ion channels (5-HT3) (**Figure 3.4**).[50]The further classification of 5-HTR associated with GPCRs has been addressed due to the difference from sequence homology, and signal transduction pathway. So far, a total of 14 5-HTR have been reported in mammals, which are subdivided into 5-HT1 (5-HT1A-1F), 5-HT2 (5-HT2A-2C), 5-HT3, 5-HT4, 5-HT5 (5-HT5A-5B), 5-HT6, and 5-HT7.

### 3.3.2 Serotonin receptors (5-HTR) in health and diseases

5-HTRs are widely distributed in the central nervous system (CNS) that are essential for regulating neurological processes including memory, cognition, sleep, as well as appetite.[51] As a result, they encouraged numerous researchers to explore the therapeutic potential to treat neurological and psychiatric diseases. In practice, 5-HT2 receptors are probably the most attractive family of 5-HTR since they have been profiled the main targets among a large number of approved drugs to treat psychiatric disorders.[52]

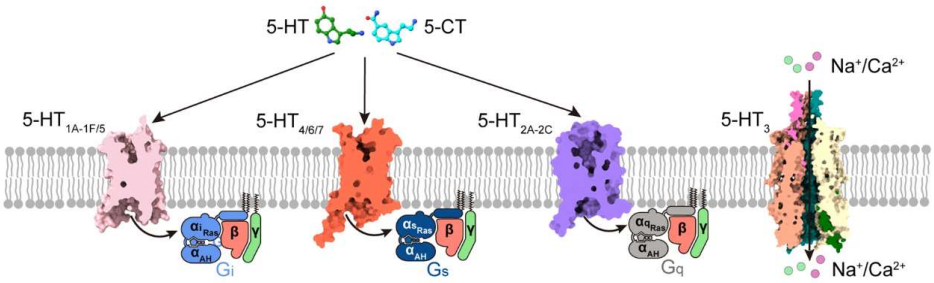


**Figure 3.4 Schematic illustration of 5-HT receptors. Reproduced from Tan *et al.*[50]**

## 3.4 Serotonin 5-HT2 receptor modulators

5-HT2 receptors comprise 5-HT2A, 5-HT2B, and 5-HT2C. The 5-HT2A receptor exhibits 41% and 46% overall sequence homology compared to 5-HT2B and 5-HT2C in humans, respectively.[53] Such high sequence identity renders it difficult for researchers to identify selective modulators.

Many psychedelic drugs possess high agonistic activity at 5-HT2A, including LSD, 25I-NBOMe, and TBG (**Figure 3.5**).[54,55] LSD was characterized a nonselective agonist at 5-HT2A due to the comparative binding affinities to other aminergic GPCRs. In order to explore new ligands with improved selectivity against other receptors, 25I-NBOMe and derivatives were synthesized, but they are often characterized as the synthetic hallucinogens. As such, focus at least has partially shifted from the exploration of more potent and selective ligands to discover novel modulators such as TBG but without hallucinogenic effect. 5-HT2A antagonists also have the remarkable potential for the treatment of Schizophrenia. Examples of atypical antipsychotics include known clozapine, aripiprazole, risperidone and zotepine. In general, 5-HT2B agonists are believed to have cardiovascular side effects, which hamper the further clinical research. In contrast, 5-HT2B antagonists are being studied the therapeutic potential to teat irritable bowel syndrome. As a case, the highly potent and selective 5-HT2B antagonist RQ 00310941 developed by RaQualia Pharma Inc. is being tested in the phase I clinic trials. 5-HT2C receptors are believed to regulate various behaviors including mood, anxiety, and appetite.[56] As a known selective 5-HT2C agonist, Lorcaserin has been marketed to treat obesity by controlling appetite.

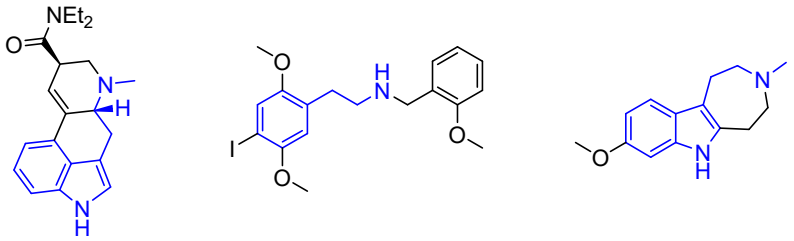


**Figure 3.5 Selected examples of potent 5-HT2A agonist**[54,55]

## 3.5 Synthesis of tropanes inspired library

In this section, I will describe my efforts to synthesise a library of diverse compounds containing tropane as the guiding natural product fragment. This will be fused to a range of secondary fragments predominantly found in natural products to access compounds for targeted screening against aminergic GPCRs and ion channels.

### 3.5.1 Indole-fused tropane analogue synthesis

The indole heterocycle frequently occurs in bioactive small molecules and natural products. Approaches to construct indole rings include Pd catalyzed annulation reaction and the well-known Fisher indole synthesis (**Table 3.1**). To examine the feasibility of the former for tropane library synthesis, we reacted tropinone and *o*-iodoaniline similar to the reported literature (entry 1). Although a decent amount of tropinone was consumed, we only observed a decomposed mixture. Instead, we turned to focus on Fisher indole synthesis via screening various conditions (entries 2-8). Inspired by the high efficiency synthesis of indole fused steroid analogues using *p*-TsOH·$H_2O$, this method was employed first.[26] To begin with, the condensation of tropinone and phenyl hydrazine led to the formation of hydrazone within 2 hours, which could be isolated and characterized by NMR. Interestingly, the further intramolecular cyclization did not occur even we extended the reaction time. Another approach by adding additives $MgSO_4$ failed to generate the desired product. We also investigated more forcing reaction conditions ranging from high temperature to strong acid under microwave irritation. Disappointedly, we are unable to observe any cyclized product suggested by LC-MS. Although L-(+) Tartaric acid-DMU at low melting has been recommended to synthesize a focused library of various indoles,[57] this protocol failed to accommodate tropinone (entry 7). Finally, we found HCl in MeOH at high concentration could dramatically improve the conversion of hydrazone into the product, which afforded compound **3.08** in good yield.

**Table 3.1 Conditions attempted to synthesize indole-fused analogues**

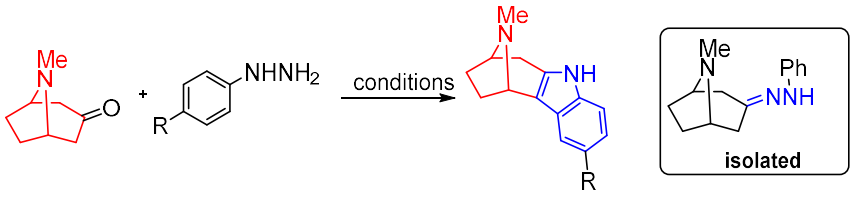


| Entry | R | Conditions | Yield (%) |
|---|---|---|---|
| 1 | | 1.0 equiv *o*-iodoaniline, 10% $Pd(OAc)_2$, 1.5 equiv DABCO, 1.6 equiv $MgSO_4$, DMF, 105 °C, 24.5 h | - |
| 2 | H | *p*-TsOH·$H_2O$, EtOH, reflux, 2 h | - |
| 3 | H | *p*-TsOH·$H_2O$, EtOH, $MgSO_4$, reflux, 4 h | - |
| 4 | H | *p*-TsOH·$H_2O$, EtOH, reflux, 2 h; sealed, 120 °C, overnight | - |
| 5 | H | 5% $H_2SO_4$ in EtOH, reflux, 24 h | - |
| 6 | H | 7% $H_2SO_4$ in 1,4-Dioxane, 130 °C, microwave, 1 h | - |
| 7 | OMe | L-(+) Tartaric acid-DMU, 70 °C, 1 h | - |
| 8 | H | HCl in MeOH (3 M), reflux, 18 h | 46 |

Under the optimized conditions, three analogues featuring different substitutions could rapidly be prepared (**Table 3.2**). The reaction between tropinone and 4-methyl phenylhydrazine afforded analogue **3.09** in moderate isolated yield. However, analogue **3.10** was generated in a lower yield even in a longer reaction time. In order to access additional analogue containing secondary amine, *N*-Boc nortropinone was reacted with 4-flouro phenylhydrazine followed by deprotection in one pot reaction, which offered analogue **3.11** in 42% isolated yield.

**Table 3.2 Scope of indole-fused tropane analogues via Fisher indole synthesis**

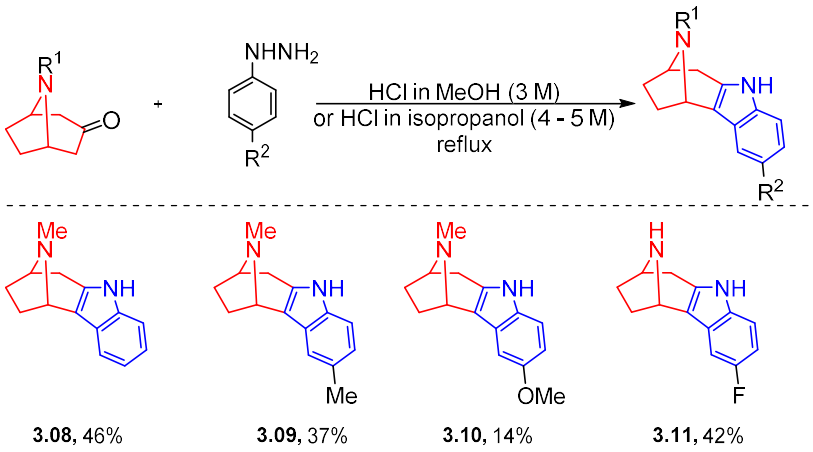


Attempts to obtain structurally relevant three-dimensional analogues, the resulting product **3.08** was treated with different oxidants in mixed solvents to obtain the spirooxindole (**Scheme 3.1**). To begin with, we prioritized *N*-Bromosuccinimide (NBS) as the testing oxidant since it has been widely used to access indole rings to obtain oxindoles. Unfortunately, this oxidant proved unsuccessful to contract compound **3.08**, the crude NMR spectra suggested bromination occurs in the aromatic ring system. More recently, Tong employed Oxone ($KHSO_5$-1/2$KHSO_4$-1/2$K_2SO_4$) as the key oxidants, which enabled the synthesis of spiroindolone collection including naturally occurring alkaloids horsfiline and rhyncophyline.[58] However, this protocol failed to transform compound **3.08** into the desired product. The major product is presumably associated with the brominated side product suggested by LC-MS.

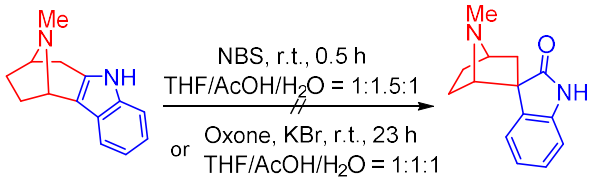


**Scheme 3.1 Conditions attempted to synthesize spirooxindole**

### 3.5.2 Quinoline-fused tropane analogue synthesis

To synthesize quinoline-fused analogues, the Friedländer and related syntheses were preferably employed due to mild reaction conditions and wide substrates scope (**Table 3.3**). Commencing the synthesis of a quinoline-fused library from tropinone and 2-aminobenzophenone under microwave irritation, which afforded analogue **3.12** in moderate yield. This condition has been extended to react with substituted 2-aminobenzophenones in good yields. Furthermore, the reaction with 2-aminoacetophenone also produced analogue **3.13** in 21% yield.

**Table 3.3 Scope of quinoline-fused tropane analogues *via* Friedländer syntheses with ketone**

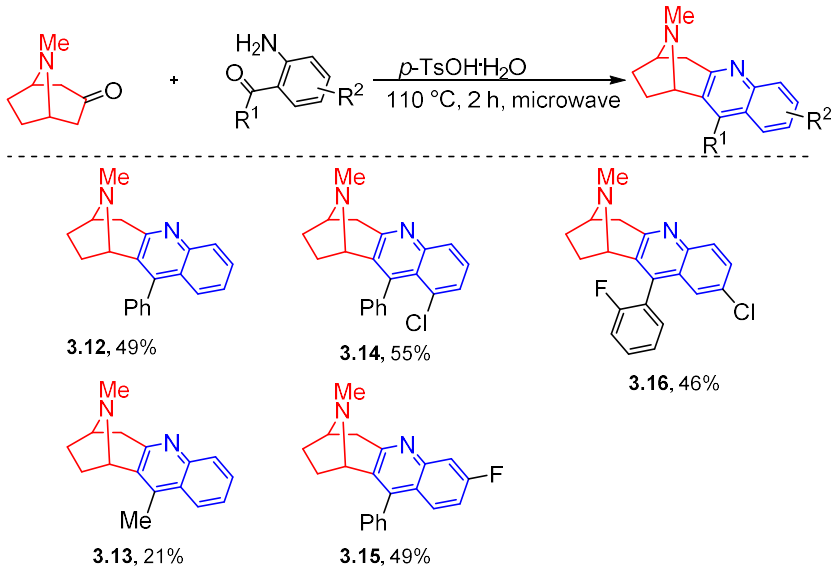


**3.12**, 49%

**3.14**, 55%

**3.16**, 46%

**3.13**, 21%

**3.15**, 49%

To increase the chance of identifying new hit compounds, it was decided to synthesize more quinoline-fused analogues. The additional substrates including unstable 2-aminobenzaldehydes, which can be produced by the reduction of 2-nitro benzaldehydes, and for use without further purification. As such, we treated the substituted 2-nitro benzaldehydes followed by Friedländer condensations, which afforded analogues (**3.17-3.19**) in satisfied yields (**Table 3.4**).

**Table 3.4 Scope of quinoline-fused tropane analogues *via* Friedländer syntheses**

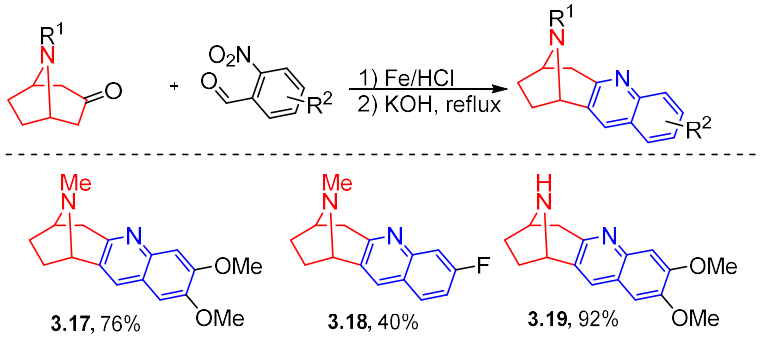


**3.17**, 76%

**3.18**, 40%

**3.19**, 92%

### 3.5.3 The preparation of α-bromoketone and β-keto ester derived *N*-Boc nortropinone

*N*-Boc nortropinone could be further functionalised to provide additional building blocks including the α-bromoketone **3.20** and β-keto ester **3.21** (**Scheme 3.2**). α-bromination of *N*-Boc nortropinone was carried out with 5,5-dibromobarbituric acid, which resulted in the synthesis of the desired product with mono α-bromination, and the side product with di- bromination suggested by LC-MS. Additionally, the unreacted *N*-Boc nortropinone was also observed. Removing the impurities by recrystallization provided the desired building block **3.20** in good yield. To synthesize the β-keto ester as another bulling block, *N*-Boc nortropinone and dimethyl carbonate were treated with NaH in refluxing THF. Due to the high conversion of *N*-Boc nortropinone, it thus provided the desired β-keto ester **3.21** in excellent yield.

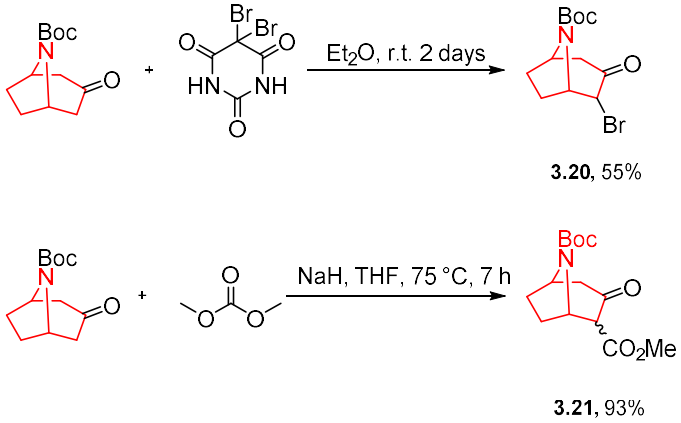


**Scheme 3.2 Synthesis of α-bromoketone and β-keto ester as building block**

### 3.5.4 Quinoxaline-fused tropane analogue synthesis

To obtain quinoxaline analogues, the initial reaction was set up with α-bromo *N*-Boc-nortropinone **3.20** and *o*-phenylenediamine in refluxing ethanol. However, conversion into the desired product was poor, possibly as a result of lacking sufficient oxygen in the solution. In a parallel experiment, the mixed solution was saturated with air at 70 °C, which ended up with the synthesis of analogue **3.22** in 45% yield. This condition has been extended to *o*-phenylenediamines bearing various functional groups (**Table 3.5**). As a result, four desired products were afforded in moderate yields.

To synthesize more analogues containing secondary amine, removing the protecting groups of quinoxaline analogues by adding HCl in MeOH (3 M), which enabled the synthesis of analogues **3.26** -**3.29** in quantitive yields.

**Table 3.5 Scope of quinoxaline-fused tropane analogues**

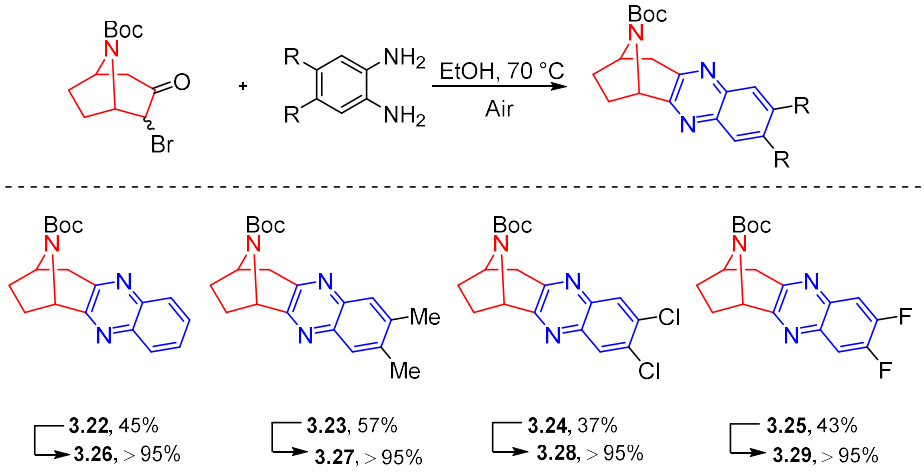


To examine additional analogue fused to pyrido[2,3-b]pyrazine, we commenced α-bromo *N*-Boc-nortropinone **3.20** and pyridine-2,3-diamine over 5 hours. It turned out to be disappointed since no product was detected under this protocol (**Scheme 3.3**).

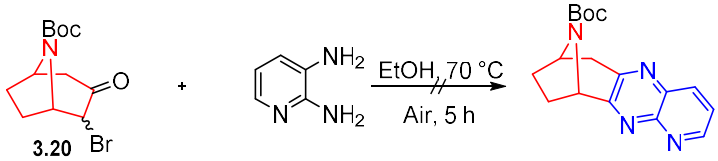


**Scheme 3.3 Condition attempted to synthesize additional analogue**

### 3.5.5 Pyrimidine-fused tropane analogues synthesis

As the *N*-Boc-nortropinone derived β-keto ester **3.21** could be prepared in high yield, it provided the ideal handle for the synthesis of pyrimidines from amidines in large scale. To maximize the chance of identifying new ligands, we covered the diverse amidines featuring different substitutions. As such, seven analogues were obtained in moderate yields. The subsequent deprotection enabled the synthesis of additional six analogues in quantitive yields (**Table 3.6**).

**Table 3.6 Scope of pyrimidines-fused tropane analogues**

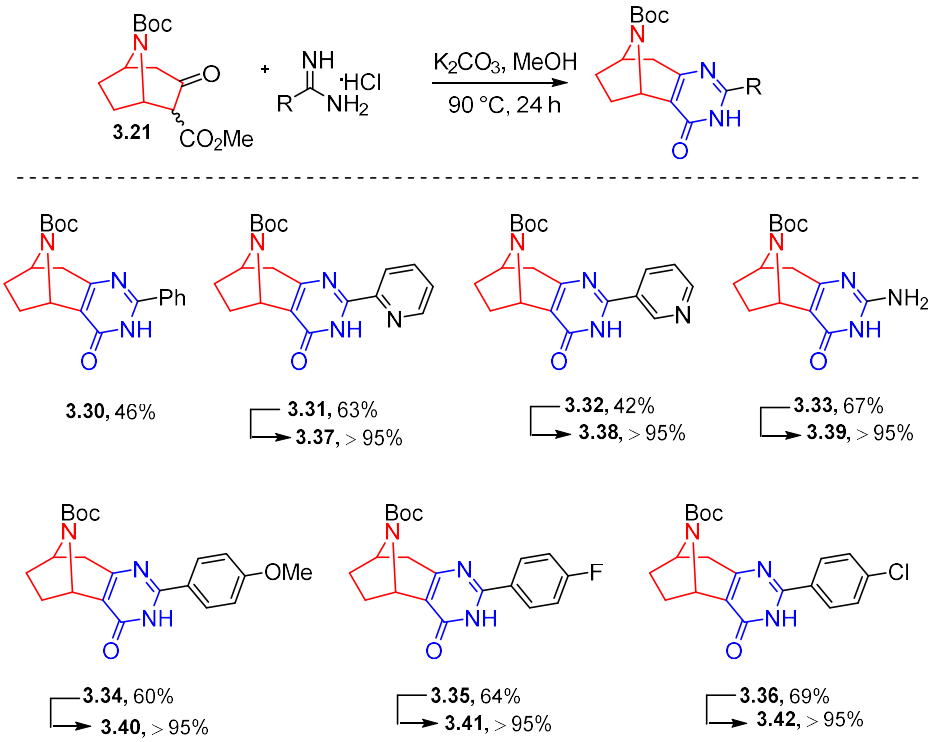

### 3.5.6 Spirocyclic tropane analogues *via* Pictet-Spengler or oxa Pictet-Spengler reaction

Synthesis of a compound library containing Tetrahydro-β-Carboline (THβC) has attracted considerable interest among medicinal chemists due to a broad range of therapeutic potentials. The methodologies to approach THβC include Pd catalyzed annulation reaction and classic Pictet-Spengler reactions mediated by acid catalysts (**Table 3.7**).[59] The Pd catalyzed annulation reaction was carried out with *N*-Boc nortropinone and tryptamine according to literature procedure. Disappointingly, this protocol led to the formation of a complex mixture (entry 1). As such, we concentrated on the exploration of Pictet-Spengler reactions *via* Lewis or Brøsted acids. However, these conditions proved inefficient to synthesize compound **3.43** since the majority of *N*-Boc nortropinone and tryptamine remained (entries 2 and 3). The use of excessive equivalents of TMSCl has demonstrated the remarkable benefits on the construction of various β-Carboline analogues.[60] We reasoned this protocol could applied to generate compound **3.43** (entry 4). As such, the high conversion of the starting material resulted in the formation of compound **3.43** in good yield.

**Table 3.7 Conditions attempted to synthesize spirocyclic tropane analogue *via* Pictet-Spengler reaction**

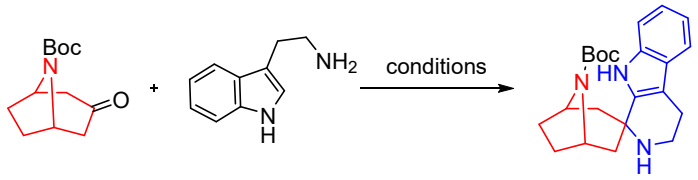


**3.43**

| Entry | Tryptamine | Condition | Time | Yield (%) |
|---|---|---|---|---|
| 1 | 1.0 equiv | $Pd(OH)_2/C$ | 24 h | - |
| 2 | 1.0 equiv | 10 mol% $I_2$, EtOH, reflux | 15.5 h | - |
| 3 | 1.0 equiv | 20 mol% *p*-TsOH·$H_2O$, EtOH, reflux | 14 h | - |
| 4 | 1.2 equiv | 5 equiv TMSCl, pyridine, 5 equiv $Et_3N$, 100 °C | 22 h | 63 |

With the optimized conditions in hand, we further scoped up the substrates featuring different substitutions (**Table 3.8**). As a case, 4-methoxyltryptamine reacted to *N*-Boc nortropinone led to the synthesis of **3.44** in a poor yield. Another analogue **3.45** could be achieved in good yield *via* a Pictet-Spengler reaction followed by the decarboxylation in one pot reaction. Interestingly, analogue **3.45** was identified insoluble in the solvents of $H_2O$, DCM, and MeOH. To determine the absolute configuration, the compound crystal was obtained as the HCl salt. However, the treatment of *N*-Boc nortropinone and 4-chlorotryptamine failed to synthesize compound **3.46** although a decent amount consumption detected by LC-MS. Moreover, we did not observe any transformation into compound **3.47** in the presence of *L*-tyrosine. In order to access more analogues containing secondary amine, starting from compounds **3.43** and **3.44** in the presence of HCl in MeOH (3 M). As a result, analogues **3.48** and **3.49** could be synthesized in quantitive yields.

**Table 3.8 Scope of spirocyclic tropane analogues *via* Pictet-Spengler reaction**

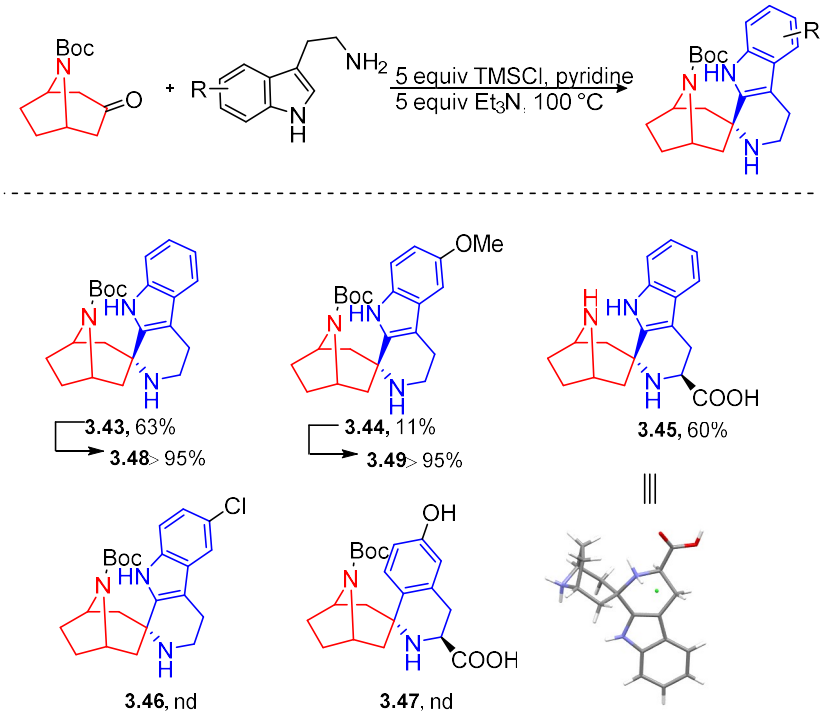


In order to examine additional analogue containing tertiary amine **3.50**, we commenced tropinone and tryptamine under the standard condition (**Scheme 3.4**). Disappointedly, only a trace amount of the desired product was detected by LC-MS.

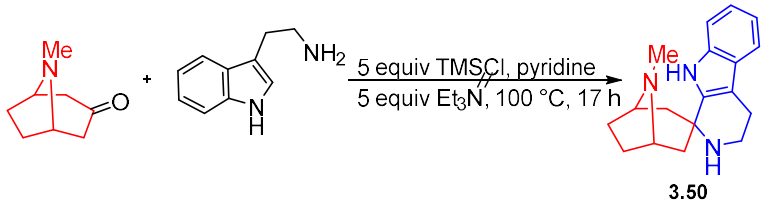


**Scheme 3.4 Condition attempted to synthesize additional analogue *via* Pictet-Spengler reaction**

Similarly to the Pictet-Spengler reaction, the oxa Pictet-Spengler reaction is involved in the condensation of ketone or aldehyde with aryl alcohol under acidic conditions. This reaction provides a straightforward approach to synthesize isochromans, and it was initially identified by Wünsh.[61] It well accommodated spirocyclic isochromans fused to the natural product fragments. As we discussed in the introduction section, $TfOH{\cdot}SiO_2$ can be used to carry out the oxa Pictet-Spengler reaction using a broad arrange of ketones.[23] However, it has been also discussed this protocol failed to accommodate basic amines. The oxa Pictet-Spengler reaction mediated by *p*-$TsOH{\cdot}H_2O$ has remarkably contributed to identify a series of potent and selective sigma receptor ligands.[62] We thus employed the similar condition to explore the synthesis of **3.51**. The test reaction was initially performed at 100 °C under $N_2$ protection, and was subsequently monitored by TLC and LC-MS. Disappointedly, the reaction suffered degradation after 4.5 hours although the formation of a small portion desired product. Lowering the reaction temperature was beneficial to improve the conversion into the desired product **3.51** (**Scheme 3.5**). The scope of tryptophol substrates could be further extended depending on the relevant biological screening if needed.

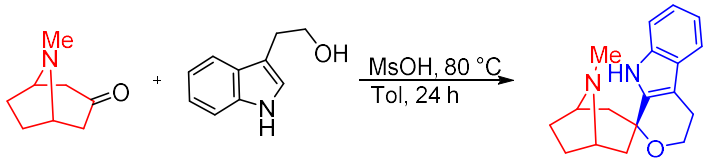


**3.51,** 60%

**Scheme 3.5 Synthesis of additional siprocyclic tropane analogue *via* oxa Pictet-Spengler reaction**

However, attempts to synthesize compound **3.53** by accessing tropinone and alcohol **3.52** was not successful since no product was observed monitored by TLC over 7 hours (**Scheme 3.6**).

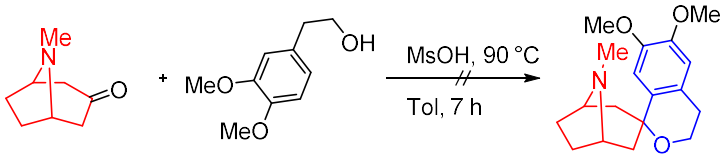


**3.52** **3.53**

**Scheme 3.6 Condition attempted to synthesize siprocyclic chromane *via* oxa Pictet-Spengler reaction**

### 3.5.7 Spirocyclic tropane analogues *via* [3+2] cycloaddition

Tosylhydrozone species served as stable and nonexplosive metal carbenoid precursors, which could be used to access C-C bond formation including cross coupling and cyclopropanation. Tosylhydrozones treated with base can react to alkene and alkyne following a [3 + 2] cycloaddition. To access additional spirocyclic scaffold, dihydropyrazole **3.55** was prepared from *N*-Boc nortropinone by first forming the N-tosyl hydrazine **3.54**, and subsequently reacting the latter with chalcone in a [3+2] cycloaddition (**Scheme 3.7**). The product was formed as a single diastereoisomer and the relative configuration confirmed using NOESY experiments (**Figure 3.6**).

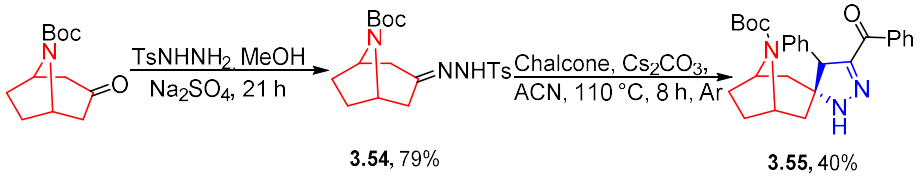


**3.54**, 79% **3.55**, 40%

**Scheme 3.7 Synthesis of pyrazole-fused analogue via [3+2] cycloaddition**

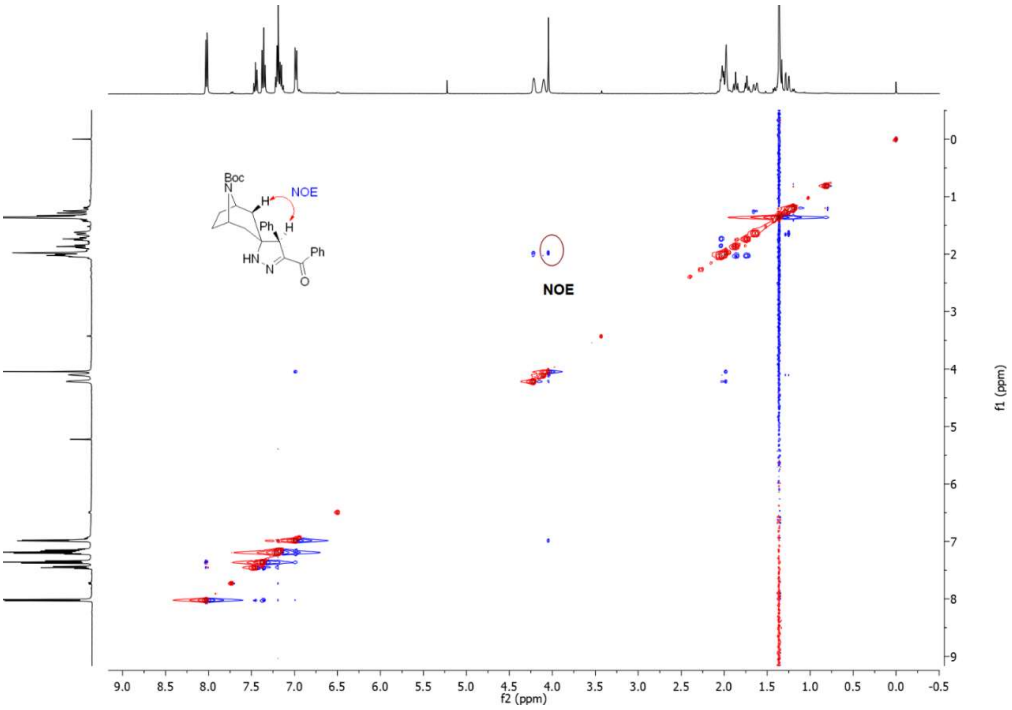


**Figure 3.6 NOESY spectra of dihydropyrazole 3.55**

### 3.5.8 Spirocyclic tropane analogues *via* reactions with anthranilamides

In an effort to synthesize spirocyclic quinazolinones, *N*-Boc-nortropinone and anthranilamide were treated with *p*-TsOH·$H_2O$ in a reflux (**Scheme 3.8**). However, the conversion is very limited over 35 hours, it only offered 42 % combined yield. This reaction is also deficient for the diasteroselectivity, and the d.r value is calculated equal to 1:2. In addition, the isolation of each diasteroisomer with high purity is challenging. Taken together, it might be worthwhile to explore other catalysts.

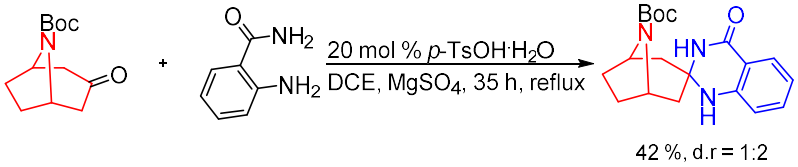


**Scheme 3.8 Condition attempted to react with anthranilamide**

$NH_4Cl$ served as the key catalyst, has demonstrated the great potentials to access a series of ketones to react with anthranilamide in high yields.[63] We thus prioritized this catalyst to access spirocyclic quinazolinones (**Table 3.9**). As a result, all analogues were obtained in high yields and high diasteroselectivity. The reaction of tropinone with anthranilamide enabled the synthesis of analogue **3.59** in 20 % yield, but only a single diasteroisomer was detected (**Figure 3.7**).

**Table 3.9 Scope of spirocyclic tropane analogues via reactions with anthranilamides**

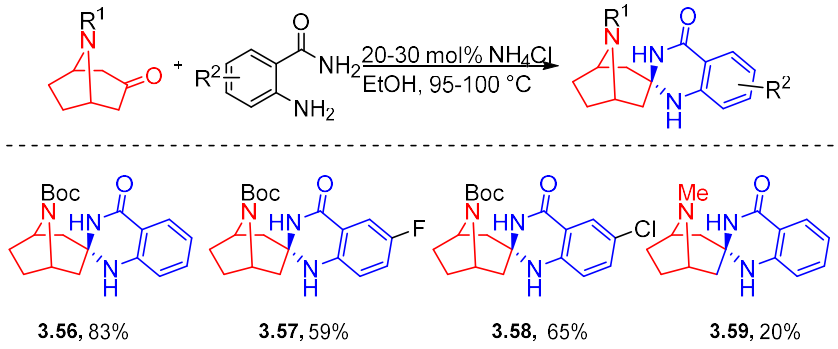


**3.56,** 83% **3.57,** 59% **3.58,** 65% **3.59,** 20%

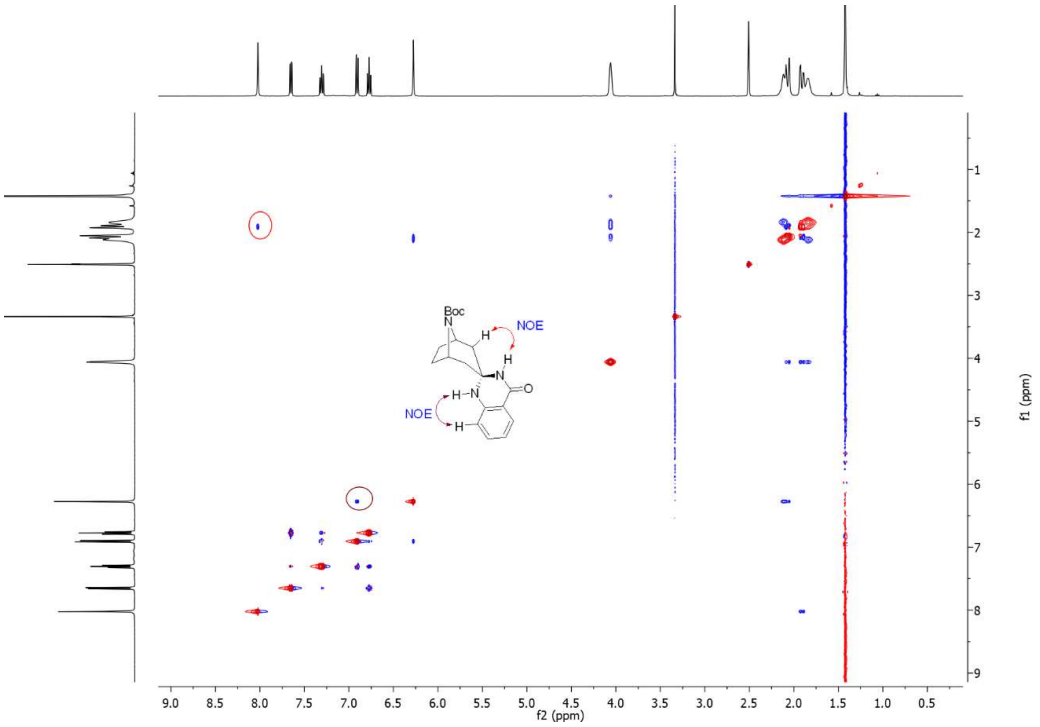


**Figure 3.7 NOESY spectra of analogue 3.56**

In an effort to generate additional analogue without protecting groups, analogue **3.56** was tested deprotection in consistent with the previous procedure. However, the product partially suffered epimerization alongside degradation, which made it difficult for further purification (**Scheme 3.9**).

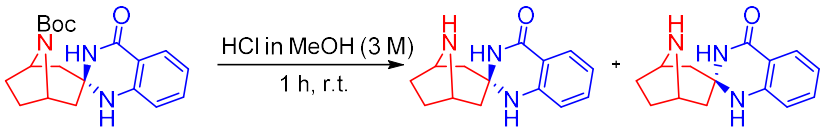


**Scheme 3.9 Example of compound 3.56 suffered epimerization**

### 3.5.9 Spirocyclic tropane analogues *via* Kabbe reaction

*N*-Boc nortropinone was reacted with 2-hydroxyacetophenones in a Kabbe reaction to produce chromanones in moderate yields as single diastereoisomers (**Table 3.10**). Initially, the crude product was purified by silica gel for column chromatograph, hexane and ethyl acetate are the eluents, which resulted in the isolation of the product **3.60** in 85% purity. It´s noted the unreacted *N*-Boc nortropinone was further removed by recrystallization in hexane. The structure of analogue **3.60** was also confirmed by x-ray crystallography. The protecting group of the products was subsequently removed with HCl in MeOH (3 M) to afford the amines in quantitative yields. Furthermore, the Kabbe reaction was also examined to access chromanone **3.64** tolerated a methyl group starting from tropinone. However, under the same protocol, the conversion was poor, as suggested by LC-MS.

**Table 3.10 Scope of spirocyclic tropane analogues via Kabbe reaction**

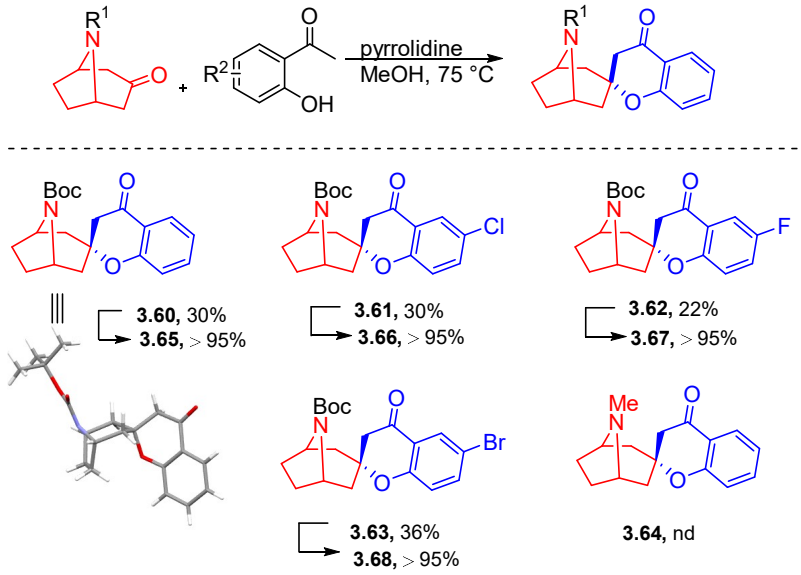

Finally, chromanone **3.60** was reacted with anthranilamide **3.69** to furnish the bis-spirocycle-containing **3.70** (**Scheme 3.10**), a motif found in natural products and recently introduced as a design strategy in compound library synthesis.[64] The structure of the product is also characterized as a single diastereoisomer suggested by 2D NOESY spectra (**Figure 3.8**).

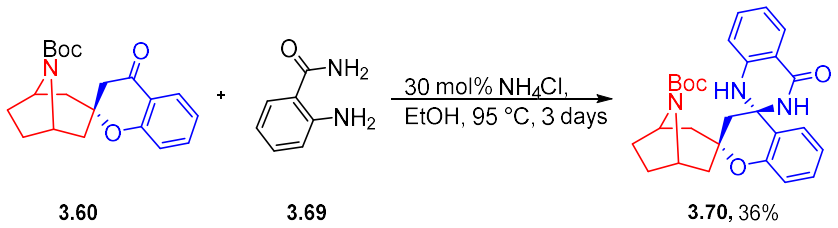


**3.60** **3.69** **3.70,** 36%

**Scheme 3.10 Synthesis of bis-spirocycle from chromanone 3.60**

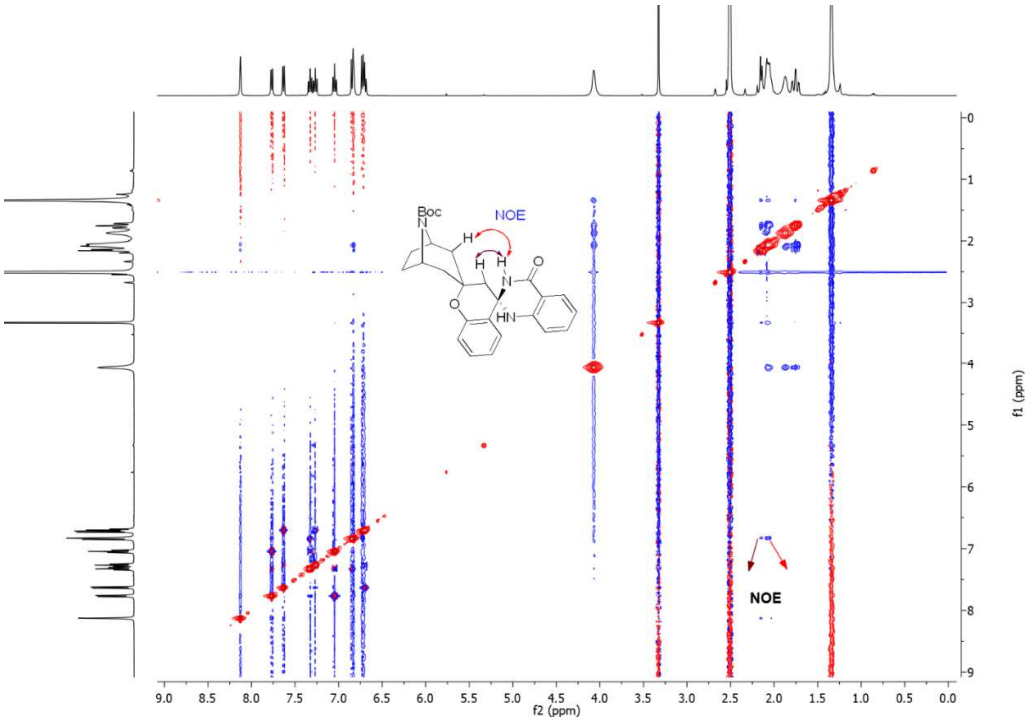


**Figure 3.8 NOESY spectra of analogue 3.70**

## 3.6 Synthesis of quinuclidines inspired library

In this section, I will describe my efforts to synthesise a library of diverse compounds containing quinuclidines. This will be also fused to a range of secondary fragments predominantly found in natural products to access spirocyclic collection. This work has been partially carried out by our former master student Nicklas Peter Hovendal under my guidance. In addition, I will also discuss unsuccessful examples failed to synthesise quinuclidine analogues with edged fusion.

### 3.6.1 Spirocyclic quinuclidine analogues *via* reactions with anthranilamide

Similar design principles were subsequently applied to access a quinuclidine-derived compound collection, with an exclusive focus on obtaining spirocyclic library compounds (**Table 3.11**). Starting from the free base of commercially available quinuclidin-3-one hydrochloric acid salt, under analogous conditions to tropinone, spirocyclic dihydroquinazolinones **3.71-3.73** were prepared in good yields. It is worth pointing out that the resulting quinazolinones have poor solubility in various solvent systems including DMSO, DCM, EtOH, as well as $H_2O$, but they can be protoned by HCl in $H_2O$. As such, the resulting quinazolinones were characterized as the HCl salts by NMR.

**Table 3.11 Scope of spirocyclic quinuclidine analogues via reactions with anthranilamide**

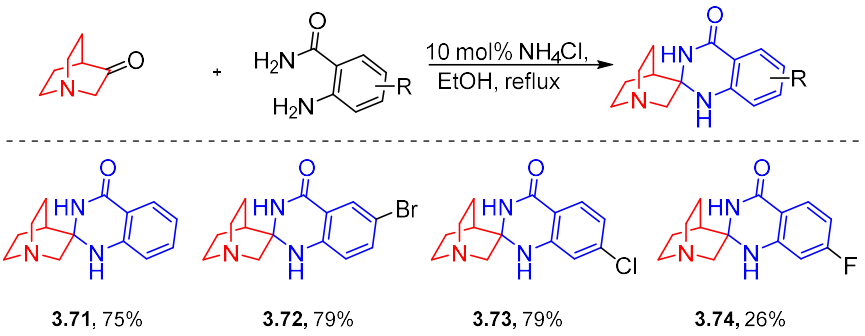


### 3.6.2 Spirocyclic quinuclidine analogues *via* Pictet-Spengler reaction

A spirocyclic β-carboline **3.76** was obtained in one step from 5-methoxytriptamine **3.75** employing the Pictet-Spengler reaction (**Scheme 3.11**). However, the oxa Pictet-Spengler reaction failed to mediate quinuclidinone into the desired spirocyclic product (**Scheme 3.12**). It´s suggested that the tertiary amine of quinuclidinone tended to be protoned with MsOH, since the pure side product **3.77** could be isolated and further characterized with NMR.

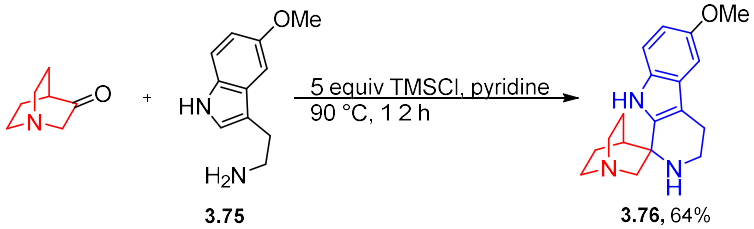


**Scheme 3.11 Synthesis of spirocyclic quinuclidine analogue via Pictet-Spengler reaction**

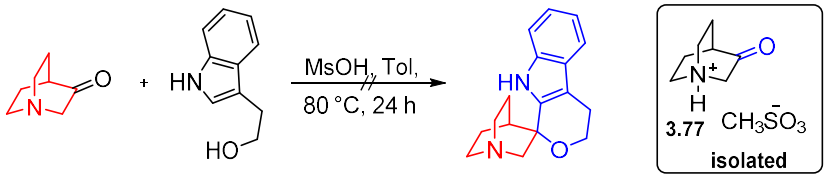


**Scheme 3.12 Condition attempted to synthesize spirocyclic quinuclidine *via* Oxa Pictet-Spengler reaction**

### 3.6.3 Spirocyclic quinuclidine analogues *via* Kabbe reaction

Quinuclidines fused to spirocyclic carbamates have contributed the identification of the first generation selective α7 nAChRs ligand **3.78**[65], and more potent and selective α7 nAChRs ligand **3.79**[66] (**Scheme 3.13**). Due to the high potency and remarkable selectivity against nAChRs, together with a panel of other targets, a spirocyclic quinuclidine-derived analogue AZD0328 was developed and studied by Astra Zeneca in the clinic trials to treat Schizophrenia, but it failed in the phase II.

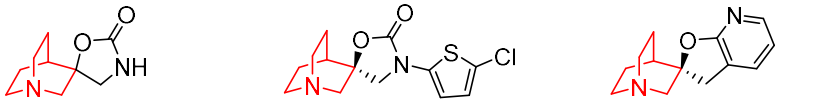

**3.78**, Ki (α7) = 190 nM
Ki (α7β2) = 16000 nM

**3.79**, Ki (α7) = 9 nM

**AZD0328**, Ki (α7) = 3 nM

**Scheme 3.13 Examples of selective α7 nAChRs ligands**

To mimic the structure relevance with novel entities to identify new amingeric GPCRs modulators in the CNS, analogues (**3.80-3.83)** are particularly interesting because they are both accessible in one pot reaction from commercially available starting material (**Table 3.12**). Employing the Kabbe reaction, spirocyclic chromanones (**16a-16d**) were also obtained in good to excellent yields.

**Table 3.12 Scope of spirocyclic quinuclidine analogues via Kabbe reaction**

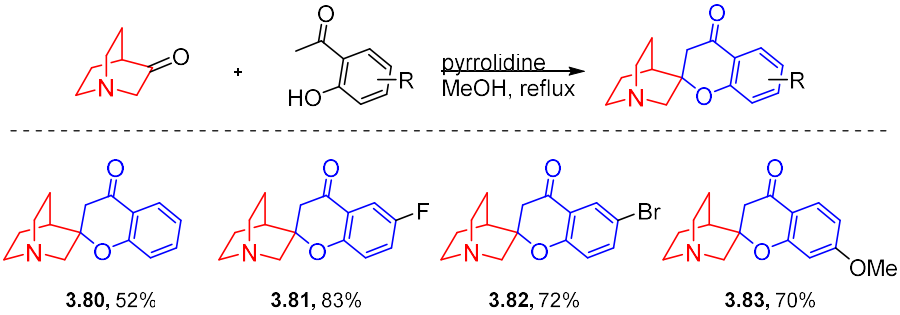


**3.80**, 52%

**3.81**, 83%

**3.82**, 72%

**3.83**, 70%

### 3.6.4 Spirocyclic γ-lactones quinuclidine analogues

The other structurally mimic could be also accessible *via* a well-established procedure. Finally, spirocyclic γ-lactones (**3.84-3.85**) were synthesized using 2-bromobenzoic acids following a lithium-halogen exchange, nucleophilic attack and cyclisation sequence (**Scheme 3.14**).

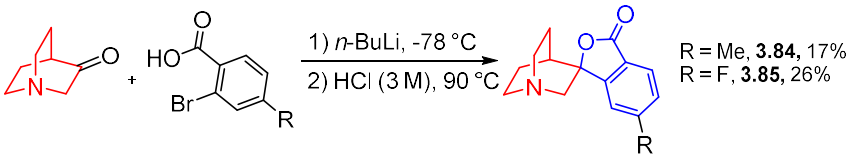


**Scheme 3.14 Synthesis of spirocyclic γ-lactones quinuclidine analogues**

### 3.6.5 Attempts to synthesize quinuclidine analogues with edged fusion

In an effort to construct **3.86** *via* a Fisher indole reaction, quinuclidinone and phenylhydrazine were reacted with HCl in MeOH (3 M). However, under these conditions, the observed intermediate hydrazone failed to go through a further rearrangement (**Scheme 3.15A**). Furthermore, Pd catalyzed annulation reaction was also examined, which resulted in a complex decomposed mixture. Attempts to synthesize **3.87** could be accessible by the condensation of quinuclidinone and β-keto ester. However, the acylation of quinuclidinone with NaH in a reflux is highly hindered, since no acrylated product observed from TLC and LC-MS (**Scheme 3.15B**). Additionally, to test the feasibility of Friedländer quinoline syntheses to approach **3.88**, 2-aminoacetophenone and quinuclidinone were treated with *p*-TsOH·$H_2O$ under a microwave irritation (**Scheme 3.15C**). Disappointedly, the reaction suffered a poor conversion up to 6 hours, and it was decided not to further optimize it.

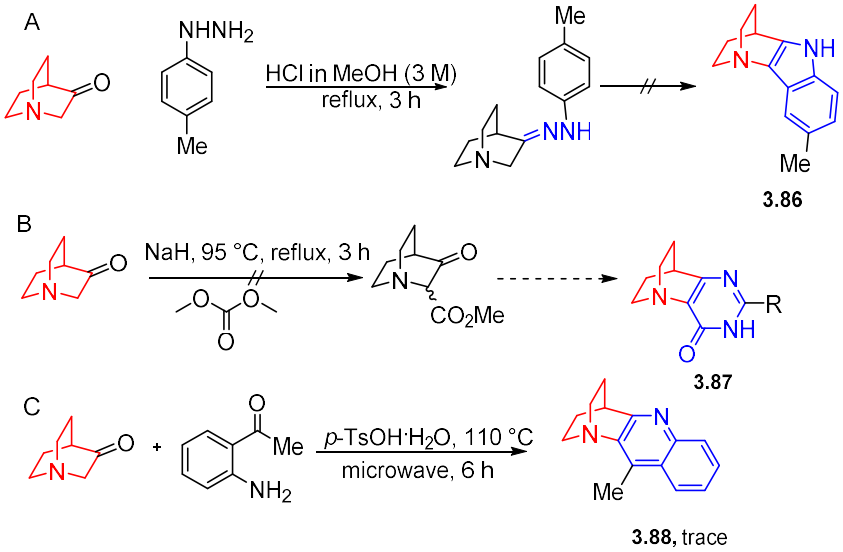


**Scheme 3.15 Conditions attempted synthesize quinuclidine analogues with edged fusion**

## 3.7 Chemoinformatic assessment

In total, the final library consisted of 64 compounds from 14 diverse pseudo-NP scaffolds, of which 10 contained spirocyclic fragment fusions. Chemoinformatic analysis of the library revealed that the vast majority of the compounds (62/64) conformed to Lipinski's *rule of five*, with many of them falling within lead-like chemical space (**Figure 3.9A**). Furthermore, the average fraction of $sp^3$ hybridized carbons ($Fsp^3$ = 0.48) was the same as for all approved drugs (**Figure 3.9B**).

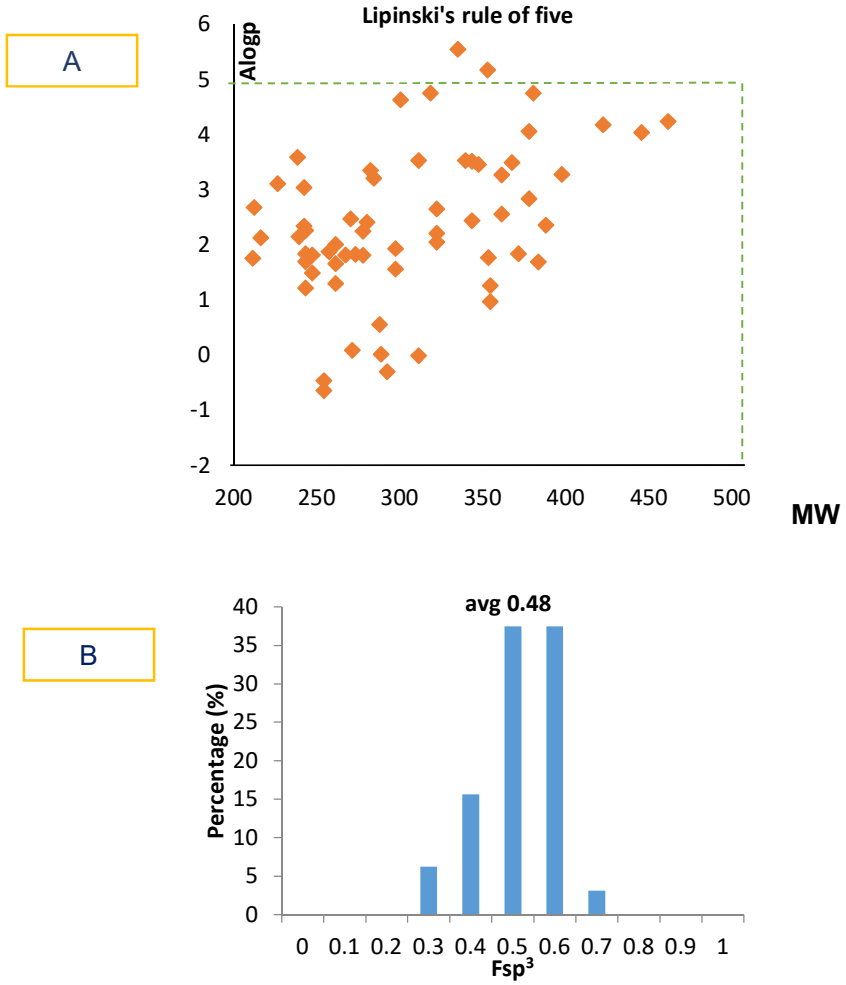


**Figure 3.9 Chemoinformatic analysis of the synthetic alkaloid-inspired compound library.** a) Evaluation of lead-likeness of the library using LLAMA (Lead-Likeness and Molecular Analysis)[67] b) fraction of sp3 hybridised carbons for the library compounds. The library has an average Fsp3 of 0.48.

## 3.8 Biological evaluation at monoaminergic receptors

To evaluate our hypothesis that these compounds would provide valuable starting points for identifying potent and selective monoaminergic GPCR ligands, we subjected them to functional screens for both agonist and antagonist activity at the 5-HT1B, 5-HT2A, and 5-HT2C serotonin receptors.[68,69] Serotonin receptors are of high clinical relevance and have been implicated in a variety of psychiatric and cognitive disorders, such as depression and schizophrenia, and in pain.[52] Despite extensive work, a significant proportion of orthosteric 5-HTR ligands (agonists and competitive antagonists) possess significant activity at a number of 5-HTR subtypes, other monoaminergic receptors or even at more distantly related off-targets, with an even greater part never having been tested for subtype-selectivity at all.[70,71] Tropane- and quinuclidine-containing compounds, including the approved drug tropisetron, have been reported to target the 5-HT3 receptor, a ligand-gated ion channel, however, activity at serotonin GPCRs is less established.[72,73] We were particularly keen to evaluate whether our diverse scaffold fusions could alter the selectivity of the primary fragments.

Interestingly, our primary screening of the entire compound library uncovered three scaffolds with activity against at least one of the 5-HT1B, 5-HT2A or 5-HT2C receptors (**Figure 3.10**, and **Table 3.13**). Notably, none of the compounds showed any activity at the two neuronal nicotinic acetylcholine receptors (nAChRs) α3β4 and α4β2 in a [3H]epibatidine competition binding assay, and only one compound **3.71** displayed >50% inhibition at 10 μM (**Table 3.14**). Furthermore, screening for functional activity at the D1R and D2R showed that none of the compounds had any agonist or antagonist activity at 10 μM (**Table 3.15**). This data suggests that a strong preference for serotonergic receptors over dopamine receptors and nAChRs for the whole family of compounds.

The quinoxaline-fused tropanes **3.27** and **3.28** displayed moderately potent agonist activity at 5-HT2A (EC50 values of 0.40 and 0.64 μM, respectively), substantially weaker (15 fold) agonist potencies at 5-HT2C, and no significant activity at 5-HT1B (at concentrations up to 10 μM) (**Figure 3.10** and **Table 3.13**). Interestingly, only the dichloro- and dimethyl-substituted quinoxalines were active, while the unsubstituted and difluoro-substituted analogues were not. In contrast, none of the quinoline-fused tropanes **3.22-3.25** were active, suggesting that the second nitrogen present in the quinoxaline ring is important for activity (**Table 3.13**). These preliminary structure-activity relationships (SAR) are an important feature of our library design and suggest potential avenues to follow in the further optimization of compounds **3.27**-**3.28** towards more potent and selective 5-HT2A agonists.

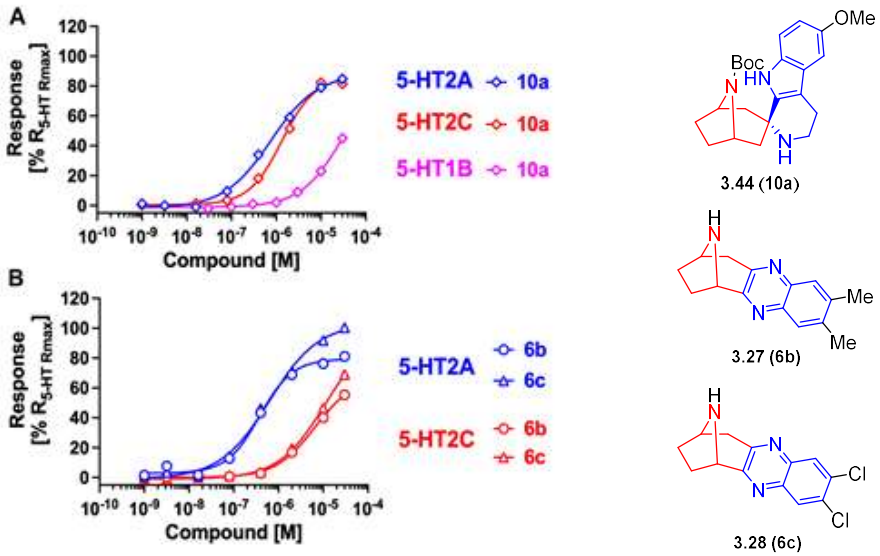


**Figure 3.10 Agonist concentration-response relationships exhibited by compound 3.43 (10a), 3.27(6b) and 3.28 (6c) at 5-HT2A and 5-HT2C.** The data are representative data obtained at stable 5-HT2A- and 5-HT2C-HEK293 cells in a Ca2+/Fluo-4 assay. For reasons of clarity, data are presented without error bars.

We focused our main attention on another lead compound coming out of the screening at the 5-HT2A, 5-HT2C and 5-HT1B receptors: the spirocyclic chromanone-fused quinuclidine (termed SCQ) **3.83**, which was identified as a moderately potent 5-HT2C antagonist (IC50 = 0.52 μM) displaying no agonist or antagonist activity at 5-HT2A (EC50 > 30 μM, IC50 > 30 μM) or 5-HT1B (EC50 > 10 μM, IC50 > 10 μM) (**Table 3.13**). The antagonist potency and selectivity profile of **3.83** prompted us to pursue it as a lead compound for further SAR study in the following chapter.

**Table 3.13 Functional properties of the synthetic alkaloid-inspired collection at the human 5-HT$_{2A}$, 5-HT$_{2C}$ and 5-HT$_{1B}$ receptors**. The compounds were characterized functionally at stable 5-HT$_{2A}$- and 5-HT$_{2C}$-HEK293 cell lines in a $Ca^{2+}$/Fluo-4 assay and at a stable 5-HT1B/GIRK2-HEK293 cell line in the FLIPR Membrane Potential Blue assay essentially as previously described. $EC_{50}$ values for agonists are given in µM (with $pEC_{50}$ ± S.E.M. values in brackets), and maximum response values ($R_{max}$) are given in % of $R_{max}$ of 5-HT determined at the same plate (in italics). $IC_{50}$ values are given in µM (with $pIC_{50}$ ± S.E.M. values in brackets). The antagonist testing was performed using 5-HT $EC_{80}$ ($EC_{70}$-$EC_{90}$) as agonist. All data for the test compounds are based on three independent experiments (n = 3).

| **Compound** | **5-HT$_{2A}$**<br>$EC_{50}$ [$pEC_{50}$ ± S.E.M.]<br>**µM**<br>*$R_{max}$ ± S.E.M.* [(n)] | **5-HT$_{2c}$**<br>$EC_{50}$ [$pEC_{50}$ ± S.E.M.]<br>**µM**<br>*$R_{max}$ ± S.E.M.* [(n)] | **5-HT$_{1B}$/GIRK2**<br>$EC_{50}$ [$pEC_{50}$ ± S.E.M.]<br>**µM**<br>*$R_{max}$ ± S.E.M.* [(n)] |
|---|---|---|---|
| 5-HT | 0.0030 [8.52 ± 0.07]<br>*100* | 0.0016 [8.79 ± 0.04]<br>*100* | 0.0011 [8.95 ± 0.06]<br>*100* |
| **3.08** | >10 [<5.0] [a] | >10 [<5.0] [a] | >10 [<5.0] [a] |
| **3.09** | >10 [<5.0] [a] | antagonist @ *10* [b] | >10 [<5.0] [a] |
| **3.10** | >10 [<5.0] [a] | >10 [<5.0] [a] | >10 [<5.0] [a] |
| **3.11** | agonist @ *3, 30* [c] | >10 [<5.0] [a] | >10 [<5.0] [a] |
| **3.12** | >10 [<5.0] [a] | >10 [<5.0] [a] | >10 [<5.0] [a] |
| **3,13** | >10 [<5.0] [a] | >10 [<5.0] [a] | >10 [<5.0] [a] |
| **3.14** | >10 [<5.0] [a] | >10 [<5.0] [a] | >10 [<5.0] [a] |
| **3.15** | >10 [<5.0] [a] | >10 [<5.0] [a] | >10 [<5.0] [a] |
| **3.16** | >10 [<5.0] [a] | >10 [<5.0] [a] | >10 [<5.0] [a] |
| **3.22** | >10 [<5.0] [a] | >10 [<5.0] [a] | >10 [<5.0] [a] |
| **3.23** | >10 [<5.0] [a] | >10 [<5.0] [a] | >10 [<5.0] [a] |
| **3.25** | >10 [<5.0] [a] | >10 [<5.0] [a] | >10 [<5.0] [a] |
| **3.26** | >10 [<5.0] [a] | >10 [<5.0] [a] | >10 [<5.0] [a] |
| **3.27** | **0.40 [6.39 ± 0.07]**<br>80 ± 10 | agonist @ *3, 10, 30* [c] | >10 [<5.0] [a]<br>>10 [<5.0] [a] |
| **3.28** | **0.64 [6.19 ± 0.10]**<br>99 ± 7 | agonist @ *3, 10, 30* [c] | >10 [<5.0] [a]<br>>10 [<5.0] [a] |
| **3.29** | >10 [<5.0] [a] | >10 [<5.0] [a] | >10 [<5.0] [a] |
| **3.34** | >10 [<5.0] [a] | >10 [<5.0] [a] | >10 [<5.0] [a] |
| **3.30** | >10 [<5.0] [a] | >10 [<5.0] [a] | >10 [<5.0] [a] |
| **3.36** | >10 [<5.0] [a] | >10 [<5.0] [a] | >10 [<5.0] [a] |
| **3.32** | >10 [<5.0] [a] | >10 [<5.0] [a] | >10 [<5.0] [a] |
| **3.35** | >10 [<5.0] [a] | >10 [<5.0] [a] | >10 [<5.0] [a] |
| **3.31** | >10 [<5.0] [a] | >10 [<5.0] [a] | >10 [<5.0] [a] |
| **3.33** | >10 [<5.0] [a] | >10 [<5.0] [a] | >10 [<5.0] [a] |
| **3.40** | >10 [<5.0] [a] | >10 [<5.0] [a] | >10 [<5.0] [a] |
| **3.39** | >10 [<5.0] [a] | >10 [<5.0] [a] | >10 [<5.0] [a] |
| **3.42** | >10 [<5.0] [a] | >10 [<5.0] [a] | >10 [<5.0] [a] |
| **3.38** | >10 [<5.0] [a] | >10 [<5.0] [a] | >10 [<5.0] [a] |
| **3.41** | >10 [<5.0] [a] | >10 [<5.0] [a] | >10 [<5.0] [a] |
| **3.37** | >10 [<5.0] [a] | >10 [<5.0] [a] | >10 [<5.0] [a] |
| **3.57** | >10 [<5.0] [a] | >10 [<5.0] [a] | >10 [<5.0] [a] |

| | | | |
|---|---|---|---|
| **3.58** | >10 [<5.0] [a] | >10 [<5.0] [a] | >10 [<5.0] [a] |
| **3.59** | >10 [<5.0] [a] | >10 [<5.0] [a] | >10 [<5.0] [a] |
| **3.44** | **0.69 [6.16 ± 0.11]**<br>82 ± 10 | **1.7 [5.776 ± 0.11]**<br>81 ± 6 | agonist @ *3, 10, 30* [c] |
| **3.43** | agonist @ *3, 10, 30* [c] | agonist @ *3, 10, 30* [c] | agonist @ *10, 30* [c] |
| **3.45** | >10 [<5.0] [a] | >10 [<5.0] [a] | >10 [<5.0] [a] |
| **3.50** | agonist @ *3, 10, 30* [c] | agonist @ *3, 10, 30* [c] | >10 [<5.0] [a] |
| **3.48** | agonist @ *10, 30* [c] | agonist @ *10, 30* [c] | >10 [<5.0] [a] |
| **3.49** | agonist @ *3, 10, 30* [c] | agonist @ *3, 10, 30* [c] | agonist @ *10, 30* [c] |
| **3.61** | >10 [<5.0] [a] | >10 [<5.0] [a] | >10 [<5.0] [a] |
| **3.60** | agonist @ *10, 30* [c] | agonist @ *3, 10, 30* [c] | >10 [<5.0] [a] |
| **3.62** | >10 [<5.0] [a] | >10 [<5.0] [a] | >10 [<5.0] [a] |
| **3.63** | >10 [<5.0] [a] | >10 [<5.0] [a] | >10 [<5.0] [a] |
| **3.65** | >10 [<5.0] [a] | >10 [<5.0] [a] | agonist @ *10, 30* [c] |
| **3.66** | >10 [<5.0] [a] | >10 [<5.0] [a] | >10 [<5.0] [a] |
| **3.67** | >10 [<5.0] [a] | >10 [<5.0] [a] | >10 [<5.0] [a] |
| **3.68** | >10 [<5.0] [a] | >10 [<5.0] [a] | >10 [<5.0] [a] |
| **3.70** | >10 [<5.0] [a] | >10 [<5.0] [a] | >10 [<5.0] [a] |
| **3.71** | >10 [<5.0] [a] | >10 [<5.0] [a] | >10 [<5.0] [a] |
| **3.72** | >10 [<5.0] [a] | >10 [<5.0] [a] | >10 [<5.0] [a] |
| **3.73** | >10 [<5.0] [a] | >10 [<5.0] [a] | agonist @ *10, 30* [c] |
| **3.74** | >10 [<5.0] [a] | >10 [<5.0] [a] | >10 [<5.0] [a] |
| **3.80** | >10 [<5.0] [a] | >10 [<5.0] [a] | >10 [<5.0] [a] |
| **3.81** | >10 [<5.0] [a] | >10 [<5.0] [a] | >10 [<5.0] [a] |
| **3.83** | **>**30 [<4.5] [a] | **$IC_{50}$ = 0.52** | >10 [<5.0] [a] |
| **3.82** | >10 [<5.0] [a] | >10 [<5.0] [a] | >10 [<5.0] [a] |

[a] The compound displayed no significant agonist or antagonist activity at the indicated concentration (10 or 30 μM). [b] The compound mediated ~50% inhibition of the 5-HT-induced response at 10 μM. [c] Weak agonist. The concentration-response curve was not completed within the tested concentration range, but the compound displayed significant agonist activity at the indicated concentrations.

**Table 3.14 Screening of alkaloid-inspired compounds (10 μM) for inhibition of binding of [3H]epibatidine to acetylcholine receptors.** Data is residual binding normalized to the DMSO control and represents the mean of two independent experiments carried out in duplicate. Nicotine (100 μM) was used as the positive control.

| Compound | α4β2 nAChR (% residual binding) | α3β4 nAChR (% residual binding) |
|---|---|---|
| **DMSO** | 100 | 100 |
| **Nicotine (100 μM)** | 0 | 0 |
| **3.12** | 81 | 83 |
| **3.13** | 101 | 85 |
| **3.14** | 81 | 88 |
| **3.15** | 86 | 84 |
| **3.16** | 83 | 79 |
| **3.17** | 58 | 80 |
| **3.19** | 88 | 80 |
| **3.42** | 97 | 77 |
| **3.38** | 74 | 76 |
| **3.26** | 92 | 78 |
| **3.27** | 71 | 93 |
| **3.28** | 88 | 83 |
| **3.29** | 64 | 78 |
| **3.59** | 90 | 97 |
| **3.41** | 97 | 94 |
| **3.37** | 101 | 89 |
| **3.39** | 90 | 85 |
| **3.40** | 91 | 83 |
| **3.68** | 56 | 70 |
| **3.66** | 62 | 82 |
| **3.65** | 78 | 82 |
| **3.67** | 70 | 82 |
| **3.84** | 81 | 71 |
| **3.85** | 70 | 63 |
| **3.80** | 68 | 69 |
| **3.82** | 54 | 54 |
| **3.71** | **41** | **40** |
| **3.81** | 68 | 70 |
| **3.72** | 92 | 56 |
| **3.73** | 62 | 45 |
| **3.74** | 94 | 87 |
| **3.83** | 67 | 68 |
| **3.76** | 92 | 89 |

**Table 3.15 Compound's activity on the dopamine receptor $D_1$ and $D_2$.** Activation or inhibition of the dopamine receptors $D_1$ (DRD1) and $D_2$ (DRD2) was assessed through measurement of $G_s$-mediated intracellular cyclic adenosine monophosphate (cAMP) accumulation in HEK 293T cells (DRD1) and arrestin2-mediated luciferase luminescence in HTLA cells (DRD2). For assessment of agonist-activity, results were normalized to the maximum response of 10 µM dopamine (DRD1) or quinpirole (DRD2) (n=3). For assessment of antagonist-activity, results were normalized to the response produced by $EC_{80}$ of the agonist dopamine (DRD1) or quinpirole (DRD2) (n≥3).

| Compound | DRD1 activation, % of 10 µM Dopamine | | DRD1 % inhibition | | DRD2 activation, % of 10 µM quinpirole | | DRD2 % inhibition | |
|---|---|---|---|---|---|---|---|---|
| | % | SEM | % | SEM | % | SEM | % | SEM |
| **Dopamine** | 100 | 4.2 | - | - | - | - | - | - |
| **R(+)SCH23390** | - | - | 93.2 | 1.8 | - | - | - | - |
| **Quinpirole** | - | - | - | - | 100 | 4.9 | - | - |
| **Benperidol** | - | - | - | - | - | - | 98.6 | 0.2 |
| **3.12** | 1.5 | 0.9 | 12 | 11.5 | -2.5 | 0.3 | 9.2 | 5.4 |
| **3.13** | 0.8 | 0.7 | 6.4 | 14.2 | -2.7 | 0.1 | 25.9 | 9.2 |
| **3.14** | 1.1 | 0.7 | 9.6 | 12.7 | -2.7 | 0.2 | 20 | 5.4 |
| **3.15** | 1.2 | 0.8 | 12.2 | 12.4 | -2.5 | 0.3 | 17.0 | 8.5 |
| **3.16** | 1.2 | 0.4 | -4.6 | 8.8 | -2.7 | 0.2 | 5.5 | 10.2 |
| **3.17** | 1.6 | 0.8 | -1 | 7.9 | -2.7 | 0.3 | -10.8 | 5.4 |
| **3.19** | 2 | 0.5 | -8 | 5.9 | -2.7 | 0.2 | 9.3 | 7.3 |
| **3.42** | 0.4 | 0.7 | 12.4 | 11.1 | -2.8 | 0.3 | -6 | 6.3 |
| **3.38** | 0.6 | 0.8 | 1.2 | 13.7 | -2.9 | 0.2 | 3 | 9.4 |
| **3.26** | 1.2 | 0.8 | 14 | 14 | -2.8 | 0.1 | 5 | 8.4 |
| **3.27** | 0.7 | 0.6 | 7.9 | 12.3 | -2.8 | 0.2 | -3.2 | 8.1 |
| **3.28** | 0.7 | 0.7 | 10.5 | 10.9 | -2.7 | 0.2 | 4.5 | 8.7 |
| **3.29** | 1.3 | 0.6 | -1.4 | 13.1 | -2.9 | 0.2 | 14.2 | 7.6 |
| **3.68** | 0.7 | 0.7 | 29.1 | 9.6 | -2.9 | 0.2 | 29.1 | 10.1 |
| **3.66** | 0.3 | 0.6 | 25.8 | 11.3 | -2.9 | 0.2 | 8.5 | 7.4 |
| **3.65** | 0.8 | 0.6 | 4.7 | 7.8 | -2.5 | 0.3 | -13.5 | 7 |
| **3.67** | 1.2 | 0.8 | 8.2 | 10.5 | -2.9 | 0.1 | -0.4 | 8.4 |
| **3.59** | 1.2 | 0.7 | 7.3 | 11.5 | -2.4 | 0.2 | 7.4 | 6.1 |
| **3.41** | 0.7 | 0.7 | 13.8 | 9 | -2.6 | 0.2 | 9.2 | 7.2 |
| **3.37** | 1.2 | 0.4 | 6.9 | 9.9 | -2.7 | 0.1 | 7.7 | 9.3 |
| **3.39** | 1.1 | 0.6 | 2.2 | 6.9 | -2.6 | 0.2 | 7 | 7 |
| **3.40** | 1.5 | 0.6 | 7.4 | 6 | -2.4 | 0.5 | 11.4 | 7.8 |
| **3.84** | 0.7 | 0.9 | 2.2 | 11 | 3.5 | 2 | -7.1 | 4.30 |
| **3.85** | 0.7 | 0.5 | 7.8 | 8.1 | -1.3 | 0.2 | 9.5 | 8.1 |
| **3.80** | 0.4 | 0.8 | 17.6 | 10.6 | -1.3 | 0.2 | 2 | 6.6 |
| **3.82** | 1.7 | 0.7 | 20.7 | 12.9 | -2.1 | 0.1 | 7.8 | 6 |
| **3.71** | 1.2 | 0.5 | 5.8 | 12.2 | -2.4 | 0 | 11.7 | 4.1 |
| **3.81** | 0 | 1.1 | 8.4 | 13.6 | -2.4 | 0.1 | 6.1 | 7.2 |
| **3.72** | 2.6 | 2 | 21.3 | 14.8 | -2.7 | 0.1 | 1.5 | 7.4 |
| **3,73** | 3.2 | 1.9 | 14.1 | 13.9 | -2.7 | 0.1 | 10.4 | 7.9 |
| **3.74** | 0.8 | 0.8 | 18.6 | 10.5 | -2.6 | 0.1 | 12.1 | 5.4 |

| | | | | | | | | |
|---|---|---|---|---|---|---|---|---|
| **3.83** | 2.3 | 1.7 | 14.3 | 9.4 | -2.1 | 0.2 | -29.9 | 10.3 |
| **3.76** | 1 | 0.6 | 7.9 | 11.4 | -2.2 | 0.1 | 11.4 | 6.1 |

# 4 Structure-activity relationship (SAR)

In this chapter, I will outline efforts to increase potency for 5-HT2C while retaining selectivity over other serotonin receptors.

## 4.1 Available modification sites for the SAR study

The hit compound **3.83** we identified is structurally composed of a basic amine, a ketone (dihydropyran-one), and an aromatic ring system. As such, the SAR study was aimed to independently explore the modification sites on the parental scaffold.

Apart from the nucleophilic addition into quinuclidine moiety of **3.83**, the late-stage functionalization to break down aliphatic C-H bond needs efficient and well-established protocols. In addition, a broad range of tertiary amines could be considered to merge chromanone for SAR study. However, it might need multiple steps to prepare many amino-ketone analogues as the building blocks. Other available modifications include accessing the dihydropyran-one ring via various synthetic pathways (**Figure 4.1)**. Ring expansion to produce medium size ring analogues (**Figure 4.1a)**, along with the reduction of ketone to produce chromane (**Figure 4.1b)**. Additionally, the alkylation of C-H bond (**Figure 4.1c)**, and the condensation of ketone followed by subsequent diversification may produce inseparable amine isomers (**Figure 4.1d)**.

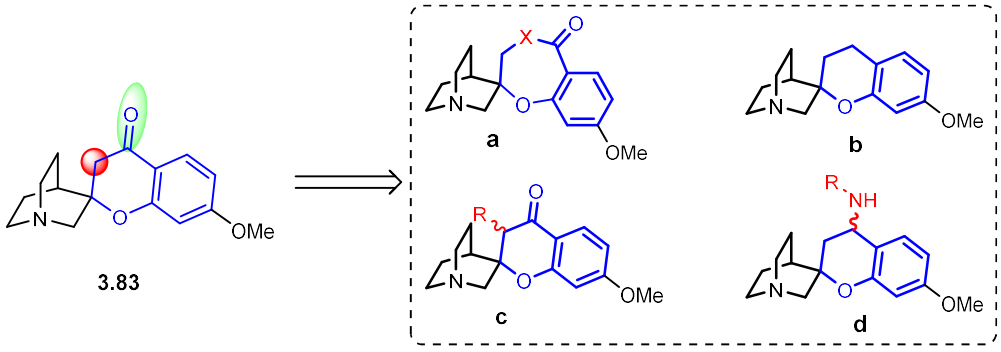


**Figure 4.1 Selected examples of modifications on dihydropyran-one**

The most accessible analogues for the SAR study are those featuring diverse substitutions on the phenyl ring. The preliminary SAR study revealed that a substituent at the 7' position might determine the potency, since **3.80-3.82** were inactive at the 5-HT2C receptor. Additionally, a large number of chromanone-fused quinuclidine analogues are readily accessible via a well-established Kabbe reaction in one-step. We thus prioritized the synthesis of a focused library containing substituents at the 7' position of phenyl ring as the first round SAR study (**Scheme 4.1)**.

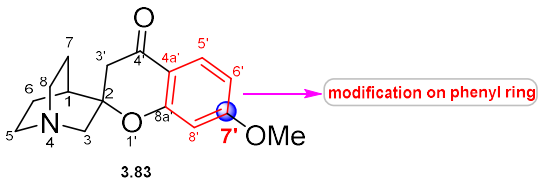


**Scheme 4.1 Sites modification on phenyl ring for SAR study**

## 4.2 Synthesis of analogues at the 7' position of phenyl ring

To study the substituents at the 7' position of phenyl ring for SAR, more analogues have been suggested. In general, analogues were synthesized *via* the established Kabbe reaction in various reaction times (**Scheme 4.2)**. To begin with, analogues with substituents including benzyloxy **4.01**, cyclopropylmethoxy **4.02**, and hydroxy **4.03** were synthesized in good yields. Additionally, alkyl-substituted analogue **4.04** was also afforded in good yield. Furthermore, the brominated analogue **4.05** was obtained in moderate yield, which could be considered as an ideal handle for cross coupling. As such, two analogues bearing the phenyl **4.06** and *para*-methoxy phenyl **4.07** were afforded in moderate yields via well-known Suzuki coupling. Lastly, four analogues containing various amines **4.08-4.11** were also prepared.

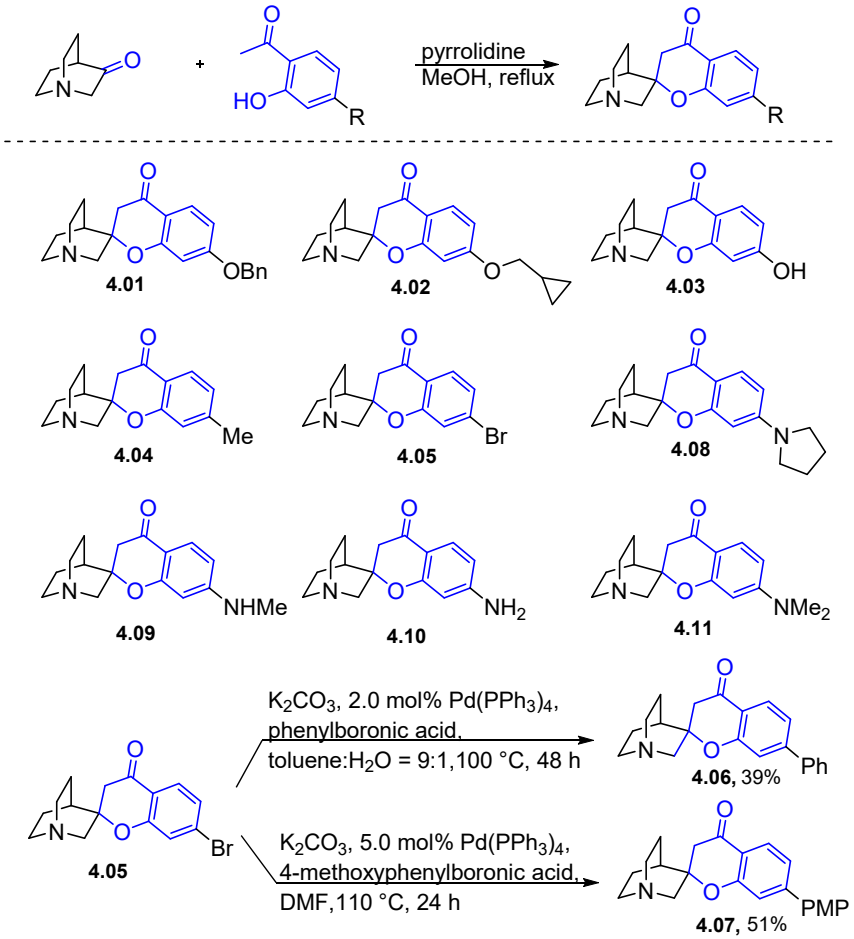


**Scheme 4.2 Synthesis of analogues at the 7' position for structure–activity relationship**

## 4.3 Biological evaluation of analogues at the 7' position of phenyl ring

With all the aforementioned analogues in hand, we further determined the antagonist activity against 5-HT2 receptors (**Table 4.1)**. In general, no ligands showed an increased potency at 5-HT2C compared to the hit **3.83**. For example, analogues bearing larger size aryl groups **4.06** and **4.07** (entries 11-12) were tested inactive at the given concentration of 10 μM. Analogues containing electron-donating groups **4.01-4.03** (entries 6-8) exhibited reduced potency. These findings suggested that among all the substituents at the 7' position, the analogue containing a methoxy group exhibited the most potent activity at 5-HT2C. Further optimization was thus explored by the functionalization of other sites, such as the ketone and tertiary amine.

**Table 4.1 Biological evaluation of analogues 3.80-3.83 and 4.01-4.11**

| Entry | Compound | R | 5-HT2A $IC_{50}$ [μM] | 5-HT2C $IC_{50}$ [μM] | 5-HT1B $IC_{50}$ [μM] |
|---|---|---|---|---|---|
| 1 | **5-HT** (agonist) | | $EC_{50}$ = 0.0030 | $EC_{50}$ = 0.0016 | $EC_{50}$ = 0.0011 |
| 2 | **3.83** | **OMe** | >30 [a] | **0.52** | **>**10 [a] |
| 3 | **3.80** | - | >10[a] | >10 [a] | >10 [a] |
| 4 | **3.81** | - | >10 [a] | >10 [a] | >10 [a] |
| 5 | **3.82** | - | >10 [a] | >10 [a] | >10 [a] |
| 6 | **4.01** | OBn | >100 [a] | 5.0 | n. d. |
| 7 | **4.02** | cyclopropylmethoxyl | >100 [a] | 1.5 | n. d. |
| 8 | **4.03** | OH | >100 [a] | 2.5 | n. d. |
| 9 | **4.04** | Me | >100 [a] | 2.5 | n. d. |
| 10 | **4.05** | Br | ~15 [b] | 2.3 | n. d. |
| 11 | **4.06** | Ph | >100 [a] | ~50 [b] | n. d. |
| 12 | **4.07** | PMP | >100 [a] | >100 [a] | n. d. |
| 13 | **4.08** | 1-pyrrolidine | >100 [a] | 8.3 | n. d. |
| 14 | **4.09** | methylamino | >100 [a] | 3.1 | n. d. |
| 15 | **4.10** | amino | >100 [a] | 6.8 | n. d. |
| 16 | **4.11** | dimethylamino | >100 [a] | 4.1 | n. d. |

[a] The compound displayed no significant agonist or antagonist activity at the indicated concentration (10, 30 or 100 μM). [b] The concentration-inhibition curve for the compound was not completed within the tested concentration range, and thus the $IC_{50}$ value represents an estimate based on visual inspection of the curve. n.d (not determined)

## 4.4 Synthesis and biological evaluation of analogues by accessing ketone or amine

From the hit **3.83**, reduction of the ketone to the methylene **4.12** or to the alcohol **4.13** (**Scheme 4.3**) produced compounds with significantly reduced 5-HT2C antagonist activity, highlighting its importance for target potency (**Table 4.2**). The alkene **4.14** was prepared from the alcohol using *p*-TsOH·$H_2O$ leading to elimination of water (**Scheme 4.3**). The subsequent screening revealed a reduced antagonist activity at 5-HT2C compared to the hit **3.83**. The preparation of *N*-quaternized **4.15** was in high yield, which tested inactive at 5-HT2C (**Table 4.2**), the latter further validating the importance of the basic nitrogen for activity of the quinuclidine scaffold against monoaminergic GPCRs. These findings supported that ketone alongside basic amine are essential for maintaining the potency against 5-HT2C.

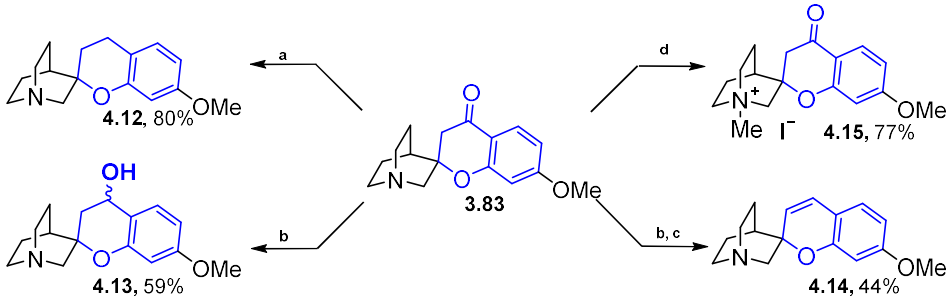


**Scheme 4.3 Synthesis of analogues employing the modifications on ketone and amine**

(**a**) Zinc, HOAc, 80 °C, 18 h; (**b**) $NaBH_4$, 0 °C to r.t.; (**c**) *p*-TsOH·$H_2O$, dioxane, 80 °C, 26 h; (**d**) $CH_3I$, acetone,12 h.

**Table 4.2 Biological evaluation of analogues 4.12-4.15**

| Entry | Compound | 5-HT2A $IC_{50}$ [μM] | 5-HT2C $IC_{50}$ [μM] | 5-HT1B $IC_{50}$ [μM] |
|---|---|---|---|---|
| **1** | **5-HT** (agonist) | $EC_{50}$ = 0.0030 | $EC_{50}$ = 0.0016 | $EC_{50}$ = 0.0011 |
| **2** | **3.83** | >30 [a] | **0.52** | >10 [a] |
| **3** | **4.12** | >100 [a] | 2.8 | n. d. |
| **4** | **4.13** | >100 [a] | 3.4 | n. d. |
| **5** | **4.14** | >100 [a] | 2.3 | n. d. |
| **6** | **4.15** | >100 [a] | >100 | n. d. |

[a] The compound displayed no significant agonist or antagonist activity at the indicated concentration (10, 30 or 100 μM). n.d (not determined)

## 4.5 Synthesis and biological evaluation of analogues with electron rich substituents

In an effort to optimize the hit compound **3.83**, it became important to figure out whether methoxy groups at other positions of the phenyl ring could increase the potency. As such, five analogues were prepared in moderate to good yields, which are composed of mono- and di-methoxy substitutions. (**Scheme 4.4**) However, none of these compounds displayed activity at the receptors 5-HT2A and 5-HT2C at concentrations up to 100 μM (**Table 4.3**). These findings highlighted its importance of the substitution at the 7' position for target potency. Lastly, two additional analogues (entries 8-9, **Table 4.3)** possessing rigid aromatic ring fusions at the 7' and its ortho position were included. Interestingly, one notable exception was spiro-chromanoquinuclidines **4.22** ((rac)-SCQ1), which was a 3-fold more potent 5-HT2C antagonist than **3.83**. While compound **4.21** showed no significant response at the given concentration up to 100 μM.

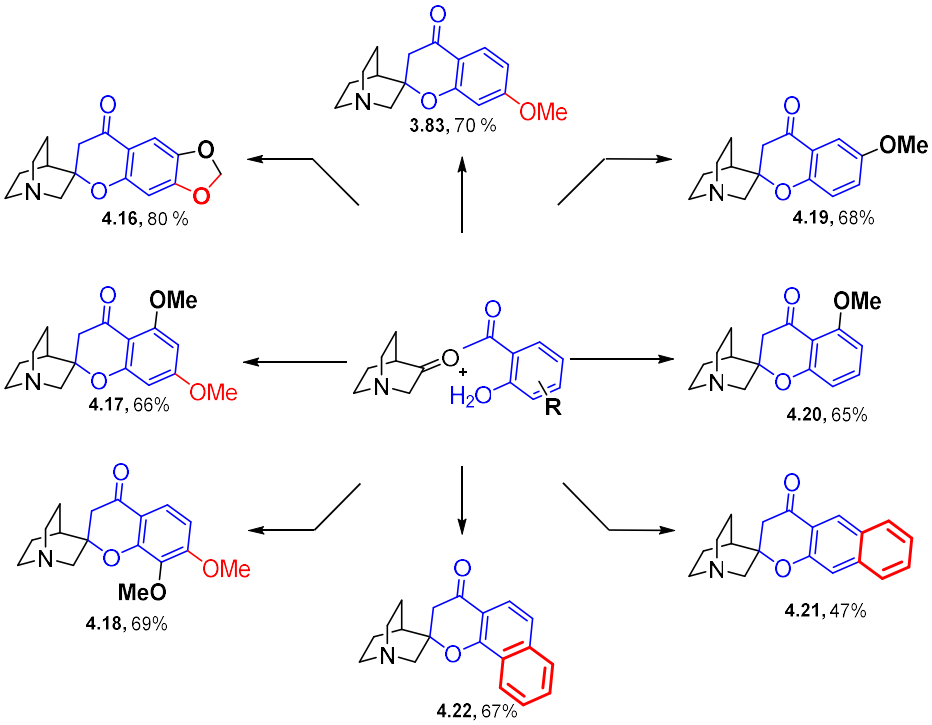


**Scheme 4.4 Synthesis of analogues employing the modifications on methoxy and naphthalene**

**Table 4.3 Biological evaluation of analogues 4.16-4.22**

| Entry | Compound | 5-HT2A $IC_{50}$ [μM] | 5-HT2C $IC_{50}$ [μM] | 5-HT1B $IC_{50}$ [μM] |
|---|---|---|---|---|
| 1 | **5-HT** (agonist) | $EC_{50}$ = 0.0030 | $EC_{50}$ = 0.0016 | $EC_{50}$ = 0.0011 |
| 2 | **3.83** | >30 [a] | **0.52** | >10 [a] |
| 3 | **4.16** | >100 [a] | >100 [a] | n. d. |
| 4 | **4.17** | >100 [a] | >100 [a] | n. d. |
| 5 | **4.18** | >100 [a] | >100 [a] | n. d. |
| 6 | **4.19** | >100 [a] | >100 [a] | n. d. |
| 7 | **4.20** | >100 [a] | >100 [a] | n. d. |
| 8 | **4.21** | ~50 [b] | >100 [a] | n. d. |
| 9 | **4.22** | ~20 [b] | **0.18** | n. d. |

## 4.6 Separation of 4.22 ((rac)-SCQ1)

All compounds so far were synthesised as racemic mixtures. However, one enantiomer of a bioactive molecule may cause severe side effects due to different pharmacological activity and toxicity. As a result, the racemate often requires resolution for each enantiomer. Apart from asymmetric catalysis, chiral resolution and chiral column chromatography are well-known methods to separate each enantiomer. Chiral resolution employing D-tartaric acid has previously been used to resolve [$^{14}C_2$]-AZD0328[74] in poor yield. However, this protocol afforded unsatisfied resolution of our enantiomers (**Figure 6.9**). Analytical HPLC experiments were initially performed on an in-house Daciel Chiralpak® AD-H column (250 x 4.6 mm; 5 µm) and eluted at 1 mL/min with heptane–isopropanol–diethylamine (95:5:0.1) for compound **3.83** and heptane–isopropanol–diethylamine (97.5:2.5:0.1) for compound **4.22** (**(rac)-SCQ1**). Although the racemate **3.83** could be closely separated in a running time of 1 h (**Figure 4.2**). However, the same column failed to get completed separation for **4.22** (**(rac)-SCQ1**) (**Figure 4.3**).

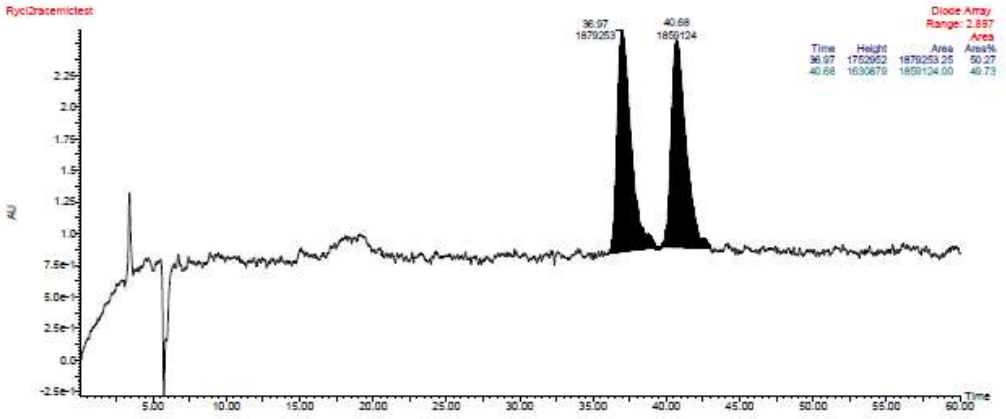


**Figure 4.2 Analytical HPLC spectrum for (rac)-3.83.**

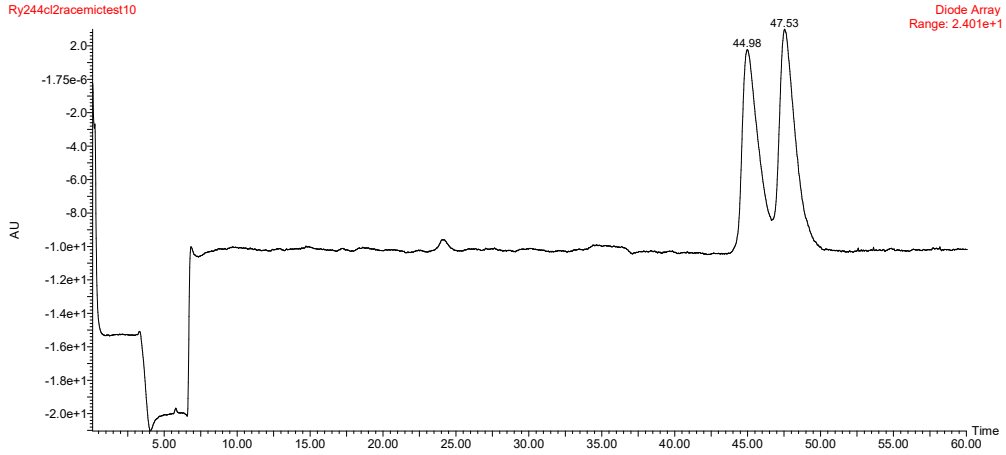


**Figure 4.3 Analytical HPLC spectrum for (rac)-SCQ1**

Separation of both enantiomers (> 99% ee) by chiral supercritical fluid chromatography (SFC) in high yield was ultimately possible in collaboration with Henrik Pedersen (Lundbeck A/S). I was able to assign the absolute stereochemistry of one enantiomer by generating a crystal and resolving the X-ray crystal structure analysis (**Scheme 4.5**). Functional receptor characterization revealed that the entire activity resided in the (*S*)-enantiomer, as (*R*)-**SCQ1** was essentially inactive at 5-HT2C (**Figure 4.7**).

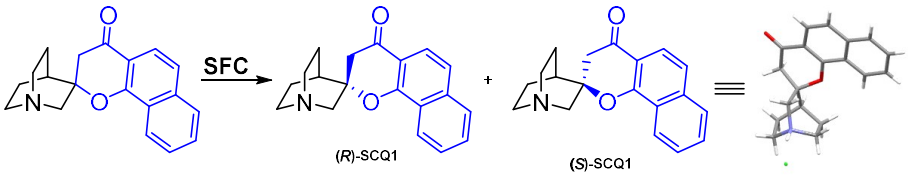


**Scheme 4.5 Separation of 4.22 ((rac)-SCQ1) by chiral SFC**

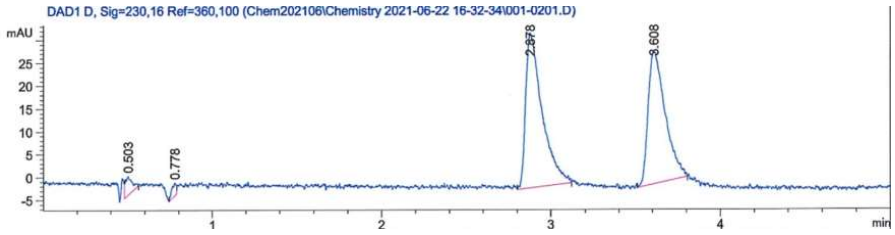


**Figure 4.4 Analytical SFC spectrum for (rac)-SCQ1**

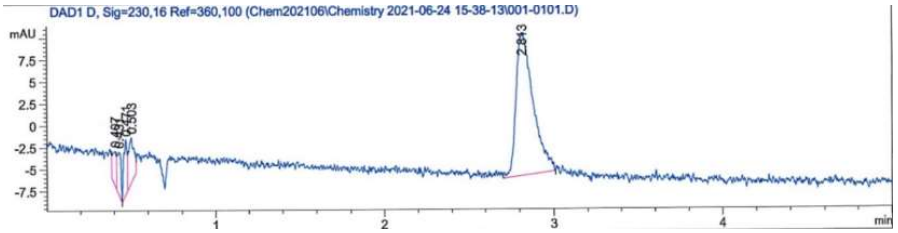


**Figure 4.5 Analytical SFC spectrum for (*R*)-SCQ1**

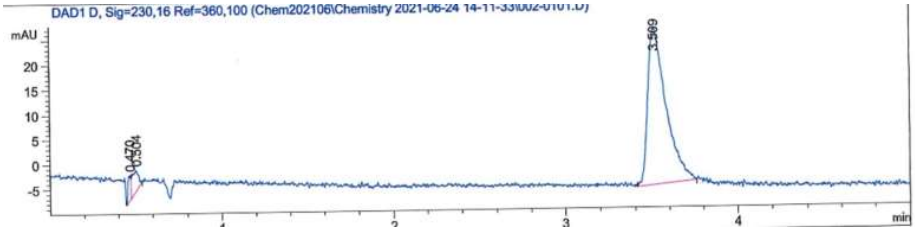


**Figure 4.6 Analytical SFC spectrum for (*S*)-SCQ1**

## 4.7 Biological evaluation of (*S*)-SCQ1 at the receptors of 5-HT and M1-M5

With (*S*)-**SCQ1** as our lead compound, we next carried out a more extensive profiling of its pharmacology in radioligand competition binding assays at a selection of serotonin receptors and at the five muscarinic acetylcholine receptor subtypes (**Table 4.4**). (*S*)-**SCQ1** (10 μM) only mediated partial inhibition of radioligand binding to six other 5-HTR subtypes (5-HT1A, 5-HT3, 5-HT4E, 5-HT5A, 5-HT6, 5-HT7) and to the M1-M5 receptors, thus displaying estimated binding IC50 values in the 1-10 μM range or higher at these receptors. In contrast, (*S*)-**SCQ1 (**10 μM) mediated complete inhibition of [3H]mesulergine binding to 5-HT2B, which prompted us to characterize its functional properties at this receptor. In an inositol phosphate 1 (IP1) assay, (*S*)-**SCQ1** mediated concentration-dependent inhibition of 5-HTinduced 5-HT2B signaling with an IC50 value of 135 nM (**Figure 4.7**). Thus, although caution should be taken when comparing antagonist properties displayed by a compound at receptors in two different functional assays, (*S*)-**SCQ1** appears to be a roughly equipotent antagonist of 5-HT2B and 5-HT2C, with notably little activity at 5-HT2A, at other 5-HTRs, at dopamine receptors (**Table 4.5**), and at M1-M5 receptors. The latter is important, as quinuclidines have been reported as privileged scaffolds displaying agonism at muscarinic acetylcholine receptors, with a large array of substituted quinuclidines including the approved drug cevimeline showing high potency against this receptor class.

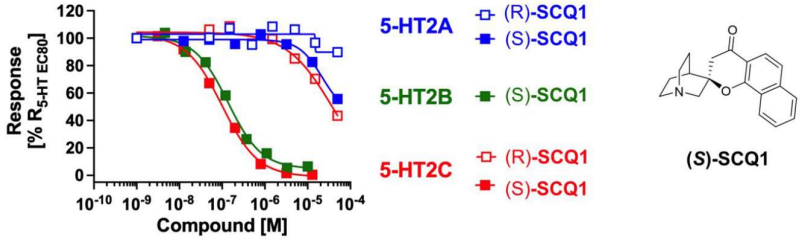


**Figure 4.7 Antagonist concentration-inhibition relationships exhibited by (*S*)-SCQ1 and (*R*)-SCQ1 at 5-HT2A, 5-HT2B and5-HT2C.** The data are representative data obtained at stable 5-HT2A- and 5-HT2C-HEK293 cells in a Ca2+/Fluo-4 assay and at 5-HT2B-CHO cells in an IP1 assay. For reasons of clarity, data are presented without error bars.

**Table 4.4 Binding properties of (*S*)-SCQ1 at serotonin and muscarinic acetylcholine receptors in radioligand competition binding assays.** (*S*)-SCQ1 was tested at an assay concentration of 10 µM using the indicated radioligands at the respective receptors, and data are given as inhibition of specific radioligand binding (in % of control, i.e. the specific radioligand binding in the absence of test compound) based on duplicate determinations. All data in the table were generated at Eurofins.

| Receptor | Radioligand | % Inhibition [@ 10 µM] |
|---|---|---|
| 5-HT1A | [$^3$H]-8-OH-DPAT | 57 |
| 5-HT2B | [$^3$H]mesulergine | 99 |
| 5-HT3 | [$^3$H]BRL 43694 | 85 |
| 5-HT4E | [$^3$H]GR 113808 | 42 |
| 5-HT5A | [$^3$H]LSD | 64 |
| 5-HT6 | [$^3$H]LSD | 57 |
| 5-HT7 | [$^3$H]LSD | 92 [67% @ 1 µM] |
| M1 | [$^3$H]pirenzepine | 67 |
| M2 | [$^3$H]AF-DX 384 | 31 |
| M3 | [$^3$H]4-DAMP | 27 |
| M4 | [$^3$H]4-DAMP | 67 |
| M5 | [$^3$H]4-DAMP | 69 |

**Table 4.5 Compound's activity on the dopamine receptor D1 and D2.** Activation or inhibition of the dopamine receptors D1 (DRD1) and D2 (DRD2) was assessed through measurement of Gs-mediated intracellular cyclic adenosine monophosphate (cAMP) accumulation in HEK 293T cells (DRD1) and arrestin2-mediated luciferase luminescence in HTLA cells (DRD2). For assessment of agonist-activity, results were normalized to the maximum response of 10 µM dopamine (DRD1) or quinpirole (DRD2) (n=3).

| Compound | DRD1 activation, % of 10 µM Dopamine | DRD1 % inhibition | DRD2 activation, % of 10 µM quinpirole | DRD2 % inhibition |
|---|---|---|---|---|
| | % | % | % | % |
| **Dopamine** | 100 | - | - | - |
| **R(+)SCH23390** | - | 93.2 | - | - |
| **Quinpirole** | - | - | 100 | - |
| **Benperidol** | - | - | - | 98.6 |
| **(S)-SCQ1** | -0.2 | 34 | 0 | -10.8 |

## 4.8 Conclusions

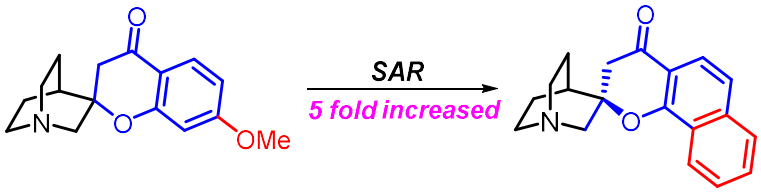


**Figure 4.8 The SAR study led to the identification of lead compound (S)-SCQ1**

The facile nature of the library synthesis enabled rapid SAR exploration, with 23 analogues prepared and screened. I can conclude that substituents at the 7' position of phenyl ring, along with ketone and basic amine are both essential to maintain the potency at 5-HT2C. Compared to other mono-substituents at 7' position of phenyl ring, compound **3.83** exhibited at least 3-fold more potent to inhibit 5-HT2C. Additionally, it is concluded that methoxy group at other position of phenyl ring led to inactive at 5-HT2C.

Replacing the phenyl ring of compound **3.83** with naphthalene **SCQ1** led to 3-fold more potent 5-HT2C antagonist than compound **3.83.** Separating the both enantiomers of **SCQ1**, which resulted in the development of the spirochromoquinuclidine analogue (*S*)-**SCQ1** that exhibited potent dual antagonist activity at 5-HT2B (IC50 = 135 nM) and 5-HT2C (IC50 = 95 nM). Notably, (*S*)-**SCQ1** exhibited >100-fold selectivity as antagonists for these receptors over the closely related 5-HT2A receptor, a pronounced subtype-selectivity not often observed for orthosteric 5-HT2 receptor ligands.

## 4.9 Perspective

Owing to the high potency of (S)-SCQ1 at 5-HT2C/5-HT2B, preferentially selective potent versus a panel of aminergic GPCRs and related nAChRs, we reasoned this lead compound is a promising starting point for further development aiming to identify more potent and selective ligands biased towards 5-HT2B and/or 5-HT2C against other aminergic GPCRs including 5-HTR and muscarinic acetylcholine receptors.

Firstly, except quinuclidine, other structurally related tertiary amines fused to chromanone **4.23** could be also envisaged (**Figure 4.9a**). Moreover, to obtain medium size ring analogue **4.24** for optimization, ring expansion of (S)-SCQ1 could provide a straightforward synthetic pathway (**Figure 4.9b**). In addition, the naphthalene could consider to be replaced by other rigid aromatic rings including the compound **4.25** (**Figure 4.9c**).

Furthermore, the high-resolution structures of ligands in complex with 5-HT2B[34] and 5-HT2C[35] have been solved, which offered the templates for docking study. As such, the profound understanding of lead compound (*S*)-SCQ1 binding to 5-HT2C and 5-HT2B *via* docking studies may favor the design of biased ligands with improved potency in the lower nanomolar range.

Finally, identification of β-arrestin biased ligands has attracted considerable interest since ligands can potentially modulate GPCRs through different signal transduction pathways. As such, it´s an inspiration to develop a potent biased ligand minimizing the side effects caused by the possible other signalling pathways.

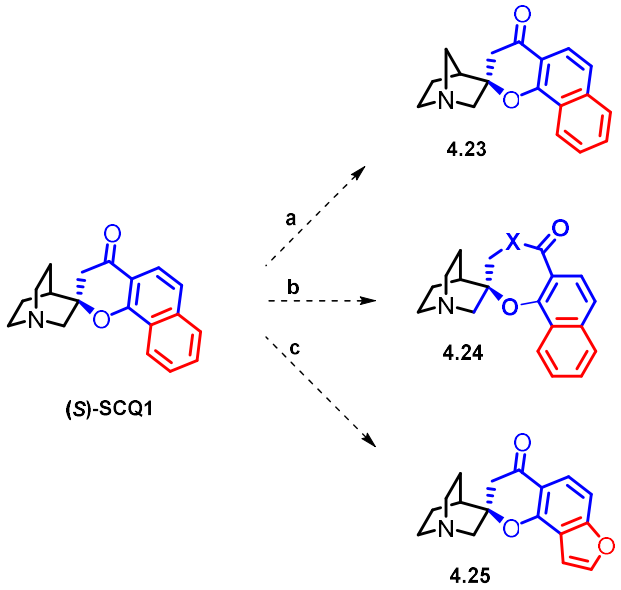


**Figure 4.9 Selected examples of modification sites on (S)-SCQ1 for SAR**

# 5 Project aim and outline

The synthesis of pseudo-natural product inspired libraries has facilitated the identification of novel biological modulators. In the previous chapter, it enabled us to discover a moderately potent 5-HT2A agonist, as well as a dual 5-HT2B/5-HT2C antagonist which exhibited high selectivity versus multiple neurological receptors, respectively. We reasoned that a similar strategy could be extended to identify other selective CNS modulators. As I will briefly describe in the following section, dopamine receptors are one of most important GPCR families, which regulate fundamental neurological processes in the mammals. As a case study, the dopamine 2 receptor (D2R) is the main target linked to a treatment of Schizophrenia.

The quinolizidine alkaloids are mainly isolated from plants, and possess a wide array of biological effects.[75] In the context of scarcity isolated from organism, naturally occurring quinolizidines have not served as a source for further chemical diversification. Alternatively, the synthesis of a quinolizidine-inspired library could provide promising candidates for biological screening. Quinolizidines display diverse neurological activities against nAChRs[76] and adrenoceptors.[77] In particular, ORM-10921 showed the excellent antagonist activities at $\alpha_{2c}$ but demonstrated moderate potency at D2R.[78] We speculated that quinolizidines could be used as a privileged scaffold, which when fused to diverse secondary NP fragments may lead to identify structurally unknown modulators targeting D2R (**Figure 5.1**).

Ketones can serve as essential building blocks, for merging a variety of aromatic or aliphatic heterocycles.[39] As such, they have been utilized to synthesize a series of pseudo natural products. Similarly, we chose octahydro-1H-quinolizin-1-one as our building block, which can be prepared in three steps in good yields. We were particularly interested in synthesizing a focused library *via* various spirocyclic fusions. In addition to diverse Pictet-Spengler reactions, we employed the oxa Pictet-Spengler reactions and subsequent ring contractions. Furthermore, we synthesized several analogues *via* Friedländer reactions.

With the resulting collections in hand, we first evaluated the inhibition and activation against D2R using a β-arrestin recruitment assay. We also determined the selectivity over dopamine 1 receptor (D1R), but using a cAMP assay. Additionally, to study the selectivity over nAChRs, we tested our collections against the human α4β2 and the rat α3β4 nAChR in a competition [3H]epibatidine binding assay.

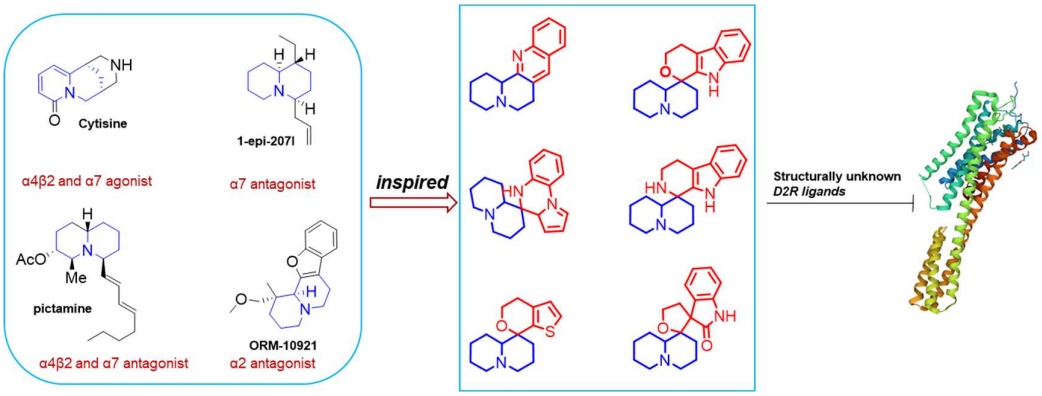


**Figure 5.1 Design strategy for quinolizidine alkaloid-inspired compound collection**

## 5.1 Introduction to dopamine 2 receptor (D2R)

### 5.1.1 Dopamine receptors classifications and D2R in health and disease

The dopamine receptors are classified as the signalling receptors belong to GPCRs. According to different physiological activities mediated by dopamine, they can subdivide into D1-liked (D1R, D5R) and D2-liked (D2R, D3R, D4R). D1-liked coupled to Gαs protein can stimulate adenylyl cyclase, which lead to the production of cAMP. D2-like receptors are coupled to Gαi/Go protein, which inhibit adenylyl cyclase and $K^+$ ion channel. Many approved drugs for the treatment of Parkinson disease (**Figure 5.2**)[79] and Schizophrenia either stimulate or inhibit D2R. However, these drugs may also cause side effects due to additional binding to other GPCRs simultaneously.

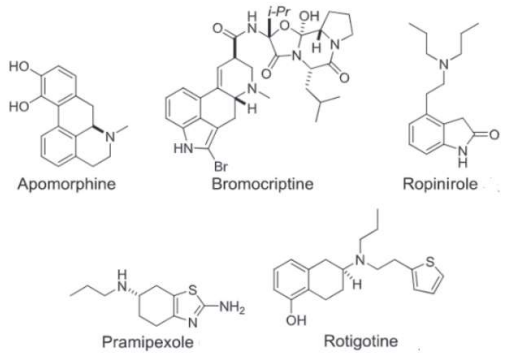


**Figure 5.2 Approved D2-like dopamine agonists. Reproduced from Ellis *et al.*[79]**

### 5.1.2 High-resolution structures of D2R and D1R

The first high-resolution structures of D2R bound to the drug risperidone[80] and D1R in complex with three agonists[81] were solved by Roth and Xu, respectively. The structures of D1R and D2R provide the templates to develop therapeutics pharmacologically efficient with reduced side effects.

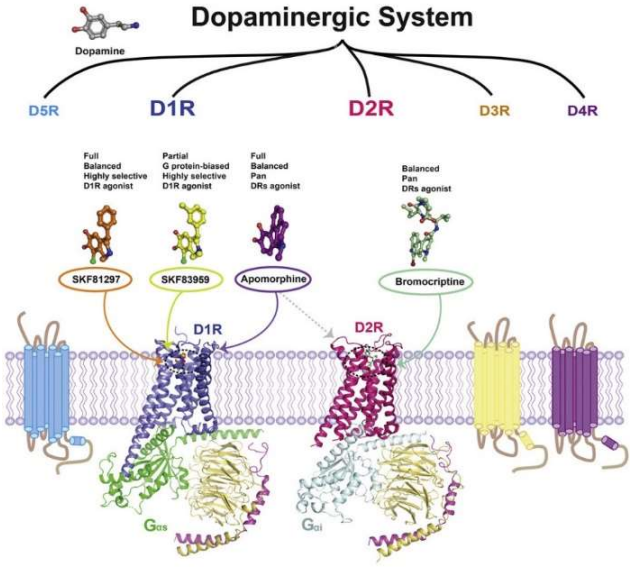


**Figure 5.3 Reproduced from Xu *et al.*[81]**

### 5.1.3 Signalling pathways of D2R

Apart from the canonical Gαi/Go signalling pathway, D2R signalling also goes through β-arrestin (**Figure 5.4**).[82] Antipsychotics mainly used in Schizophrenia, block both G-protein dependent (Gαi/o) signalling and G-protein independent (β-arrestin) signalling. The new generation antipsychotics, such as aripiprazole engages partial agonism at D2R. Jin in cooperation with Roth has revealed the first β-arrestin biased ligands at D2R based on privileged aripiprazole scaffolds.[83]

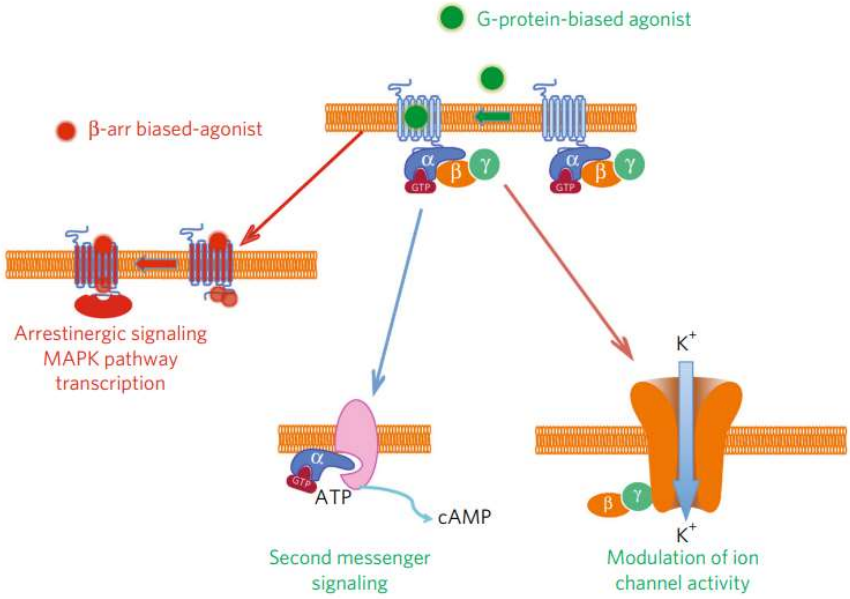


**Figure 5.4 The representative signalling pathways modulated by G-protein and β-arrestin. Reproduced from Jin *et al.*[83]**

## 5.2 Quinolizidines occurrence and pharmacological potentials

### 5.2.1 Naturally occurring quinolizidine alkaloids

The quinolizidine alkaloids frequently occurs in many plants family such as the roots of *Sophora flavescens*, the seeds and leaves of *Sophora alopecuroides L*, as well as the *Fabaceae* family.[84,85]The chemical structures of quinolizidine alkaloids are diverse, and often divided in lupinine, sparteine, matrine, aloerine, cytisine, and boehmeriasin families (**Figure 5.5)**. Owing to their inherent diverse biological and pharmacological properties, quinolizidine alkaloids have been widely explored to treat a broad spectrum of human diseases.

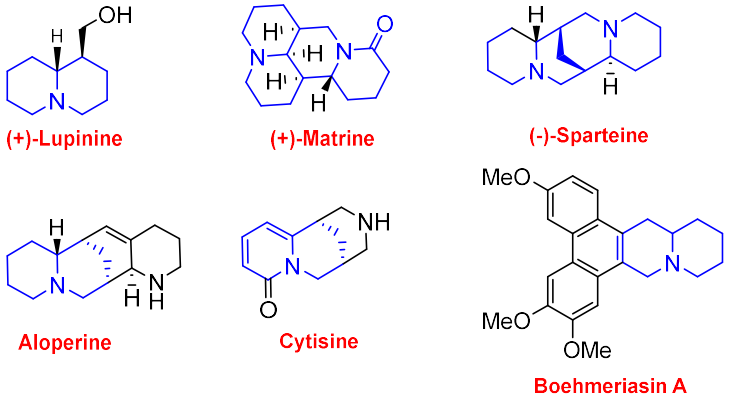


**Figure 5.5 The selected examples of quinolizidine alkaloid families**

### 5.2.2 Antiviral activity

Aloperine was first extracted from the seeds and leaves of *Sophora alopecuroides L*., and has been found in *Sophorae flavescentis* together with *Leptorhabdos parviflora Benth*.[85] A new class of anti-HIV-1 entry inhibitors ($EC_{50}$ = 0.69 μM) was identified from aloperine derivatives.[86] As a lead hepatitis C virus (HCV) inhibitor, aloperine was accessed with the late-staged functionalization for SAR study. As such, the new HCV inhibitor ($EC_{50}$ = 3.56 μM) particularly possesses a good oral pharmacokinetic and safety profile.[87] Interestingly, the equal potency against HCV ($EC_{50}$ = 3.2 μM) was also determined based on matrinic ethanol derivatives.[88]

### 5.2.3 Antimalarial activity

Malaria is a severe infectious disease that frequently occurs in the tropical area including sub-Saharan Africa. Taramelli *et al.* devised a competitive chemotherapy which the two enantiomers (+)-AM1 and (-)-AM1 have demonstrated the high potency ($IC_{50}$ = 16–53 nM) against chloroquine-sensitive and resistant *P.falciparum* strains (**Figure 5.6)**.[89]

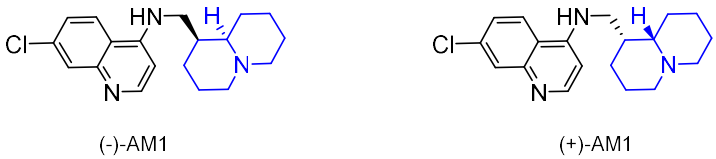


**Figure 5.6 The selected examples of quinolizidine mimics with antimalarial activities**

### 5.2.4 Anticancer activity

The natural quinolizidine alkaloids have attracted enormous attention in the last decades due to the diverse pharmacological potential including anticancer ability. The phenanthro quinolizidine (-)-(*R*) boehmeriasin A, for example, has displayed potent cytotoxicity against several human cancer assays *in vitro*.[90]

### 5.2.5 Neurological activities

Many quinolizidine alkaloids are endowed with multiple neurological activities (**Figure 5.7**). As a low cost and high affinity partial agonist at nicotinic acetylcholine receptors (nAChRs) α4β2, cytisine has been widely used to treat smoking cessation in eastern Europe. Pictamine was found to block two neuronal nAChRs at the micromolar concentrations α4β2 ($IC_{50}$ = 1.5 μM) and α7 ($IC_{50}$ = 1.3 μM), respectively.[91] The synthetic quinolizidine (1-epi-207I) was characterized to be a relatively selective α7 inhibitor ($IC_{50}$ = 0.6 μM) over α4β2 and α3β4.[91] ORM-10921 was originally profiled and studied as the potent and selective $\alpha_{2c}$ adrenoceptors antagonist. It also possess high affinity to human D1-liked receptors, human 5-HT1A and 5-HT2B. Additionally, it shows moderate potency at human D2-liked receptors.[78]

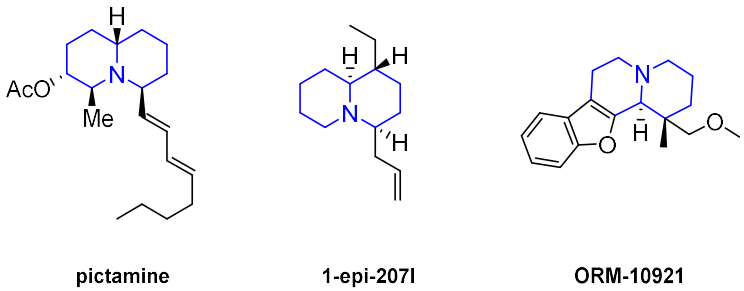


pictamine 1-epi-207I ORM-10921

**Figure 5.7 Structures of quinolizidines with neurological activities**

## 5.3 Synthesis of quinolizidines inspired library

In this section, I will describe my efforts to synthesise a library of diverse compounds containing quinolizidines fused to secondary fragments predominantly found in natural products or bioactive small molecules.

### 5.3.1 The preparation of octahydro-1H-quinolizin-1-one

Although the quinolizidines inspired library could be approached *via* various synthetic routes of the collection, those reported compound collections are often lack of scaffold diversity. To overcome the diversity concerns, octahydro-1H-quinolizin-1-one was proposed as the building block due to the remarkable potentials for merging secondary fragments. We initially noted the building block octahydro-1H-quinolizin-1-one is commercially available, but no suppliers could offer it at a reasonable price. In contrast, Barker delivered the synthetic pathway in four steps **(Scheme 5.1)**.[92]

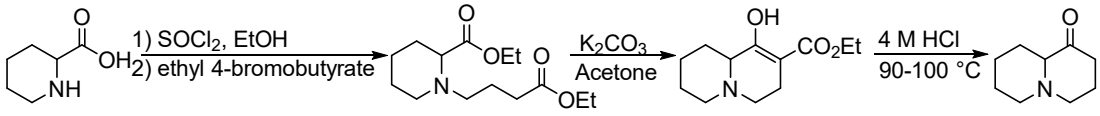


**Scheme 5.1 The delivered synthesis route of key building block**[92]

We began our syntheses from economically available reagent **5.01**, the alkylation with ethyl 4-bromobutyrate gave us diester **5.02** in a high isolated yield. The following Dieckman condensation was accessed in the presence of tBuOK,[93] which provided the β-keto ester as an inseparable mixture of keto **5.03** and enol forms **5.04**. We finally performed the hydrolysis and decarboxylation under the referred condition. In the reported procedure, no information about the purification was provided. Due to the strong hydrophilicity, the desired ketone **5.05** was extracted with a mixed solvent (*i*PrOH:$CHCl_3$ = 1:9) over eight times. This provided a good isolated yield. The overall yield in three steps **(Scheme 5.2)** we calculated is 66%, which is in consistent with the reference. Octahydro-1H-quinolizin-1-one tends to decomposed at the room temperature. As such, it is recommended to prepare it fresh each time or store in the freezer according to our laboraory experience.

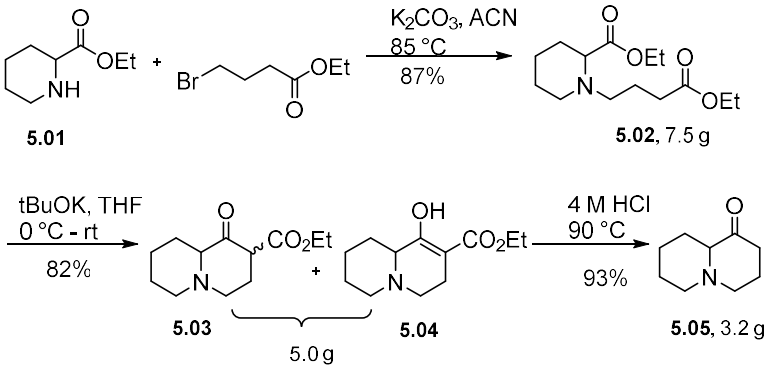


**Scheme 5.2 Synthesis of ketone building blocks for library synthesis**

### 5.3.2 Spirocyclic quinolizidine analogues *via* oxa Pictet-Spengler reaction

The synthesis of spirocyclic library using the oxa Pictet-Spengler reactions has led to identify several biologically active modulators. In our previous study, MsOH mediated the essential cyclization based on tropinone and tryptophol was reported. We prioritized this protocol to explore the synthesis of quinolizidine-inspired collections (**Table 5.1**).

To begin with, we tested the oxa Pictet-Spengler reactions with tryptophol and 5-methoxytryptophol since they are economically available from the chemical supplier combi-blocks. Products **5.06** and **5.08** were both achievable under the standard reaction conditions, which gave us the isolated yields of 50% and 18%, respectively. More types of tryptophols were synthesized by the reduction of substituted acetyl acetic acid treated with LAH. These alcohols were reacted with Octahydro-1H-quinolizin-1-one **5.05**, which yielded three analogues featuring different substitutions. In general, it provides us the spirocyclic products in moderate isolated yield. Interestingly, we only detected and isolated one single diastereoisomer, of which the relative configuration was determined by 2D NOE NMR spectra (**Figure 5.8**). We subsequently explored the feasibility of other aromatic alcohol species to extend our collections.

It was decided to generate compound **5.11** following the similar condition, albeit in relatively lower yield (< 5%). In a paralleled experiment, the isolated yield was slightly improved (9%) under Dean-Stark conditions. This protocol failed to obtain compound **5.12**, though a trace amount of conversion could be observed from the LC-MS.

**Table 5.1 Synthesis of oxa Pictet-Spengler adducts of quinolizidinone**

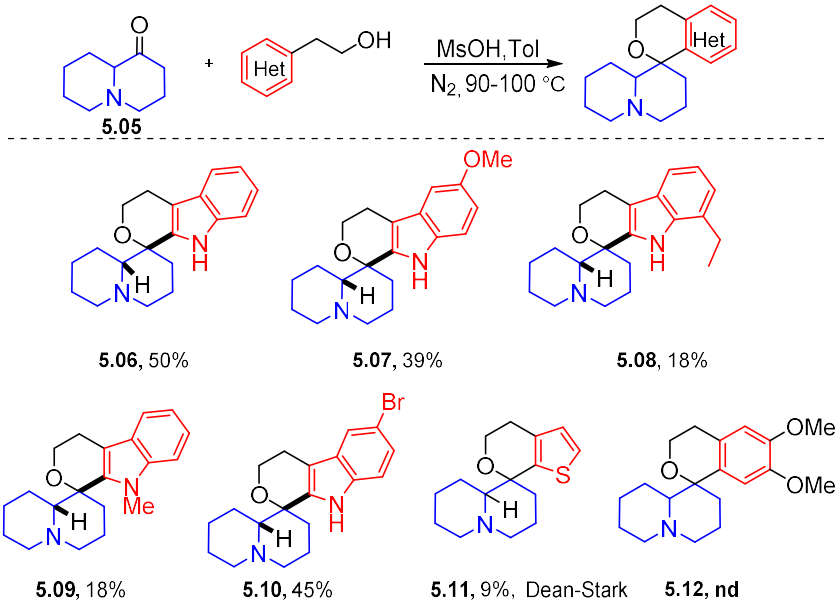

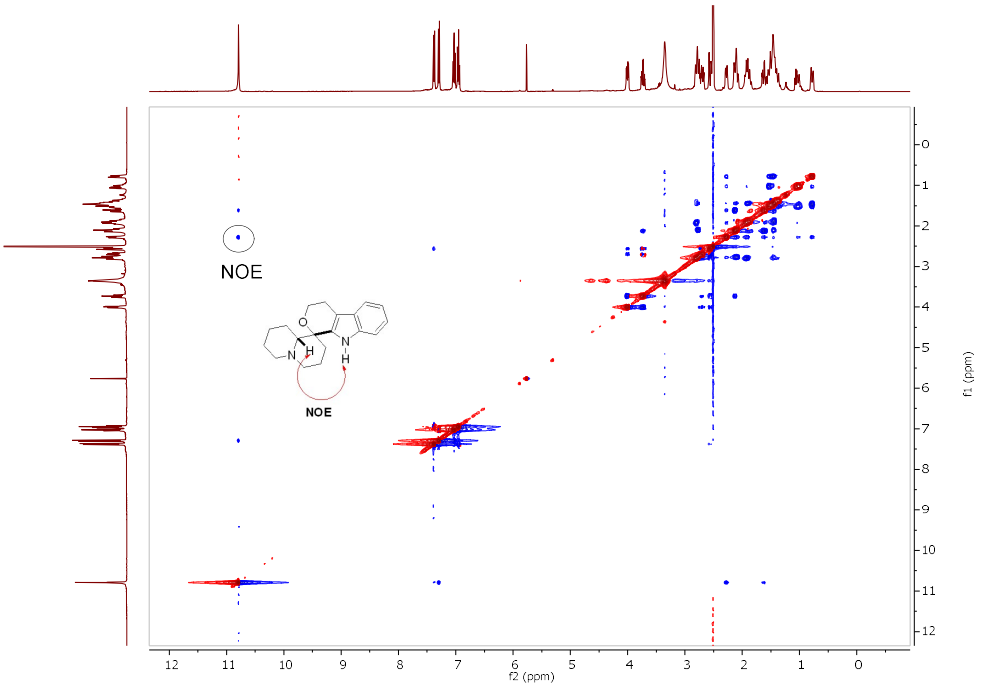


**Figure 5.8 2D NOE NMR spectra of compound 5.06**

### 5.3.3 Synthesis of spiroindolones

The construction of a quaternary carbon center or an aza quaternary carbon center has attracted tremendous attention among the synthetic chemists. Spiroindolones are widely founded in many alkaloids family such as horsfiline and rhyncophyline (**Figure 5.9**).[94]

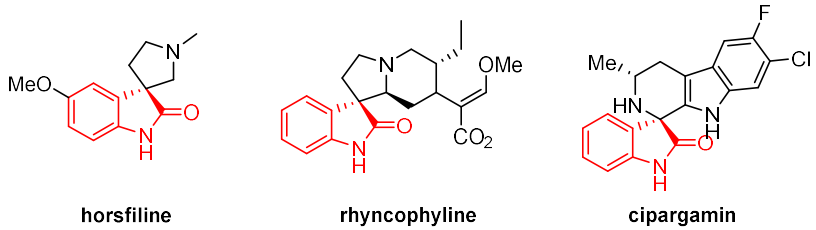


**Figure 5.9 Structures of natural products or approved drug containing spirocyclic indolones**

Although numerous methodologies have been developed, chemical oxidation of indoles is the strategical approach to achieve such transformations. N-bromosuccinimide (NBS) mediated the oxidation of the indole ring on the Tetrahydro-β-Carboline (THβC) resulted in the total synthesis of alkaloid (-)-horsfiline.[95] In addition, sterol fused oxindoles were accessed *via* bromination mediated by NBS and subsequent ring rearrangement in the acidic environment in our group.[26] However, such protocol proved to be inefficient to access compound **5.06**, the main product that we determined as the brominated side product. Oxone ($KHSO_5$-$1/2KHSO_4$-$1/2K_2SO_4$) served as a cheap and green oxidant, has the great potential for various chemical oxidations.[96] It also has been recently employed to synthesize alkaloid (±)-horsfiline and (±)-coeruescine.[58] Following the similar protocol, we reported the synthesis of five analogues **5.13-5.17** featuring various substitutions (**Table 5.2**). Although one single diastereoisomer was detected and separated, the relative configuration needs to be further confirmed with X-Ray crystallography.

**Table 5.2 Synthesis of spiroindolones via an oxidative ring contraction**

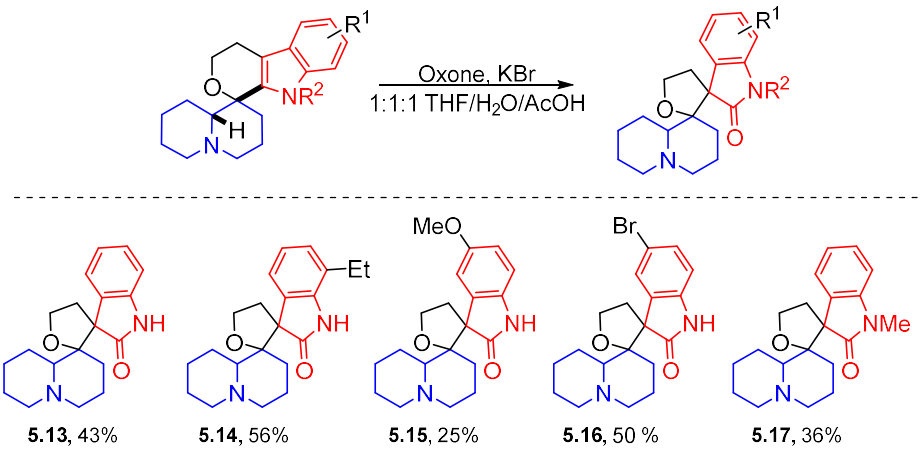

### 5.3.4 Spirocyclic quinolizidine analogues *via* Pictet-Spengler reaction

THβC is one of the most popular chemical structure naturally existing in numerous alkaloid families, as well as multiple biologically active molecules.[97] In particular, it may have therapeutic potentials for the treatment of neurological disorders due to various signalling transduction in the CNS (**Figure 5.10).**[98,99] To the best of our knowledge, no ligands compromised THβC show potent affinity to dopamine receptors. As such, we propose the combination this privileged structures with Octahydro-1H-quinolizin-1-one **5.5** may lead to discover novel dopamine receptors modulators.

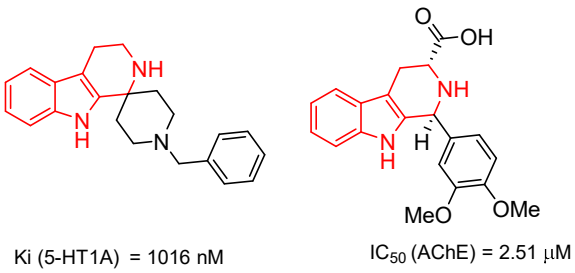


**Figure 5.10 Selected examples of ligands in the CNS contain privileged THβC**

Attempts to synthesize analogues **5.18-5.21** *via* Pictet-Spengler reactions were carried out according to a previously reported protocol **(Table 5.3)**.[60] As a result, four analogues bearing different substitution patterns were generated in good isolated yields. Only one single diastereomer was detected, and the subsequent analysis from the 2D NOE NMR spectra confirmed the relative configuration (**Figure 5.11**).

**Table 5.3 Synthesis of Pictet-Spengler adducts of quinolizidinone**

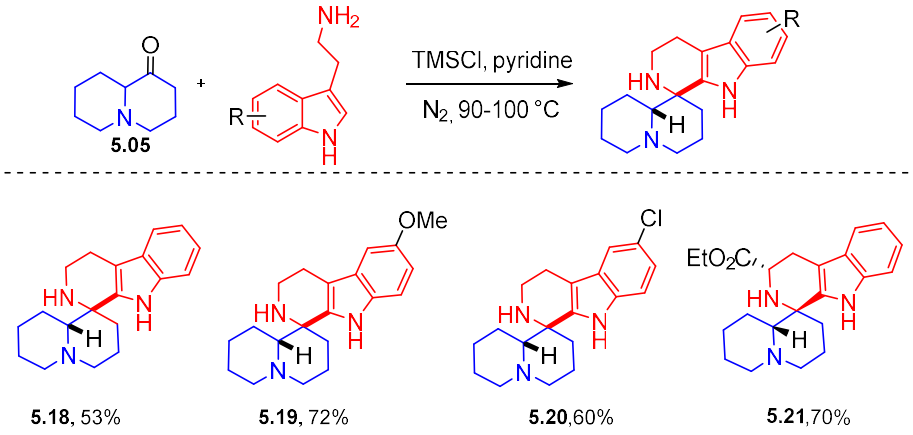

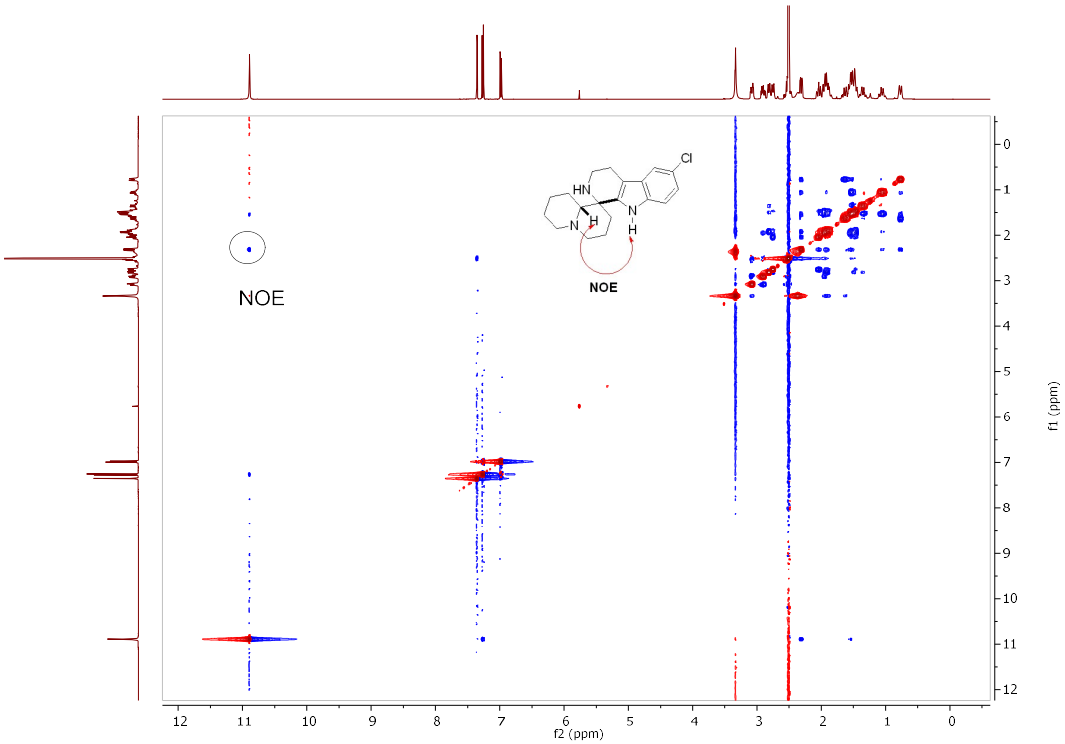


**Figure 5.11 2D NOE NMR Spectra of analogue 5.20**

### 5.3.5 Spirocyclic quinolizidines *via* Pictet-Spengler reaction with pyrroloquinoxalines

There is no doubt that the Pictet-Spengler reactions can applied to construct other spirocyclic heterocycles. The pyrroloquinoxaline skeletons extensively occurs in drug-like molecules, and they have been profiled to display the highly potent antagonism at adenosine $A_3$ receptor and excellent agonism at serotonin 5-HT3 receptor[100] (**Figure 5.12**), respectively. These findings suggest that Octahydro-1H-quinolizin-1-one **5.05** fused to pyrroloquinoxaline may result in identifying new ligands at other aminergic receptors.

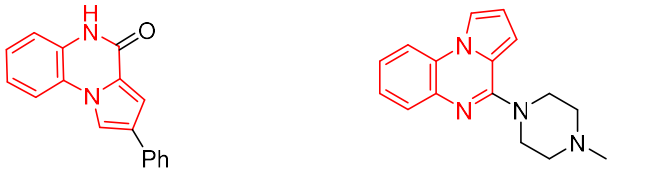


**5.22**, $IC_{50}$ ($A_3$) = 9.5 nM **5.23**, $IC_{50}$ (5-HT3) = 0.37 nM

**Figure 5.12 Selected examples of neurological active ligands contain pyrroloquinoxaline**

To test the feasibility of the proposed reaction, we initially tested the Pictet-Spengler reaction conditions (20 mol% TfOH for 4 hours). Disappointingly, poor conversion of the substrates to **5.24** was detected. We pursued further optimization by adding additional 80 mol% TfOH. Additionally, the reaction time was prolonged to 20 hours with good conversions. Using this optimized protocol, we reported the synthesis of three analogues **5.24-5.26** in a mild isolated yield (**Table 5.4**) with a complete diastereocontrol (**Figure 5.13)**.

**Table 5.4 Synthesis of aza Pictet-Spengler adducts of quinolizidinone**

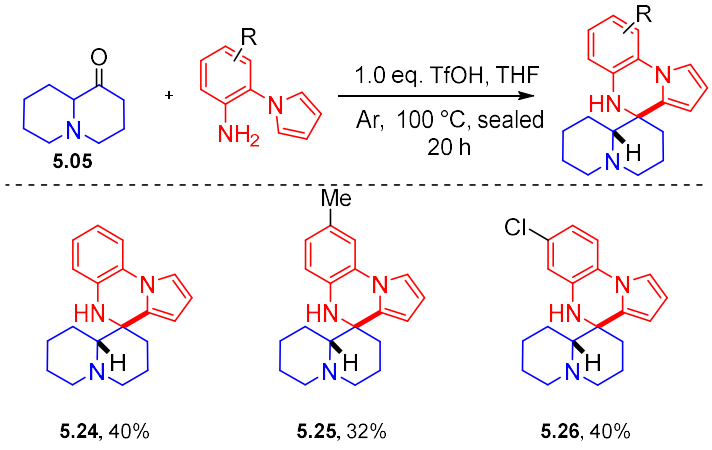


**5.24**, 40% **5.25**, 32% **5.26**, 40%

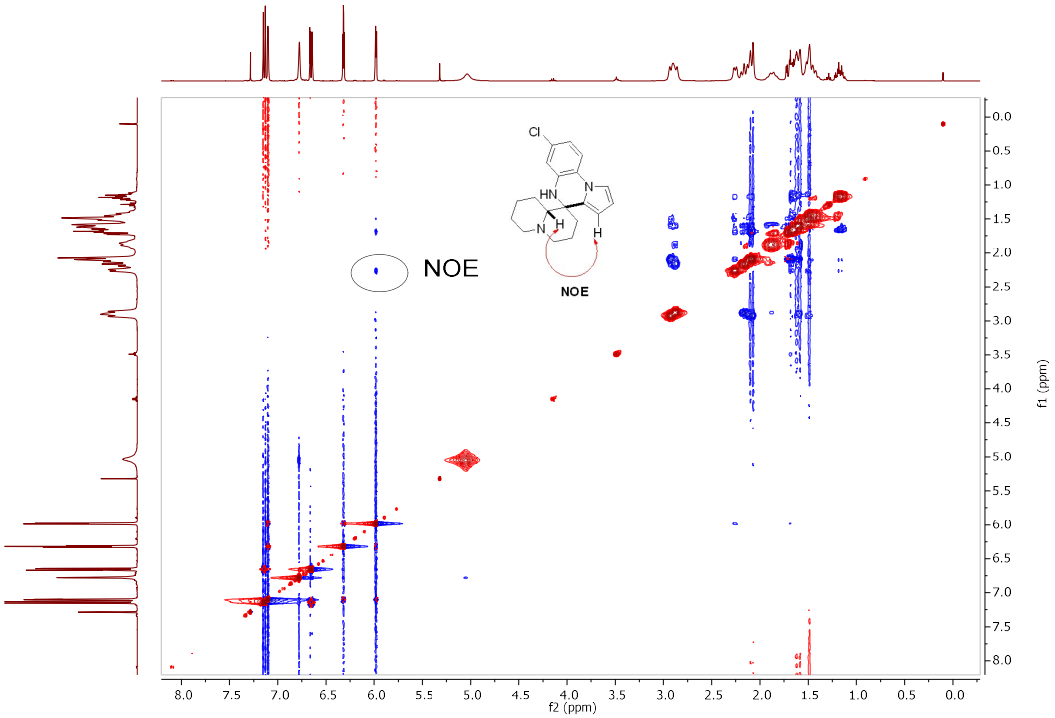


**Figure 5.13 2D NOE NMR Spectra of analogue**

### 5.3.6 Attempts to synthesize other spirocyclic analogues

To examine the new spirocyclic fusion *via* olefin metathesis, the spiro-lactam **5.29** was proposed to be prepared in three steps (**Scheme 5.3**). The alkylation of the Octahydro-1H-quinolizin-1-one **5.05** with a Grignard reagent afforded the tertiary alcohol **5.27** as a mixture of diasteroisomers, which were separable by flash column chromatography. To examine the feasibility of the ester coupling, we employed DCC as the reagent. Disappointedly, the activation of the acid failed to react with the tertiary alcohol **5.27**, possibly due to steric hindrance. Surprisingly, we isolated the intermediate **5.30** and further confirmed the structure with NMR.

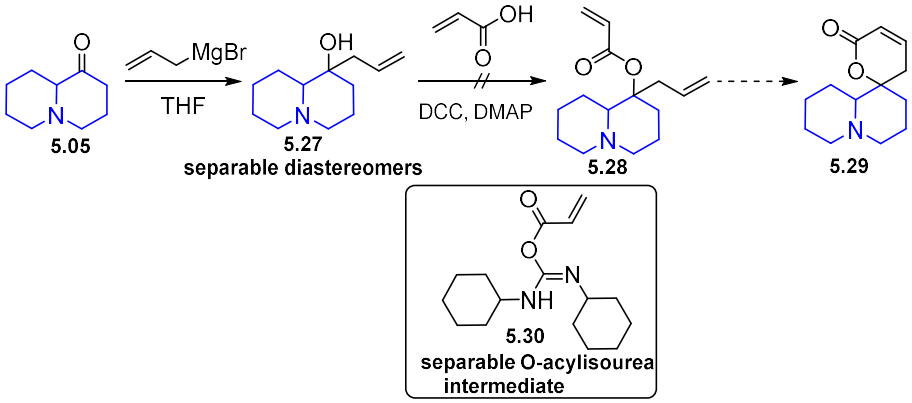


**Scheme 5.3 The proposed synthetic routes to spiro-lactam**

Syntheses of medium-sized heterocycles have attracted considerable interests due to their broad therapeutic potentials. Kozmin illustrated the oxidative cleavage of the indole ring to produce ketoamides based on the indoloquinolizidine alkaloid mimics.[101] $NaIO_4$, served as the common oxidant to the Witkop oxidation has been examined to access **5.06**. Unfortunately, despite the excellent conversion monitored by LC-MS under our optimized condition, the product **5.31** suffered the degradation from silica column chromatography (**Scheme 5.4**).

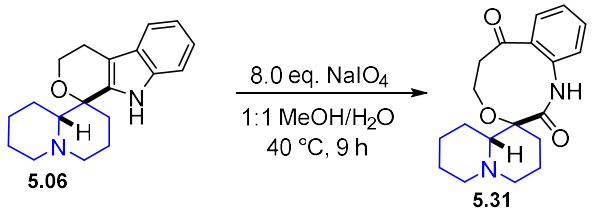


**Scheme 5.4 An effort to synthesize medium-sized heterocycle of ring oxidative cleavage**

The recombination of fragments bearing different linkers may favor the identification of various biological signalling pathways. Encouraged by the synthesis of analogues **5.13-5.17** displaying an impressive 3D profile, we sought to extend this collection with other linkers (**Scheme 5.5**). The methylation of THβC enabled the synthesis of compound **5.32** in an excellent isolated yield. However, under the aforementioned condition, compound **5.32** failed to transform into compound **5.33**. In addition, we examined the acetylation of THβC on compound **5.6**. Disappointedly, the analysis of LC-MS suggests the amide coupling is highly hindered.

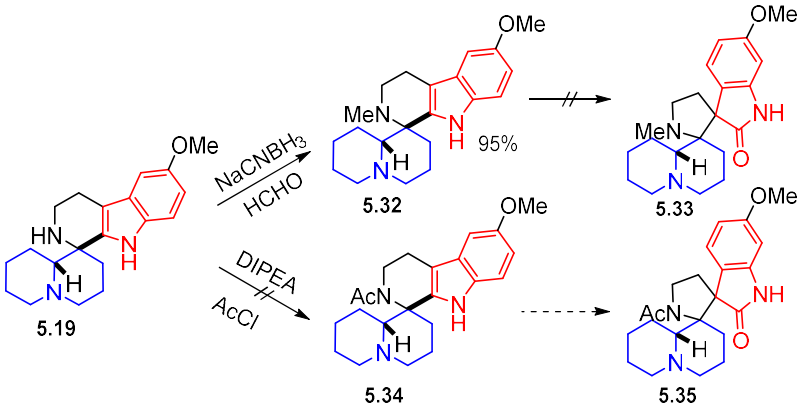


**Scheme 5.5 Attempts to synthesize other spiroindolones via an oxidative ring contraction**

### 5.3.7 Quinolizidines analogues synthesis *via* Friedlander reaction

Quinolizidines fused to several aryl heterocycles by edged fusion has previously been reported in the discovery of non-selective adrenergic receptor antagonists (**Figure 5.14)**.[77] However, to address the structural and biological diversity, there is an unfulfilled need for the synthesis of a library with new edged fusions to identify new CNS ligands.

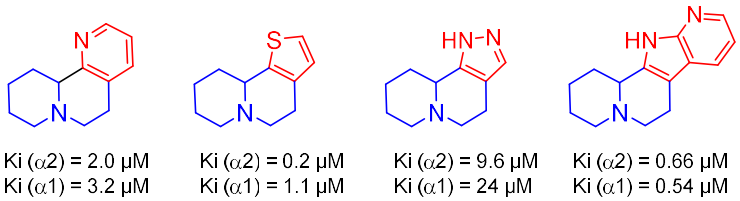


**Figure 5.14 Selected examples of antagonists against adrenergic receptor based on quinolizidines**

We previously reported the synthesis of compounds **3.17-3.19** employing the Friedländer reaction in good yields. We reasoned this protocol could been extended to synthesize analogues **5.36-5.38 (Table 5.5)**. The synthetic work for this collection was initially assigned to our former master student Annika Garcia Eriksen under my guidance. Here, we reported three analogues bearing different substitutions in relatively low yields.

**Table 5.5 Synthesis of Friedländer quinoline adducts of quinolizidinone**

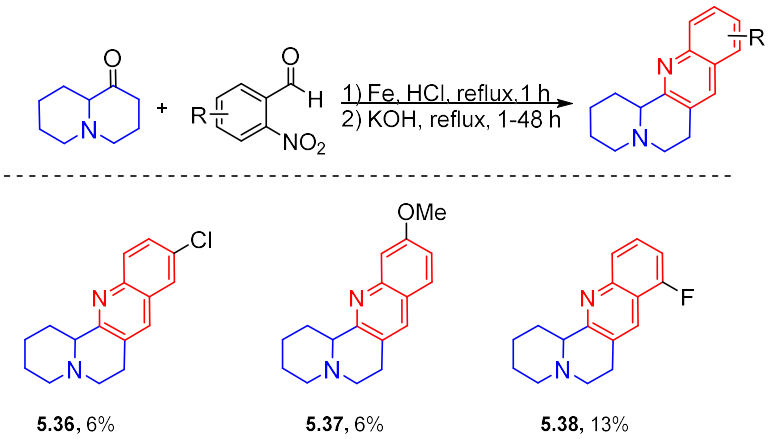

## 5.4 Biological evaluation

Quinolizidines are found in many nAChRs ligands and potent adrenergic receptors ligands, but less studied as the core scaffolds of dopamine receptors modulators. Our interest is to identify new and selective D2R ligands by merging the privileged quinolizidines with natural products fragments. As such, the resulting compound collections were initially assessed the inhibition and activation against D2R using a PRESTO-Tango assay in a mouse model **(Table 5.6)**. As a result, compounds **5.38** ($IC_{50}$ = 0.76 μM) and **5.36** ($IC_{50}$ = 0.48 μM) exhibited the good inhibition. In addition, six analogues were found to exhibit the moderate antagonism.

To determine the selectivity over D1R, the compound collections were tested the inhibition with a cAMP accumulation assay. Impressively, the majority of hit compounds demonstrated the lower inhibition at D1R (≤ 50%) at the given concentration of 10 μM except compound **5.36** ($IC_{50}$ = 5.0 μM) (**Table 5.7**). In parallel, all the compounds did not display significant antagonism response at 10 μM (**Table 5.7**).

To exemplify the selectivity evaluation over other CNS receptors, we tested our collections against nAChRs because they are well known to target many quinolizidine alkaloids. Targeted screening against human α4β2 and the rat α3β4 nAChRs were assessed in a competition [3H]epibatidine binding assay. Surprisingly, none of these compounds showed decent active at the given concentrations of 10 μM. (**Table 5.8**).

**Table 5.6 Antagonist evaluation of quinolizidines inspired library on the dopamine receptor D1R and D2R.** Activation or inhibition of the dopamine receptors D1R was assessed through measurement of Gs-mediated intracellular cAMP in HEK 293T cells; D2R was assessed through measurement β-arrestin-mediated luciferase luminescence in HTLA cells. n.d. (not determined).

| Entry | compound | D2R (*β*-arrestin) | D1R (cAMP) |
|---|---|---|---|
| | | IC50 (μM) n=3 | IC50 (μM) n=3 |
| **1** | **5.38** | 0.76 | n.d. |
| **2** | **5.37** | 5.9 | n.d. |
| **3** | **5.36** | 0.48 | 5.0 |
| **4** | **5.18** | 10.0 | n.d. |
| **5** | **5.20** | 3.1 | n.d. |
| **6** | **5.21** | 8.9 | n.d. |
| **7** | **5.10** | 3.1 | n.d. |
| **8** | **5.08** | 4.9 | 41 |

**Table 5.7 Compound's activity on the dopamine receptor $D_1$ and $D_2$.** Activation or inhibition of the dopamine receptors $D_1$ (DRD1) and $D_2$ (DRD2) was assessed through measurement of $G_s$-mediated intracellular cyclic adenosine monophosphate (cAMP) accumulation in HEK 293T cells (DRD1) and arrestin2-mediated luciferase luminescence in HTLA cells (DRD2). For assessment of agonist-activity, results were normalized to the maximum response of 10 µM dopamine (DRD1) or quinpirole (DRD2) (n=3). For assessment of antagonist-activity, results were normalized to the response produced by $EC_{80}$ of the agonist dopamine (DRD1) or quinpirole (DRD2) (n≥3).

| Compound | DRD1 activation, % of 10 µM Dopamine | | DRD1 % inhibition | | DRD2 activation, % of 10 µM quinpirole | | DRD2 % inhibition | |
|---|---|---|---|---|---|---|---|---|
| | % | SEM | % | SEM | % | SEM | % | SEM |
| **Dopamine** | 100 | 4.2 | - | - | - | - | - | - |
| **R(+)SCH23390** | - | - | 93.2 | 1.8 | - | - | - | - |
| **Quinpirole** | - | - | - | - | 100 | 4.9 | - | - |
| **Benperidol** | - | - | - | - | - | - | 98.6 | 0.2 |
| **5.18** | 1.7 | 1 | 9.9 | 12.4 | -2.7 | 0.1 | 58.4 | 17.1 |
| **5.06** | 2.1 | 0.7 | 12.9 | 13.7 | -2.7 | 0.1 | 33.6 | 8.9 |
| **5.07** | 0.4 | 0.5 | 11.3 | 11.6 | -2.5 | 0.1 | -2.9 | 4.4 |
| **5.11** | 0.4 | 0.7 | 5.9 | 11.3 | -2.8 | 0.1 | 4.2 | 4.1 |
| **5.20** | 2.7 | 1.3 | 20.3 | 13.5 | -2.8 | 0.1 | 99.3 | 0.5 |
| **5.21** | 2 | 0.8 | 9.8 | 7.7 | -2.8 | 0.1 | 88 | 4.9 |
| **5.32** | 0.3 | 0.7 | 2.2 | 8.4 | -2.7 | 0.1 | 20.2 | 7.8 |
| **5.19** | 0.2 | 0.8 | 12.8 | 11.7 | -2.7 | 0.1 | 23 | 11.4 |
| **5.10** | 1.6 | 1.4 | 18.9 | 14.4 | -2.8 | 0.1 | 97.9 | 0.7 |
| **5.08** | 1.9 | 0.8 | 12.8 | 13 | -2.8 | 0.1 | 89.8 | 7 |
| **5.09** | 1 | 0.8 | 6.5 | 14.6 | -2.7 | 0.1 | 25.3 | 12.4 |
| **5.13** | 1.7 | 1 | 12.1 | 11.4 | -2.5 | 0.1 | 9.6 | 8.9 |
| **5.14** | 1.4 | 0.6 | 10.9 | 11.4 | -2.7 | 0 | 11.7 | 6 |
| **5.16** | 1 | 0.6 | 0.7 | 8.4 | -2.5 | 0.1 | -0.8 | 8.1 |
| **5.15** | 1.3 | 0.7 | 11.5 | 10.3 | -2.1 | 0.1 | 3 | 7.2 |
| **5.38** | 1.2 | 1.4 | 4 | 10.7 | -2.5 | 0.1 | 97.3 | 0.9 |
| **5.37** | 0.9 | 0.6 | 45.2 | 10.1 | -2.5 | 0.1 | 91.2 | 3.3 |
| **5.36** | 0.5 | 0.8 | 66.8 | 10.1 | -2.5 | 0.1 | 92.7 | 5.4 |

**Table 5.8 Screening of alkaloid-inspired compounds (10 μM) for inhibition of binding of [3H]epibatidine to acetylcholine receptors**. Data is residual binding normalized to the DMSO control and represents the mean of two independent experiments carried out in duplicate. Nicotine (100 μM) was used as the positive control.

| Compound | α4β2 nAChR (% residual binding) | α3β4 nAChR (% residual binding) |
|---|---|---|
| **DMSO** | 100 | 100 |
| **Nicotine (100 μM)** | 0 | 0 |
| **5.38** | 88 | 67 |
| **5.37** | 89 | 65 |
| **5.36** | 80 | 79 |
| **5.18** | 88 | 61 |
| **5.11** | 96 | 70 |
| **5.13** | 91 | 57 |
| **5.14** | 94 | 79 |
| **5.20** | 88 | 54 |
| **5.21** | 95 | 55 |
| **5.32** | 85 | 55 |
| **5.16** | 92 | 56 |
| **5.09** | 95 | 67 |
| **5.18** | 88 | 55 |
| **5.10** | 87 | 58 |
| **5.08** | 91 | 68 |
| **5.07** | 93 | 60 |

## 5.5 Conclusions

We report the synthesis of a diverse quinolizidine alkaloid inspired library containing 22 compounds, of which eight analogues composed of three distinct scaffolds showed the antagonist activation ($IC_{50} \leq$ 10 μM) against D2R using a β-arrestin recruitment assay. Employing the Pictet-Spengler reactions for the synthesis of THβC analogues, of which three analogues demonstrated the imbibition at the concentrations ranging from 3.1 μM to10 μM. An increasing potency may benefit from the electron withdrawing groups on the THβC, such as **5.20**. Because 5-OMe on the THβC **5.19** was found to possess the lower response of antagonism, and demonstrated little inhibition against D1R at the given concentration of 10 μM. Although six compounds were generated *via* oxa Pictet-Spenggler reactions, of which two compounds were identified as the hits and demonstrated the similar potency. In the presence of Friedländer reaction, three analogues featuring various substitutions were synthesized. As such, they were both identified as the hits, in particular two analogues featuring halogen substitution in the different position displayed the higher potency ($IC_{50} \leq 1$ μM). One analogue **5.38** was suggested highly selective versus D1R due to the neglected response inhibition.

Taken together, these findings suggest Octahydro-1H-quinolizin-1-one served as the building block, fused to the secondary natural fragments, which facilitated the identification of the novel D2R antagonist ligands. The preliminary SAR study suggested the quinoline-fused quinolizidines are the promising selective ligands versus D1R, α4β2 and α3β4 nAChRs.

# 6 Experimental

**Table 6.1 X-ray diffraction**

Single-crystals of **3.45**, **3.60** and **(*S*)-4.22** were immersed in polybutene oil (Aldrich, >90%) and mounted on a nylon loop, which was attached to a SuperNova Dual Source CCD-diffractometer. Data were collected using Cu K$\alpha$ ( $\lambda$ = 1.5406 Å) radiation at 120(1) K**.** Using Olex2, the structure was solved with the SHELXT structure solution program using Intrinsic Phasing and refined with the SHELXL shelxl refinement package using Least Squares minimization. **All non-hydrogen atoms were refined anisotropically.** The absolute configuration of **3.45, and (*S*)-4.22** was determined by anomalous dispersion methods using Bayesian statistics on Bijvoet differences implemented in the program *PLATON*. The obtained probability values for **3.60** were: P2(true):1.000, P3(true):1.000, P3(rac-twin): 0.2E-19, P3(false): 0.7E-73 based on 1622 Bijvoet pairs (**Figure 6.1**).The values for **(*S*)-4.22** were: P2(true): 1.000 ,P3(true): 1.000, P3(rac-twin): 0, P3(false): 0 based on 1209 Bijvoet pairs (**Figure 6.2**)

| Compound | **3.45** | **3.60** | **(*S*)-4.22** |
|---|---|---|---|
| CCDC number | 2111735 | 2111736 | 2111738 |
| Temperature/K | 120 | 120 | 120 |
| Crystal system | monoclinic | orthorhombic | monoclinic |
| Space group | $P2_1/n$ | $P2_12_12_1$ | $P2_1$ |
| $a$ / Å | 7.4671(2) | 9.99970(10) | 7.21570(10) |
| $b$ / Å | 28.9549(4) | 10.34580(10) | 6.74930(10) |
| $c$ / Å | 9.1589(2) | 17.4234(2) | 18.2887(2) |
| $\alpha$ / ° | 90 | 90 | 90 |
| $\beta$ / ° | 96.952(2) | 90 | 99.2130(10) |
| $\gamma$ / ° | 90 | 90 | 90 |
| Volume / Å$^3$ | 1965.68(7) | 1802.54(3) | 879.19(2) |
| $Z$ | 4 | 4 | 2 |
| $\rho_{calc}$ / gcm$^{-3}$ | 1.359 | 1.265 | 1.382 |
| $\mu$ / mm$^{-1}$ | 3.163 | 0.711 | 2.128 |
| F(000) | 848.0 | 736.0 | 388.0 |
| Crystal size / mm$^3$ | 0.73 × 0.3 × 0.1 | 0.35 × 0.1 × 0.1 | 0.7 × 0.5 × 0.2 |
| Radiation | Cu Kα ($\lambda$ = 1.54184) | Cu Kα ($\lambda$ = 1.54184) | Cu Kα ($\lambda$ = 1.54184) |
| 2$\Theta$ range for data collection / ° | 10.198 to 153.764 | 9.944 to 153.488 | 9.798 to 144.816 |
| Index ranges | -8 ≤ h ≤ 9, -36 ≤ k ≤ 36, -11 ≤ l ≤ 11 | -12 ≤ h ≤ 12, -13 ≤ k ≤ 13, -21 ≤ l ≤ 21 | -8 ≤ h ≤ 8, -8 ≤ k ≤ 7, -22 ≤ l ≤ 22 |
| Reflections collected | 50209 | 46495 | 12640 |
| Independent reflections | 4131 [$R_{int}$ = 0.0724, $R_{sigma}$ = 0.0215] | 3794 [$R_{int}$ = 0.0595, $R_{sigma}$ = 0.0188] | 3382 [$R_{int}$ = 0.0292, $R_{sigma}$ = 0.0175] |
| Data/restraints/parameters | 4131/0/253 | 3794/0/229 | 3382/1/232 |
| Goodness-of-fit on $F^2$ | 1.080 | 1.085 | 1.034 |
| Final $R$ indexes [I>=2σ (I)] | $R_1$ = 0.0503, $wR_2$ = 0.1189 | $R_1$ = 0.0291, $wR_2$ = 0.0733 | $R_1$ = 0.0295, $wR_2$ = 0.0792 |
| Final $R$ indexes [all data] | $R_1$ = 0.0515, $wR_2$ = 0.1196 | $R_1$ = 0.0305, $wR_2$ = 0.0746 | $R_1$ = 0.0295, $wR_2$ = 0.0792 |
| Largest diff. peak / hole / e Å$^{-3}$ | 0.50/-0.49 | 0.16/-0.20 | 0.23/-0.18 |
| Flack parameter | | -0.06(6) | -0.006(9) |

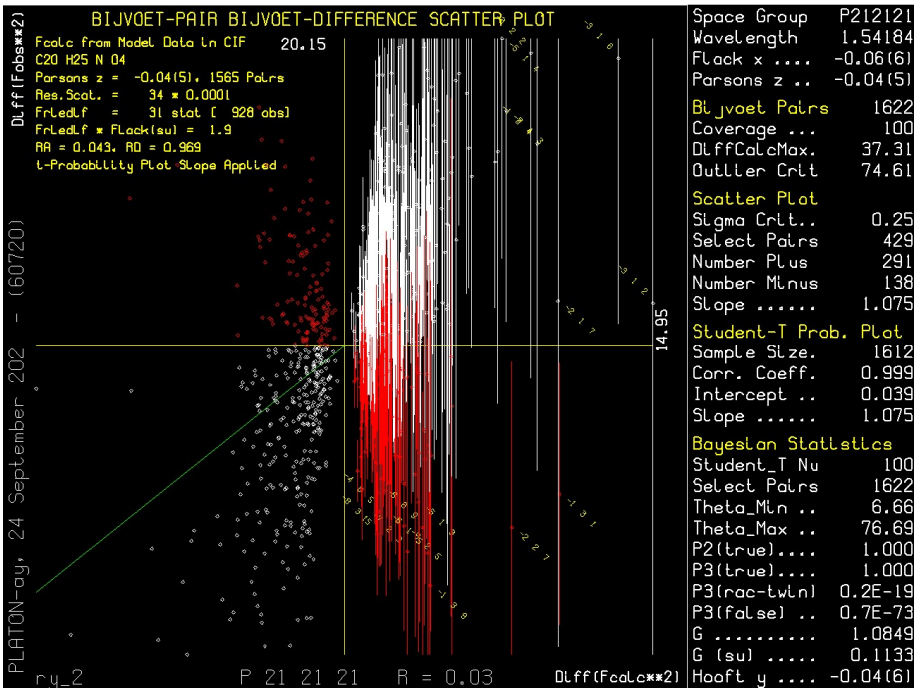


**Figure 6.1 Bijvoet-pair Bijvoet-diffrence scatter plot for 3.45**

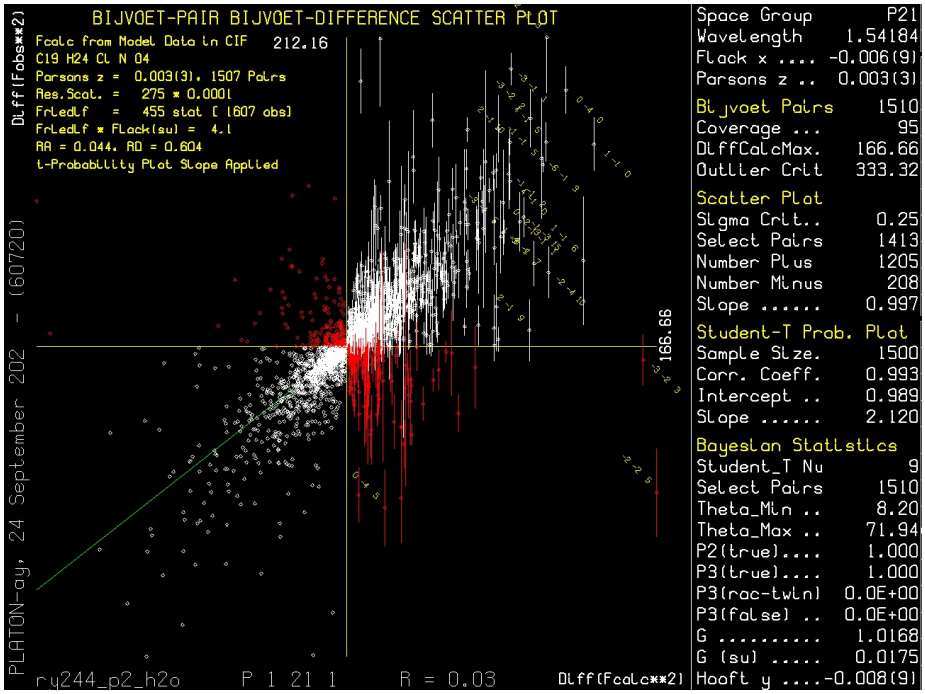


**Figure 6.2 Bijvoet-pair Bijvoet-diffrence scatter plot for (*S*)-4.22**

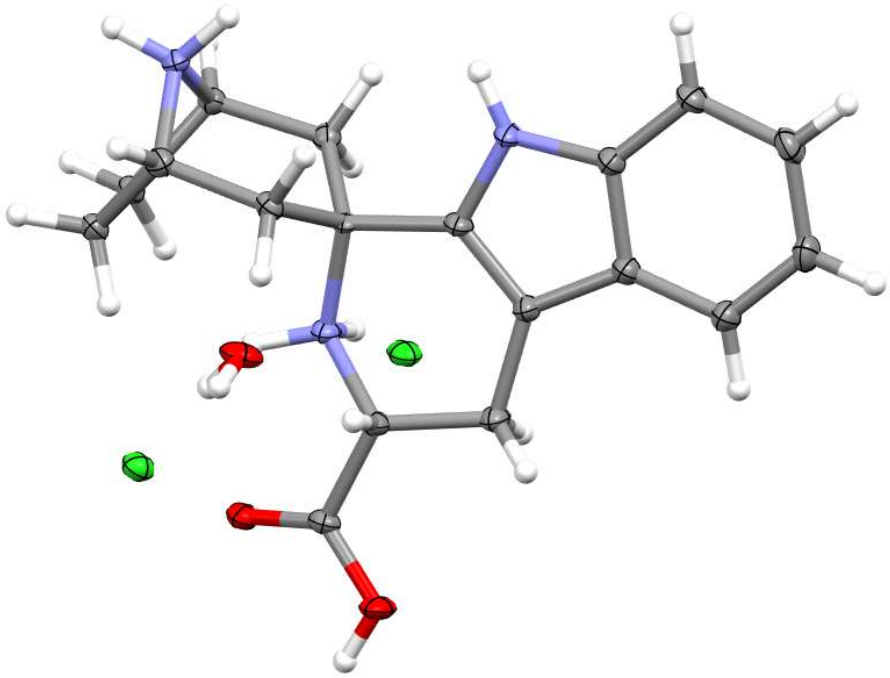

**Figure 6.3 X-ray crystal structure of 3.45**

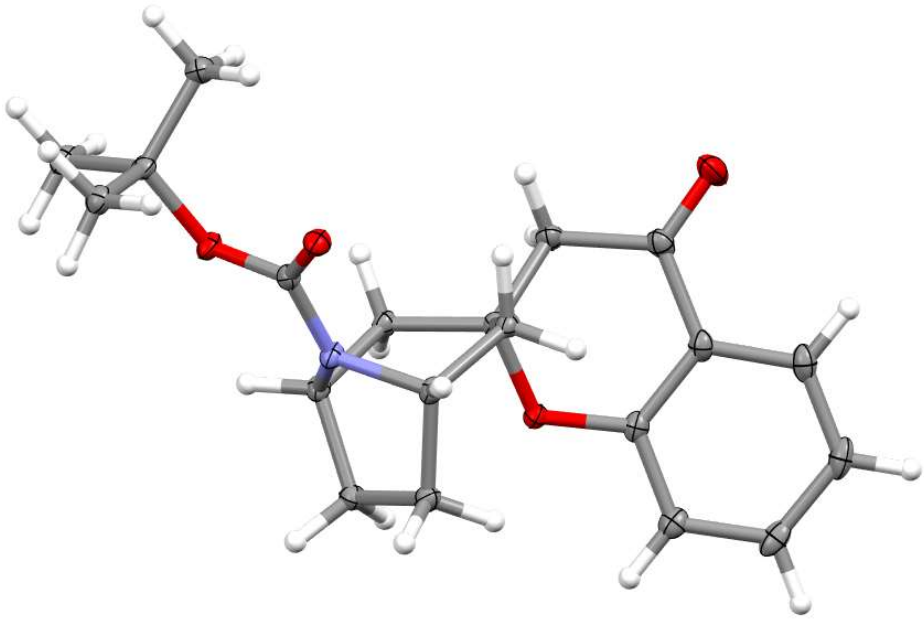

**Figure 6.4 X-ray crystal structure of 3.60**

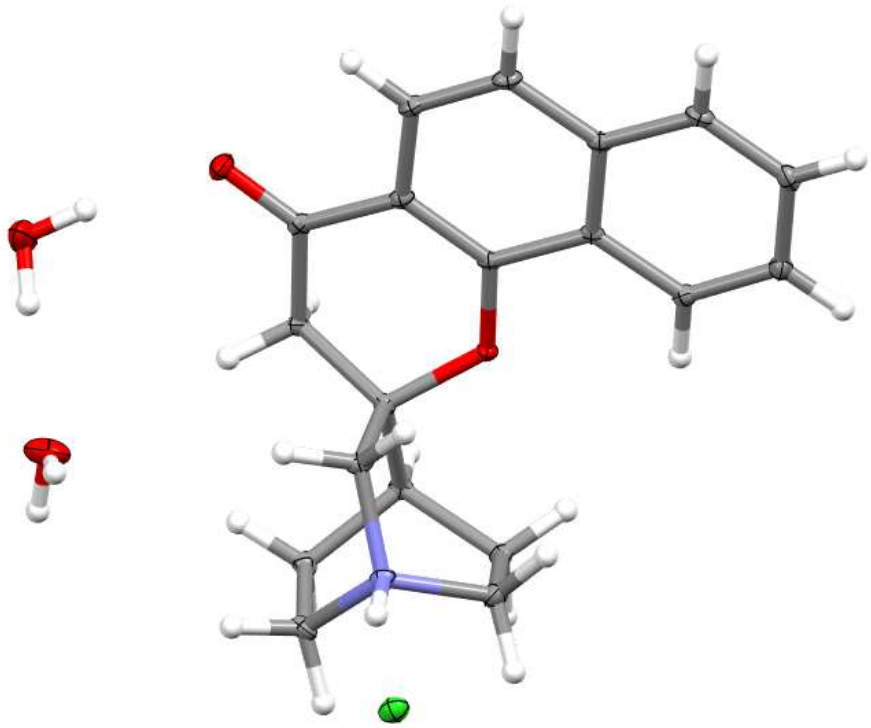

**Figure 6.5 X-ray crystal structure of (S)-4.22**

Data File C:\Chem32\1\Data\Chem202106\Chemistry 2021-06-22 16-32-34\001-0201.D
Sample Name: RY244AD20EtOH01DEA

```
==========================================================================
Acq. Operator   : SYSTEM                          Seq. Line :   2
Acq. Instrument : SFC                             Location :   1
Injection Date  : 06/22/2021 16:38:52                 Inj :   1
                                                Inj Volume : Inj prog
Method          : C:\Chem32\1\Data\Chem202106\Chemistry 2021-06-22 16-32-34\SFC_20_pos1_
                  A4ml5min.M (Sequence Method)
Last changed    : 06/22/2021 16:32:34 by SYSTEM
```

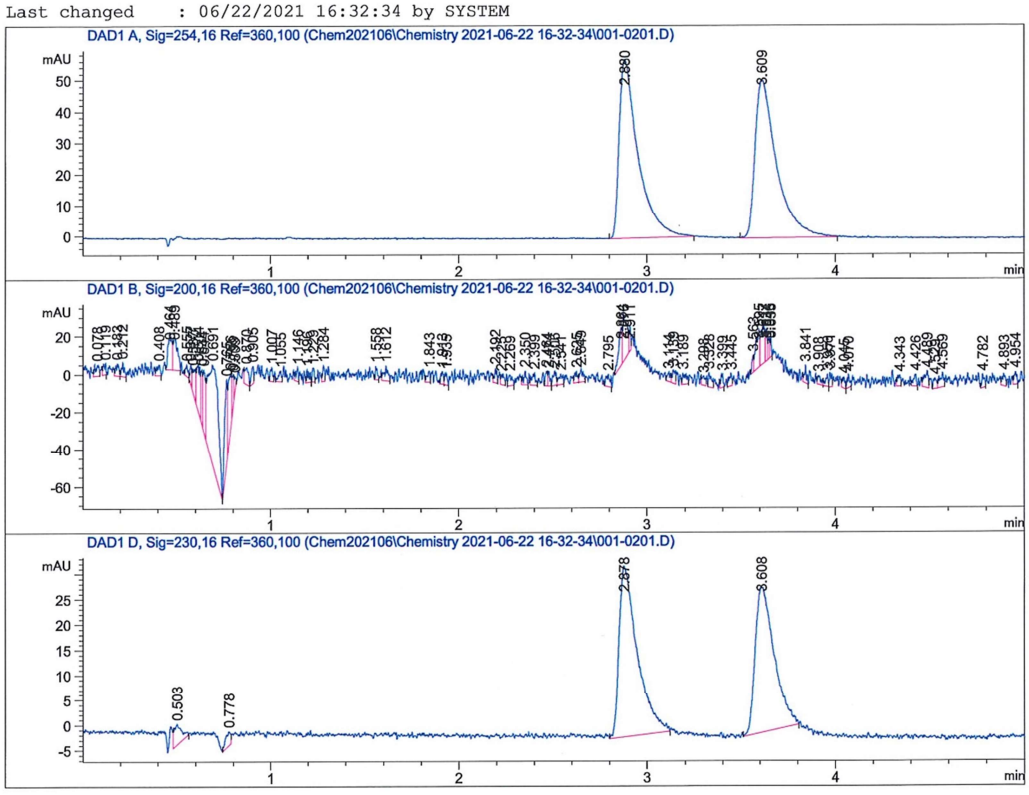


```
==========================================================================
                        Area Percent Report
==========================================================================

Sorted By             :      Signal
Multiplier            :      1.0000
Dilution              :      1.0000
Use Multiplier & Dilution Factor with ISTDs


Signal 1: DAD1 A, Sig=254,16 Ref=360,100
```



**Figure 6.6 Analytical SFC spectrum for (rac)-SCQ1**

Data File C:\Chem32\1\Data\Chem202106\Chemistry 2021-06-24 15-38-13\001-0101.D
Sample Name: RY244p1AD20EtOH01DEA

| | | | |
|---|---|---|---|
| Acq. Operator | : SYSTEM | Seq. Line : | 1 |
| Acq. Instrument | : SFC | Location : | 1 |
| Injection Date | : 06/24/2021 15:40:45 | Inj : | 1 |
| | | Inj Volume : | Inj prog |

Method : C:\Chem32\1\Data\Chem202106\Chemistry 2021-06-24 15-38-13\SFC_20_pos1_A4ml5min.M (Sequence Method)

Last changed : 06/24/2021 15:38:13 by SYSTEM

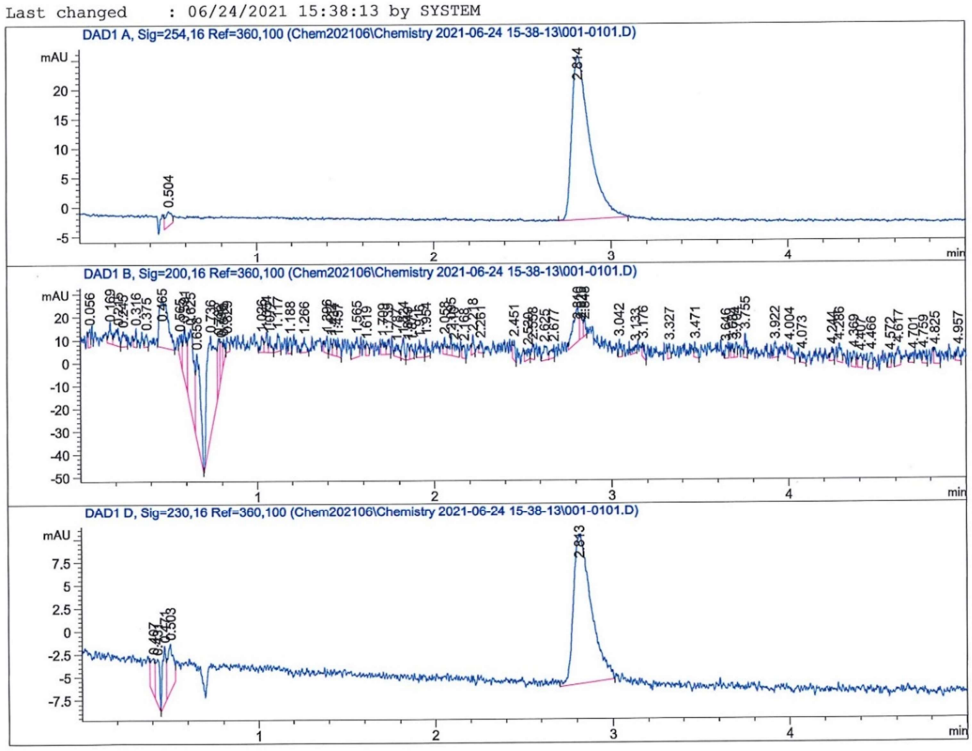


Area Percent Report

Sorted By : Signal
Multiplier : 1.0000
Dilution : 1.0000
Use Multiplier & Dilution Factor with ISTDs

Signal 1: DAD1 A, Sig=254,16 Ref=360,100



**Figure 6.7 Analytical SFC spectrum for (R)- SCQ1**

Data File C:\Chem32\1\Data\Chem202106\Chemistry 2021-06-24 14-11-33\002-0101.D
Sample Name: RY244p2AD20EtOH01DEA

| | | | |
|---|---|---|---|
| Acq. Operator | : SYSTEM | Seq. Line : | 1 |
| Acq. Instrument | : SFC | Location : | 2 |
| Injection Date | : 06/24/2021 14:14:02 | Inj : | 1 |
| | | Inj Volume : | Inj prog |

Method : C:\Chem32\1\Data\Chem202106\Chemistry 2021-06-24 14-11-33\SFC_20_pos1_A4ml5min.M (Sequence Method)

Last changed : 06/24/2021 14:11:33 by SYSTEM

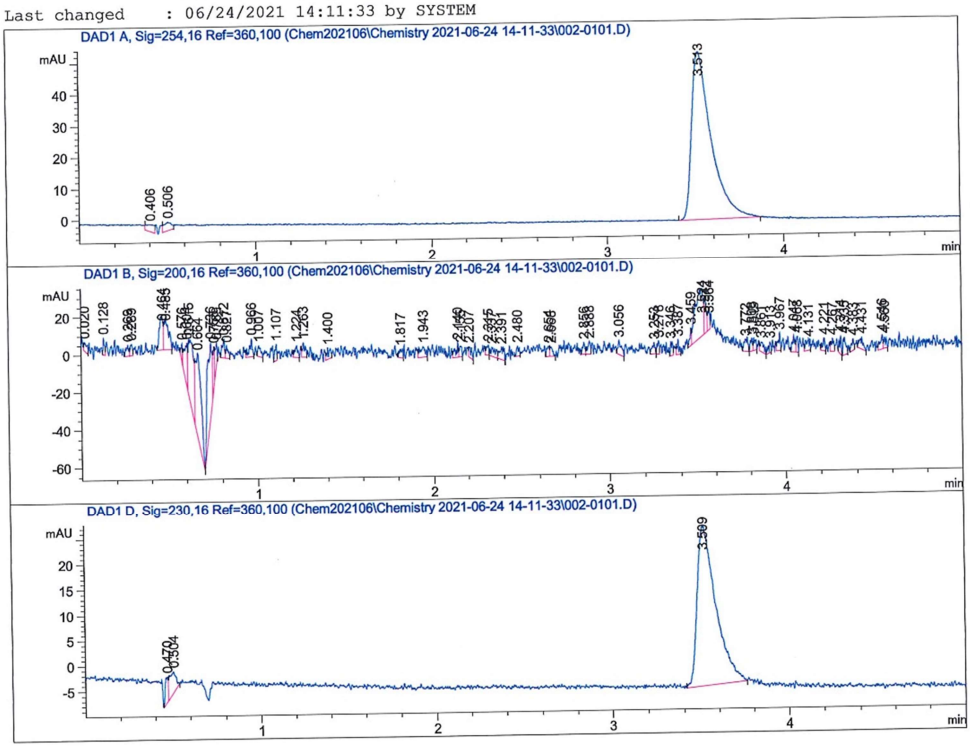


Area Percent Report

Sorted By : Signal
Multiplier : 1.0000
Dilution : 1.0000
Use Multiplier & Dilution Factor with ISTDs

Signal 1: DAD1 A, Sig=254,16 Ref=360,100



**Figure 6.8 Analytical SFC spectrum for (*S*)- SCQ1**

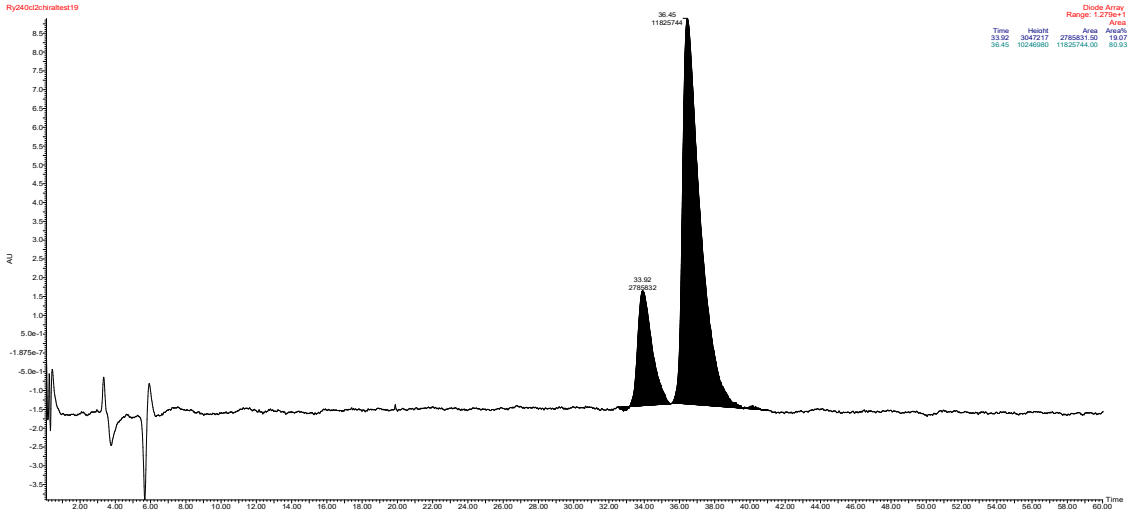


**Figure 6.9 Chiral resolution employing D-tartaric acid to separate compound 3.83**

*5-HTR Pharmacology*. The compounds were characterized functionally at stable 5-$HT_{2A}$- and 5-$HT_{2C}$-HEK293 cell lines in the $Ca^{2+}$/Fluo-4 assay and at a stable 5-$HT_{1B}$/GIRK2-HEK293 cell line in the essentially as previously described.[102,103] The testing of (*S*)-SCQ1 in various radio ligand binding assays and at a 5-HT2B-CHO cell line in an IP1 assay were carried out by Eurofins.

*$Ca^{2+}$/Fluo-4 Assay*. The 5-$HT_{2A}$- and 5-$HT_{2C}$-HEK293 cells[104] were cultured a humidified atmosphere at 37 ºC and 5% $CO_2$ in Dulbeccos Modified Eagle Medium (DMEM) supplemented with penicillin (100 U/mL), streptomycin (100 µg/mL), 5% dialyzed fetal bovine serum and 1 mg/mL G-418. The day before the assay, the cells were split into poly-D-lysine-coated black 96-well plates with clear bottom (6 x $10^4$ cells/well). The following day the culture medium was aspirated and the cells were incubated in 50 µL assay buffer [HBSS containing 20 mM HEPES, 1 mM $CaCl_2$, 1 mM $MgCl_2$ and 2.5 mM probenecid, pH 7.4] supplemented with 6 mM Fluo–4/AM at 37 °C for 1 h. Then the buffer was aspirated, the cells were washed once with 100 µL assay buffer, and then 100 µL assay buffer was added to the cells (in the antagonist experiments the test compound was added at this point). The 96-well plate was assayed in a FLEXStation$^3$ (Molecular Devices) measuring emission [in fluorescence units (FU)] at 525 nm caused by excitation at 485 nm before and up to 90 s after addition of 33.3 µL agonist solution in assay buffer.

*FLIPR® Membrane Potential Blue (FMP) Assay.* 5-$HT_{1B}$/GIRK2-HEK293 cell[103] were cultured in DMEM supplemented with penicillin (100 U/mL), streptomycin (100 µg/mL), 5% dialyzed fetal bovine serum, 1 mg/mL G-418 and 300 µg/mL hygromycin B. The day before the assay, the cell lines were split into poly-D-lysine-coated black 96-well plates (6 x $10^4$ cells/well) with clear bottom in culture medium supplemented with the appropriate combination of antibiotics. 16-24 h later, the culture medium was aspirated, and the cells were washed once with 100 µL assay buffer (132 mM NaCl, 1 mM KCl, 1 mM $CaCl_2$, 1 mM $MgCl_2$, 11 mM HEPES, 10 mM D-Glucose, pH 7.4 with NaOH). 100 µL assay buffer supplemented with FMP dye (0.5 mg/ml) was added to each well (in the antagonist experiments, the antagonist was added to this buffer), after which the cells were incubated at 37 °C for 40 min. The plate was assayed in a FLEXStation$^3$ Benchtop Multi-Mode Microplate Reader (Molecular Devices), where fluorescence levels in the wells were recorded continuously from 20 s before to 70 s after the addition of agonist using excitation and emission wavelengths of 525 nm and 565 nm.

*Data analysis.* The data analysis was performed in GraphPad Prism 8.0 (GraphPad Software, Inc.). Concentration-response and concentration-inhibition curves were fitted to nonlinear regression curves fit with variable slopes: *$Y = Bottom + (Top-Bottom)/(1+10^{\wedge}((LogEC_{50}-X)*n_H))$* and *$Y = Bottom + (Top - Bottom)/(1+10^{\wedge}((LogIC_{50}-X)*n_H)$*, respectively, where Y is the response, Top and Bottom values are plateaus in the units of the response axis, X is the test compound concentration, $EC_{50}$ is the test compound concentration that yields a response half way between Bottom and Top, $IC_{50}$ is the test compound concentration yielding inhibition to a response half way between Bottom and Top, and $n_H$ is the Hill slope.

*[$^3$H]epibatidine competitive binding assay.* The compounds were tested for binding at the human α4β2 and the rat α3β4 nAChR in a competition [$^3$H]epibatidine binding assay performed essentially as previously described.[105] Membranes were prepared from α4β2- or α3β4-expressing HEK293 cell lines[106] by harvesting at 90% confluency and homogenization for 10 s using an Ultra-Turrax homogenizer (IKA-Labortechnik, Staufen, Germany) in 30 mL of ice-cold assay buffer (140 mM NaCl, 1.5 mM KCl, 2 mM $CaCl_2$, 1 mM $MgCl_2$, 25 mM HEPES, pH 7.4). After centrifugation at 50,000 x g at 4 °C for 30 min, the supernatant was discarded. The protein pellet was resuspended in 30 mL of ice-cold assay buffer and homogenized for another 10 s. After centrifugation at 50,000 x g at 4 °C for 30 min, the supernatant was discarded again, and the membrane protein pellet was stored at -80 °C. One the assay day, the frozen membrane protein pellet was resuspended by the appropriate volume ice-cold assay buffer and homogenized for 10 seconds. The protein concentration was quantified by the Bradford assay (Bio-Rad, Hercules, CA).

For compound testing on α4β2, 4.5-5 µg of membrane proteins were incubated with ~30 pM [$^3$H]epibatidine (55 Ci/mmol, PerkinElmer, Waltham, MA) in the absence of test compound, or the presence of a test compound (in an assay concentration of 5 µM or 10 µM) or 100 µM nicotine (St. Louis, MO) in a total volume of 2 mL in assay buffer. For screening on α3β4 nAChR, 1.17-3.7 µg of membrane proteins were incubated with 300 pM [$^3$H]epibatidine in the absence of test compound, or the presence of a test compound (in an assay concentration of 5 µM or 10 µM) or 100 µM nicotine (St. Louis, MO in a total volume of 1 mL in assay buffer. The incubation was performed at room temperature while shaking for 2.5 hours. Whatman GF/C filters (PerkinElmer) were prepared by pre-soaking with 0.2% polyethyleneimine for 30 min. The reaction mixtures were harvested using a Brandell M-48T cell harvester (Alpha Biotech, London, UK), followed by 3 times of washing with 5 ml ice-cold washing buffer (0.9% NaCl, 10 mM Tris-HCl, pH 7.4). Filters were then transferred to scintillation vials containing 3 ml OptiFluor$^{TM}$ (PerkinElmer), and the radioactivity was measured by liquid scintillation counting using a Tri-Carb® 4910 TR (PerkinElmer). The bound/free ratios of [$^3$H]epibatidine in all reactions were confirmed to be around or less than 10%.

*Cell maintenance and transfection (DRD1 and DRD2 assays).* HEK 293T cells were maintained in Dulbecco's Modified Eagle Medium (DMEM) supplemented with 10% (v/v) fetal bovine serum (FBS), 100 U/mL penicillin and 100 µg/mL streptomycin and incubated at 37 °C and 5% $CO_2$ in a humidified incubator. HTLA cells (A HEK-293 cell line stably expressing a tTA-dependent luciferase reporter and a $\beta$-arrestin2-TEV fusion gene) were maintained in Dulbecco modified Eagle medium (DMEM) supplemented with 10% (v/v) fetal bovine serum (FBS), 100 U/mL penicillin, 100 µg/mL streptomycin, 100 µg/mL hygromycin and 2 µg/mL puromycin and incubated at 37 °C and 5% $CO_2$ in a humidified incubator. Before experiments, cells were plated onto 15 cm culture dishes, and the day after transfected at approximately 50% confluency, with 10 µg either dopamine receptor $D_1$ (DRD1) in PcDNA3.1 vector (cDNA.org) (HEK 293T cells) or dopamine receptor $D_2$ (DRD2)-Tango (from Brian Roth, Addgene plasmid # 66269; http://n2t.hnet/addgene:66269; RRID:Addgene_66269) (HTLA cells) using polyethylenimine. After approximately 48 hours, the cells were used for experiments or frozen in FBS with 10% DMSO for later use in experiments.

*cAMP assay.* To determine the compound's ability to activate or inhibit the $G_s$-coupled DRD1, cyclic adenosine monophosphate (cAMP) concentration was determined using HEK 293T cells transiently transfected with DRD1. The determination of intracellular cAMP was obtained using a time-resolved Förster resonance energy transfer (FRET)-based detection kit (CisBio, PerkinElmer) according to manufacturer's protocol. 10,000 cells/well in Hank's balanced salt solution supplemented with 20 mM HEPES, 1 mM $MgCl_2$ and 1 mM $CaCl_2$, pH 7.4 (HBSS) were added in a 384 well low-volume white microplate (GR-784075, Greiner). To test for agonist-activity, 10 µM concentrations of compounds in HBSS were added, followed by a 45-minute incubation at room temperature. To test for antagonist-activity, cells were pre-incubated with compounds at 10 µM concentration in HBSS for 30 minutes at room temperature, followed by a further 45-minute incubation at room temperature with 36 nM ($EC_{80}$) of dopamine in HBSS added to the wells. Reactions were stopped according to manufacturer's instructions, and fluorescence was measured by an Envision plate reader (PerkinElmer), using a time resolved fluorescence protocol that measures light emission at 620 and 665 nm. The results were analyzed using GraphPad Prism (version 9).

*PRESTO-Tango assay*. To determine the compound's ability to activate or inhibit the DRD2, $\beta$-arrestin2-mediated luminescence from luciferase was determined using HTLA cells transiently transfected with DRD2-tango. The assay was adopted from Kroeze, *et al.* (2015)[104] with minor changes. 25,000 cells/well in DMEM supplemented with 1% dialyzed FBS, 100 U/mL penicillin and 100 µg/mL streptomycin, were added in a 384-well flat clear bottom white polystyrene microplate (Corning). To test for agonist activity, 10 µM concentrations of compounds were added, followed by a 40-hour incubation at 37 °C and 5% $CO_2$ in a humidified incubator. To test for antagonist activity, cells were pre-incubated with 10 µM concentrations of compounds for 30 minutes at 37 °C and 5% $CO_2$ in a humidified incubator, followed by a further 40-hour incubation at room temperature with 32 nM ($EC_{80}$) of quinpirole added to the wells. Lastly, BrightGlo (Promega) was added according to manufacturer's instructions. The reaction was incubated for 15 minutes at room temperature, and luminescence was measured by an Enspire instrument at 384 nm. Results were analyzed using GraphPad Prism (version 9).

## General directions

All reactions were run under a $N_2$ atmosphere and were monitored by thin layer chromatography (TLC) and/or reversed-phase ultra-performance liquid chromatography mass spectrometry (RP-UPLC-MS). Commercially available reagents were used without further purification, all solvents were of HPLC quality and dry solvents were obtained from a PureSolv system.

Analytical TLC was conducted on Merck aluminium sheets covered with silica (C60). The plates were either visualized under UV-light or stained by dipping in a developing agent followed by heating. $KMnO_4$ [$KMnO_4$ (3 g) in water (300 mL), $K_2CO_3$ (20 g) and 5% aqueous NaOH (5 mL)] were used as developing agents. Flash column chromatography was performed using Merck Geduran® Si 60 (40-63 µm) silica gel.

All new compounds were characterized by NMR, MS (ESI) and HRMS (ESI) (byproducts were not fully characterized). For the recording of $^1$H NMR and $^{13}$C NMR a Bruker Ascend with a Prodigy cryoprobe (operating at 400 MHz or 800 MHz for proton and 100 MHz or 200 MHz for carbon) were used. The chemical shifts (δ) are reported in parts per million (ppm) and the coupling constants (J) in Hz. Spectra were referenced using the residual solvent peaks of the respective solvent; DMSO-$d_6$ (δ 2.50 ppm for $^1$H NMR and δ 40.0 ppm for $^{13}$C NMR), $CDCl_3$ (δ 7.26 ppm for $^1$H NMR and δ 77.16 ppm for $^{13}$C NMR), $CD_3OD$ (δ 3.31 ppm for $^1$H NMR and δ 49.00 ppm for $^{13}$C NMR), $D_2O$ (δ 4.79 ppm for $^1$H NMR).The following abbreviations were used to report peak multiplicities: s = singlet, d = doublet, t = triplet, q = quartet, dd = doublet of doublets, m = multiplet, br = broad singlet.

Analytical RP-UPLC-MS (ESI) analysis was performed on a S2 Waters AQUITY RP-UPLC system equipped with a diode array detector using an Thermo Accucore C18 column (d 2.6 µm, 2.1 x 50 mm; column temp: 50 °C; flow: 1.0 mL/min). Eluents A (0.1% $HCO_2H$ in $H_2O$) and B (0.1% $HCO_2H$ in MeCN) were used in a linear gradient (5% B to 100% B) in 2.4 min and then held for 0.1 min at 100% B (total run time: 2.6 min). The LC system was coupled to a SQD mass spectrometer.

Preparative RP-HPLC was carried out on a Waters Alliance reversed-phase HPLC system consisting of a Waters 2545 Binary Gradient Module equipped with an xBridge BEH C18 OBD Prep Column (130 A, 5 µm, 30 x 150 mm) operating at 20 °C and a flow rate of 20 mL/min, a Waters Photodiode Array Detector (detecting at 210-600 nm), a Waters UV Fraction Manager, and a Waters 2767 Sample Manager. Eluents A1 (0.1% $HCO_2H$ in $H_2O$) and B1 (0.1% $HCO_2H$ in MeCN) were used. Analytical LC-HRMS (ESI) analysis was performed on a Waters Alliance 2695 system. Samples were injected directly and the LC system was coupled to a Waters LCT Premier XE Micromass equipped with a Lock Mass probe operating in positive electrospray mode. Eluents A (0.1%$HCO_2H$ in $H_2O$) and B (0.1% $HCO_2H$ in MeCN) were used in a 1:1 ratio for a total run time of 2 min.

Analytical SFC was conducted on an Aurora Fusion A5/Agilent SFC system operating at 4 mL/min at 40 °C and 150 bar back pressure. The column was an Diacel AD-Chiralpak 3µ, (150 × 4.6 mm). The eluent was $CO_2$ (80%) and 96% ethanol + 0.1% diethylamine (20%).

Preparative SFC was performed on a Shimadzu Nexera Prep system operating at 60 mL/min at 40 °C and 100 bar backpressure using stacked injections. The column was a Diacel AD Chiralpak 5µ (250 × 20 mm). The eluent was $CO_2$ (80%) and 96% ethanol + 0.1% diethylamine (20%). UV detection was performed at 254 nM.

Optical rotation was carried out using a Perkin-Elmer polarimeter 341. The temperature for all recordings was approximately 20 °C.

**General procedure I**

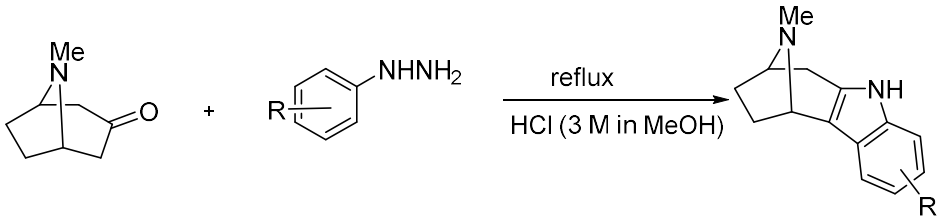


To a solution of phenylhydrazines (0.6 mmol, 1.2 equiv) in 6 mL HCl (3 M in MeOH) was added tropinone (69.6 mg, 0.5 mmol), the mixture was refluxed overnight under $N_2$. The resulting residue was quenched by $NaHCO_3$ (20 mL), DCM (10 mL) was added, the two layers were separated, the aqueous phase was extracted with DCM (10 mL), the combined organic phase was dried over anhydrous $Na_2SO_4$, and concentrated *in vacuo*. The crude was purified by flash column chromatography on silica gel (DCM: MeOH: $Et_3N$ = 100:5:1 to 100:10:1) to afford the product as a solid.

**(10*S**)-11-methyl-5,6,7,8,9,10-hexahydro-7,10-epiminocyclohepta[b]indole 3.08**

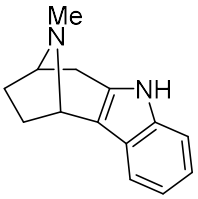


18 hours, yellow solid (49.0 mg, 46%).

$^1$H NMR (400 MHz, $CDCl_3$) δ 8.05 (bs, 1H), 7.47 (dd, *J* = 7.0, 1.8 Hz, 1H), 7.33 – 7.28 (m, 1H), 7.15 – 7.04 (m, 2H), 4.24 (d, *J* = 4.7 Hz, 1H), 3.67 – 3.51 (m, 1H), 3.23 (dd, *J* = 16.4, 4.4 Hz, 1H), 2.40 (s, 3H), 2.37 – 2.25 (m, 3H), 1.94 (t, *J* = 9.2 Hz, 1H), 1.63 – 1.49 (m, 1H); $^{13}$C NMR (101 MHz, $CDCl_3$) δ 136.18, 129.24, 125.91, 121.29, 119.57, 117.41, 112.96, 111.03, 58.04, 58.00, 35.66, 35.08, 29.49, 28.77.

HRMS (ESI+) m/z found 213.1386 [M+H]+, $C_{14}H_{17}N_2$ calculated 213.1392 (Δ = -2.8 ppm).

**(10*S**)-11-methyl-5,6,7,8,9,10-hexahydro-7,10-epiminocyclohepta[b]indole 3.09**

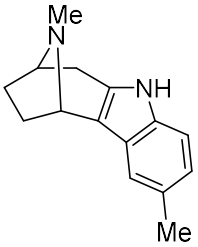


12 hours, yellow solid (42.0 mg, 37%).

$^1$H NMR (400 MHz, $CDCl_3$) δ 7.85 (s, 1H), 7.26 (d, *J* = 2.5 Hz, 1H), 7.18 (d, *J* = 8.2 Hz, 1H), 7.02 – 6.79 (m, 1H), 4.20 (d, *J* = 4.7 Hz, 1H), 3.65 – 3.52 (m, 1H), 3.21 (dd, *J* = 16.4, 4.4 Hz, 1H), 2.44 (s, 3H), 2.39 (s, 3H), 2.34 – 2.24 (m, 3H), 1.92 (t, *J* = 9.2 Hz, 1H), 1.65 – 1.47 (m, 1H); $^{13}$C NMR (101 MHz, $CDCl_3$) δ 134.31, 129.36, 128.77, 126.38, 122.67, 117.27, 112.87, 110.49, 57.60, 57.57, 46.21, 35.34, 29.87, 28.42, 21.61.

HRMS (ESI+) m/z found 227.1542 [M+H]+, $C_{15}H_{19}N_2$ calculated 227.1548 (Δ = -2.6 ppm).

**(10S*)-2-methoxy-11-methyl-5,6,7,8,9,10-hexahydro-7,10-epiminocyclohepta[b]indole 3.10**

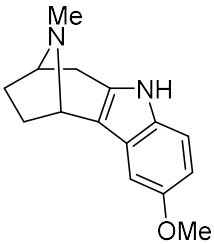


29 hours, yellow solid (16.4 mg, 14%).

$^1$H NMR (400 MHz, $CDCl_3$) δ 8.31 (s, 1H), 7.19 (d, *J* = 8.7 Hz, 1H), 6.90 (d, *J* = 2.4 Hz, 1H), 6.77 (dd, *J* = 8.7, 2.5 Hz, 1H), 4.31 (d, *J* = 4.9 Hz, 1H), 3.84 (s, 3H), 3.26 (dd, *J* = 16.8, 4.4 Hz, 1H), 2.57 – 2.20 (m, 6H), 2.07 – 1.85 (m, 1H), 1.71 – 1.57 (m, 1H); $^{13}$C NMR (101 MHz, $CDCl_3$) δ 154.20, 131.25, 129.81, 126.08, 112.32, 111.68, 111.15, 99.65, 77.48, 58.19, 56.04, 35.46, 34.88, 29.26, 28.77.

HRMS (ESI+) m/z found 243.1494 [M+H]+, $C_{15}H_{19}N_2O$ calculated 243.1497 (Δ = -1.2 ppm).

**(10*S**)-2-fluoro-5,6,7,8,9,10-hexahydro-7,10-epiminocyclohepta[b]indole 3.11**

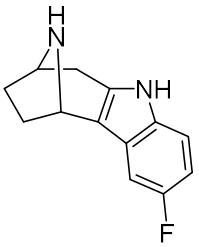

N-Boc-nortropinone (225.3 mg, 1.0 mmol) was reacted with 4-Fluorophenylhydrazine hydrochloride (194.4 mg, 1.2 mmol) at reflux in 10 mL HCl (4-5 M in isopropanol) for 17.5 hours to give a yellow solid (105.9 mg, 42%).

$^1$H NMR (400 MHz, DMSO-$d_6$) δ 10.84 (s, 1H), 7.42 – 7.06 (m, 2H), 6.87 – 6.54 (m, 1H), 4.38 (d, $J$ = 4.9 Hz, 1H), 3.85 (dd, $J$ = 7.4, 4.4 Hz, 1H), 3.10 (dd, $J$ = 16.2, 4.5 Hz, 1H), 2.44 (d, $J$ = 16.2 Hz, 1H), 2.05 – 1.86 (m, 2H), 1.83 – 1.73 (m, 1H), 1.47 (ddd, $J$ = 11.4, 7.8, 5.9 Hz, 1H); $^{13}$C NMR (101 MHz, DMSO-$d_6$) δ 157.23 (d, $J$ = 230.2 Hz), 133.94, 132.59, 125.17 (d, $J$ = 10.1 Hz), 116.85 (d, $J$ = 4.5 Hz), 111.92 (d, $J$ = 9.9 Hz), 107.82 (d, $J$ = 25.7 Hz), 102.12 (d, $J$ = 23.2 Hz), 52.80, 51.54, 37.03, 33.96, 29.75.

$^{19}$F NMR (377 MHz, $CDCl_3$) δ -125.7

HRMS (ESI+) m/z found 217.1140 [M+H]+, $C_{13}H_{14}FN_2$ calculated 217.1141(Δ = -0.46 ppm).

## General procedure II

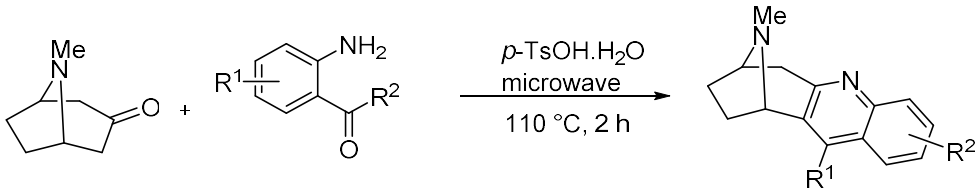


To a 0.5 – 2.0 mL Biotage microwave vial charged a magnetic stirring bar was added tropinone (42.8 mg, 0.3 mmol), amino-benzophenone or amino-acetonephenone (0.45 mol 1.5 equiv.), and $p$-TsOH.$H_2O$ (0.33 mol 1.1 equiv.).The vial was heated at 110 °C via microwave irradiation for 2 hours. After cooling to room temperature, the resulting residue was dissolved in DCM and washed with saturated $NaHCO_3$ twice, the collected organic layer was dried over anhydrous $Na_2SO_4$, and concentrated under reduced pressure. The crude was further purified by flash column chromatography on silica gel (DCM:MeOH = 100:1 to 5:1) to deliver a solid product.

**(10*S**)-12-methyl-11-phenyl-7,8,9,10-tetrahydro-6H-7,10-epiminocyclohepta[b]quinoline 3.12**

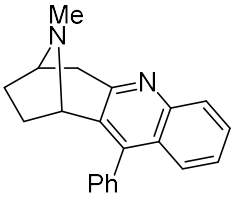

Yellow solid (43.0 mg, 48%).

$^1$H NMR (400 MHz, $CDCl_3$) δ 8.01 (dd, $J$ = 8.5, 1.0 Hz, 1H), 7.61 (td, $J$ = 5.1, 2.4 Hz, 1H), 7.57 – 7.46 (m, 3H), 7.34 (dd, $J$ = 4.2, 1.4 Hz, 2H), 7.29 (dd, $J$ = 7.0, 1.8 Hz, 1H), 7.24 – 7.21 (m, 1H), 3.89 (d, $J$ = 6.0 Hz, 1H), 3.68 – 3.52 (m, 2H), 2.91 (d, $J$ = 17.8 Hz, 1H), 2.36 (s, 3H), 2.33 – 2.16 (m, 2H), 1.83 – 1.69 (m, 2H); $^{13}$C NMR (101 MHz, $CDCl_3$) δ 155.91, 146.91, 144.10, 135.98, 132.28, 129.77, 129.47, 128.76, 128.62, 128.57, 128.10, 126.84, 126.24, 125.79, 60.97, 58.94, 38.59, 37.22, 34.05, 29.29.

HRMS (ESI+) m/z found 301.1698 [M+H]+, $C_{21}H_{21}N_2$ calculated 301.1705 (Δ = -2.3 ppm).

**(10*S**)-11,12-dimethyl-7,8,9,10-tetrahydro-6H-7,10-epiminocyclohepta[b]quinoline 3.13**

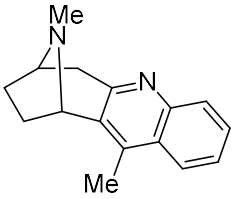

Yellow solid. (14.5 mg. 21%).

$^1$H NMR (400 MHz, $CDCl_3$) δ 8.00 – 7.93 (m, 2H), 7.66 – 7.59 (m, 1H), 7.52 – 7.45 (m, 1H), 4.42 (d, *J* = 6.2 Hz, 1H), 3.70 – 3.62 (m, 1H), 3.58 – 3.48 (m, 1H), 2.79 (d, *J* = 17.9 Hz, 1H), 2.60 (d, *J* = 0.8 Hz, 3H), 2.45 (d, *J* = 0.8 Hz, 3H), 2.43 – 2.27 (m, 2H), 1.77 – 1.60 (m, 2H); $^{13}$C NMR (101 MHz, $CDCl_3$) δ 155.42, 146.62, 138.64, 132.66, 129.17, 128.54, 127.17, 125.66, 123.67, 60.69, 58.53, 38.54, 37.38, 33.18, 29.22, 12.93.

HRMS (ESI+) m/z found 239.1542 [M+H]+, $C_{16}H_{19}N_2$ calculated 239.1548 (Δ = -2.5 ppm).

**(10*S**)-1-chloro-12-methyl-11-phenyl-7,8,9,10-tetrahydro-6H-7,10-epiminocyclohepta[b]quinoline 3.14**

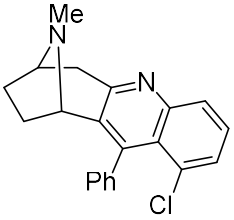

Yellow solid (55.0 mg. 55%).

$^1$H NMR (400 MHz, $CDCl_3$) δ 7.94 (d, *J* = 8.9 Hz, 1H), 7.59 – 7.48 (m, 4H), 7.30 (d, *J* = 2.4 Hz, 1H), 7.28 – 7.25 (m, 1H), 7.22 – 7.18 (m, 1H), 3.88 (d, *J* = 5.8 Hz, 1H), 3.64 (t, *J* = 6.0 Hz, 1H), 3.60 – 3.48 (m, 1H), 2.89 (d, *J* = 18.0 Hz, 1H), 2.36 (s, 3H), 2.31 – 2.15 (m, 2H), 1.84 – 1.68 (m, 2H); $^{13}$C NMR (101 MHz, $CDCl_3$) δ 156.29, 145.31, 143.28, 135.20, 131.66, 130.23, 129.68, 129.36, 129.01, 128.85, 128.45, 127.58, 125.03, 61.08, 59.02, 38.72, 37.37, 33.89, 29.19.

HRMS (ESI+) m/z found 335.1310 [M+H]+, $C_{21}H_{20}ClN_2$ calculated 335.1315 (Δ = -1.5 ppm).

**(10S*)-3-fluoro-12-methyl-11-phenyl-7,8,9,10-tetrahydro-6H-7,10-epiminocyclohepta[b] quinoline 3.15**

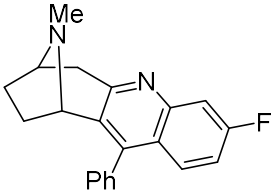

Yellow solid (48.9 mg, 49%).

$^1$H NMR (400 MHz, $CDCl_3$) δ 8.01 (d, *J* = 8.4 Hz, 1H), 7.66 – 7.59 (m, 1H), 7.38 – 7.29 (m, 2H), 7.28 – 7.16 (m, 4H), 3.91 (d, *J* = 5.6 Hz, 1H), 3.68 (t, *J* = 5.9 Hz, 1H), 3.63 – 3.51 (m, 1H), 2.93 (d, *J* = 18.1 Hz, 1H), 2.38 (s, 3H), 2.32 – 2.17 (m, 2H), 1.87 – 1.64 (m, 2H); $^{13}$C NMR (101 MHz, $CDCl_3$) δ 162.64 (d, *J* = 247.7 Hz), 155.52, 146.97, 143.15, 132.09, 131.61 (d, *J* = 3.6 Hz), 131.39 (d, *J* = 8.1 Hz), 131.20 (d, *J* = 8.0 Hz), 128.99, 128.69, 126.81, 126.05, 125.99, 116.03 (d, *J* = 20.1 Hz), 115.81 (d, *J* = 20.0 Hz), 61.06, 59.05, 38.55, 37.13, 33.90, 29.13.

$^{19}$F NMR (377 MHz, $CDCl_3$) δ -113.2;

HRMS (ESI+) m/z found 319.1604 [M+H]+, $C_{21}H_{20}FN_2$ calculated 319.1611 (Δ = -2.2 ppm).

**(10S*)-2-chloro-11-(2-fluorophenyl)-12-methyl-7,8,9,10-tetrahydro-6H-7,10-epiminocyclohepta[b]quinoline 3.16**

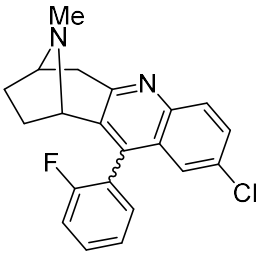

Yellow solid (47.0 mg, 46%).

$^1$H NMR (400 MHz, $CDCl_3$) δ major isomer 7.94 (d, *J* = 8.9 Hz, 1H), 7.59 – 7.48 (m, 2H), 7.37 – 7.30 (m, 1H), 7.29 – 7.25 (m, 1H), 7.25 – 7.14 (m, 2H), 2.91 (d, *J* = 18.1 Hz, 1H), 2.36 (s, 3H), 2.31 – 2.11 (m, 2H), 1.91– 1.66 (m, 2H); minor isomer 7.95 (d, *J* = 8.9 Hz, 1H),7.59 – 7.48 (m, 2H), 7.37 – 7.30 (m, 1H), 7.29 – 7.25 (m, 1H), 7.25 – 7.14 (m, 2H), 2.87 (d, *J* = 18.1 Hz, 1H), 2.40 (s, 3H), 2.31 – 2.11 (m, 2H),

1.91– 1.66 (m, 2H). $^{13}$C NMR (101 MHz, $CDCl_3$) δ major isomer 160.16 (d, *J* = 246.7 Hz), 156.18, 145.26, 137.39, 133.94, 132.02, 131.25 (d, *J* = 3.2 Hz), 130.96 (d, *J* = 7.9 Hz), 130.36, 129.89, 127.41, 124.82 (d, *J* = 3.6 Hz), 124.42, 122.50 (d, *J* = 17.6 Hz), 116.35 (d, *J* = 21.7 Hz), 61.35, 58.91, 38.64, 37.32, 32.52 (d, *J* = 2.6 Hz), 29.24; minor isomer δ 159.14 (d, *J* = 247.2 Hz), 156.03, 131.70 (d, *J* = 3.1 Hz), 130.99 (d, *J* = 7.9 Hz), 130.40, 129.94, 127.41124.73 (d, *J* = 3.7 Hz), 124.32, 122.42 (d, *J* = 17.3 Hz), 116.49 (d, *J* = 21.5 Hz), 61.09, 58.30, 37.27, 36.01, 34.06, 29.64.

$^{19}$F NMR (377 MHz, $CDCl_3$) δ -112.7.

HRMS (ESI+) m/z found 353.1216 [M+H]+, $C_{21}H_{19}FClN_2$ calculated 353.1221 (Δ = -1.4 ppm).

## General procedure III

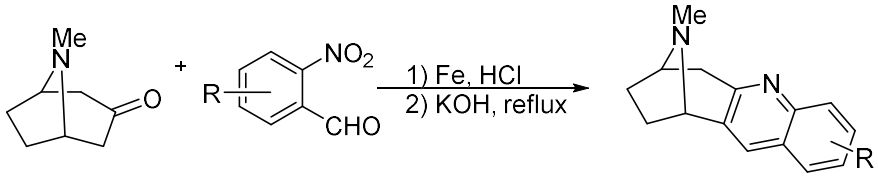


To a solution of nitrobenzaldehyde (1.0 mmol, 1.0 equiv) in EtOH (4 mL) was added Fe (560 mg, 10.0 equiv) and Con. HCl (3 drops), the mixture was refluxed for 1 hour. The brown precipitate was filtered off through a celite plug, KOH (112.0 mg, 2.0 mmol) and tropinone (68.8 mg, 0.5 mmol) dissolved in EtOH (5 mL) were added into the filtrate, the resulting solution was heated at reflux for 4-5 hours. The crude was quenched by saturated $NaHCO_3$ (20 mL). The resulting solution was extracted with EtOAc (2×20 mL), the combined organic phase was dried over anhydrous $Na_2SO_4$, the solvent was removed under reduced pressure, further purification was performed by flash column chromatography on silica gel (EtOAc: MeOH = 100:5 to 100:10) to afford the final product.

**(10S*)-2,3-dimethoxy-12-methyl-7,8,9,10-tetrahydro-6H-7,10-epiminocyclohepta[b]quinoline 3.17**

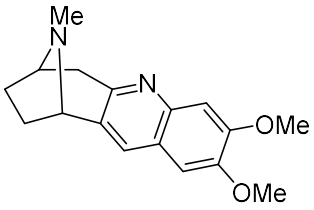


5 hours, pale white solid (108.4 mg, 76%).

$^1$H NMR (400 MHz, $CDCl_3$) δ 7.57 (s, 1H), 7.31 (s, 1H), 6.96 (s, 1H), 4.08 (d, *J* = 6.2 Hz, 1H), 3.97 (d, *J* = 4.3 Hz, 6H), 3.71 – 3.63 (m, 1H), 3.50 – 3.36 (m, 1H), 2.83 – 2.67 (m, 1H), 2.48 – 2.26 (m, 5H), 1.83 – 1.74 (m, 1H), 1.74 – 1.62 (m, 1H); $^{13}$C NMR (101 MHz, $CDCl_3$) δ 152.76, 152.22, 149.52, 144.34, 132.11, 131.18, 122.64, 107.39, 104.88, 63.73, 58.76, 56.20, 56.14, 37.14, 36.45, 34.57, 29.24.

HRMS (ESI+) m/z found 285.1599 [M+H]+, $C_{17}H_{21}N_2O_2$ calculated 285.1603 (Δ = -1.4 ppm).

**(10S*)-3-fluoro-12-methyl-7,8,9,10-tetrahydro-6H-7,10-epiminocyclohepta[b]quinoline 3.18**

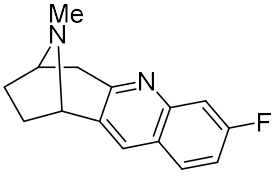


5 hours, pale yellow solid 5 hours (48. 7 mg, 40%).

$^1$H NMR (400 MHz, $CDCl_3$) δ 8.03 – 7.91 (m, 1H), 7.71 (s, 1H), 7.46 – 7.39 (m, 1H), 7.38 – 7.32 (m, 1H), 4.22 (d, *J* = 6.3 Hz, 1H), 3.77 (t, *J* = 6.2 Hz, 1H), 3.55 – 3.45 (m, 1H), 2.88 (d, *J* = 18.2 Hz, 1H), 2.51 (s, 4H), 2.40 (q, *J* = 11.7, 10.7 Hz, 1H), 1.89 – 1.67 (m, 2H); $^{13}$C NMR (101 MHz, $CDCl_3$) δ 160.42 (d, *J* = 247.5 Hz), 154.61, 152.71, 144.69, 132.10 (d, *J* = 4.8 Hz), 131.07 (d, *J* = 9.2 Hz), 127.88 (d, *J* = 9.9 Hz), 119.49 (d, *J* = 25.7 Hz), 110.42 (d, *J* = 21.6 Hz), 63.91, 58.92, 37.37, 36.44, 34.26, 29.12.

$^{19}$F NMR (377 MHz, $CDCl_3$) δ -114.2

HRMS (ESI+) m/z found 243.1304 [M+H]+, $C_{15}H_{16}FN_2$ calculated 243.1298 (Δ = 2.5 ppm).

**(10S*)-2,3-dimethoxy-7,8,9,10-tetrahydro-6H-7,10-epiminocyclohepta[b]quinoline hydrochloride 3.19**

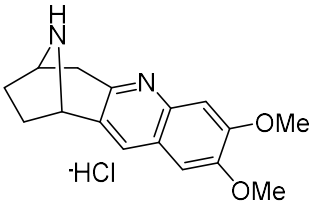


*N*-Boc-nortropinone (112.6 mg,0.5 mmol) was reacted with prepared aldehyde (1.0 mol, 2.0 equiv) for 6 hours according to general procedure III to give a yellow solid (170.0 mg), the resulting yellow solid (37.0 mg) was dissolved in 2 mL HCl (3 M in MeOH) and stirred at room temperature for 1 hour to yield a white solid (30.6 mg, 92 % for 2 steps).

$^1$H NMR (400 MHz, $D_2O$) δ 8.69 (s, 1H), 7.52 (s, 1H), 7.35 (s, 1H), 5.33 (d, *J* = 4.9 Hz, 1H), 4.69 (d, *J* = 6.0 Hz, 1H), 4.05 (s, 3H), 3.99 (s, 3H), 3.90 (dd, *J* = 19.3, 5.1 Hz, 1H), 3.53 (d, *J* = 19.2 Hz, 1H), 2.65 – 2.43 (m, 2H), 2.33 (t, *J* = 10.3 Hz, 1H), 2.19 – 1.97 (m, 1H); $^{13}$C NMR (101 MHz, $D_2O$) δ 156.85, 151.32, 144.83, 140.62, 136.66, 127.66, 124.46, 106.33, 98.67, 56.77, 56.51, 56.30, 53.19, 33.87, 32.90, 26.38.

HRMS (ESI+) m/z found [M+H]+ 271.1448; $C_{16}H_{19}N_2O_2$ calculated 271.1447 (Δ = 0.37 ppm).

**Synthesis of α-bromo ketone 3.20**

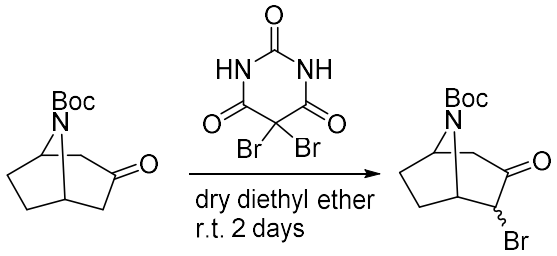


To a solution of N-Boc-nortropinone (2.3 g, 10.0 mmol) in dry diethyl, ether (20 mL) was added dibromo-barbituric acid (1.6 g, 5.5 mmol). The mixture was stirred at room temperature under $N_2$, a white precipitate was formed after 12 hours, the mixture continued to be stirred for 36 hours. The precipitate was filtered off, washing with dry diethyl ether. The filtrate was concentrated under reduced pressure, the crude was purified by column chromatography on silica gel (hexane: ethyl acetate = 10:1 to 6:1) to yield a white solid. The resulting residue still contained unreacted *N*-Boc-nortropinone and was thus further purified by recrystallization with hexane to yield a colorless crystal (1.5 g, 50%). $^1$H NMR (400 MHz, $CDCl_3$) δ 4.92 – 4.48 (m, 2H), 4.06 (s, 1H), 3.48 – 3.16 (m, 1H), 2.40 – 2.15 (m, 1H), 2.15 – 1.96 (m, 1H), 1.78 – 1.66 (m, 1H), 1.65 – 1.57 (m, 1H), 1.51 (s, 9H); $^{13}$C NMR (101 MHz, $CDCl_3$) δ 201.70, 80.68, 58.05, 52.84, 52.37, 52.37, 44.47, 28.51, 27.96, 27.95.

**Synthesis of β-ketoester 3.21**

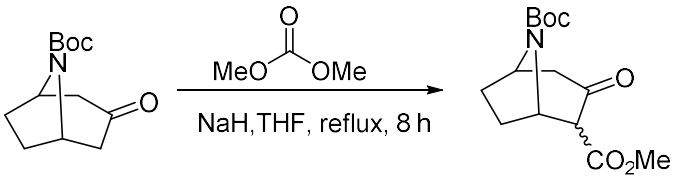


A 50 mL round bottom flask with oven-dried, *N*-Boc-nortropinone (450.6 mg, 2.0 mmol) was dissolved in dry THF (20 mL), NaH (60 wt% in mineral oil, 400.0 mg, 10.0 mmol) was slowly added at 0 °C. Dimethyl carbonate (540.2 mg, 6.0 mmol) was added to the solution, and the mixture then was refluxed and monitored by TLC. After 8 hours, the reaction was cooled to 0 °C and quenched with saturated $NH_4Cl$ (50 mL), the mixture was added DCM (20 mL), the aqueous phase was extracted with DCM (20 mL), the combined organic phase was dried over anhydrous $Na_2SO_4$, and concentrated *in vacuo*. The crude was dried under high vacuum to give the product as a colorless oil for use without further purification (531.0 mg, 94%).

**General procedure IV**

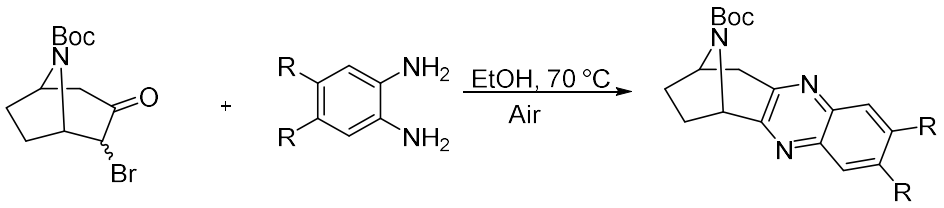


A 25 mL oven-dried two neck round flask containing a magnetic stirring bar attached a reflux condenser was placed α-bromo ketone **3.20** (151.2 mg, 0.5 mmol), 1,2-diamine (2.0 equiv, 1.0 mmol) dissolved in absolute ethanol (5 mL) was added. The mixture was saturated with air and heated to 70 °C overnight, the resulting residue was purified by column chromatography on silica gel (hexane: ethyl acetate = 5:1 to 3:1) to yield a solid compound.

***tert*-butyl (6S*)-7,8,9,10-tetrahydro-6H-6,9-epiminocyclohepta[b]quinoxaline-12-carboxylate 3.22**

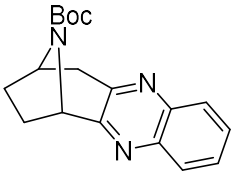


12 hours, white solid (70.0 mg, 45%)

$^1$H NMR (400 MHz, $CDCl_3$) δ 8.04 – 7.94 (m, 2H), 7.74 – 7.66 (m, 2H), 5.29 (d, $J$ = 7.0 Hz, 1H), 4.76 (s, 1H), 3.73 – 3.57 (m, 1H), 2.98 (d, $J$ = 18.0 Hz, 1H), 2.44 – 2.29 (m, 2H), 2.05 – 1.92 (m, 1H), 1.77 – 1.67 (m, 1H), 1.40 (s, 9H); $^{13}$C NMR (101 MHz, $CDCl_3$) δ 155.57, 153.79, 151.72, 141.84, 140.59, 129.68, 129.61, 128.97, 128.38, 80.54, 60.02, 52.68, 39.97, 38.87, 28.48.

HRMS (ESI+) m/z found 312.1707 [M+H]+, $C_{18}H_{22}N_3O_2$ calculated 312.1712 (Δ = -1.6 ppm).

***tert*-butyl (6S*)-2,3-dimethyl-7,8,9,10-tetrahydro-6H-6,9-epiminocyclohepta[b]quinoxaline-12-carboxylate 3.23**

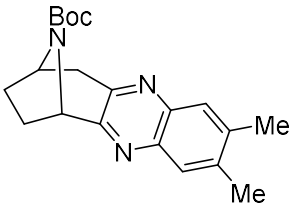


15 hours, white solid (96.6 mg, 57%)

$^1$H NMR (400 MHz, $CDCl_3$) δ 7.71 (d, *J* = 12.0 Hz, 2H), 5.24 (s, 1H), 4.73 (s, 1H), 3.60 (d, *J* = 17.3 Hz, 1H), 2.92 (d, *J* = 17.7 Hz, 1H), 2.45 (s, 6H), 2.39 – 2.22 (m, 2H), 2.01 – 1.89 (m, 1H), 1.76 – 1.64 (m, 1H), 1.39 (s, 9H); $^{13}$C NMR (101 MHz, $CDCl_3$) δ 154.53, 153.84, 150.35, 140.84, 140.05, 139.96, 139.46, 128.02, 127.49, 80.37, 59.81.52.48, 39.83, 33.89, 29.00, 28.46, 20.44, 20.43.

HRMS (ESI+) m/z found 362.1840 [M+Na]+, $C_{20}H_{26}N_3NaO_2$ calculated 362.1844 (Δ = - 1.1 ppm).

***tert*-butyl (6S*)-2,3-dichloro-7,8,9,10-tetrahydro-6H-6,9-epiminocyclohepta[b]quinoxaline-12-carboxylate 3.24**

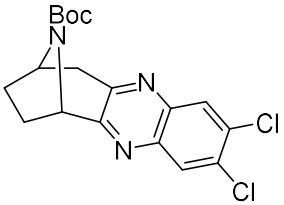


15 hours, white solid (70.0 mg, 37%).

$^1$H NMR (400 MHz, $CDCl_3$) δ 8.12 (s, 1H), 8.09 (s, 1H), 5.25 (d, *J* = 5.7 Hz, 1H), 4.75 (s, 1H), 3.60 (d, *J* = 18.0 Hz, 1H), 2.95 (d, *J* = 18.2 Hz, 1H), 2.44 – 2.29 (m, 2H), 2.00 – 1.90 (m, 1H), 1.76 – 1.67 (m, 1H), 1.41 (s, 9H); $^{13}$C NMR (101 MHz, $CDCl_3$) δ 156.78, 153.76, 153.26, 140.71, 139.39, 134.14, 134.04, 129.71, 129.20, 80.76, 59.91, 52.64, 40.02, 33.71, 29.20, 28.48.

HRMS (ESI+) m/z found 380.0931 [M+H]+, $C_{18}H_{20}Cl_2N_3O_2$ calculated 380.0933 (Δ = -0.53 ppm).

***tert*-butyl (6S*)-2,3-difluoro-7,8,9,10-tetrahydro-6H-6,9-epiminocyclohepta[b]quinoxaline-12-carboxylate 3.25**

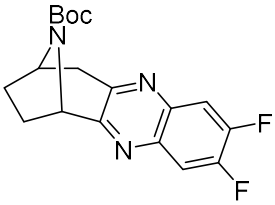


48 hours, white solid (75.4 mg, 43%).

$^1$H NMR (400 MHz, $CDCl_3$) δ 7.80 – 7.67 (m, 2H), 5.26 (d, *J* = 5.7 Hz, 1H), 4.75 (s, 1H), 3.60 (d, *J* = 17.5 Hz, 1H), 2.95 (d, *J* = 18.0 Hz, 1H), 2.44 – 2.28 (m, 2H), 2.00 – 1.92 (m, 1H), 1.77 – 1.63 (m, 1H), 1.42 (s, 9H), $^{13}$C NMR (101 MHz, $CDCl_3$) δ 155.94, 153.76, 153.40 (dd, *J* = 17.8, 7.2 Hz), 152.15, 150.84 (dd, *J* = 17.9, 7.3 Hz), 139.22 (dd, *J* = 9.8, 1.8 Hz), 114.53 (dd, *J* = 45.8, 16.0 Hz), 80.66, 59.82, 52.53, 39.86, 33.74, 29.18 28.46.

$^{19}$F NMR (377 MHz, $CDCl_3$) δ -130.56 – 130.86 (m).

HRMS (ESI+) m/z found 348.1522 [M+H]+, $C_{18}H_{20}F_2N_3O_2$ calculated 348.1524 (Δ = -0.57 ppm).

**(6S*)-7,8,9,10-tetrahydro-6H-6,9-epiminocyclohepta[b]quinoxaline hydrochloride 3.26**

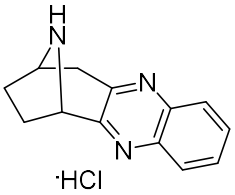


Compound **3.22** (15.6 mg, 0.05 mol) was dissolved in HCl (3 M in MeOH) and stirred at r.t. for 1 hour to yield the titled product as a brown solid (12.3mg, >95%).

$^1$H NMR (400 MHz, MeOD) δ 8.16 – 8.02 (m, 2H), 7.96 – 7.78 (m, 2H), 5.15 (d, *J* = 5.4 Hz, 1H), 4.66 (d, *J* = 6.3 Hz, 1H), 3.79 (d, *J* = 17.7 Hz, 1H), 3.39 – 3.33 (m, 1H), 2.68 – 2.47 (m, 2H), 2.39 – 2.23 (m, 1H), 2.18 – 1.98 (m, 1H); $^{13}$C NMR (101 MHz, MeOD) δ 151.64, 149.02, 142.63, 142.28, 132.52, 131.95, 130.07, 128.77, 61.50, 55.88, 38.33, 32.69, 28.06.

HRMS (ESI+) m/z found 212.1186 [M+H]+, $C_{13}H_{14}N_3$ calculated 212.1188 (Δ = -0.94 ppm).

**(6S*)-2,3-dimethyl-7,8,9,10-tetrahydro-6H-6,9-epiminocyclohepta[b]quinoxaline hydrochloride 3.27**

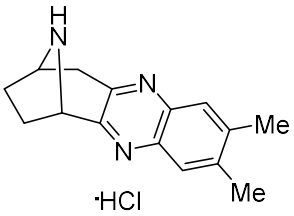

Compound **3.23** (17.0 mg, 0.05 mol) was was dissolved in HCl (3 M in MeOH) and stirred at r.t. for 1 hour to yield the title product as a brown solid (13.6 mg, >95%).

$^1$H NMR (400 MHz, $D_2O$) δ 7.22 (d, *J* = 16.1 Hz, 2H), 5.08 (d, *J* = 5.0 Hz, 1H), 4.69 (d, *J* = 5.4 Hz, 1H), 3.79 – 3.64 (m, 1H), 3.21 (d, *J* = 18.6 Hz, 1H), 2.67 – 2.51 (m, 2H), 2.36 – 2.25 (m, 1H), 2.19 (s, 6H), 2.01 (d, *J* = 13.5 Hz, 1H); $^{13}$C NMR (101 MHz, $D_2O$) δ 148.17, 145.81, 143.06, 142.52, 139.62, 138.44, 125.65, 125.06, 59.45, 54.25, 36.51, 31.47, 26.50, 19.37, 19.33.

HRMS (ESI+) m/z found 239.1404 [M+H]+, $C_{15}H_{18}N_3$ calculated 239.1422 (Δ = -7.5 ppm).

**(6S*)-2,3-dichloro-7,8,9,10-tetrahydro-6H-6,9-epiminocyclohepta[b]quinoxaline hydrochloride 3.28**

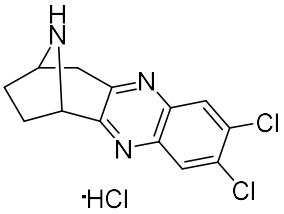

Compound **3.24** (19.0 mg, 0.05 mol) was dissolved in HCl (3 M in MeOH) and stirred at r.t. for 1 hour to yield the title product as a brown solid (16.0 mg, >95%).

$^1$H NMR (400 MHz, MeOD) δ 8.25 (d, *J* = 13.6 Hz, 2H), 5.11 (d, *J* = 6.0 Hz, 1H), 4.65 (d, *J* = 6.2 Hz, 1H), 3.81 – 3.62 (m, 1H), 3.34 (d, *J* = 6.4 Hz, 1H), 2.66 – 2.44 (m, 2H), 2.38 – 2.22 (m, 1H), 2.17 – 1.93 (m, 1H); $^{13}$C NMR (101 MHz, MeOD) δ 152.82, 151.17, 142.50, 140.86, 136.05, 135.59, 130.79, 130.37, 61.43, 55.83, 38.63, 32.49, 28.01.

HRMS (ESI+) m/z found 280.0400 [M+H]+, $C_{13}H_{12}Cl_2N_3$ calculated 280.0408 (Δ = -2.9 ppm).

**(6S*)-2,3-difluoro-7,8,9,10-tetrahydro-6H-6,9-epiminocyclohepta[b]quinoxaline hydrochloride 3.29**

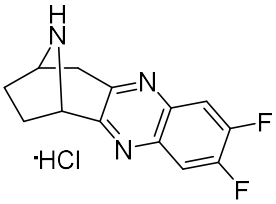

Compound **3.25** (17.4 mg, 0.05 mol) was dissolved in HCl (3 M in MeOH) and stirred at r.t. for 1 hour to yield the titled product as a brown solid (14.0 mg, >95%) .

$^1$H NMR (400 MHz, MeOD) δ 8.10 – 7.71 (m, 2H), 5.09 (s, 1H), 4.63 (s, 1H), 3.68 (s, 1H), 2.54 (s, 2H), 2.30 (s, 1H), 2.07 (s, 1H); $^{13}$C NMR (201 MHz, MeOD) δ 154.49 (dd, *J* = 59.8, 15.7 Hz), 153.22 (dd, *J* = 59.1, 15.8 Hz), 151.72, 149.88, 141.33 (d, *J* = 11.2 Hz), 139.91-137.63 (m), 115.88 (dd, *J* = 17.4, 5.8 Hz), 115.48 (dd, *J* = 18.0, 4.0 Hz), 61.62, 56.34, 38.93, 33.00, 28.44.

$^{19}$F NMR (377 MHz, MeOD) δ -131.29 – -131.53 (m); -131.92 – -132.15 (m).

HRMS (ESI+) m/z found 248.0999 [M+H]+, $C_{13}H_{12}F_2N_3$ calculated 248.0999 (Δ = 0 ppm).

***tert*-butyl (5S*)-4-oxo-2-phenyl-4,5,6,7,8,9-hexahydro-3H-5,8-epiminocyclohepta[d]pyrimidine-10-carboxylate 3.30**

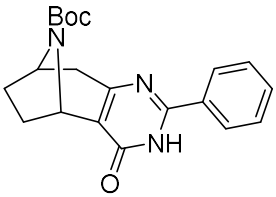

White solid (80.9 mg, 46%).

$^1$H NMR (400 MHz, $CDCl_3$) δ 12.85 (s, 1H), 8.19 (d, *J* = 7.2 Hz, 2H), 7.60 – 7.43 (m, 3H), 5.30 – 5.19 (m, 1H), 4.58 (s, 1H), 3.34 (d, *J* = 17.0 Hz, 1H), 2.57 (d, *J* = 18.1 Hz, 1H), 2.39 – 2.25 (m, 1H), 2.26 – 2.11 (m, 1H), 1.95 (t, *J* = 10.2 Hz, 1H), 1.69 (s, 1H), 1.44 (s, 9H); $^{13}$C NMR (101 MHz, $CDCl_3$) δ 162.27, 160.46, 155.47, 153.82, 132.24, 131.74, 129.16, 127.92, 124.92, 80.18, 52.01, 50.30, 39.76, 34.94, 29.88, 28.58.

HRMS (ESI+) m/z found 354.1814 [M+H]+, $C_{20}H_{24}N_3O_3$ calculated 354.1818 (Δ = -1.1 ppm)

***tert*-butyl (5S*)-4-oxo-2-(pyridin-2-yl)-4,5,6,7,8,9-hexahydro-3H-5,8-epiminocyclohepta[d]pyrimidine-10-carboxylate 3.31**

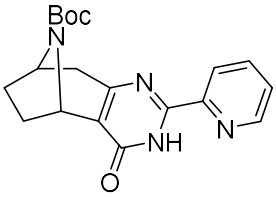

White solid (111.9 mg, 63%).

$^1$H NMR (400 MHz, $CDCl_3$) δ 10.98 (s, 1H), 8.42 (d, *J* = 7.9 Hz, 1H), 7.95 – 7.81 (m, 1H), 7.57 – 7.40 (m, 1H), 5.26 (d, *J* = 5.8 Hz, 1H), 4.59 (s, 1H), 3.33 (d, *J* = 18.1 Hz, 1H), 2.51 (d, *J* = 18.1 Hz, 1H), 2.35 – 2.22 (m, 1H), 2.21 – 2.09 (m, 1H), 2.01 – 1.93 (m, 1H), 1.71 – 1.61 (m, 1H), 1.43 (s, 9H); $^{13}$C NMR (101 MHz, $CDCl_3$) δ 159.45, 153.90, 151.84, 151.77, 148.96, 147.66, 137.94, 127.32, 126.65, 122.20, 80.14, 51.85, 50.94, 39.64, 34.98, 29.55, 28.54.

HRMS (ESI+) m/z found 355.1769 [M+H]+, $C_{19}H_{23}N_4O_3$ calculated 355.1770 (Δ = -0.28 ppm).

***tert*-butyl (5S*)-4-oxo-2-(pyridin-3-yl)-4,5,6,7,8,9-hexahydro-3H-5,8-epiminocyclohepta[d]pyrimidine-10-carboxylate 3.32**

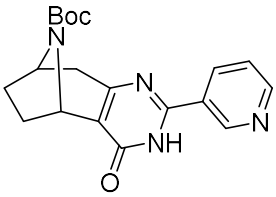

White solid (75.2 mg, 42%).

$^1$H NMR (400 MHz, $CDCl_3$) δ 13.72 (br, 1H), 9.52 (s, 1H), 8.76 (d, *J* = 4.8 Hz, 2H), 8.61 (d, *J* = 7.8 Hz, 2H), 7.62 – 7.41 (m, 1H), 5.26 (d, *J* = 5.9 Hz, 1H), 4.84 – 4.27 (m, 1H), 3.54 – 3.21 (m, 1H), 2.56 (d, *J* = 18.2 Hz, 1H), 2.39 – 2.13 (m, 2H), 2.05 – 1.85 (m, 1H), 1.80 – 1.61 (m, 1H), 1.43 (s, 9H); $^{13}$C NMR (101 MHz, $CDCl_3$) δ 163.17, 161.38, 153.74, 151.92, 149.12, 135.58, 128.81, 124.99, 123.73, 80.16, 52.09, 50.27, 39.73, 34.42, 29.82, 28.50.

HRMS (ESI+) m/z found 355.1761 [M+H]+, $C_{19}H_{23}N_4O_3$ calculated 355.1770 (Δ = -2.5 ppm).

***tert*-butyl (5S*)-2-amino-4-oxo-4,5,6,7,8,9-hexahydro-3H-5,8-epiminocyclohepta[d]pyrimidine-10-carboxylate 3.33**

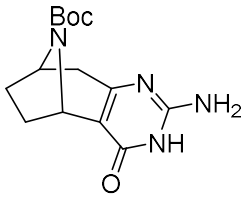

White solid (98.0 mg, 67%).

$^1$H NMR (400 MHz, MeOD) δ 4.99 (d, *J* = 5.7 Hz, 1H), 4.49 – 4.37 (m, 1H), 3.03 (br , 1H), 2.33 – 2.17 (m, 2H), 2.12 – 1.99 (m, 1H), 1.90 – 1.79 (m, 1H), 1.74 – 1.61 (m, 1H), 1.43 (s, 9H); $^{13}$C NMR (101 MHz, MeOD) δ 164.35, 158.44, 155.91, 155.45, 115.93, 81.35, 53.57 (52.94), 52.08 (51.30), 39.15 (38.61), 35.64 (35.28), 30.42 (29.87), 28.62.

**Note:** peaks corresponding to rotamers are listed in brackets and underlined.

HRMS (ESI+) m/z found 293.1611 [M+H]+, $C_{14}H_{21}N_4O_3$ calculated 293.1614 (Δ = -1.0 ppm).

***tert*-butyl (5S*)-2-(4-methoxyphenyl)-4-oxo-4,5,6,7,8,9-hexahydro-3H-5,8-epiminocyclohepta[d]pyrimidine-10-carboxylate 3.34**

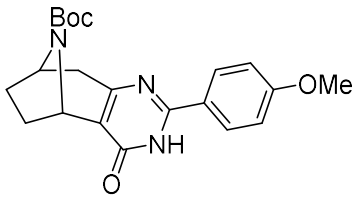

White solid (115.7 mg, 60%).

$^1$H NMR (400 MHz, $CDCl_3$) δ 12.57 (br, 1H), 8.16 (d, *J* = 8.7 Hz, 2H), 7.08 – 6.93 (m, 2H), 5.25 (s, 1H), 4.58 (s, 1H), 3.89 (s, 3H), 3.33 (d, *J* = 14.6 Hz, 1H), 2.53 (d, *J* = 18.1 Hz, 1H), 2.37 – 2.12 (m, 2H), 2.00 – 1.88 (m, 1H), 1.74 – 1.62 (m, 1H), 1.44 (s, 9H); $^{13}$C NMR (101 MHz, $CDCl_3$) δ 162.94, 162.22, 155.09, 153.78, 129.62, 123.93, 114.51, 80.07, 55.66, 52.06, 50.48, 39.72, 34.46, 29.63, 28.56.

HRMS (ESI+) m/z found 384.1918 [M+H]+, $C_{21}H_{26}N_3O_4$ calculated 384.1923 (Δ = -1.3 ppm).

***tert*-butyl (5S*)-2-(4-fluorophenyl)-4-oxo-4,5,6,7,8,9-hexahydro-3H-5,8-epiminocyclohepta[d]pyrimidine-10-carboxylate 3.35**

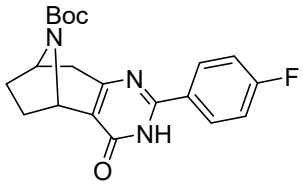

White solid (118.9 mg, 64%).

$^1$H NMR (400 MHz, $CDCl_3$) δ 13.38 (br, 1H), 8.41 – 8.17 (m, 2H), 7.20 (t, *J* = 8.5 Hz, 2H), 5.29 – 5.12 (m, 1H), 4.84 – 4.36 (m, 1H),3.32 (d, *J* = 17.3 Hz, 1H), 2.54 (d, *J* = 18.2 Hz, 1H), 2.31 (q, *J* = 11.0, 10.3 Hz, 1H), 2.24 – 2.11 (m, 1H), 2.07 – 1.91 (m, 1H), 1.79 – 1.61 (m, 1H), 1.44 (s, 9H); $^{13}$C NMR (101 MHz, $CDCl_3$) δ 165.27 (d, *J* = 253.5 Hz), 162.66, 159.90, 154.40, 153.74, 130.37 (d, *J* = 8.9 Hz), 128.02, 124.58, 116.18 (d, *J* = 22.0 Hz), 80.14, 52., 50.69, 39.76, 34.90, 29.71, 28.51.

HRMS (ESI+) m/z found 372.1721 [M+H]+, $C_{20}H_{23}FN_3O_3$ calculated 372.1723 (Δ = -0.54 ppm).

***tert*-butyl (5S*)-2-(4-chlorophenyl)-4-oxo-4,5,6,7,8,9-hexahydro-3H-5,8-epiminocyclohepta[d]pyrimidine-10-carboxylate 3.36**

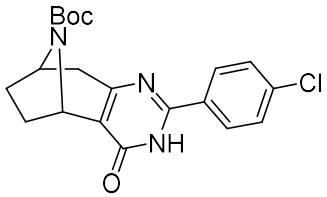

White solid (132.9 mg, 69%).

$^1$H NMR (400 MHz, $CDCl_3$) δ 13.40 (br, 1H), 8.21 (d, *J* = 8.5 Hz, 2H), 7.49 (d, *J* = 8.5 Hz, 2H), 5.27 (d, *J* = 19.1 Hz, 1H), 4.60 (s, 1H), 3.33 (d, *J* = 19.8 Hz, 1H), 2.52 (d, *J* = 18.2 Hz, 1H), 2.41 – 2.24 (m, 1H), 2.25 – 2.10 (m, 1H), 2.04 – 1.85 (m, 1H), 1.80 – 1.60 (m, 1H), 1.44 (s, 9H), $^{13}$C NMR (101 MHz,

$CDCl_3$) δ 162.68, 160.83, 154.21, 153.76, 138.37, 130.50, 129.28, 129.26, 124.88, 80.14, 51.88, 50.70, 39.87, 34.50, 29.83, 28.53.

HRMS (ESI+) m/z found 388.1425 [M+H]+, $C_{20}H_{23}ClN_3O_3$ calculated 388.1428 (Δ = -0.77 ppm).

## General procedure VI

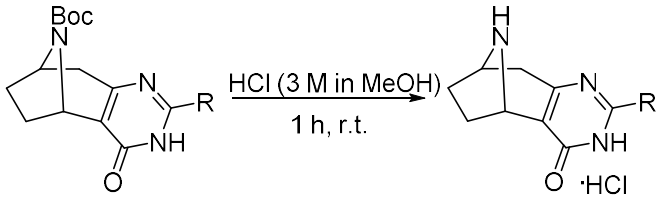


To a 5 mL oven-dried round bottom flask containing a magnetic stirring bar, compound **3.31-3.36** (0.5 mmol) was added 2 mL HCl (3 M in MeOH), the mixture was stirred at room temperature for 1-2 hours. After removal of the solvent, the residue was dried *in vacuo* overnight to give the product as a solid compound (>95%).

**(5S*)-2-(pyridin-2-yl)-3,5,6,7,8,9-hexahydro-4H-5,8-epiminocyclohepta[d]pyrimidin-4-one hydrochloride 3.37**

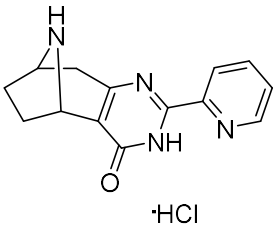


Brown solid (145.0 mg, >95%).

$^1$H NMR (400 MHz, MeOD) δ 8.89 (d, *J* = 4.4 Hz, 1H), 8.74 (d, *J* = 7.1 Hz, 1H), 8.51 (d, *J* = 7.1 Hz, 1H), 8.00 (t, *J* = 5.5 Hz, 1H), 5.10 (d, *J* = 4.6 Hz, 1H), 4.52 (s, 1H), 3.56 (d, *J* = 17.6 Hz, 1H), 3.07 (d, *J* = 18.3 Hz, 1H), 2.59 – 2.18 (m, 3H), 2.04 (d, *J* = 9.5 Hz, 1H); $^{13}$C NMR (101 MHz, MeOD) δ 164.97, 160.43, 155.86, 148.12, 146.66, 145.09, 129.43, 125.83, 119.93, 55.28, 53.04, 38.91, 33.71, 28.68.

HRMS (ESI+) m/z found 255.1244 [M+H]+, $C_{14}H_{15}N_4O$ calculated 255.1246 (Δ = -0.78 ppm).

**(5S*)-2-(pyridin-3-yl)-3,5,6,7,8,9-hexahydro-4H-5,8-epiminocyclohepta[d]pyrimidin-4-one hydrochloride 3.38**

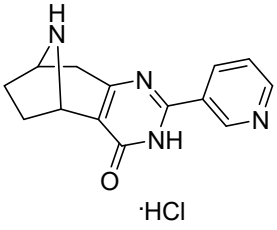


Brown solid (147.0 mg, >95%).

$^1$H NMR (400 MHz, $D_2O$) δ 9.34 (s, 1H), 9.10 – 8.92 (m, 2H), 8.35 – 8.09 (m, 1H), 5.03 (d, *J* = 4.7 Hz, 1H), 4.55 – 4.47 (m, 1H), 3.55 – 3.37 (m, 1H), 2.96 (d, *J* = 19.1 Hz, 1H), 2.54 – 2.18 (m, 3H), 2.06 – 1.83 (m, 1H).

$^{13}$C NMR (101 MHz, $D_2O$) δ 161.91, 156.90, 152.96, 144.66, 144.27, 141.71, 131.35, 127.49, 120.37, 53.52, 51.19, 36.77, 32.03, 27.01.

HRMS (ESI+) m/z found 255.1244 [M+H]+, $C_{14}H_{15}N_4O$ calculated 255.1246 (Δ = -0.78 ppm)

**(5S*)-2-amino-3,5,6,7,8,9-hexahydro-4H-5,8-epiminocyclohepta[d]pyrimidin-4-one hydrochloride 3.39**

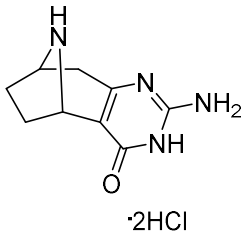


White solid (117.0 mg, >95%).

$^1$H NMR (400 MHz, DMSO-$d_6$) δ 9.73 (s, 1H), 9.47 (s, 1H), 8.10 (s, 2H), 4.63 (s, 1H), 4.24 (s, 1H), 3.19 – 3.10 (m, 1H), 2.65 – 2.54 (m, 1H), 2.23 – 2.04 (m, 2H), 2.02 – 1.91 (m, 1H), 1.88 – 1.73 (m, 1H); $^{13}$C NMR (101 MHz, DMSO-$d_6$) δ 158.47, 153.37, 110.70, 52.57, 50.37, 34.67, 32.68, 27.43.

HRMS (ESI+) m/z found 193.1088 [M+H]+, $C_9H_{13}N_4O$ calculated 193.1089 (Δ = -0.52 ppm).

**(5S*)-2-(4-methoxyphenyl)-3,5,6,7,8,9-hexahydro-4H-5,8-epiminocyclohepta[d]pyrimidin-4-one hydrochloride 3.40**

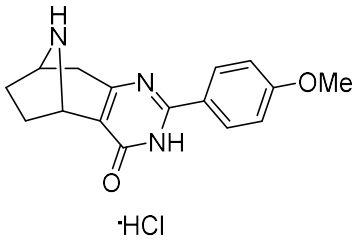


Brown solid (159.0 mg, >95%).

$^1$H NMR (400 MHz, DMSO-$d_6$) δ 9.91 (s, 1H), 9.52 (s, 1H), 8.08 (d, $J$ = 7.7 Hz, 2H), 7.06 (d, $J$ = 7.9 Hz, 2H), 4.76 (s, 1H), 4.27 (s, 1H), 3.83 (s, 3H), 3.26 (d, $J$ = 17.7 Hz, 1H), 2.70 (d, $J$ = 18.1 Hz, 1H), 2.22 (s, 2H), 2.00 (d, $J$ = 9.8 Hz, 1H), 1.84 (s, 1H); $^{13}$C NMR (101 MHz, DMSO-$d_6$) δ 162.64, 160.46, 156.72, 156.08, 129.95, 124.02, 118.53, 114.51, 55.95, 53.07, 50.66, 37.92, 32.74, 27.65.

HRMS (ESI+) m/z found 284.1394 [M+H]+, $C_{16}H_{18}N_3O_2$ calculated 284.1399 (Δ = -1.8 ppm)

**(5S*)-2-(4-fluorophenyl)-3,5,6,7,8,9-hexahydro-4H-5,8-epiminocyclohepta[d]pyrimidin-4-one hydrochloride 3.41**

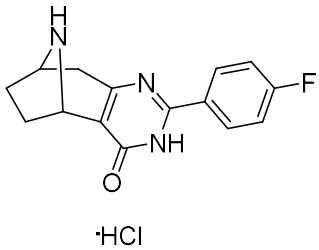


Brown solid (153.0 mg, >95%)

$^1$H NMR (400 MHz, MeOD) δ 8.19 – 7.97 (m, 2H), 7.35 (t, $J$ = 8.4 Hz, 2H), 5.00 (d, $J$ = 5.1 Hz, 1H), 4.47 (t, $J$ = 5.9 Hz, 1H), 3.51 – 3.38 (m, 1H), 2.94 (d, $J$ = 18.9 Hz, 1H), 2.54 – 2.23 (m, 3H), 2.07 (d, $J$ = 12.3 Hz, 1H); $^{13}$C NMR (101 MHz, MeOD) δ 167.10 (d, $J$ = 253.3 Hz), 161.74, 159.07, 155.69, 132.15 (d, $J$ = 9.4 Hz), 128.01 (d, $J$ = 3.2 Hz), 120.28, 117.35 (d, $J$ = 22.6 Hz), 55.05, 52.66, 37.74, 33.62, 28.58.

$^{19}$F NMR (377 MHz, MeOD) δ -108.0

HRMS (ESI+) m/z found 272.1196 [M+H]+, $C_{15}H_{15}FN_3O$ calculated 272.1199 (Δ = -1.1 ppm).

**(5S*)-2-(4-chlorophenyl)-3,5,6,7,8,9-hexahydro-4H-5,8-epiminocyclohepta[d]pyrimidin-4-one hydrochloride 3.42**

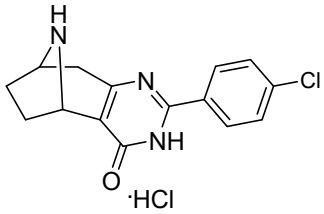

Brown solid (161.0 mg, >95%).

$^1$H NMR (400 MHz, MeOD) δ 8.03 (d, *J* = 7.4 Hz, 2H), 7.65 (d, *J* = 5.7 Hz, 2H), 4.49 (s, 1H), 3.49 (d, *J* = 15.3 Hz, 1H), 3.08 – 2.89 (m, 1H), 3.56 – 2.20 (m, 3H), 2.08 (s, 1H); $^{13}$C NMR (101 MHz, MeOD) δ 161.58, 159.66, 154.00, 141.05, 131.40, 130.64, 129.16, 120.76, 54.91, 52.59, 37.09, 33.66, 28.73.

HRMS (ESI+) m/z found 288.0897[M+H]+, $C_{14}H_{15}N_4O$ calculated 288.0904 (Δ = -2.4 ppm).

## General procedure VII

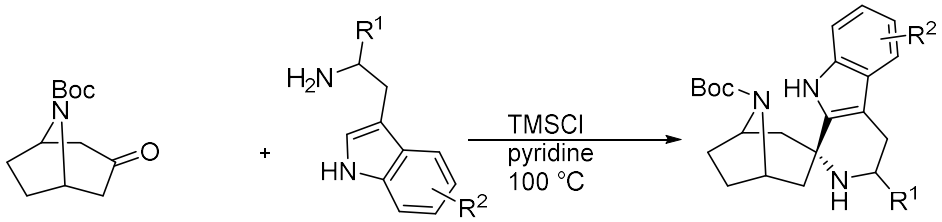

*N*-Boc-nortropinone (225.3 mg, 1.0 mmol), amines (1.2 mmol, 1.2 equiv) were dissolved in pyridine (2.0 mL), TMSCl (631 μL, 5.0 mmol) was added dropwise to the solution. The reaction was heated to 100 °C overnight, and monitored by TLC (DCM: MeOH = 10:1). After cooling to room temperature, trimethylamine (701 μL, 5.0 mmol) was added followed by water (4 mL). The mixture was further vigorously stirred for 2 hours, and the formed precipitate was washed with diethyl ether, which was dried *in vacuo* overnight to yield the product as a white solid.

***tert*-butyl (1S,3S)-2',3',4',9'-tetrahydro-8-azaspiro[bicyclo[3.2.1]octane-3,1'-pyrido[3,4-b]indole]-8-carboxylate 3.43**

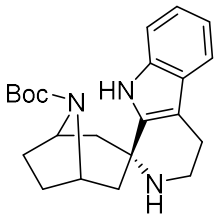

*N*-Boc-nortropinone (1.0 mmol) was reacted with tryptamine (192.2 mg, 1.2 mmol) for 22 hours to give the titled product as a white solid (233.0 mg, 63%).

$^1$H NMR (400 MHz, $CDCl_3$) δ 7.75 (s, 1H), 7.45 (d, *J* = 7.7 Hz, 1H), 7.28 – 7.24 (m, 1H), 7.17 – 7.11 (m, 1H), 7.07 (t, *J* = 7.4 Hz, 1H), 4.30 (s, 2H), 3.14 (t, *J* = 5.7 Hz, 2H), 2.66 (t, *J* = 5.7 Hz, 2H), 2.49 – 2.04 (m, 4H), 2.00 – 1.90 (m, 2H), 1.70 (s, 2H), 1.59 – 1.52 (m, 9H); $^{13}$C NMR (101 MHz, $CDCl_3$) δ 154.25, 140.30, 135.58, 127.48, 121.98, 119.48, 118.21, 110.88, 109.63, 79.55, 53.59, 52.35, 41.90, 39.14, 28.71, 28.39, 23.05.

HRMS (ESI+) m/z found 368.2328 [M+H]+ $C_{22}H_{30}N_3O_2$ calculated 368.2338 (Δ = -2.7 ppm).

**tert-butyl (1S,3S)-6'-methoxy-2',3',4',9'-tetrahydro-8-azaspiro[bicyclo[3.2.1]octane-3,1'-pyrido[3,4-b]indole]-8-carboxylate 3.44**

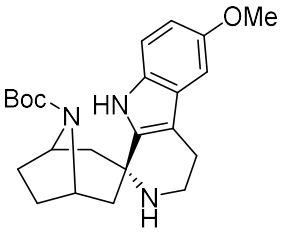


*N*-Boc-nortropinone (1.0 mmol) was reacted with 5-methoxytryptamine (228.2 mg, 1.2 mmol) for 16.5 hours to give the titled product as a white solid (43.9 mg, 11%). $^1$H NMR (400 MHz, $CDCl_3$) δ 7.81 (s, 1H), 7.15 (d, *J* = 8.7 Hz, 1H), 6.91 (d, *J* = 2.5 Hz, 1H), 6.80 (dd, *J* = 8.7, 2.4 Hz, 1H), 4.30 (s, 2H), 3.84 (s, 3H), 3.14 (t, *J* = 5.7 Hz, 2H), 2.62 (t, *J* = 5.7 Hz, 2H), 2.08 (d, *J* = 7.4 Hz, 4H), 1.98 – 1.88 (m, 2H), 1.55 (s, 9H); $^{13}$C NMR (101 MHz, $CDCl_3$) δ 154.21, 154.12, 141.33, 130.70, 127.80, 111.67, 111.57, 109.37, 100.60, 79.53, 56.18, 52.46, 41.93, 39.12, 28.70, 23.10.

HRMS (ESI+) m/z found 398.2412 [M+H]+, $C_{23}H_{32}N_3O_3$ calculated 398.2444 (Δ = -8.0 ppm).

**(1S,3S,3'S)-2',3',4',9'-tetrahydro-8-azaspiro[bicyclo[3.2.1]octane-3,1'-pyrido[3,4-b]indole]-3'-carboxylic acid 3.47**

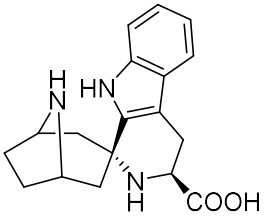


*N*-Boc-nortropinone (1.0 mmol) was reacted with *L*-tryptophan (245.1 mg, 1.2 mmol)for 19 hours to give the titled product as a white solid (185.4 mg, 60%). $^1$H NMR (400 MHz, $D_2O$) δ 7.45 (d, *J* = 7.8 Hz, 1H), 7.32 (d, *J* = 8.1 Hz, 1H), 7.17 – 6.96 (m, 2H), 3.46 (s, 1H), 3.37 – 3.23 (m, 1H), 3.14 (s, 1H), 3.00 – 2.87 (m, 1H), 2.64 – 2.47 (m, 1H), 2.32 – 2.14 (m, 1H), 2.02 – 1.60 (m, 5H), 1.51 – 1.37 (m, 2H); $^{13}$C NMR (101 MHz, $D_2O$) δ 180.15, 140.26, 136.00, 126.40, 121.61, 119.15, 117.90, 111.24, 107.88, 53.03, 43.43, 38.39, 27.65, 27.50, 24.60.

HRMS (ESI+) m/z found 312.1708 [M+H]+, $C_{18}H_{22}N_3O_2$ calculated 312.1712 (Δ = -1.3 ppm); **$[\alpha]^{20}_D$ = +18.3** (*c* = 1.0, $H_2O$).

**(1S,3S)-2',3',4',9'-tetrahydro-8-azaspiro[bicyclo[3.2.1]octane-3,1'-pyrido[3,4-b]indole] hydrochloride 3.48**

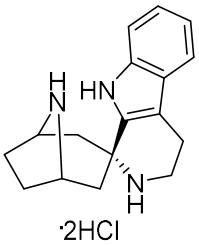


Compound **3.43** (18.4 mg, 0.05 mol) was stirred at r.t. for 1 hour to yield the titled product according to General procedure III as a brown solid (14.0 mg, >95%) . $^1$H NMR (400 MHz, $D_2O$) δ 7.52 (dd, *J* = 36.2, 7.6 Hz, 2H), 7.35 – 7.08 (m, 2H), 4.30 (s, 2H), 3.68 (d, *J* = 5.9 Hz, 2H), 3.07 (d, *J* = 5.8 Hz, 2H), 2.95 – 2.76 (m, 2H), 2.57 (d, *J* = 16.8 Hz, 2H), 2.47 – 2.35 (m, 2H), 2.27 – 2.14 (m, 2H);$^{13}$C NMR (101 MHz, $D_2O$) δ 148.17, 145.81, 143.06, 142.52, 139.62, 138.44, 125.65, 125.06, 59.45, 54.25, 36.51, 31.47, 26.50, 19.37, 19.33.

HRMS (ESI+) m/z found [M+H]+ 268.1813, $C_{17}H_{22}N_3$ calculated 268.1814 (Δ = -0.37 ppm).

**(1S,3S)-6'-methoxy-2',3',4',9'-tetrahydro-8-azaspiro[bicyclo[3.2.1]octane-3,1'-pyrido[3,4-b]indole] hydrochloride 3.49**

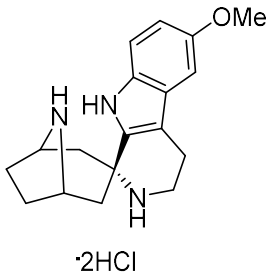


Compound **3.44** (20.0 mg, 0.05 mol) was stirred at r.t. for 1 hour to yield the titled product according to General procedure III as a brown solid (15.0 mg, >95% ).

$^1$H NMR (400 MHz, $D_2O$) δ 7.41 (d, *J* = 8.8 Hz, 1H), 7.13 (d, *J* = 2.2 Hz, 1H), 6.96 (dd, *J* = 8.8, 2.3 Hz, 1H), 4.34 (s, 2H), 3.73 (t, *J* = 6.0 Hz, 2H), 3.07 (t, *J* = 6.0 Hz, 2H), 2.95 – 2.80 (m, 2H), 2.73 – 2.56 (m, 2H), 2.51 – 2.36 (m, 2H), 2.32 – 2.09 (m, 2H); $^{13}$C NMR (101 MHz, $D_2O$) δ 153.28, 132.09, 131.61, 125.40, 113.21, 112.73, 107.63, 100.90, 55.95, 54.81, 53.09, 39.75, 37.08, 24.73, 17.47.

HRMS (ESI+) m/z found 298.1917 [M+H]+, $C_{18}H_{24}N_3O$ calculated 298.1919 (Δ = -0.67 ppm).

**(1S,3S)-8-methyl-4',9'-dihydro-3'H-8-azaspiro[bicyclo[3.2.1]octane-3,1'-pyrano[3,4-b]indole] 3.51**

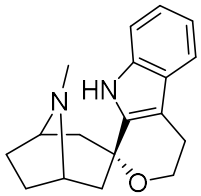


To a solution of tropinone (41.8 mg, 0.3 mmol) in dry toluene (2.0 mL) was added tryptophol (53.2 mg, 0.33 mmol) and methanesulfonic acid (22.0 µL, 1.1 equiv), the mixture was then stirred at 80 °C under an inert $N_2$ atmosphere. A white precipitate was formed after 24 hours, which was washed with a minimal amount of EtOAc. The solid was basified with saturated $NaHCO_3$, the aqueous phase was extracted with EtOAc (2×), dried over $Na_2SO_4$, the combined organic layer was concentrated under reduced pressure. The product was dried under high vacuum to yield a white solid (50.7 mg, 60%).

$^1$H NMR (400 MHz, DMSO-$d_6$) δ 10.83 (s, 1H), 7.33 (d, *J* = 7.7 Hz, 1H), 7.23 (d, *J* = 8.1 Hz, 1H), 7.03 – 6.97 (m, 1H), 6.95 – 6.89 (m, 1H), 3.91 – 3.80 (m, 2H), 3.11 (s, 2H), 2.62 (t, *J* = 5.4 Hz, 2H), 2.24 (s, 3H), 2.21 – 2.12 (m, 2H), 2.04 (t, *J* = 6.3 Hz, 2H), 1.96 – 1.85 (m, 4H); $^{13}$C NMR (101 MHz, DMSO-$d_6$) δ 139.74, 136.27, 126.72, 121.09, 118.71, 117.95, 111.61, 106.55, 72.86, 60.63, 58.81, 41.79, 40.80, 25.87, 22.32.

HRMS (ESI+) m/z found 283.1807 [M+H]+, $C_{18}H_{23}N_2O$ calculated 283.1810 (Δ = -1.1 ppm).

## Synthesis of tosylhydrazine 3.54

**tert-butyl (1S*)3-(2-tosylhydrazineylidene)-8-azabicyclo[3.2.1]octane-8-carboxylate 3.54**

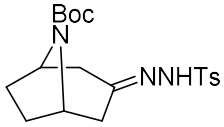


To a 10 mL round bottom flask was added $Na_2SO_4$ (142.6 mg, 3.0 mmol). *N*-Boc-nortropinone **2** (450.6 mg, 2.0 mmol) dissolved in MeOH (5 mL) was added and the mixture treated with $TsNHNH_2$ (391.0 mg, 2.1mmol) was stirred at room temperature overnight. After 21 hours, $Na_2SO_4$ was filtered off, the filtrate was concentrated, and the resulting crude was purified by column chromatography on silica gel (MeOH:DCM = 1:15) to give a white solid (618.0 mg, 79%).

$^1$H NMR (400 MHz, $CDCl_3$) δ 7.84 – 7.78 (m, 2H), 7.30 (d, *J* = 8.1 Hz, 2H), 2.54 (d, *J* = 15.4 Hz, 2H), 2.42 (s, 3H), 2.34 (d, *J* = 15.2 Hz, 1H), 2.28 – 2.16 (m, 1H), 1.91 (d, *J* = 7.5 Hz, 2H), 1.56 – 1.50 (m, 1H), 1.44 (s, 9H), 1.39 – 1.31 (m, 1H); $^{13}$C NMR (101 MHz, $CDCl_3$) δ 153.35, 144.37, 135.39, 129.77, 128.21, 80.26, 77.52, 77.20, 76.88, 53.51, 52.33, 41.11, 34.23, 29.19, 28.61, 28.08, 21.79.

HRMS (ESI+) m/z found 394.1795 [M+H]+, $C_{19}H_{28}N_3O_4S$ calculated 394.1801 (Δ = -1.5 ppm).

**tert-butyl (1S*,3S*)-5'-benzoyl-4'-phenyl-2',4'-dihydro-8-azaspiro[bicyclo[3.2.1]octane-3,3'-pyrazole]-8-carboxylate 3.55**

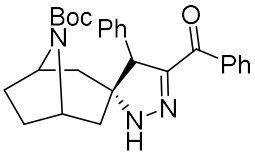

To a 10 mL oven-dried vial containing a magnetic stirring bar was added compound **2c** (117.9 mg, 0.3 mmol), together with $Cs_2CO_3$ (97.8 mg, 0.3 mmol). Chalcone (31.3 mg, 0.15 mmol) dissolved in $CH_3CN$ (3 mL) was added. The mixture was stirred at 110 °C in an inert argon atmosphere. After 8 hours, the solvent was removed under reduced pressure, and the crude mixture was purified via column chromatography on silica gel using hexane/ethyl acetate (8:1 to 5:1) to yield the product as a white solid (30.0 mg, 45%).

$^1$H NMR (400 MHz, $CDCl_3$) δ 8.16 – 8.03 (m, 2H), 7.56 – 7.49 (m, 1H), 7.46 – 7.39 (m, 2H), 7.30 – 7.25 (m, 2H), 7.25 – 7.20 (m, 1H), 7.09 – 7.02 (m, 2H), 4.33 – 4.26 (m, 1H), 4.17 (s, 1H), 4.12 (s, 1H), 2.13 – 2.02 (m, 4H), 1.98 – 1.90 (m, 1H), 1.82 (d, *J* = 8.1 Hz, 1H), 1.69 (d, *J* = 3.6 Hz, 1H), 1.43 (s, 9H), 1.36 – 1.31 (m, 1H); $^{13}$C NMR (101 MHz, $CDCl_3$) δ 187.38, 153.43, 152.26, 137.44, 135.51, 132.48, 130.00, 128.81, 128.49, 128.18, 127.67, 79.88, 68.70, 62.26, 53.40, 52.78, 44.28, 37.51, 28.57, 28.04, 27.17.

HRMS (ESI+) m/z found 446.2444 [M+H]+, $C_{27}H_{32}N_3O_3$ calculated 446.2444 (Δ = 0 ppm).

## General procedure VIII

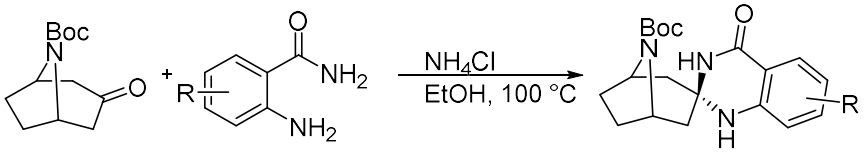

To a 10 mL oven-dried round bottom flask charged a reflux condenser was added *N*-Boc-nortropinone (135.2 mg, 0.6 mmol) and diverse 2-aminobenzamide analogues (0.5 mmol, 1.0 equiv) followed by $NH_4Cl$ (5.3 mg, 0.1 mmol). The resulting mixture was dissolved in absolute ethanol (3 mL) and heated to 100 °C overnight. After cooling to room temperature, the solvent was removed under reduced pressure, and the crude was purified by column chromatography on silica gel using MeOH/DCM (0.5% to 2.5%) to yield a single diastereoisomer as a white solid.

**tert-butyl (1S,3R)-4'-oxo-3',4'-dihydro-1'H-8-azaspiro[bicyclo[3.2.1]octane-3,2'-quinazoline]-8-carboxylate 3.56**

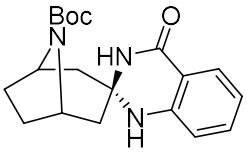

24 hours, white solid (143.0 mg, 83%).

$^1$H NMR (400 MHz, DMSO-$d_6$) δ 8.01 (s, 1H), 7.64 (dd, *J* = 7.8, 1.5 Hz, 1H), 7.37 – 7.24 (m, 1H), 6.90 (d, *J* = 8.1 Hz, 1H), 6.83 – 6.70 (m, 1H), 6.26 (s, 1H), 4.05 (d, *J* = 5.3 Hz, 2H), 2.17 – 2.01 (m, 4H), 1.96 – 1.75 (m, 4H), 1.41 (s, 9H).

$^{13}$C NMR (101 MHz, DMSO-$d_6$) δ 164.13, 152.75, 145.87, 133.54, 127.47, 118.68, 117.58, 117.51, 79.05, 66.53, 53.18 (52.31), 42.24 (41.51), 28.66 (27.57).

**Note:** peaks corresponding to rotamers are listed in brackets and underlined.

HRMS (ESI+) m/z found 344.1970 [M+Na]+, $C_{19}H_{25}N_3O_3Na$ calculated 344.1974 (Δ = -0.10 ppm).

***tert*-butyl (1S,3R)-7'-fluoro-4'-oxo-3',4'-dihydro-1'H-8-azaspiro[bicyclo[3.2.1]octane-3,2'-quinazoline]-8-carboxylate 3.57**

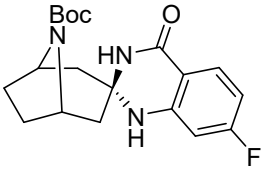

21 hours, white solid (107.3 mg, 59%).

$^1$H NMR (400 MHz, $CDCl_3$) δ 7.87 (dd, *J* = 8.7, 6.3 Hz, 1H), 6.79 (s, 1H), 6.62 – 6.52 (m, 1H), 6.40 (dd, *J* = 9.8, 2.4 Hz, 1H), 4.72 (s, 1H), 4.26 (s, 2H), 2.25 (d, *J* = 14.3 Hz, 2H), 2.13 – 1.87 (m, 6H), 1.45 (s, 9H); $^{13}$C NMR (101 MHz, $CDCl_3$) δ 166.70 (d, *J* = 252.3 Hz), 164.01, 153.25, 146.70 (d, *J* = 12.3 Hz), 131.04 (d, *J* = 11.2 Hz), 113.59 (d, *J* = 0.8 Hz), 107.94 (d, *J* = 22.5 Hz), 103.05 (d, *J* = 24.8 Hz), 80.17, 68.06, 52.59, 42.77, 28.57.

$^{19}$F NMR (377 MHz, $CDCl_3$) δ -105.1.

HRMS (ESI+) m/z found 362.1841 [M+H]+, $C_{19}H_{25}FN_3O_3$ calculated 362.1880 (Δ = -10.8 ppm).

***tert*-butyl (1S,3R)-7'-chloro-4'-oxo-3',4'-dihydro-1'H-8-azaspiro[bicyclo[3.2.1]octane-3,2'-quinazoline]-8-carboxylate 3.58**

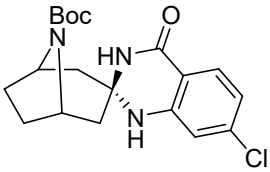

48 hours, white solid (122.0 mg, 65%)

$^1$H NMR (400 MHz, $CDCl_3$) δ 7.82 (d, *J* = 8.3 Hz, 1H), 6.87 (dd, *J* = 8.3, 1.8 Hz, 1H), 6.74 (d, *J* = 1.7 Hz, 1H), 6.52 (s, 1H), 4.60 (s, 1H), 4.27 (s, 2H), 2.26 (d, *J* = 14.3 Hz, 2H), 2.16 – 1.98 (m, 4H), 1.95 (t, *J* = 7.3 Hz, 2H), 1.46 (s, 9H); $^{13}$C NMR (101 MHz, $CDCl_3$) δ 163.87, 153.24, 145.64, 140.00, 129.88, 120.84, 116.48, 115.76, 80.23, 68.12, 52.60, 42.96, 28.58, 27.55.

HRMS (ESI+) m/z found 378.1583 [M+H]+, $C_{19}H_{25}ClN_3O_3$ calculated 378.1584 (Δ = -0.26 ppm).

**(1S,3R)-8-methyl-1'H-8-azaspiro[bicyclo[3.2.1]octane-3,2'-quinazolin]-4'(3'H)-one 3.59**

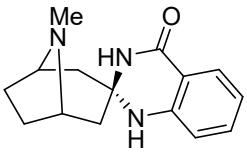

Tropinone **1** (139.2 mg, 1.0 mmol) was reacted with 2-aminobenzamide (1.2 mmol, 1.2 equiv) followed by the addition of catalyst $NH_4Cl$ (0.3 mmol, 0.3 equiv) in EtOH at 95 °C for 37 hours to yield a brown solid (51.6 mg, 20%).

$^1$H NMR (400 MHz, $CDCl_3$) δ 7.89 (dd, *J* = 7.8, 1.5 Hz, 1H), 7.37 – 7.29 (m, 1H), 6.94 – 6.82 (m, 1H), 6.71 (d, *J* = 8.0 Hz, 1H), 6.36 (s, 1H), 4.39 (s, 1H), 3.27 (dd, *J* = 5.4, 2.8 Hz, 2H), 2.34 (s, 3H), 2.25 (dd, *J* = 14.4, 4.3 Hz, 2H), 2.21 – 2.11 (m, 4H), 1.92 (d, *J* = 8.4 Hz, 2H);$^{13}$C NMR (101 MHz, $CDCl_3$) δ 164.50, 144.89, 133.98, 128.37, 120.30, 117.32, 116.70, 67.02, 60.22, 43.85, 39.69, 25.90.

HRMS (ESI+) m/z found 258.1602 [M+H]+, $C_{15}H_{20}N_3O$ calculated 258.1606 (Δ = -1.6 ppm).

## General procedure IX

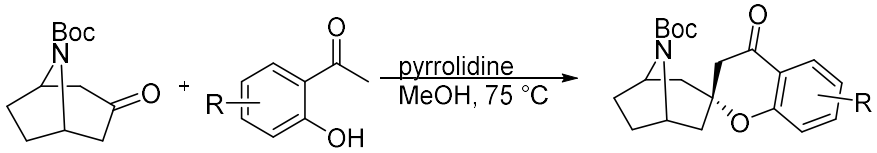


To a solution of substituted 1-(2-hydroxyphenyl) ethan-1-one (1.0 mmol) in anhydrous MeOH (10 mL) was added pyrrolidine (167 μL, 2.0 mmol). The mixture was stirred at room temperature for 20 mins followed by the addition of *N*-Boc-nortropinone **2** (225.3 mg, 1.0 mmol), and was subsequently heated to reflux under $N_2$. The mixture

was monitored by TLC (ethyl acetate: hexane = 1:6) until no further transformation of ketone, the solvent was removed under reduced pressure. The resulting residue was purified by column chromatography on silica gel (ethyl acetate: hexane = 10:1 to 6:1) to afford a white solid which was recrystallized with hexane to yield the titled product.

***tert*-butyl (1S,3S)-4'-oxo-8-azaspiro[bicyclo[3.2.1]octane-3,2'-chromane]-8-carboxylate 3.60**

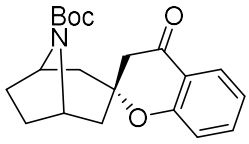


72 hours, white solid (104.0 mg, 30%).

$^1$H NMR (400 MHz, $CDCl_3$) δ 7.85 (dd, *J* = 7.8, 1.7 Hz, 1H), 7.60 – 7.42 (m, 1H), 7.04 – 6.97 (m, 1H), 6.92 (d, *J* = 8.3 Hz, 1H), 4.22 (s, 2H), 2.58 (s, 2H), 2.20 – 2.09 (m, 4H), 1.97 (dd, *J* = 8.6, 4.4 Hz, 2H), 1.89 (dd, *J* = 15.0, 3.6 Hz, 2H), 1.45 (s, 9H); $^{13}$C NMR (101 MHz, $CDCl_3$) δ 192.00, 159.32, 153.43, 136.59, 126.59, 121.32, 120.93, 118.37, 80.44, 79.74, 52.54, 50.96, 39.15, 28.59, 27.89.

HRMS (ESI+) m/z found 344.1862 [M+H]+, $C_{20}H_{26}NO_4$ calculated 344.1862 (Δ = 0 ppm)

***tert*-butyl (1S,3S)-6'-chloro-4'-oxo-8-azaspiro[bicyclo[3.2.1]octane-3,2'-chromane]-8-carboxylate 3.61**

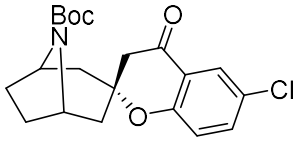


*N*-Boc-nortropinone **2** (1.0 equiv, 0.5 mmol) was reacted with 5'-chloro-2'-hydroxyacetophenone (85.3 mg, 0.5 mmol) for 36 hours to give the product as a white solid (56.7 mg, 30%).

$^1$H NMR (400 MHz, $CDCl_3$) δ 7.81 (d, *J* = 2.7 Hz, 1H), 7.46 – 7.41 (m, 1H), 6.89 (d, *J* = 8.8 Hz, 1H), 4.22 (s, 2H), 2.58 (s, 2H), 2.18 – 2.11 (m, 2H), 2.10 – 1.95 (m, 4H), 1.89 (d, *J* = 14.2 Hz, 2H), 1.45 (s, 9H); $^{13}$C NMR (101 MHz, $CDCl_3$) δ 190.86, 157.72, 153.40, 136.40, 126.93, 126.03, 121.67, 120.06, 80.97, 79.85, 50.66, 28.59.

HRMS (ESI+) m/z found 378.1470 [M+H]+, $C_{20}H_{25}ClNO_4$ calculated 378.1472 (Δ = -0.53 ppm).

***tert*-butyl (1S,3S)-6'-fluoro-4'-oxo-8-azaspiro[bicyclo[3.2.1]octane-3,2'-chromane]-8-carboxylate 3.62**

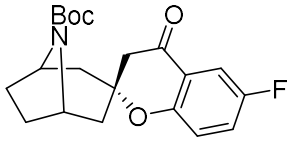


48 hours, white solid (78.8 mg, 22%).

$^1$H NMR (400 MHz, $CDCl_3$) δ 7.50 (dd, *J* = 8.1, 3.2 Hz, 1H), 7.25 – 7.18 (m, 1H), 6.90 (dd, *J* = 9.0, 4.1 Hz, 1H), 4.27 – 4.16 (m, 2H), 2.57 (s, 2H), 2.18 – 2.12 (m, 2H), 2.11 – 2.05 (m, 2H), 2.04 – 1.95 (m, 2H), 1.88 (dd, *J* = 14.9, 3.7 Hz, 2H), 1.45 (s, 9H); $^{13}$C NMR (101 MHz, $CDCl_3$) δ 191.20 (d, *J* = 2.0 Hz), 157.26 (d, *J* = 242.0 Hz), 155.47 (d, *J* = 1.8 Hz), 153.40, 124.01 (d, *J* = 24.4 Hz), 121.28 (d, *J* = 6.4 Hz), 119.92 (d, *J* = 7.3 Hz), 111.76 (d, *J* = 23.4 Hz), 80.75, 79.80, 52.47, 50.70, 39.01, 28.58, 27.88.

$^{19}$F NMR (377 MHz, $CDCl_3$) δ -121.6.

HRMS (ESI+) m/z found 362.1764 [M+H]+, $C_{20}H_{25}FNO_4$ calculated 362.1768 (Δ = -1.1 ppm).

***tert*-butyl (1S,3S)-6'-bromo-4'-oxo-8-azaspiro[bicyclo[3.2.1]octane-3,2'-chromane]-8-carboxylate 3.63**

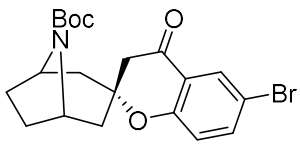


72 hours, white solid (151.1 mg, 36%).

$^1$H NMR (400 MHz, $CDCl_3$) δ 7.95 (d, *J* = 2.6 Hz, 1H), 7.65 – 7.52 (m, 1H), 6.83 (d, *J* = 8.8 Hz, 1H), 4.21 (s, 2H), 2.57 (s, 2H), 2.17 – 2.11 (m, 2H), 2.09 – 2.02 (m, 2H), 2.02 – 1.93 (m, 2H), 1.88 (dd, *J* = 15.0, 3.7 Hz, 2H), 1.45 (s, 9H); $^{13}$C

NMR (101 MHz, $CDCl_3$) δ 190.70, 158.16, 153.37, 139.17, 129.10, 122.13, 120.42, 114.01, 80.97, 79.83, 50.60, 39.06, 28.57.

HRMS (ESI+) m/z found 444.0783 [M+Na]+, $C_{20}H_{24}BrNO_4Na$ calculated 444.0786 (Δ = -0.67 ppm)

## General procedure X

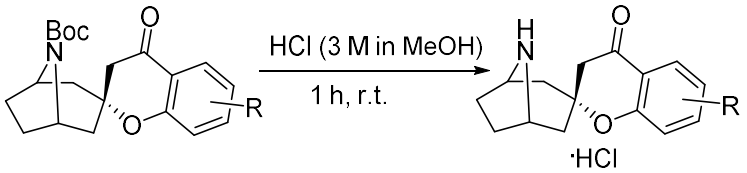


To a 5 mL oven-dried round bottom flask containing chromane **3.60-3.63** (0.03 – 0.12 mmol) was added 2 mL HCl (3 M in MeOH) and the mixture was stirred at room temperature for 1 hour. After removal of the solvent, the residue was dried under high vacuum overnight to yield a solid compound without further purification (>95%).

**(1S,3S)-8-azaspiro[bicyclo[3.2.1]octane-3,2'-chroman]-4'-one one hydrochloride 3.65**

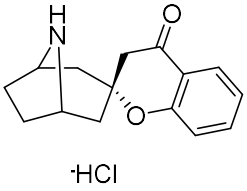


Grey solid (8.3 mg, >95%).

$^1$H NMR (400 MHz, MeOD) δ 7.83 (d, *J* = 7.5 Hz, 1H), 7.61 (t, *J* = 7.3 Hz, 1H), 7.08 (q, *J* = 7.4 Hz, 2H), 4.10 (s, 2H), 2.75 (s, 2H), 2.60 – 2.34 (m, 4H), 2.30 – 1.98 (m, 4H); $^{13}$C NMR (101 MHz, MeOD) δ 192.48, 159.87, 138.23, 127.26, 123.01, 121.92, 119.60, 79.03, 55.64, 50.22, 38.18, 26.92.

HRMS (ESI+) m/z found 244.1335 [M+H]+ $C_{15}H_{18}NO_2$ calculated 244.1338 (Δ = -1.2 ppm).

**(1S,3S)-6'-chloro-8-azaspiro[bicyclo[3.2.1]octane-3,2'-chroman]-4'-one hydrochloride 3.66**

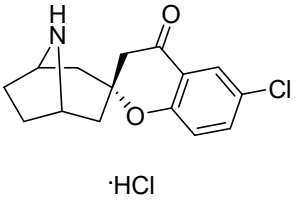


Yellow solid (24.0 mg, >95%).

$^1$H NMR (400 MHz, MeOD) δ 7.75 (br, 1H), 7.58 (br, 1H), 7.10 (br, 1H), 4.11 (br, 2H), 2.75 (br, 2H), 2.45 (br, 4H), 2.17 (br, 4H); $^{13}$C NMR (101 MHz, MeOD) δ 191.07, 158.22, 137.80, 128.22, 126.37, 122.73, 121.90, 79.43, 55.81, 49.96, 38.32, 27.17.

HRMS (ESI+) m/z found 278.0942 [M+H]+, $C_{15}H_{17}ClNO_2$ calculated 278.0948 (Δ = -2.2 ppm).

**(1S,3S)-6'-fluoro-8-azaspiro[bicyclo[3.2.1]octane-3,2'-chroman]-4'-one hydrochloride 3.67**

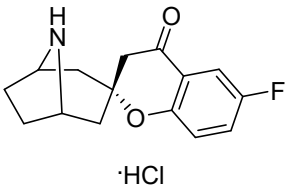


Yellow solid (17.8 mg, >95%).

$^1$H NMR (400 MHz, MeOD) δ 7.49 (d, *J* = 7.6 Hz, 1H), 7.40 (br, 1H), 7.13 (br, 1H), 4.12 (br, 2H), 2.76 (br, 2H), 2.48 (br, 4H), 2.18 (br, 4H); $^{13}$C NMR (101 MHz, MeOD) δ 191.48, 158.78 (d, *J* = 241.2 Hz), 156.02, 125.42 (d, *J* = 24.7 Hz), 122.42 (d, *J* = 6.3 Hz), 121.83 (d, *J* = 7.5 Hz), 112.11 (d, *J* = 23.8 Hz), 79.29, 55.81, 50.02, 38.24, 27.13.

$^{19}$F NMR (377 MHz, MeOD) δ -123.0

HRMS (ESI+) m/z found 262.1249 [M+H]+, $C_{15}H_{17}FNO_2$ calculated 262.1243 (Δ = 2.2 ppm).

**(1S,3S)-6'-bromo-8-azaspiro[bicyclo[3.2.1]octane-3,2'-chroman]-4'-one hydrochloride 3.68**

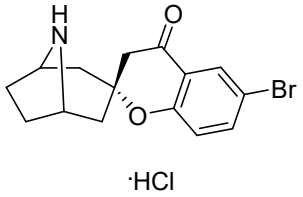

Brown solid (37.0 mg, >95%).

$^1$H NMR (400 MHz, MeOD) δ 7.93 (d, *J* = 2.0 Hz, 1H), 7.74 (dd, *J* = 8.4, 2.3 Hz, 1H), 7.07 (d, *J* = 8.4 Hz, 1H), 4.13 (s, 2H), 2.79 (s, 2H), 2.57 – 2.38 (m, 4H), 2.18 (d, *J* = 13.9 Hz, 4H), $^{13}$C NMR (101 MHz, MeOD) δ 191.11, 158.82, 140.61, 129.63, 123.30, 121.99, 115.36, 79.57, 55.53, 49.82, 38.09, 26.87.

HRMS (ESI+) m/z found [M+H]+ 322.0443, $C_{15}H_{17}BrNO_2$ calculated 322.0443 (Δ = 0 ppm).

***tert*-butyl (1S*,3S*)-4''-oxo-3'',4''-dihydro-1''H-8-azadispiro[bicyclo[3.2.1]octane-3,2'-chromane-4',2''-quinazoline]-8-carboxylate 3.70**

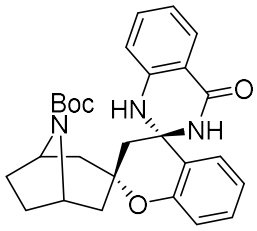

A 10 mL round bottom flask with oven-dried attached a condenser was placed **3.60** (171.0 mg, 0.5 mmol), together 2-aminobenzamide (81.6 mg, 0.6mmol) dissolved in ethanol was added, followed by $NH_4Cl$ (9.6 mg, 0.3 equiv). The mixture was heated to 95 °C for 3 days, after removal of the solvent, the crude was washed with 1M HCl (10 mL), the aqueous phase was extracted with EtOAc (2×), dried over $Na_2SO_4$, the combined organic layer was concentrated, the resulting residue was purified by column chromatography on silica gel using MeOH/DCM (0.5% to 2.5%) to yield the product as a white solid (81.6 mg, 36%).

$^1$H NMR (400 MHz, $CDCl_3$) δ 7.94 – 7.86 (m, 1H), 7.86 – 7.72 (m, 1H), 7.38 – 7.27 (m, 2H), 7.04 – 6.97 (m, 1H), 6.91 – 6.85 (m, 1H), 6.85 – 6.79 (m, 1H), 6.63 (d, *J* = 8.0 Hz, 1H), 5.96 (s, 1H), 4.22 (d, *J* = 7.1 Hz, 2H), 2.36 – 2.23 (m, 2H), 2.18 (s, 1H), 2.09 (s, 1H), 2.06 – 1.99 (m, 1H), 1.92 (d, *J* = 7.1 Hz, 5H), 1.41 (s, 9H); $^{13}$C NMR (101 MHz, $CDCl_3$) δ 163.81, 153.36, 153.26, 144.87, 134.66, 131.71, 128.87, 128.61, 123.24, 121.85, 119.65, 118.17, 115.09, 79.70, 76.24, 66.66, 52.74, 48.92, 39.84, 28.56, 28.03.

HRMS (ESI+) m/z found 462.2388 [M+H]+, $C_{27}H_{32}N_3O_4$ calculated 462.2393 (Δ = -1.1 ppm).

## General procedure XI

Quinuclidine-3-one (1.0 mmol, 1.0 equiv,) was reacted with anthranilamide **3.69** (1.0 equiv) and $NH_4Cl$ (0.1equiv), the mixture was heated to 80 ºC to yield a white precipitate. The resulting residue was washed with MeOH (30 mL), DCM (30 mL), and ethyl acetate (30 mL) to give the title compound as a white solid. The resulting white product was dissolved in HCl (12 M), the solvent was removed under reduced pressure, and the product was characterized.

**(1S*,2R*,4S*)-1'H-4-azaspiro[bicyclo[2.2.2]octane-2,2'-quinazolin]-4'(3'H)-one hydrochloride 3.71**

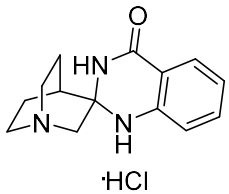

Quinuclidine-3-one **(**1.0 equiv, 1.35 mmol) was reacted with anthranilamide **3.69** (184.2 mg, 1.35 mmol) for 2 days to give a white solid (182.3 mg, 75%).

$^1$H NMR (400 MHz, DMSO-$d_6$) δ 10.87 (s, 1H), 8.80 – 8.35 (m, 1H), 7.61 (dd, *J* = 7.8, 1.5 Hz, 1H), 7.48 (d, *J* = 1.6 Hz, 1H), 7.41 – 7.19 (m, 1H), 6.85 (d, *J* = 8.0 Hz, 1H), 6.81 – 6.57 (m, 1H), 3.50 – 3.08 (m, 6H), 2.33 – 2.22 (m, 1H),2.17 – 1.88 (m, 2H), 1.86 – 1.54 (m, 2H); $^{13}$C NMR (101 MHz, DMSO) δ 163.15, 145.82, 134.26, 127.72, 118.18, 115.07, 114.88, 67.32, 58.10, 45.43, 45.37, 30.23, 18.56, 18.11.

HRMS (ESI+) m/z found 244.1439 [M+H]+ , $C_{15}H_{18}N_3O$ calculated 244.1450 (Δ = -4.5 ppm)

**(1S*, 2R*, 4S*)-7'-bromo-1'H-4-azaspiro[bicyclo[2.2.2]octane-2,2'-quinazolin]-4'(3'H)-one hydrochloride 3.72**

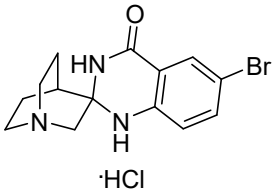


Quinuclidine-3-one (1.0 equiv, 1.46 mmol) was reacted with 2-amino-5-bromobenzamide (315 mg, 1.46 mmol) for 3 days to give a white solid (370 mg, 79%).

$^1$H NMR (400 MHz, DMSO-$d_6$) δ 11.09 (s, 1H), 8.81 (s, 1H), 7.97 (s, 1H), 7.66 (d, *J* = 2.4 Hz, 1H), 7.45 (dd, *J* = 8.6, 2.4 Hz, 1H), 6.89 (d, *J* = 8.6 Hz, 1H), 3.44 – 3.17 (m, 6H), 2.37 – 2.22 (m, 1H), 2.12 – 1.90 (m, 2H), 1.84 – 1.59 (m, 2H); $^{13}$C NMR (101 MHz, DMSO) δ 161.93, 144.99, 136.64, 129.73, 117.50, 116.45, 108.98, 67.50, 57.74, 45.35, 45.32, 30.40, 18.54, 18.02.

HRMS (ESI+) m/z found 324.0537 [M+H], $C_{14}H_{17}BrN_3O$ calculated 324.0535 (Δ = - 0.6 ppm)

**(1S*,2R*,4S*)-7'-chloro-1'H-4-azaspiro[bicyclo[2.2.2]octane-2,2'-quinazolin]-4'(3'H)-one hydrochloride 3.73**

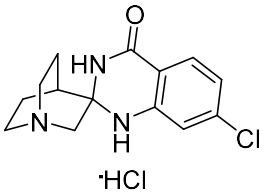


Quinuclidine-3-one (1.0 equiv, 0.80 mmol) was reacted with 2-amino-4-chlorobenzamide (136.2 mg, 0.80 mmol) with a reaction time of 3 days to give a white solid (173.0 mg, 79%) .

$^1$H NMR (400 MHz, DMSO-$d_6$) δ 10.98 (s, 1H), 8.74 (s, 1H), 8.04 (s, 1H), 7.60 (d, *J* = 8.3 Hz, 1H), 6.95 (d, *J* = 2.0 Hz, 1H), 6.75 (dd, *J* = 8.3, 2.0 Hz, 1H), 3.45 – 3.16 (m, 6H), 2.34 – 2.23 (m, 1H), 2.15 – 2.04 (m, 1H), 2.03 – 1.92 (m, 1H), 1.82 – 1.62 (m, 2H); $^{13}$C NMR (101 MHz, DMSO) δ 162.36, 146.95, 138.62, 129.72, 118.09, 114.21, 113.54, 67.63, 57.88, 55.37, 45.37, 30.61, 18.54, 18.06.

HRMS (ESI+) m/z found 278.1056 [M+H]+ , $C_{14}H_{17}ClN_3O$ calculated 278.1060 (Δ = -1.4 ppm).

**(1S*, 2R*, 4S*)-7'-fluoro-1'H-4-azaspiro[bicyclo[2.2.2]octane-2,2'-quinazolin]-4'(3'H)-one hydrochloride 3.74**

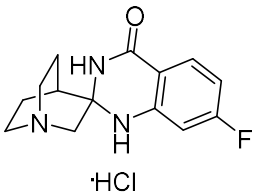


Quinuclidine-3-one (1.0 equiv, 1.41 mmol) was reacted with 2-amino-4-flurobenzamide (217.8 mg, 1.41 mmol) with a reaction time of 3 days to give a white solid (102.0 mg, 28 %).

$^1$H NMR (400 MHz, DMSO-$d_6$) δ 10.96 (s, 1H), 8.79 – 8.48 (m, 1H), 7.66 (dd, *J* = 8.6, 6.6 Hz, 1H), 6.65 (dd, *J* = 10.7, 2.5 Hz, 1H), 6.57 – 6.49 (m, 1H), 3.41 – 3.19 (m, 6H), 2.33 – 2.21 (m, 1H), 2.12 – 1.89 (m, 2H), 1.81 – 1.59 (m, 2H); $^{13}$C NMR (201 MHz, DMSO) δ 166.20 (d, *J* = 248.0 Hz), 162.38, 147.84 (d, *J* = 12.8 Hz), 130.73 (d, *J* = 11.5 Hz), 111.54, 105.65 (d, *J* = 23.0 Hz), 100.90 (d, *J* = 25.0 Hz), 67.66, 57.95, 45.38 (d, *J* = 5.5 Hz), 30.59, 18.54, 18.10.

$^{19}$F NMR (377 MHz, MeOD) δ -106.1

HRMS (ESI+) m/z found [M+H]+ 262.1357, $C_{14}H_{17}FN_3O$ calculated 262.1356 (Δ = 0.38 ppm)

**(1S*, 2R*, 4S*)-6'-methoxy-2',3',4',9'-tetrahydro-4-azaspiro[bicyclo[2.2.2]octane-2,1'-pyrido[3,4-b]indole] 3.76**

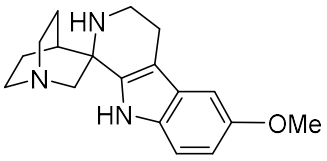

To a solution of Quinuclidine-3-one (150.0 mg, 1.2 mmol) in pyridine (3 mL) was added 5-Methoxytryptamine **3.75** (190.0 mg, 1.0 mmol), followed by dropwise addition of TMSCl (634 µL, 5.0 equiv). The mixture was heated to 90 °C for 12 hours under an $N_2$ atmosphere, and the solvent was removed under reduced pressure. The resulting residue was purified by column chromatography on silica gel using DCM/MeOH/$Et_3N$ (10:1:0.1 to 5:1:0.1) to yield the product as a white foam (190.0 mg, 64%).

$^1$H NMR (400 MHz, DMSO) δ 10.41 (s, 1H), 7.23 (d, *J* = 8.6 Hz, 1H), 6.82 (d, *J* = 2.5 Hz, 1H), 6.67 (dd, *J* = 8.7, 2.5 Hz, 1H), 3.73 (s, 3H), 3.22 – 3.13 (m, 3H), 3.10 – 3.03 (m, 1H), 3.02 – 2.93 (m, 1H), 2.85 – 2.76 (m, 1H), 2.74 – 2.66 (m, 2H), 2.65 – 2.57 (m, 1H), 2.57 – 2.45 (m, 2H), 2.14 – 2.02 (m, 1H), 2.02 – 1.93 (m, 1H), 1.90 – 1.76 (m, 1H), 1.53 – 1.39 (m, 1H), 1.29 – 1.12 (m, 1H); $^{13}$C NMR (101 MHz, DMSO) δ 153.45, 141.57, 131.04, 127.74, 112.03, 110.59, 107.86, 99.97, 61.93, 55.82, 53.15, 49.06, 46.90, 46.86, 39.16, 30.70, 23.11, 22.76.

HRMS (ESI+) m/z found 298.1919 [M+H]+, $C_{18}H_{24}N_3O$ calculated 298.1919 (Δ = 0 ppm).

## General procedure XII

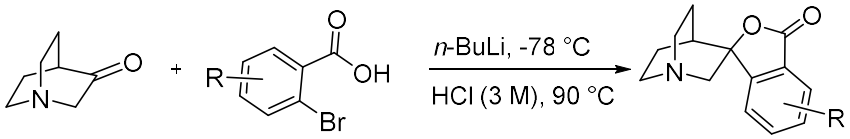


To a solution of the substituted *o*-bromo benzoic acid (2.0 mmol, 1.0 eqiuv.) in dry THF (5 mL) at -78 °C was added *n*-butyllithium (2.5 M in hexane, 1.6 mL, 4.0 mmol) over 15 mins. The resulting solution was stirred for an additional 2 hours at -78 °C before 3-Quinuclidone **16** (250.2 mg, 2.0 mmol) dissolved in dry THF (3 mL) was added dropwise over 15 mins. The mixture was stirred for 2 hours at -78 °C, then warmed to room temperature, $H_2O$ (15 mL) and diethyl ether (10 mL) were added sequentially, the basic layer was acidified with 3 M HCl to pH (2-3). The mixture was stirred for 1 hour at 90 °C before cooling to ambient temperature, diethyl ether (10 mL) was added. The acidic layer was washed with excessive saturated $NaHCO_3$ and extracted with DCM (2× 30 mL), the collected organic layer was dried over $Na_2SO_4$, and concentrated in vacuo to yield a solid product without further purification.

**(1R*,2S*,4R*)-6'-methyl-3'H-4-azaspiro[bicyclo[2.2.2]octane-2,1'-isobenzofuran]-3'-one 3.84**

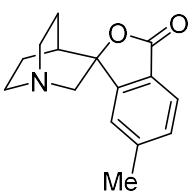

white solid (40.6 mg, 17%).

$^1$H NMR (400 MHz, $CDCl_3$) δ 7.74 (d, *J* = 7.8 Hz, 1H), 7.44 – 7.28 (m, 2H), 3.35 – 3.22 (m, 2H), 3.13 – 2.96 (m, 4H), 2.50 (s, 3H), 2.34 – 2.21 (m, 1H), 2.18 – 2.06 (m, 1H), 1.89 (s, 1H), 1.81 – 1.69 (m, 1H), 1.58 – 1.46 (m, 1H); $^{13}$C NMR (101 MHz, $CDCl_3$) δ 169.97, 153.23, 145.39, 130.48, 125.86, 123.81, 122.80, 86.76, 60.49, 46.85, 46.53, 32.38, 22.69, 22.46, 22.43.

HRMS (ESI+) m/z found 244.1329 [M+H]+, $C_{15}H_{18}NO_2$ calculated 244.1338 (Δ = -3.7 ppm).

**(1R*,2S*,4R*)-6'-fluoro-3'H-4-azaspiro[bicyclo[2.2.2]octane-2,1'-isobenzofuran]-3'-one 3.85**

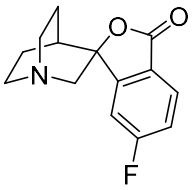

white solid (63.3 mg, 26%).

$^{1}$H NMR (400 MHz, $CDCl_3$) δ 7.91 – 7.77 (m, 1H), 7.34 – 7.09 (m, 2H), 3.34 – 3.20 (m, 2H), 3.11 – 2.92 (m, 4H), 2.31 – 2.17 (m, 1H), 2.09 – 1.97 (m, 1H), 1.95 – 1.88 (m, 1H), 1.82 – 1.69 (m, 1H), 1.60 – 1.45 (m, 1H); $^{13}$C NMR (101 MHz, $CDCl_3$) δ 168.21 (d, *J* = 80.2 Hz), 155.38 (d, *J* = 9.4 Hz), 128.40 (d, *J* = 10.6 Hz), 122.40 (d, *J* = 1.6 Hz), 117.41 (d, *J* = 23.9 Hz), 109.89 (d, *J* = 24.7 Hz), 86.53, 60.41, 46.75, 46.45, 32.35, 22.56, 22.27. $^{19}$F NMR (377 MHz, $CDCl_3$) δ -102.4.

HRMS (ESI+) m/z found 248.1077 [M+H]+ , $C_{14}H_{15}FNO_2$ calculated 248.1097 (Δ = -8.1 ppm).

**(1R*,2S*,4R*)-4-azaspiro[bicyclo[2.2.2]octane-2,2'-chroman]-4'-one 3.80**

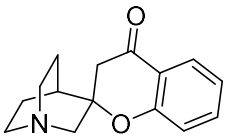

Quinuclidine-3-one (1.0 equiv, 0.87 mmol) was reacted with 2'-hydroxyacetophenone (117.9 mg, 0.87mmol) at reflux for 24 hours to give an amber crystal as the product according to the General Procedure IX (110.0 mg, 52.0%) .

$^{1}$H NMR (400 MHz, $CDCl_3$) δ 7.90 – 7.80 (m, 1H), 7.59 – 7.42 (m, 1H), 7.06 – 6.90 (m, 2H), 3.30 – 3.23 (m, 1H), 3.13 – 3.03 (m, 1H), 3.00 – 2.79 (m, 6H), 2.27 – 2.20 (m, 1H), 2.07 – 1.96 (m, 1H), 1.70 – 1.60 (m, 2H), 1.48 – 1.35 (m, 1H); $^{13}$C NMR (101 MHz, $CDCl_3$) δ 192.10, 159.74, 136.71, 126.74, 121.54, 121.03, 118.51, 80.73, 60.88, 46.69, 46.66, 45.32, 27.91, 22.32, 20.96.

HRMS (ESI+) m/z found 244.1329 [M+H]+, $C_{15}H_{18}NO_2$ calculated 244.1338 (Δ = -3.7 ppm).

**(1R*,2S*,4R*)-6'-fluoro-4-azaspiro[bicyclo[2.2.2]octane-2,2'-chroman]-4'-one 3.81**

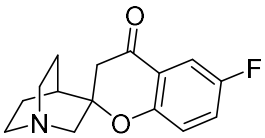

Quinuclidine-3-one (1.0 equiv, 1.3 mmol) was reacted with 4'-fluoro-2'-hydroxyacetophenone (201.0 mg, 1.30 mmol) at reflux to give an amber crystal as the product according to the General Procedure IX (291.0 mg, 83%) .

$^{1}$H NMR (400 MHz, $CDCl_3$) δ 7.53 – 7.45 (m, 1H), 7.24 – 7.18 (m, 1H), 6.99 – 6.94 (m, 1H), 3.23 – 3.16 (m, 1H), 3.05 – 2.96 (m, 1H), 2.94 – 2.71 (m, 6H), 2.22 – 2.13 (m, 1H), 1.97 – 1.86 (m, 1H), 1.67 – 1.54 (m, 2H), 1.41 – 1.30 (m, 1H); $^{13}$C NMR (101 MHz, $CDCl_3$) δ 191.59 (d, *J* = 1.7 Hz), 157.32 (d, *J* = 242.1 Hz), 156.03 (d, *J* = 1.7 Hz), 124.06 (d, *J* = 24.4 Hz), 121.46 (d, *J* = 6.4 Hz), 120.11 (d, *J* = 7.3 Hz), 111.83 (d, *J* = 23.4 Hz).

$^{19}$F NMR (377 MHz, $CDCl_3$) δ -121.6.

HRMS (ESI+) m/z found 262.1239 [M+H]+ , $C_{15}H_{17}FNO_2$ calculated 262.1243 (Δ = -1.5 ppm).

**(1R*,2S*,4R*)-6'-bromo-4-azaspiro[bicyclo[2.2.2]octane-2,2'-chroman]-4'-one 3.82**

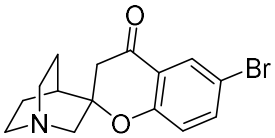

Quinuclidine-3-one (1.0 equiv, 1.2 mmol) was reacted with 5'-bromo-2'-hydroxyacetophenone (253.4 mg, 1.2 mmol) at reflux to give an amber crystal as the product according to the General Procedure IX (274.0 mg, 72%).

$^{1}$H NMR (400 MHz, $CDCl_3$) δ 7.99 – 7.89 (m, 1H), 7.61 – 7.52 (m, 1H), 6.93 – 6.86 (m, 1H), 3.24 – 3.17 (m, 1H), 3.05 – 2.97 (m, 1H), 2.95 – 2.73 (m, 6H), 2.23 – 2.14 (m, 1H), 1.97 – 1.86 (m, 1H),

1.67 – 1.53 (m, 2H), 1.41 – 1.31 (m, 1H); $^{13}$C NMR (101 MHz, $CDCl_3$) δ 191.14, 158.75, 139.17, 129.16, 122.25, 120.55, 114.00, 81.55, 61.04, 46.67, 46.65, 44.99, 27.82, 22.54, 21.10.

HRMS (ESI+) m/z found 324.0423 [M+H]+, $C_{15}H_{17}BrNO_2$ calculated 322.0443 (Δ = -6.2 ppm).

**(1R*,2S*,4R*)-7'-methoxy-4-azaspiro[bicyclo[2.2.2]octane-2,2'-chroman]-4'-one 3.83**

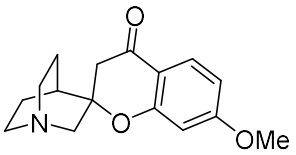

Quinuclidine-3-one (1.0 equiv, 10.0 mmol) was reacted with 4'-methoxyl-2'-hydroxyacetophenone (1.66 g, 10.0 mmol) for 41 hours to yield a yellow solid according to the General Procedure IX (1.83 g, 70%).

$^1$H NMR (400 MHz, $CDCl_3$) δ 7.78 (d, *J* = 8.8 Hz, 1H), 6.56 (dd, *J* = 8.8, 2.4 Hz, 1H), 6.42 (d, *J* = 2.4 Hz, 1H), 3.84 (s, 3H), 3.20 (dd, *J* = 14.5, 2.2 Hz, 1H), 3.13 – 2.97 (m, 1H), 2.95 – 2.71 (m, 6H), 2.28 – 2.15 (m, 1H), 2.10 – 1.86 (m, 1H), 1.70 – 1.51 (m, 1H), 1.47 – 1.28 (m, 1H); $^{13}$C NMR (101 MHz, $CDCl_3$) δ 190.66, 166.61, 161.86, 128.43, 114.93, 109.68, 101.55, 81.28, 61.14, 55.78, 46.74, 46.68, 45.09, 28.18, 22.68, 21.18.

HRMS (ESI+) m/z found 274.1443 [M+H]+, $C_{16}H_{20}NO_3$ calculated 274.1443 (Δ = 0 ppm).

**(1R*,2S*,4R*)-7'-(benzyloxy)-4-azaspiro[bicyclo[2.2.2]octane-2,2'-chroman]-4'-one 4.01**

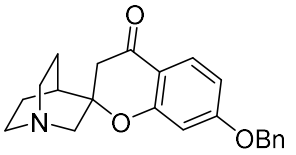

Quinuclidine-3-one (1.0 equiv, 0.5 mmol) was reacted with 4'-benzyloxy-2'-hydroxyacetophenone (242.0 mg, 1.0 mmol) for 13 hours to yield a white solid according to the General Procedure IX (40.0 mg, 23%).

$^1$H NMR (400 MHz, $CDCl_3$) δ 7.79 (d, *J* = 8.8 Hz, 1H), 7.44 – 7.31 (m, 5H), 6.63 (dd, *J* = 8.8, 2.4 Hz, 1H), 6.52 (d, *J* = 2.4 Hz, 1H), 5.09 (s, 2H), 3.19 (dd, *J* = 14.6, 2.1 Hz, 1H), 3.08 – 2.97 (m, 1H), 2.94 – 2.69 (m, 6H), 2.23 – 2.16 (m, 1H), 2.03 – 1.92 (m, 1H), 1.67 – 1.57 (m, 2H), 1.45 – 1.31 (m, 1H); $^{13}$C NMR (101 MHz, $CDCl_3$) δ 190.75, 165.66, 161.84, 136.01, 128.82, 128.46, 128.44, 127.65, 115.13, 110.13, 102.57, 81.38, 70.45, 61.22, 46.75, 46.70, 45.11, 28.16, 22.76, 21.24.

HRMS (ESI+) m/z found 350.1763 [M+H]+ , $C_{22}H_{24}NO_3$ calculated 350.1756 (Δ = 2.0 ppm).

**(1R*,2S*,4R*)-7'-(cyclopropylmethoxy)-4-azaspiro[bicyclo[2.2.2]octane-2,2'-chroman]-4'-one 4.02**

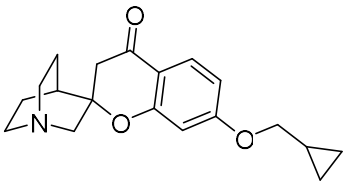

Quinuclidine-3-one (1.0 equiv, 1.0 mmol) was reacted with 5'cyclopropylmethoxy-2'-hydroxyacetophenone (206.2 mg, 1.0 mmol) for 17 hours, yellow solid according to the General Procedure IX (198.2 mg, 63%).

$^1$H NMR (400 MHz, $CDCl_3$) δ 7.69 (d, *J* = 8.7 Hz, 1H), 6.49 (dd, *J* = 8.8, 2.4 Hz, 1H), 6.34 (d, *J* = 2.3 Hz, 1H), 3.77 (d, *J* = 6.9 Hz, 2H), 3.11 (dd, *J* = 14.6, 2.1 Hz, 1H), 2.98 – 2.89 (m, 1H), 2.87 – 2.64 (m, 6H), 2.12 (q, *J* = 3.1 Hz, 1H), 1.96 – 1.85 (m, 1H), 1.60 – 1.47 (m, 2H), 1.35 – 1.25 (m, 1H), 1.24 – 1.13 (m, 1H), 0.65 – 0.54 (m, 2H), 0.36 – 0.23 (m, 2H); $^{13}$C NMR (101 MHz, $CDCl_3$) δ 190.69, 165.97, 161.83, 128.32, 114.77, 109.99, 102.02, 81.26, 73.24, 61.18, 46.71, 46.66, 45.06, 28.14, 25.76, 22.73, 21.22, 10.09, 3.36, 3.34

HRMS (ESI+) m/z found [M+H]+ 314.1752 , $C_{19}H_{24}NO_3$ calculated 314.1756 (Δ = -1.3 ppm).

**(1R*,2S*,4R*)-7'-hydroxy-4-azaspiro[bicyclo[2.2.2]octane-2,2'-chroman]-4'-one 4.03**

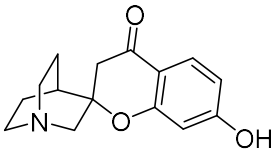

Quinuclidine-3-one (1.0 equiv, 1.0 mmol) was reacted with 5'-hydroxyl-2'-hydroxyacetophenone (1.52 g, 1.0 mmol) for 5 days to yield a white solid according to the General Procedure IX (142.5 mg, 55%).

$^1$H NMR (400 MHz, MeOD) δ 7.67 (d, *J* = 8.7 Hz, 1H), 6.47 (dd, *J* = 8.7, 2.3 Hz, 1H), 6.35 (d, *J* = 2.3 Hz, 1H), 3.14 (dd, *J* = 14.5, 2.1 Hz, 1H), 3.06 – 2.77 (m, 7H), 2.25 – 2.17 (m, 1H), 2.08 – 1.96 (m, 1H), 1.75 – 1.65 (m, 2H), 1.57 – 1.41 (m, 1H); $^{13}$C NMR (101 MHz, MeOD) δ 192.68, 163.43, 129.36, 114.73, 111.85, 104.43, 81.77, 61.22, 49.64, 47.30, 47.10, 45.33, 29.11, 22.86, 21.64.

HRMS (ESI+) m/z found [M+H]+ 260.1284 , $C_{15}H_{18}NO_3$ calculated 260.1287 (Δ = -1.1 ppm).

**(1R*,2S*,4R*)-7'-methyl-4-azaspiro[bicyclo[2.2.2]octane-2,2'-chroman]-4'-one 4.04**

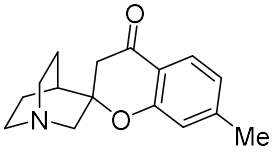

Quinuclidine-3-one (1.0 equiv, 0.5 mmol) was reacted with 4'-methyl-2'-hydroxyacetophenone (75.1 mg, 0.5.0 mmol) for 34.5 hours to yield a yellow solid according to the General Procedure IX (96.7 mg, 75%).

$^1$H NMR (400 MHz, $CDCl_3$) δ 7.71 (d, *J* = 7.8 Hz, 1H), 6.87 – 6.65 (m, 2H), 3.20 (dd, *J* = 14.6, 2.2 Hz, 1H), 3.09 – 2.97 (m, 1H), 2.95 – 2.73 (m, 6H), 2.34 (s, 3H), 2.24 – 2.10 (m, 1H), 2.03 – 1.91 (m, 1H), 1.67 – 1.55 (m, 2H), 1.44 – 1.30 (m, 1H); $^{13}$C NMR (101 MHz, $CDCl_3$) δ 191.82, 159.85, 148.11, 126.52, 122.71, 118.77, 118.49, 80.76, 61.07, 46.70, 46.66, 45.29, 28.00, 22.53, 22.06, 21.11.

HRMS (ESI+) m/z found 258.1496 [M+H]+, $C_{16}H_{20}NO_2$ calculated 258.1494 (Δ = 0.77 ppm).

**(1R*,2S*,4R*)-7'-bromo-4-azaspiro[bicyclo[2.2.2]octane-2,2'-chroman]-4'-one 4.05**

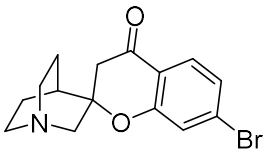

Quinuclidine-3-one (1.0 equiv, 5.0 mmol) was reacted with 4'-bromo-2'-hydroxyacetophenone (1.08 g, 5.0 mmol) at reflux for 24 hours to give an amber crystal according to General Procedure IX (1.142 g, 71%).

$^1$H NMR (400 MHz, DMSO) δ 7.63 (d, *J* = 8.3 Hz, 1H), 7.37 (d, *J* = 1.8 Hz, 1H), 7.24 (dd, *J* = 8.4, 1.8 Hz, 1H), 3.07 – 2.91 (m, 3H), 2.88 – 2.71 (m, 3H), 2.67 (t, *J* = 8.2 Hz, 2H), 2.05 – 2.00 (m, 1H), 1.86 – 1.74 (m, 1H), 1.60 – 1.44 (m, 2H), 1.35 – 1.25 (m, 1H);$^{13}$C NMR (101 MHz, DMSO) δ 191.82, 160.30, 130.09, 127.99, 124.88, 121.63, 120.23, 82.55, 60.62, 46.48, 46.26, 44.79, 28.09, 22.34, 21.08.

HRMS (ESI+) m/z found [M+H]+ 322.0423, $C_{15}H_{17}BrNO_2$ calculated 322.0443 (Δ = -6.2 ppm).

**(1R*,2S*,4R*)-7'-phenyl-4-azaspiro[bicyclo[2.2.2]octane-2,2'-chroman]-4'-one formate 4.06**

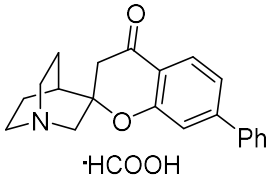

To a 10 mL oven-dried vial containing a magnetic stirring bar, compound **4.05** (96.6 mg, 0.3 mmol), $K_2CO_3$ (62.2 mg, 0.45 mmol), $Pd(PPh_3)_4$ (6.9 mg, 2.0 mol%) and phenylboronic acid (54.8 mg, 0.45 mmol) was added 5 mL (toluene:$H_2O$ = 9:1). The mixture was heated to 100 °C for 48 hours under argon atmosphere, the solvent was removed under reduced pressure, and the crude was purified by preparative HPLC to yield the title product formate salt as white power (48.4 mg, 39%).

$^1$H NMR (400 MHz, DMSO) δ 8.32 (s, 2H), 7.80 – 7.70 (m, 3H), 7.52 – 7.40 (m, 3H), 7.39 – 7.33 (m, 2H), 3.09 – 2.94 (m, 3H), 2.93 – 2.67 (m, 5H), 2.14 – 2.07 (m, 1H), 1.95 – 1.82 (m, 1H), 1.66 – 1.48 (m, 2H), 1.41 – 1.27

(m, 1H).[13]C NMR (101 MHz, DMSO) δ 192.01, 160.11, 148.52, 138.93, 129.52, 129.23, 127.50, 126.92, 120.20, 119.92, 116.53, 81.45, 60.28, 46.31, 46.09, 44.86, 28.00, 22.02, 20.88.

HRMS (ESI+) m/z found 320.1642 [M+H]+, $C_{21}H_{22}NO_2$ calculated 320.1651 (Δ = -2.8 ppm).

**(1R*,2S*,4R*)-7'-(4-methoxyphenyl)-4-azaspiro[bicyclo[2.2.2]octane-2,2'-chroman]-4'-one 4.07**

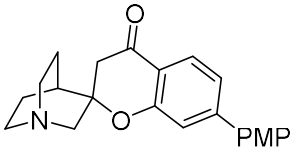


To a 10 mL oven-dried vial containing a magnetic stirring bar, compound **4.05** (96.6 mg, 0.3 mmol), $K_2CO_3$ (62.2mg, 0.45 mmol), $Pd(PPh_3)_4$ (13.6 mg, 5.0 mol%) and 4-methoxyl phenylboronic acid (68.4 mg, 0.45 mmol) were added dry DMF (3.0 mL). The reaction mixture was stirred at 110 °C for 24 hours under an argon atmosphere, the solvent was removed under reduced pressure, and the crude was purified by recrystallization with MeOH to yield a white solid (56.1 mg, 51%).

[1]H NMR (400 MHz, $CDCl_3$) δ 7.87 (d, *J* = 8.2 Hz, 1H), 7.61 – 7.52 (m, 2H), 7.22 (dd, *J* = 8.2, 1.7 Hz, 1H), 7.17 (d, *J* = 1.7 Hz, 1H), 7.04 – 6.93 (m, 2H), 3.86 (s, 3H), 3.27 (d, *J* = 14.3 Hz, 1H), 3.15 – 3.02 (m, 1H), 3.00 – 2.71 (m, 6H), 2.26 (t, *J* = 3.2 Hz, 1H), 2.04 (t, *J* = 12.1 Hz, 1H), 1.72 – 1.59 (m, 2H), 1.46 – 1.35 (m, 1H); [13]C NMR (101 MHz, $CDCl_3$) δ 191.72, 160.38, 160.13, 149.19, 131.94, 128.50, 127.18, 119.99, 119.30, 115.85, 114.54, 80.93, 61.08, 55.54, 46.74, 46.69, 45.34, 28.05, 22.51, 21.12.

HRMS (ESI+) m/z found [M+H]+ 350.1754 , $C_{22}H_{23}NO_3$ calculated 350.1756 (Δ = -0.6 ppm).

**(1R*,2S*,4R*)-7'-(pyrrolidin-1-yl)-4-azaspiro[bicyclo[2.2.2]octane-2,2'-chroman]-4'-one 4.08**

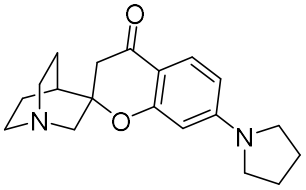


Quinuclidine-3-one (1.0 equiv, 1.0 mmol) was reacted with 5'-fluoro-2'-hydroxyacetophenone (154.1 mg, 1.0 mmol) at reflux for 24 hours to give an amber crystal as the product according to the General Procedure IX (190.8 mg, 61%).

[1]H NMR (400 MHz, $CDCl_3$) δ 7.69 (d, *J* = 8.8 Hz, 1H), 6.20 (dd, *J* = 8.8, 2.3 Hz, 1H), 5.95 (d, *J* = 2.3 Hz, 1H), 3.38 – 3.30 (m, 4H), 3.15 (dd, *J* = 14.5, 2.1 Hz, 1H), 3.05 – 2.95 (m, 1H), 2.92 – 2.70 (m, 6H), 2.23 – 2.18 (m, 1H), 2.06 – 1.97 (m, 5H), 1.68 – 1.52 (m, 2H), 1.40 – 1.29 (m, 1H); [13]C NMR (101 MHz, $CDCl_3$) δ 189.73, 161.65, 153.80, 128.34, 110.50, 106.72, 97.98, 80.48, 61.35, 47.81, 46.81, 46.73, 45.09, 28.44, 25.48, 22.92, 21.34.

HRMS (ESI+) m/z found 313.1915 [M+H]+ , $C_{19}H_{25}N_2O_2$ calculated 313.1916 (Δ = -0.32ppm).

**(1R*,2S*,4R*)-7'-(methylamino)-4-azaspiro[bicyclo[2.2.2]octane-2,2'-chroman]-4'-one 4.09**

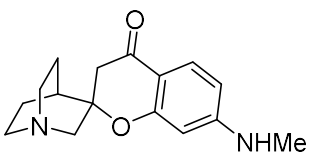


Quinuclidine-3-one (1.0 equiv, 0.45 mmol) was reacted with 4'-methylamino -2'-hydroxyacetophenone (74.2 mg, 0.45 mmol) for 3 days to yield a yellow solid according to the General Procedure IX (66.6 mg, 45%)

[1]H NMR (400 MHz, DMSO-$d_6$) δ 7.42 (d, *J* = 8.7 Hz, 1H), 6.76 (d, *J* = 4.9 Hz, 1H), 6.23 (dd, *J* = 8.7, 2.2 Hz, 1H), 5.95 (d, *J* = 2.1 Hz, 1H), 2.95 – 2.59 (m, 11H), 2.06 – 1.98 (m, 1H), 1.93 – 1.76 (m, 1H), 1.60 – 1.41 (m, 2H), 1.33 – 1.22 (m, 1H); [13]C NMR (101 MHz, DMSO-$d_6$) δ 189.03, 162.12, 156.99, 127.58, 121.23, 110.37, 96.69, 80.77, 61.20, 46.64, 46.41, 44.81, 29.59, 28.50, 22.81, 21.35.

HRMS (ESI+) m/z found 273.1599 [M+H]+ , $C_{16}H_{21}N_2O_2$ calculated 273.1603 (Δ = -1.5 ppm).

**(1R*,2S*,4R*)-7'-amino-4-azaspiro[bicyclo[2.2.2]octane-2,2'-chroman]-4'-one 4.10**

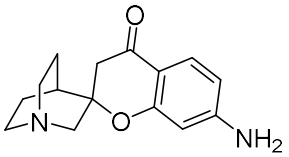

Quinuclidine-3-one (1.0 equiv, 1.0 mmol) was reacted with 4'-amino-2'-hydroxyacetophenone (151.2 mg, 1.0 mmol) for 24 hours to yield a yellow solid (71.0 mg, 21%) according to the General Procedure IX.

$^1$H NMR (400 MHz, MeOD) δ 7.56 (d, *J* = 8.7 Hz, 1H), 6.32 (dd, *J* = 8.7, 2.1 Hz, 1H), 6.15 (d, *J* = 2.1 Hz, 1H), 3.15 (dd, *J* = 14.3, 2.1 Hz, 1H), 3.05 – 2.79 (m, 7H), 2.21 (q, *J* = 3.1 Hz, 1H), 2.12 – 2.01 (m, 1H), 1.76 – 1.67 (m, 2H), 1.56 – 1.46 (m, 1H); $^{13}$C NMR (101 MHz, MeOD) δ 191.73, 163.50, 158.84, 129.31, 111.82, 110.22, 100.71, 81.01, 61.14, 47.31, 47.11, 45.14, , 29.25, 22.80, 21.52.

HRMS (ESI+) m/z found 259.1442 [M+H]+ , $C_{15}H_{19}N_2O_2$ calculated 259.1447 (Δ = -1.9 ppm).

**(1R*,2S*,4R*)-7'-(dimethylamino)-4-azaspiro[bicyclo[2.2.2]octane-2,2'-chroman]-4'-one 4.11**

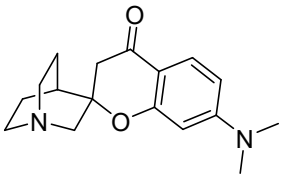

Quinuclidine-3-one (1.0 equiv, 0.4 mmol) was reacted with 4'-dimethylamino-2'-hydroxyacetophenone (50.0 mg, 0.4 mmol) for 3 days to yield a yellow solid according to the General Procedure IX (57.2 mg, 50%).

$^1$H NMR (400 MHz, $CDCl_3$) δ 7.72 (dd, *J* = 9.0, 0.5 Hz, 1H), 6.36 (dd, *J* = 9.0, 2.4 Hz, 1H), 6.08 (d, *J* = 2.4 Hz, 1H), 3.27 (dd, *J* = 14.6, 2.0 Hz, 1H), 3.17 – 3.07 (m, 1H), 3.05 (s, 6H), 2.98 – 2.84 (m, 4H), 2.80 (d, *J* = 3.9 Hz, 2H), 2.33 – 2.22 (m, 1H), 2.17 – 2.05 (m, 1H), 1.77 – 1.63 (m, 2H), 1.51 – 1.41 (m, 1H); $^{13}$C NMR (101 MHz, $CDCl_3$) δ 189.12, 161.28, 156.41, 128.36, 110.62, 106.62, 98.10, 79.96, 60.58, 46.63, 46.53, 44.93, 40.24, 28.39, 22.17, 20.75.

HRMS (ESI+) m/z found 287.1758 [M+H]+, $C_{17}H_{23}N_2O_2$ calculated 287.1760 (Δ = -0.7 ppm).

**(1R*,2S*,4R*)-7'-methoxy-4-azaspiro[bicyclo[2.2.2]octane-2,2'-chromane] 4.12**

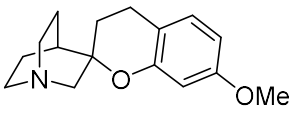

To a solution of compound **3.83** (81.9 mg, 0.3 mmol) in acetic acid (6.0 mL) was added zinc (588.4 mg, 9.0 mmol), the mixture was stirred at 80 °C under nitrogen atmosphere for 18 hours. The mixture was filtered off through a celite plug, the filtrate was concentrated, the resulting residue was added saturated $NaHCO_3$ (20 mL), and extracted with DCM (2×10 mL), the combined organic layer was dried with $NaSO_4$, the solvent was evaporated under reduced pressure to yield a brown oil compound (64.8 mg, 80%).$^1$H NMR (400 MHz, $CDCl_3$) δ 6.93 (d, *J* = 8.4 Hz, 1H), 6.44 (dd, *J* = 8.4, 2.6 Hz, 1H), 6.38 (d, *J* = 2.6 Hz, 1H), 3.75 (s, 3H), 3.11 – 2.98 (m, 2H), 2.97 – 2.65 (m, 6H), 2.15 – 2.07 (m, 1H), 2.05 – 1.99 (m, 1H), 1.98 – 1.91 (m, 2H), 1.74 – 1.58 (m, 2H), 1.42 – 1.34 (m, 1H) ; $^{13}$C NMR (101 MHz, $CDCl_3$) δ 159.34, 154.64, 129.86, 113.52, 107.33, 102.20, 75.43, 61.49, 55.42, 47.07, 46.64, 29.27, 28.07, 22.91, 21.41, 21.04.HRMS (ESI+) m/z found 260.1642 [M+H]+, $C_{16}H_{22}NO_2$ calculated 260.1651 (Δ = -3.5 ppm).

**(1R*,2S*,4R*)-7'-methoxy-4-azaspiro[bicyclo[2.2.2]octane-2,2'-chroman]-4'-ol 4.13**

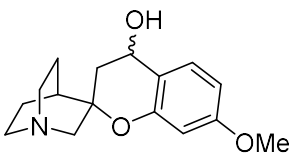

To a solution of **3.83** (47.8 mg, 1.75 mmol) in MeOH (10.0 mL) was added $NaBH_4$ (132.4 mg, 3.5 mmol) at 0 °C, the mixture was stirred at room temperature under nitrogen atmosphere overnight. After 24 hours, the reaction was quenched with saturated $NH_4Cl$ (20.0 mL) at 0 °C, the aqueous phase was extracted with

($CHCl_3$/isopropanol) several times. The collected organic layer was dried over $Na_2SO_4$ and concentered *in vacuo* to yield the product as a white solid (238.8 mg, 59%, d.r. 1:1).

$^1$H NMR (400 MHz, DMSO-$d_6$) δ 7.31 – 7.17 (m, 1H), 6.52 – 6.44 (m, 1H), 6.31 (dd, *J* = 6.0, 2.5 Hz, 1H), 5.25 (s, 1H), 4.69 – 4.54 (m, 1H), 3.69 (d, *J* = 2.2 Hz, 3H), 2.91 – 2.66 (m, 6H), 2.31 – 2.18 (m, 1H), 2.10 (dd, *J* = 13.9, 5.4 Hz, 0.5H), 1.97 – 1.89 (m, 1.5H), 1.87 – 1.76 (m, 1H), 1.76 – 1.61 (m, 1H), 1.60 – 1.47 (m, 1H), 1.35 – 1.25 (m, 1H). $^{13}$C NMR (101 MHz, $CDCl_3$) δ 160.89, 160.87, 153.41, 152.96, 130.38, 129.80, 117.01, 116.96, 108.70, 108.56, 101.98, 101.93, 75.23, 74.74, 62.76, 62.31, 60.31, 58.84, 55.50, 46.73, 46.55, 46.25, 46.16, 38.21, 38.10, 30.21, 28.21, 21.78, 21.07, 20.01, 19.53.

HRMS (ESI+) m/z found 276.1592 [M+H]+ , $C_{16}H_{22}NO_3$ calculated 276.1600 (Δ = -3.2 ppm).

**(1R*,2S*,4R*)-7'-methoxy-4-azaspiro[bicyclo[2.2.2]octane-2,2'-chromene] 4.14**

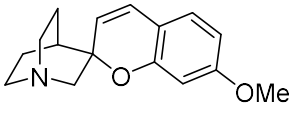


To a solution of **3.83** (79.0 mg, 0.25 mmol) in dioxane (10 mL) was added *p*-TsOH·$H_2O$ (43.0 mg, 0.25 mmol) , the mixture was stirred at 80 °C for 26 hours before quenching with 5% NaOH (10 mL). The mixture was extracted with EtOAc (10 mL), the organic phase was dried over $NaSO_4$, and concentrated in vacuo, the resulting crude was purified by column chromatography on silica gel (EtOAc/MeOH/$Et_3N$ = 1:10:0.1) to give a brown oil (57.8 mg, 75%). $^1$H NMR (400 MHz, $CDCl_3$) δ 7.05 – 6.73 (m, 1H), 6.49 – 6.31 (m, 3H), 5.68 (d, *J* = 9.7 Hz, 1H), 3.77 (s, 3H), 3.17 (dd, *J* = 14.5, 2.1 Hz, 1H), 3.10 – 2.71 (m, 5H), 2.14 – 1.99 (m, 2H), 1.73 – 1.60 (m, 1H), 1.51 – 1.39 (m, 1H), 1.33 1.26 (m, 1H); $^{13}$C NMR (101 MHz, $CDCl_3$) δ 160.92, 153.92, 127.09, 126.57, 124.17, 115.40, 107.02, 102.19, 77.01, 63.22, 55.44, 47.00, 46.98, 30.61, 22.10, 20.79.

HRMS (ESI+) m/z found 258.1489 [M+H]+ , $C_{16}H_{20}NO_2$ calculated 258.1494 (Δ = -1.9 ppm).

**(1R*,2S*,4R*)-7'-methoxy-4-methyl-4'-oxo-4-azaspiro[bicyclo[2.2.2]octane-2,2'-chroman]-4-ium 4.15**

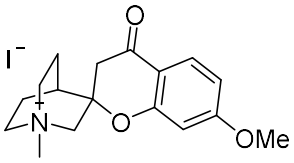


To a solution of **3.83** (136.6 mg, 0.50 mmol) in dry acetone (1.5 mL) was added MeI (322.5 μL, 10.0 mmol), and the mixture was stirred at room temperature overnight. The solvent was removed under reduced pressure after 12 hours, and the crude was washed with acetone and dried *in vacuo* to yield the title product as white power (159.0 mg, 77%).

$^1$H NMR (400 MHz, DMSO) δ 7.70 (d, *J* = 8.8 Hz, 1H), 6.71 (dd, *J* = 8.8, 2.4 Hz, 1H), 6.65 (d, *J* = 2.4 Hz, 1H), 3.84 (s, 3H), 3.77 – 3.60 (m, 2H), 3.58 – 3.34 (m, 4H), 3.15 (d, *J* = 17.0 Hz, 1H), 3.08 – 2.91 (m, 4H), 2.41 (d, *J* = 3.5 Hz, 1H), 2.19 (d, *J* = 6.8 Hz, 1H), 2.01 – 1.90 (m, 2H), 1.88 – 1.75 (m, 1H).

$^{13}$C NMR (101 MHz, DMSO) δ 188.85, 166.54, 160.56, 128.29, 114.64, 110.68, 102.51, 79.82, 65.95, 56.46, 55.82, 55.73, 51.36, 43.76, 27.64, 20.19, 19.62.

HRMS (ESI+) m/z found 288.1600[M]+, $C_{17}H_{23}NIO_3$ calculated 288.1594 (Δ = 2.1 ppm).

**(1R*,2S*,4R*)-4-azaspiro[bicyclo[2.2.2]octane-2,6'-[1,3]dioxolo[4,5-g]chromen]-8'(7'H)-one 4.16**

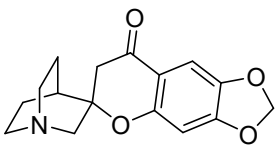


Quinuclidine-3-one (1.0 equiv, 1.0 mmol) was reacted with 1-(6-hydroxybenzo[d][1,3]dioxol-5-yl)ethan-1-one (180.0 mg, 1.0 mmol) for 3 days to yield a yellow solid according to the General Procedure IX (231.4 mg, 80%).

$^1$H NMR (400 MHz, DMSO-$d_6$) δ 7.06 (s, 1H), 6.67 (s, 1H), 6.07 (dd, $J$ = 6.4, 0.8 Hz, 2H), 2.94 – 2.88 (m, 1H), 2.87 – 2.67 (m, 5H), 2.64 (t, $J$ = 7.8 Hz, 2H), 2.04 (t, $J$ = 3.2 Hz, 1H), 1.86 – 1.71 (m, 1H), 1.60 – 1.40 (m, 2H), 1.33 – 1.22 (m, 1H); $^{13}$C NMR (101 MHz, DMSO-$d_6$) δ 190.46, 157.67, 154.68, 142.97, 114.30, 102.99, 102.63, 99.38, 81.94, 60.89, 46.55, 46.35, 44.47, 27.99, 22.59, 21.22.

HRMS (ESI+) m/z found 288.1235[M+H]+ , $C_{16}H_{18}NO_4$ calculated 288.1236 (Δ = -0.42 ppm).

**(1R*,2S*,4R*)-5',7'-dimethoxy-4-azaspiro[bicyclo[2.2.2]octane-2,2'-chroman]-4'-one 4.17**

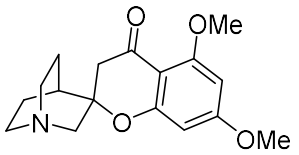


Quinuclidine-3-one (1.0 equiv, 1.0 mmol) was reacted with 4', 6'-dimethoxyl-2'-hydroxyacetophenone (1.96 g, 1.0 mmol) for 14 hours to yield a yellow solid according to the according to the General Procedure IX (200.6 mg, 66%).

$^1$H NMR (400 MHz, $CDCl_3$) δ 6.07 (d, $J$ = 2.3 Hz, 1H), 6.03 (d, $J$ = 2.3 Hz, 1H), 3.86 (s, 3H), 3.82 (s, 3H), 3.13 (dd, $J$ = 14.5, 2.1 Hz, 1H), 3.04 – 2.94 (m, 1H), 2.93 – 2.68 (m, 6H), 2.26 – 2.16 (m, 1H), 2.05 – 1.92 (m, 1H), 1.65 – 1.53 (m, 2H), 1.43 – 1.31 (m, 1H); $^{13}$C NMR (101 MHz, $CDCl_3$) δ 189.29, 166.31, 163.36, 162.04, 105.87, 94.10, 92.75, 80.44, 60.99, 56.21, 55.70, 46.75, 46.66, 46.64, 28.21, 22.69, 21.13.

HRMS (ESI+) m/z found 304.1549 [M+H]+, $C_{17}H_{22}NO_4$ calculated 304.1549 (Δ = 0 ppm).

**(1R*,2S*,4R*)-7',8'-dimethoxy-4-azaspiro[bicyclo[2.2.2]octane-2,2'-chroman]-4'-one 4.18**

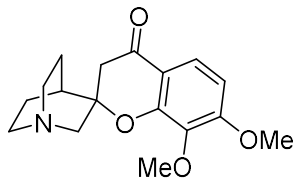


Quinuclidine-3-one (1.0 equiv, 1.0 mmol) was reacted with 3', 4'-dimethoxyl-2'-hydroxyacetophenone (1.96 g, 1.0 mmol) for 18 hours to yield a yellow solid according to the General Procedure IX (208.5 mg, 69%).

$^1$H NMR (400 MHz, $CDCl_3$) δ 7.60 (d, $J$ = 8.9 Hz, 1H), 6.59 (d, $J$ = 8.9 Hz, 1H), 3.90 (s, 3H), 3.88 (s, 3H), 3.20 (dd, $J$ = 14.5, 2.1 Hz, 1H), 3.08 – 2.98 (m, 1H), 2.94 – 2.70 (m, 6H), 2.21 – 2.15 (m, 1H), 2.12 – 2.00 (m, 1H), 1.66 – 1.54 (m, 2H), 1.43 – 1.31 (m, 1H); $^{13}$C NMR (101 MHz, $CDCl_3$) δ 191.14, 159.19, 153.75, 137.63, 122.53, 116.27, 105.36, 81.67, 61.13, 61.07, 56.28, 46.79, 46.63, 45.33, 28.64, 22.82, 21.24.

HRMS (ESI+) m/z found 304.1549 [M+H]+ , $C_{17}H_{22}NO_4$ calculated 304.1549 (Δ = 0 ppm).

**(1R*,2S*,4R*)-6'-methoxy-4-azaspiro[bicyclo[2.2.2]octane-2,2'-chroman]-4'-one 4.19**

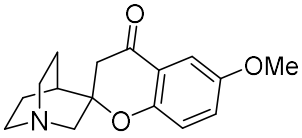


Quinuclidine-3-one **16** (1.0 equiv, 1.0 mmol) was reacted with 5'-methoxyl-2'-hydroxyacetophenone (166.2 mg, 1.0 mmol) for 17 hours to yield a yellow solid according to the General Procedure IX (185.0mg, 68%).

$^1$H NMR (400 MHz, $CDCl_3$) δ 7.26 (d, $J$ = 3.2 Hz, 1H), 7.09 (dd, $J$ = 9.0, 3.2 Hz, 1H), 6.91 (d, $J$ = 9.0 Hz, 1H), 3.78 (s, 3H), 3.18 (dd, $J$ = 14.5, 2.2 Hz, 1H), 3.05 – 2.96 (m, 1H), 2.93 – 2.71 (m, 6H), 2.21 – 2.16 (m, 1H), 2.01 – 1.89 (m, 1H), 1.64 – 1.56 (m, 2H), 1.39 – 1.30 (m, 1H); $^{13}$C NMR (101 MHz, $CDCl_3$) δ 192.41, 154.42, 154.07, 125.58, 120.82, 119.74, 107.25, 80.85, 61.18, 55.92, 46.74, 46.72, 45.30, 27.84, 22.66, 21.18.

HRMS (ESI+) m/z found 274.1442 [M+H]+ , $C_{16}H_{20}NO_3$ calculated 274.1443 (Δ = -0.36 ppm).

**(1R*,2S*,4R*)-5'-methoxy-4-azaspiro[bicyclo[2.2.2]octane-2,2'-chroman]-4'-one 4.20**

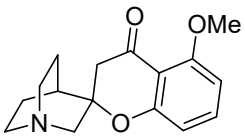

Quinuclidine-3-one (1.0 equiv, 1.0 mmol) was reacted with 6'-methoxyl-2'-hydroxyacetophenone (166.2 mg, 1.0 mmol) for 14 hours to yield a yellow solid according to the General Procedure IX (177.9 mg, 65%).

$^1$H NMR (400 MHz, $CDCl_3$) δ 7.37 (t, *J* = 8.4 Hz, 1H), 6.57 (dd, *J* = 8.3, 1.0 Hz, 1H), 6.49 (dd, *J* = 8.4, 1.0 Hz, 1H), 3.20 (dd, *J* = 14.5, 2.1 Hz, 1H), 3.08 – 2.99 (m, 1H), 2.97 – 2.74 (m, 6H), 2.29 – 2.14 (m, 1H), 2.10 – 1.90 (m, 1H), 1.70 – 1.55 (m, 2H), 1.51 – 1.30 (m, 1H); $^{13}$C NMR (101 MHz, $CDCl_3$) δ 190.58, 161.31, 160.49, 136.42, 111.20, 110.55, 103.96, 79.92, 60.56, 56.27, 46.78, 46.63, 46.53, 27.95, 22.18, 20.77.

HRMS (ESI+) m/z found 274.1443 [M+H]+, $C_{16}H_{20}NO_3$ calculated 274.1443 (Δ = 0 ppm).

**(1'R*,2S*,4'R*)-4'-azaspiro[benzo[g]chromene-2,2'-bicyclo[2.2.2]octan]-4(3H)-one 4.21**

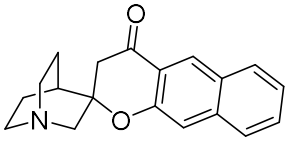

Quinuclidine-3-one (1.0 equiv, 0.16 mmol) was reacted with 1-(3-hydroxynaphthalen-2-yl)ethan-1-one (20.0 mg, 0.16 mmol) for 16.5 hours to yield a yellow solid according to the General Procedure IX (22.0 mg, 47%).

$^1$H NMR (400 MHz, $CDCl_3$) δ 8.46 (s, 1H), 7.88 (d, *J* = 8.3 Hz, 1H), 7.71 (d, *J* = 8.3 Hz, 1H), 7.55 – 7.48 (m, 1H), 7.40 – 7.33 (m, 2H), 3.36 – 3.28 (m, 1H), 3.19 – 3.08 (m, 1H), 3.05 – 2.78 (m, 6H), 2.20 (p, *J* = 3.1 Hz, 1H), 2.13 – 2.01 (m, 1H), 1.72 – 1.62 (m, 2H), 1.44 – 1.34 (m, 1H); $^{13}$C NMR (101 MHz, $CDCl_3$) δ 192.90, 154.95, 138.36, 130.23, 129.42, 128.77, 128.55, 126.71, 124.99, 121.66, 113.49, 80.21, 60.95, 46.75, 46.69, 46.07, 28.36, 22.39, 20.92.

HRMS (ESI+) m/z found [M+H]+ 294.1492, $C_{19}H_{20}NO_2$ calculated 294.1494 (Δ = -0.7 ppm).

**(1'R*,2S*,4'R*)-4'-azaspiro[benzo[h]chromene-2,2'-bicyclo[2.2.2]octan]-4(3H)-one 18t**

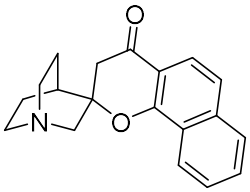

Quinuclidine-3-one (1.0 equiv, 1.0 mmol) was reacted with 1-(1-hydroxynaphthalen-2-yl)ethan-1-one (186.2 mg, 1.0 mmol) for 24 hours to yield a yellow solid according to the General Procedure IX (197.6 mg, 67%).

$^1$H NMR (400 MHz, $CDCl_3$) δ 8.29 (d, *J* = 8.3 Hz, 1H), 7.81 (dd, *J* = 11.5, 8.4 Hz, 2H), 7.65 – 7.59 (m, 1H), 7.57 – 7.50 (m, 1H),7.39 (dd, *J* = 8.7, 0.7 Hz, 1H), 3.36 (dd, *J* = 14.6, 2.1 Hz, 1H), 3.18 – 3.08 (m, 1H), 3.03 – 2.75 (m, 6H), 2.34 (p, *J* = 3.2 Hz, 1H), 2.11 – 1.98 (m, 1H), 1.72 – 1.61 (m, 2H), 1.47 – 1.35 (m, 1H); $^{13}$C NMR (101 MHz, $CDCl_3$) δ 191.73, 157.89, 137.97, 129.73, 128.18, 126.52, 125.37, 123.28, 121.50, 120.94, 115.53, 82.33, 61.32, 46.85, 46.68, 44.85, 28.41, 22.77, 21.72.HRMS (ESI+) m/z found [M+H]+ 294.1493, $C_{19}H_{20}NO_2$ calculated 294.1494 (Δ = -0.34 ppm).

## The separation of racemate 18t with Supercritical fluid chromatography

The recamate **SCQ1** (150.0 mg, 0.38 mmol) was separated by Prep SFC to yield each enantiomer (*S*)-**SCQ1** (51.3 mg, 34%,>95% *ee*), **$[\alpha]^{20}_D$ = -35.1** (*c* = 1.0, $CHCl_3$) and (*R*)-**SCQ1** (67.2 mg, 45%, >95% *ee*), **$[\alpha]^{20}_D$ = +43.2** (*c* = 1.0, $CHCl_3$) as a light yellow solid.

**The preparation of diester 5.02**

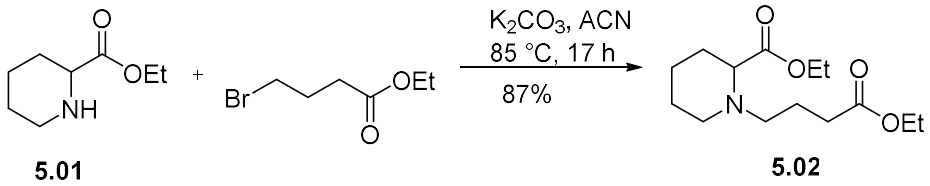


**5.01** **5.02**

A mixture of compound **5.01**(5.0 g, 31.9 mmol) and ethyl-4-bromo-butunoate (5 mL, 35 mmol) was dissolved in dry acetonitrile (100 mL), $K_2CO_3$ (11.8 g, 87.5 mmol) was added, the resulting mixture was refluxed under $N_2$ protection overnight. After 17 hours, the mixture was cooled to room temperature, the precipitate was filtered off, the filtrater was concentrated under vacuum. The crude was purified by column chromatography on silica gel (hexane: ethyl acetate = 10:1 to 6:1) to yield the product as a colorless oil (7.5 g, 87%).

$^1$H NMR (400 MHz, $CDCl_3$) δ 4.19 – 3.94 (m, 4H), 3.13 – 2.91 (m, 2H), 2.55 – 2.42 (m, 1H), 2.34 – 2.04 (m, 4H), 1.81 – 1.62 (m, 4H), 1.62 – 1.48 (m, 3H), 1.38 – 1.25 (m, 1H), 1.25 – 1.12 (m, 6H). $^{13}$C NMR (101 MHz, $CDCl_3$) δ 173.70, 173.56, 65.04, 60.31, 60.22, 55.58, 50.24, 32.16, 29.57, 25.31, 22.53, 22.10, 14.30, 14.26.

**The preparation of hexahydro-2H-quinolizin-1(6H)-one 5.05**

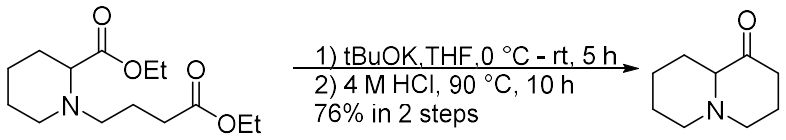


**5.02** **5.05**

$^t$BuOK (6.2 g, 55.2 mmol) dissolved in dry THF (100 mL) was added diester **5.02** (7.5 g, 27.6 mmol) in dry THF (20 mL) at 0 ºC, the resulting mixture was stirred at room temperature and monitored by TCL. After 5 hours, the solvent was removed under reduced pressure. The resulting mixture was dissolved in $H_2O$ (100 mL) at 0 ºC, and added HCl (1 M) until the pH reached 9-10. The aqueous solution was extracted with DCM (125 mLx4). The combined organic layer was concentrated under reduced pressure and further dried *in vacuo* overnight to get the product as a brown oil (5.1 g, 82%). The resulting intermediate was dissolved in HCl (45 mL, 4 M) and heated to 90 ºC under $N_2$ protection monitored by LC-MS and TLC. After 10 hours, the mixture was basified with statured $NaHCO_3$ and NaOH until at 0 ºC pH become 9-10. The aqueous phase was extracted with (iPrOH/$CHCl_3$ = 9:1) over 8 times, the collected organic layer was concentrated at 30 ºC, and further dried under the high vacuum for 2-3 hours to yield the ketone **5.05** as a brown oil (3.2 g, 93%).

$^1$H NMR (400 MHz, $CDCl_3$) δ 3.02 – 2.82 (m, 2H), 2.52 – 2.33 (m, 3H), 2.32 – 2.21 (m, 1H), 2.18 – 2.09 (m, 1H), 2.05 – 1.88 (m, 3H), 1.84 – 1.73 (m, 1H), 1.64 – 1.45 (m, 2H), 1.43 – 1.30 (m, 1H), 1.27 – 1.12 (m, 1H).$^{13}$C NMR (101 MHz, $CDCl_3$) δ 207.34, 71.05, 56.97, 54.89, 39.27, 25.67, 25.47, 24.22, 23.83.

**(1R*,9a'R*)-3',4,4',7',8',9,9',9a'-octahydro-2'H,3H,6'H-spiro[pyrano[3,4-b]indole-1,1'-quinolizine] 5.06**

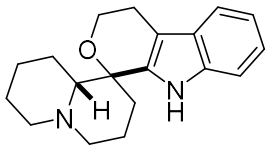

Ketone **5.05** (306 mg, 2.0 mmol) was reacted with tryptophol (1.2 equiv, 2.4 mmol) at 100 °C for 24 hours to yield a light yellow solid (295 mg, 50%).[1]H NMR (400 MHz, DMSO-$d_6$) δ 10.78 (s, 1H), 7.37 (d, $J$ = 7.7 Hz, 1H), 7.29 (d, $J$ = 7.9 Hz, 1H), 7.06 – 6.99 (m, 1H), 6.98 – 6.90 (m, 1H), 4.00 (dd, $J$ = 11.2, 5.2 Hz, 1H), 3.82 – 3.66 (m, 1H), 2.84 – 2.72 (m, 2H), 2.72 – 2.64 (m, 1H), 2.59 – 2.53 (m, 1H), 2.27 (d, $J$ = 10.2 Hz, 1H), 2.17 – 2.04 (m, 2H), 2.01 – 1.80 (m, 2H), 1.70 – 1.32 (m, 6H), 1.11 – 0.97 (m, 1H), 0.77 (d, $J$ = 14.1 Hz, 1H).[13]C NMR (101 MHz, DMSO-$d_6$) δ 137.56, 136.21, 126.71, 121.04, 118.81, 117.99, 111.55, 107.49, 74.27, 68.55, 59.74, 57.40, 56.50, 32.89, 25.75, 25.06, 24.76, 22.55, 20.90.

HRMS (ESI+) m/z found 297.1968 [M+H]+, $C_{19}H_{25}N_2O$ calculated 297.1967 (Δ = 0.34 ppm).

(1R*****,9a'R*****)-6-methoxy-3',4,4',7',8',9,9',9a'-octahydro-2'H,3H,6'H-spiro[pyrano[3,4-b]indole-1,1'-quinolizine] **5.07**

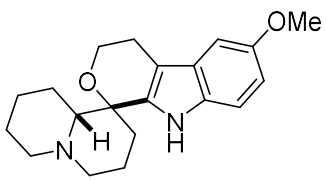

Ketone **5.05** (92 mg, 0.6 mmol) was reacted with 5-methoxytryptophol (1.2 equiv, 0.72 mmol) at 90 °C for 18 hours to yield a light yellow solid (76.2 mg, 39%).

[1]H NMR (400 MHz, DMSO-$d_6$) δ 10.60 (s, 1H), 7.16 (d, $J$ = 8.7 Hz, 1H), 6.87 (d, $J$ = 2.4 Hz, 1H), 6.66 (dd, $J$ = 8.7, 2.5 Hz, 1H), 4.04 – 3.94 (m, 1H), 3.73 (s, 3H), 3.72 – 3.67 (m, 1H), 2.77 (t, $J$ = 12.7 Hz, 2H), 2.71 – 2.61 (m, 1H), 2.56 – 2.52 (m, 1H), 2.23 (d, $J$ = 10.5 Hz, 1H), 2.16 – 2.03 (m, 2H), 1.96 – 1.80 (m, 2H), 1.65 – 1.33 (m, 6H), 1.11 – 0.97 (m, 1H), 0.83 – 0.72 (m, 1H).

[13]C NMR (101 MHz, DMSO-$d_6$) δ 153.55, 138.30, 131.24, 126.98, 112.09, 110.84, 107.37, 100.23, 74.28, 68.60, 59.76, 57.38, 56.48, 55.83, 32.91, 25.74, 25.02, 24.75, 22.63, 20.87.

HRMS (ESI+) m/z found 327.2077 [M+H]+, $C_{20}H_{27}N_2O_2$ calculated 327.2072 (Δ = 1.53 ppm).

**(1R*,9a'R*)-8-ethyl-3',4,4',7',8',9,9',9a'-octahydro-2'H,3H,6'H-spiro[pyrano[3,4-b]indole-1,1'-quinolizine] 5.08**

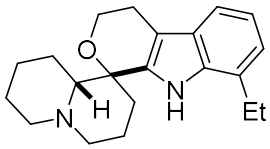

Ketone **5.05** (306 mg, 2.0 mmol) was reacted with 7-ethyltryptophol (1.2 equiv, 2.4 mmol) at 100 °C for 24 hours to yield a light yellow solid (117 mg, 18%).

[1]H NMR (400 MHz, DMSO-$d_6$) δ 10.46 (s, 1H), 7.20 (dd, $J$ = 7.5, 1.4 Hz, 1H), 6.92 – 6.87 (m, 1H), 6.87 – 6.84 (m, 1H), 3.99 (dd, $J$ = 11.2, 5.2 Hz, 1H), 3.76 – 3.64 (m, 1H), 2.90 – 2.83 (m, 2H), 2.82 – 2.64 (m, 3H), 2.58 – 2.52 (m, 1H), 2.47 – 2.39 (m, 1H), 2.21 – 2.13 (m, 1H), 2.12 – 2.05 (m, 1H), 2.01 – 1.83 (m, 2H), 1.82 – 1.71 (m, 1H), 1.57 – 1.33 (m, 5H), 1.25 (t, $J$ = 7.5 Hz, 3H), 1.08 – 0.96 (m, 1H), 0.78 (d, $J$ = 13.6 Hz, 1H).

[13]C NMR (101 MHz, DMSO-$d_6$) δ 137.38, 134.86, 127.06, 126.56, 119.92, 119.13, 115.57, 108.00, 74.49, 67.94, 59.65, 57.41, 56.34, 32.52, 25.85, 25.09, 24.85, 24.16, 22.68, 21.01, 15.02.

HRMS (ESI+) m/z found 325.2280 [M+H]+, $C_{19}H_{25}N_2O$ calculated 325.2280 (Δ = 0 ppm).

**(1R*,9a'R*)-9-methyl-3',4,4',7',8',9,9',9a'-octahydro-2'H,3H,6'H-spiro[pyrano[3,4-b]indole-1,1'-quinolizine] 5.09**

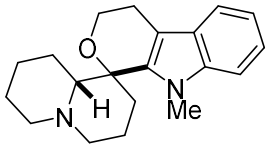


Ketone **5.05** (260 mg, 1.7 mmol) was reacted with *N*-methyl tryptophol (1.2 equiv, 2.0 mmol) at 100 - 115 °C for 3 days to yield a light yellow solid (92.2 mg, 18%).

$^1$H NMR (400 MHz, DMSO-$d_6$) δ 7.44 – 7.37 (m, 2H), 7.15 – 7.09 (m, 1H), 7.04 – 6.98 (m, 1H), 4.02 – 3.95 (m, 1H), 3.80 (s, 1H), 3.74 – 3.66 (m, 1H), 2.82 – 2.68 (m, 3H), 2.63 – 2.55 (m, 1H), 2.46 – 2.40 (m, 1H), 2.19 – 2.08 (m, 2H), 2.01 – 1.87 (m, 2H), 1.85 – 1.75 (m, 1H), 1.57 – 1.41 (m, 4H), 1.41 – 1.31 (m, 1H), 1.15 – 1.02 (m, 1H), 0.83 – 0.71 (m, 1H). $^{13}$C NMR (101 MHz, DMSO-$d_6$) δ 137.72, 137.26, 126.18, 121.60, 119.26, 118.11, 109.91, 109.43, 75.36, 67.43, 58.99, 57.32, 56.45, 32.58, 31.27, 25.73, 25.31, 24.63, 22.79, 21.05.

HRMS (ESI+) m/z found 311.2125 [M+H]+, $C_{20}H_{27}N_2O$ calculated 311.2123 (Δ = 0.64 ppm).

**(1R*,9a'R*)-6-bromo-3',4,4',7',8',9,9',9a'-octahydro-2'H,3H,6'H-spiro[pyrano[3,4-b]indole-1,1'-quinolizine] 5.10**

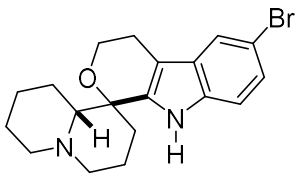


Ketone **5.05** (126 mg, 0.82 mmol) was reacted with 5-bromotryptophol (1.2 equiv, 0.9 mmol) at 95 - 100 °C for 2 days to yield a light yellow (134.1 mg, 45%).

$^1$H NMR (400 MHz, DMSO-$d_6$) δ 11.04 (s, 1H), 7.56 (d, $J$ = 1.9 Hz, 1H), 7.25 (d, $J$ = 8.5 Hz, 1H), 7.16 – 7.10 (m, 1H), 4.02 – 3.95 (m, 1H), 3.75 – 3.66 (m, 1H), 2.82 – 2.72 (m, 2H), 2.71 – 2.61 (m, 1H), 2.59 – 2.52 (m, 1H), 2.29 – 2.20 (m, 1H), 2.16 – 2.03 (m, 2H), 1.95 – 1.80 (m, 2H), 1.62 – 1.33 (m, 6H), 1.08 – 0.95 (m, 1H), 0.78 – 0.67 (m, 1H).$^{13}$C NMR (101 MHz, DMSO-$d_6$) δ 139.38, 134.90, 128.57, 123.43, 120.41, 113.48, 111.45, 107.53, 74.25, 68.48, 59.63, 57.38, 56.47, 32.82, 25.73, 25.06, 24.75, 22.36, 20.84.

HRMS (ESI+) m/z found 375.1072 [M+H]+, $C_{19}H_{24}BrN_2O$ calculated 375.1072 (Δ = 0 ppm).

**3,4,4',5',7,8,9,9a-octahydro-2H,6H-spiro[quinolizine-1,7'-thieno[2,3-c]pyran] 5.11**

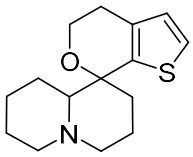


A mixture of ketone **5.05** (153.1 mg, 1.0 mmol) and 2-(thiophen-3-yl) ethan-1-ol (153.8 mg, 1.2 mmol) was dissolved in dry toluene (6 mL), MsOH (81 μL, 1.2 mmol) was added. The mixture was heated with Dean-Stark under 115 °C and under $N_2$ protection. After 22 hours, the reaction was quenched with $NaHCO_3$ solution and extracted with ethyl acetate with two times, the combined organic phase was dried over $Na_2SO_4$, and concentrated under reduced pressure and further purified by column chromatography on silica gel (DCM:MeOH:$NH_3$ = 100:1:0.1 to 20:1:0.1) to yield the product as a yellow solid (23.7 mg, 9%).

$^1$H NMR (400 MHz, DMSO-$d_6$) δ 7.36 (d, $J$ = 5.0 Hz, 1H), 6.81 (d, $J$ = 5.0 Hz, 1H), 4.01 – 3.84 (m, 1H), 3.74 – 3.59 (m, 1H), 2.80 – 2.71 (m, 2H), 2.70 – 2.56 (m, 1H), 2.28 – 2.18 (m, 1H), 2.10 – 1.98 (m, 1H), 1.95 – 1.79 (m, 3H), 1.62 – 1.29 (m, 7H), 1.09 – 0.98 (m, 1H), 0.99 – 0.88 (m, 1H).$^{13}$C NMR (101 MHz, DMSO-$d_6$) δ 140.09, 134.85, 127.37, 123.65, 75.87, 72.32, 59.20, 57.18, 56.51, 36.61, 26.58, 25.67, 24.70, 24.59, 21.07.

HRMS (ESI+) m/z found 264.1417 [M+H]+, $C_{15}H_{22}NOS$ calculated 264.1422 (Δ = -1.89 ppm).

**General procedure for synthesis of bis-spirocycle quinolizdines from ring contraction XIII**

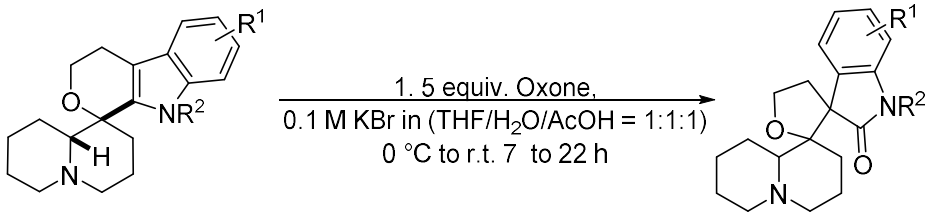


**5.06-5.10** **5.13-5.17**

A mixture of compound **5.06-5.10** (0.2 mmol, 1.0 equiv.) was dissolved in 2 mL KBr (0.1M in HOAc: $H_2O$: THF = 1:1:1) at ºC, oxone (92.1 mg, 0.3 mmol) was added. The reaction mixture was stirred at room temperature and monitored by LC-MS and TLC, and the resulting mixture was quenched with saturated $NaHCO_3$ and 5 mL saturated $Na_2SO_3$ until the pH become 9-10, and extracted with ethyl acetate twice. The combined organic layer was dried over $Na_2SO_4$ and concentrated under reduced pressure. The resulting crude was purified by column chromatography on silica gel (DCM:MeOH:$NH_3$ = 100:1:0.1 to 20:1:0.1) to yield the product as a solid or colorless oil.

**3'',4',4'',5',7'',8'',9'',9a''-octahydro-2''H,6''H-dispiro[indoline-3,3'-furan-2',1''-quinolizin]-2-one 5.13**

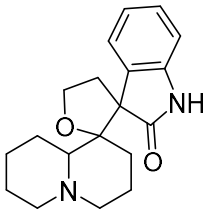


Compound **5.06** (29.6 mg, 0.1 mmol) was reacted with oxone (46.1 mg, 0.15 mmol) for 22 hour to yield a white solid (13.5 mg, 43 %).

$^1$H NMR (400 MHz, MeOD) δ 7.51 (d, *J* = 7.6 Hz, 1H), 7.44 – 7.33 (m, 2H), 7.31 – 7.23 (m, 1H), 4.44 – 4.21 (m, 1H), 3.96 – 3.61 (m, 1H), 3.25 – 3.07 (m, 1H), 2.93 – 2.76 (m, 2H), 2.66 (dd, *J* = 10.3, 2.1 Hz, 1H), 2.47 – 2.33 (m, 1H), 2.24 – 2.11 (m, 2H), 2.08 – 1.93 (m, 1H), 1.92 – 1.82 (m, 1H), 1.77 – 1.68 (m, 1H), 1.66 – 1.38 (m, 6H), 1.37 – 1.19 (m, 1H). $^{13}$C NMR (101 MHz, MeOD) δ 184.00, 153.30, 142.07, 130.57, 127.85, 123.40, 121.61, 81.55, 78.11, 68.13, 58.87, 57.80, 57.34, 39.39, 29.48, 26.38, 26.27, 25.36, 20.73.

HRMS (ESI+) m/z found 313.1912 [M+H]+, $C_{19}H_{25}N_2O_2$ calculated 313.1916 (Δ = -1.28 ppm).

**7-ethyl-3'',4',4'',5',7'',8'',9'',9a''-octahydro-2''H,6''H-dispiro[indoline-3,3'-furan-2',1''-quinolizin]-2-one 5.14**

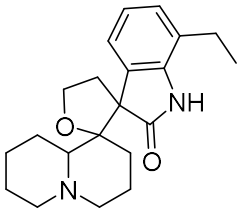


22 h, white solid (38 mg, 56%).

$^1$H NMR (400 MHz, DMSO-$d_6$) δ 7.25 – 7.04 (m, 3H), 5.86 (d, *J* = 1.6 Hz, 1H), 4.20 – 4.05 (m, 1H), 3.72 – 3.62 (m, 1H), 3.06 – 2.99 (m, 1H), 2.93 – 2.86 (m, 1H), 2.83 – 2.64 (m, 3H), 2.61 – 2.54 (m, 1H), 2.36 – 2.26 (m, 1H), 2.07 – 1.94 (m, 2H), 1.82 – 1.74 (m, 2H), 1.62 (d, *J* = 12.2 Hz, 1H), 1.50 – 1.31 (m, 5H), 1.27 – 1.18 (m, 4H), 1.18 – 1.09 (m, 1H).$^{13}$C NMR (101 MHz, DMSO-$d_6$) δ 181.34, 150.46, 141.85, 136.32, 129.23, 126.48, 120.25, 80.35, 76.84, 66.65, 57.84, 56.51, 56.36, 39.16, 28.41, 25.93, 25.47, 24.91, 24.16, 20.05, 15.86.

HRMS (ESI+) m/z found 341.2231 [M+H]+, $C_{21}H_{29}N_2O_2$ calculated 341.2229 (Δ = 0.59 ppm).

**5-methoxy-3'',4',4'',5',7'',8'',9'',9a''-octahydro-2''H,6''H-dispiro[indoline-3,3'-furan-2',1''-quinolizin]-2-one 5.15**

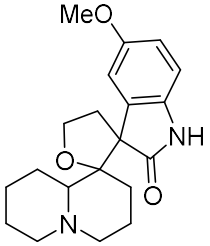


7 h, white solid (17.2 mg, 25 %).

$^{1}$H NMR (400 MHz, DMSO-$d_6$) δ 7.41 (d, $J$ = 8.3 Hz, 1H), 6.98 (d, $J$ = 2.5 Hz, 1H), 6.86 (dd, $J$ = 8.4, 2.6 Hz, 1H), 5.90 (d, J = 1.5 Hz, 1H), 4.18 – 4.04 (m, 1H), 3.76 (s, 3H), 3.72 – 3.62 (m, 1H), 3.07 – 2.92 (m, 1H), 2.79 – 2.62 (m, 2H), 2.52 – 2.45 (m, 1H), 2.36 – 2.24 (m, 1H), 2.03 – 1.87 (m, 2H), 1.85 – 1.69 (m, 2H), 1.60 (d, $J$ = 12.4 Hz, 1H), 1.52 – 1.28 (m, 5H), 1.27 – 1.16 (m, 1H), 1.17 – 1.03 (m, 1H). $^{13}$C NMR (101 MHz, DMSO-$d_6$) δ 180.76, 158.66, 146.15, 143.63, 121.41, 113.90, 109.44, 80.45, 76.76, 66.59, 57.88, 56.46, 56.41, 56.04, 39.10, 28.55, 25.94, 25.28, 25.02, 20.09.

HRMS (ESI+) m/z found 343.2016 [M+H]+, $C_{20}H_{27}N_2O_3$ calculated 343.2021 (Δ = -1.46 ppm).

**5-bromo-3'',4',4'',5',7'',8'',9'',9a''-octahydro-2''H,6''H-dispiro[indoline-3,3'-furan-2',1''-quinolizin]-2-one 5.16**

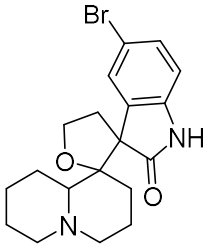


7 h, pale white solid (39.1 mg, 50%).

$^{1}$H NMR (400 MHz, DMSO-$d_6$) δ 7.57 (d, $J$ = 2.0 Hz, 1H), 7.53 (dd, $J$ = 8.1, 2.0 Hz, 1H), 7.48 (d, $J$ = 8.1 Hz, 1H), 6.07 (d, $J$ = 1.4 Hz, 1H), 4.15 – 4.04 (m, 1H), 3.78 – 3.44 (m, 1H), 3.11 – 2.92 (m, 1H), 2.84 – 2.59 (m, 2H), 2.44 – 2.24 (m, 1H), 2.04 – 1.90 (m, 2H), 1.83 – 1.66 (m, 2H), 1.61 (d, $J$ = 12.0 Hz, 1H), 1.53 – 1.29 (m, 6H), 1.28 – 1.17 (m, 1H), 1.16 – 1.02 (m, 1H). $^{13}$C NMR (101 MHz, DMSO-$d_6$) δ 183.46, 151.92, 144.41, 132.25, 126.06, 122.89, 119.47, 80.75, 76.86, 66.50, 57.83, 56.42, 56.32, 38.74, 28.30, 25.89, 25.26, 24.98, 19.99.

HRMS (ESI+) m/z found 391.1013 [M+H]+, $C_{19}H_{24}BrN_2O_2$ calculated 391.1021 (Δ = -2.05 ppm).

**1-methyl-3'',4',4'',5',7'',8'',9'',9a''-octahydro-2''H,6''H-dispiro[indoline-3,3'-furan-2',1''-quinolizin]-2-one 5.17**

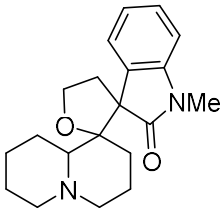


22 h, colorless oil (23.4 mg, 36%).

$^{1}$H NMR (400 MHz, DMSO-$d_6$) δ 7.32 (d, $J$ = 7.5 Hz, 1H), 7.27 (t, $J$ = 7.7 Hz, 1H), 7.02 (t, $J$ = 7.5 Hz, 1H), 6.96 (d, $J$ = 7.8 Hz, 1H), 4.15 (q, $J$ = 7.9 Hz, 1H), 4.04 – 3.95 (m, 1H), 3.10 (s, 3H), 2.68 – 2.58 (m, 1H), 2.57 – 2.45 (m, 2H), 2.45 – 2.35 (m, 1H), 2.28 – 2.16 (m, 1H), 2.14 – 2.02 (m, 1H), 1.85 – 1.72 (m, 2H), 1.74 – 1.64 (m, 1H), 1.64 – 1.54 (m, 2H), 1.54 – 1.29 (m, 4H), 1.24 – 1.03 (m, 2H).$^{13}$C NMR (101 MHz, DMSO-$d_6$) δ 178.49, 144.05, 129.60, 128.38, 125.32, 121.92, 108.49, 85.87, 66.13, 64.42, 60.45, 55.73, 49.03, 37.93, 29.85, 26.39, 25.35, 22.36, 22.22, 21.86.

HRMS (ESI+) m/z found 327.2078 [M+H]+, $C_{20}H_{27}N_2O_2$ calculated 327.2072 (Δ = 1.83 ppm).

**(1R*,9a'R*)-2,3,3',4,4',7',8',9,9',9a'-decahydro-2'H,6'H-spiro[pyrido[3,4-b]indole-1,1'-quinolizine] 5.18**

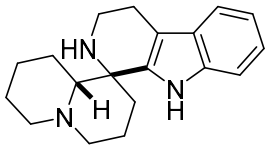

Ketone **5.05** (92 mg, 0.6 mmol) was reacted with tryptamine (1.0 equiv, 0.5 mmol) at 100 ºC for 14 hours to yield a white solid according to the General Procedure VII (78.0 mg, 53%).

$^1$H NMR (400 MHz, DMSO-$d_6$) δ 10.64 (s, 1H), 7.32 (d, $J$ = 7.7 Hz, 1H), 7.25 (d, $J$ = 8.0 Hz, 1H), 7.02 – 6.95 (m, 1H), 6.94 – 6.85 (m, 1H), 3.13 – 3.02 (m, 1H), 2.97 – 2.87 (m, 1H), 2.85 – 2.71 (m, 2H), 2.61 – 2.53 (m, 1H), 2.40 – 2.25 (m, 2H), 2.09 – 1.99 (m, 1H), 2.00 – 1.81 (m, 3H), 1.69 – 1.42 (m, 5H), 1.42 – 1.26 (m, 1H), 1.12 – 0.98 (m, 1H), 0.85 – 0.71 (m, 1H). $^{13}$C NMR (101 MHz, DMSO-$d_6$) δ 139.16, 136.17, 127.21, 120.54, 118.46, 117.74, 111.31, 108.42, 69.05, 57.46, 57.08, 55.14, 34.14, 25.87, 25.65, 24.67, 23.01, 20.97.HRMS (ESI+) m/z found 296.2117 [M+H]+, $C_{15}H_{30}N_3$ calculated 296.2126 (Δ = 0.34 ppm).

**(1R*,9a'R*)-6-methoxy-2,3,3',4,4',7',8',9,9',9a'-decahydro-2'H,6'H-spiro[pyrido[3,4-b]indole-1,1'-quinolizine] 5.19**

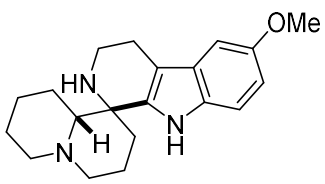

Ketone **5.05** (276 mg ,1.8 mmol) was reacted with 2-(5-methoxy-1H-indol-3-yl)ethan-1-amine (1.0 equiv, 1.5 mmol) at 100 ºC for 12 hours to yield a white solid according to the General Procedure VII (350 mg, 72%).

$^1$H NMR (400 MHz, DMSO-$d_6$) δ 10.46 (s, 1H), 7.13 (d, $J$ = 8.6 Hz, 1H), 6.82 (d, $J$ = 2.4 Hz, 1H), 6.62 (dd, $J$ = 8.7, 2.4 Hz, 1H), 3.72 (s, 3H), 3.12 – 3.02 (m, 1H), 2.96 – 2.87 (m, 1H), 2.77 (dd, $J$ = 26.1, 11.1 Hz, 2H), 2.58 – 2.52 (m, 1H), 2.29 (dd, $J$ = 10.9, 2.8 Hz, 2H), 2.08 – 1.99 (m, 1H), 1.97 – 1.79 (m, 3H), 1.67 – 1.42 (m, 5H), 1.40 – 1.29 (m, 1H), 1.11 – 0.96 (m, 1H), 0.86 – 0.75 (m, 1H). $^{13}$C NMR (101 MHz, DMSO-$d_6$) δ 153.38, 139.97, 131.25, 127.47, 111.84, 110.25, 108.34, 100.15, 69.12, 57.46, 57.08, 55.85, 55.17, 34.19, 25.88, 25.63, 24.68, 23.11, 20.96.

HRMS (ESI+) m/z found 326.2234 [M+H]+, $C_{20}H_{28}N_3O$ calculated 326.2232 (Δ = 0.6 ppm).

**(1R*,9a'R*)-6-chloro-2,3,3',4,4',7',8',9,9',9a'-decahydro-2'H,6'H-spiro[pyrido[3,4-b]indole-1,1'-quinolizine] 5.20**

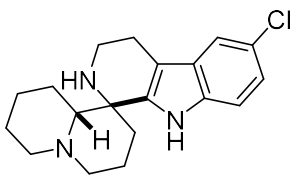

ketone **5.05** (276 mg ,1.8 mmol) was reacted with 2-(5-chloro-1H-indol-3-yl)ethan-1-amine hydrochloride (1.0 equiv, 1.5 mmol) at 95 ºC for 13 hours to yield a white solid according to the General Procedure VII (295 mg, 60%).

$^1$H NMR (400 MHz, DMSO-$d_6$) δ 10.88 (s, 1H), 7.35 (d, $J$ = 2.1 Hz, 1H), 7.26 (d, $J$ = 8.5 Hz, 1H), 6.97 (dd, $J$ = 8.5, 2.1 Hz, 1H), 3.14 – 3.01 (m, 1H), 2.96 – 2.85 (m, 1H), 2.85 – 2.78 (m, 1H), 2.78 – 2.72 (m, 1H), 2.58 – 2.52 (m, 1H), 2.43 – 2.25 (m, 2H), 2.11 – 1.81 (m, 4H), 1.69 – 1.41 (m, 5H), 1.41 – 1.28 (m, 1H), 1.14 – 0.97 (m, 1H), 0.81 – 0.71 (m, 1H). $^{13}$C NMR (101 MHz, DMSO-$d_6$) δ 141.17, 134.61, 128.35, 123.19, 120.34, 117.07, 112.70, 108.54, 68.96, 57.42, 57.03, 39.15, 34.02, 25.81, 25.63, 24.62, 22.81, 20.86.

HRMS (ESI+) m/z found 330.1733 [M+H]+, $C_{19}H_{27}ClN_3$ calculated 330.1737 (Δ = -1.21 ppm).

**ethyl (1R*,3S*,9a'R*)-2,3,3',4,4',7',8',9,9',9a'-decahydro-2'H,6'H-spiro[pyrido[3,4-b]indole-1,1'-quinolizine]-3-carboxylate 5.21**

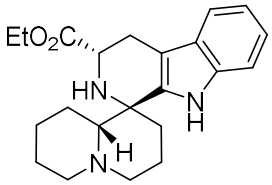

Ketone **5.05** (184 mg, 1.2 mmol) was reacted with D-Tryptophan ethyl ester hydrochloride (1.0 equiv, 1.0 mmol) at 95 ºC for 15 hours to yield a yellow solid according to the General Procedure VII (257.6 mg, 70%).

$^1$H NMR (400 MHz, DMSO-$d_6$) δ 10.77 (s, 1H), 7.37 (d, $J$ = 7.6 Hz, 1H), 7.27 (d, $J$ = 7.9 Hz, 1H), 7.04 – 6.98 (m, 1H), 6.93 (t, $J$ = 7.3 Hz, 1H), 4.30 – 4.13 (m, 2H), 3.79 (dd, $J$ = 11.1, 3.7 Hz, 1H), 2.93 (dd, $J$ = 14.5, 3.8 Hz, 1H), 2.88 – 2.74 (m, 2H), 2.63 (s, 1H), 2.57 (dd, $J$ = 14.5, 11.0 Hz, 1H), 2.36 (dd, $J$ = 10.9, 2.8 Hz, 1H), 2.11 – 1.99 (m, 2H), 1.98 – 1.88 (m, 1H), 1.82 – 1.70 (m, 1H), 1.66 – 1.44 (m, 5H), 1.27 (t, $J$ = 7.1 Hz, 3H), 1.14 – 0.99 (m, 1H), 0.82 – 0.70 (m, 1H). $^{13}$C NMR (101 MHz, DMSO-$d_6$) δ 173.49, 138.81, 136.48, 126.90, 120.89, 118.76, 117.86, 111.45, 107.06, 68.47, 61.05, 57.30, 56.90, 55.75, 51.71, 33.15, 26.26, 25.79, 25.35, 24.43, 21.12, 14.66.
HRMS (ESI+) m/z found 390.2162 [M+Na]+, $C_{22}H_{29}N_3O_2Na$ calculated 390.2157 (Δ = 1.28 ppm).

**(1R*,9a'R*)-6-methoxy-2-methyl-2,3,3',4,4',7',8',9,9',9a'-decahydro-2'H,6'H-spiro[pyrido[3,4-b]indole-1,1'-quinolizine] 5.32**

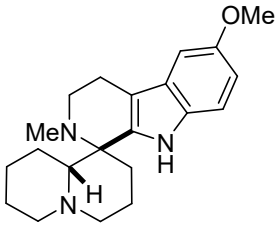

A mixture of compound **5.19** (94.3 mg, 0.29 mmol) and $NaBH_3CN$ (44 mg, 0.7 mmol) was dissolved in MeOH (3.5 mL) and treated with 0.35 mL of formaldehyde (24. 5% solution in water) at 0 ºC. The mixture was stirred at room temperature for 2.5 hours and quenched with 1.5 mL HCl (2 M). The mixture was basified with KOH to pH = 10 to 11 and extracted with DCM with 3 times to give the product as a white solid (95.0 mg, 95%).

$^1$H NMR (400 MHz, DMSO-$d_6$) δ 10.43 (s, 1H), 7.22 – 7.00 (m, 1H), 6.80 (d, $J$ = 2.4 Hz, 1H), 6.63 (dd, $J$ = 8.7, 2.5 Hz, 1H), 3.72 (s, 3H), 2.96 – 2.58 (m, 8H), 2.48 – 2.39 (m, 2H), 2.37 – 2.12 (m, 2H), 2.08 – 1.74 (m, 2H), 1.71 – 1.34 (m, 6H), 1.16 – 0.89 (m, 2H). $^{13}$C NMR (101 MHz, DMSO-$d_6$) δ 153.37, 141.17, 131.30, 126.92, 111.96, 110.55, 108.86, 100.06, 70.75, 58.77, 58.50, 56.45, 55.85, 49.00, 43.46, 29.75, 26.47, 26.16, 25.33, 23.88, 22.38.
HRMS (ESI+) m/z found 340.2385 [M+H]+, $C_{21}H_{30}N_3O$ calculated 340.2389 (Δ = -1.18 ppm).

**General procedure for synthesis of pyrrolidine fused quinolizdines XV**

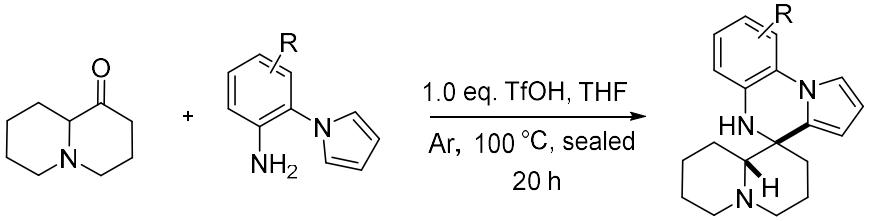


**5.05** **5.24-5.26**

A mixture of ketone **5.05** (76.6 mg, 0.5 mmol) and substituted 2-(1H-pyrrol-1-yl)aniline (0.5 mmol, 1.05 equiv) was evacuated and backfill with argon three times, the mixture was dissolved in dry THF (4 mL) and added with TfOH (44 μL, 1 .0 equiv). The solution was sealed and heated to 100 ºC overnight. The reaction was monitored

by TCL and LC- MS until complete consumption of ketone **5.05**, the reaction was quenched with $NaHCO_3$ solution at 0 °C. The aqueous solution was extracted with DCM two times, and the combined oraganic layer was dried over $Na_2SO_4$. The crude was concentrated under reduced pressure and further purified by column chromatography on silica gel (hexane: ethyl acetate = 5:1 to 3:1) to yield the product as a solid.

**(4R*,9a'R*)-3',4',7',8',9',9a'-hexahydro-2'H,5H,6'H-spiro[pyrrolo[1,2-a]quinoxaline-4,1'-quinolizine] 5.24**

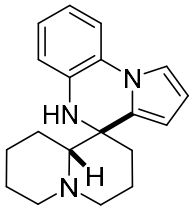

Pale white solid (58.6 mg, 40%).

$^1$H NMR (400 MHz, $CDCl_3$) δ 7.23 (dd, *J* = 7.9, 1.2 Hz, 1H), 7.14 (dd, *J* = 2.9, 1.6 Hz, 1H), 6.96 – 6.87 (m, 1H), 6.76 (d, *J* = 7.7 Hz, 1H), 6.72 – 6.64 (m, 1H), 6.29 (t, *J* = 3.2 Hz, 1H), 5.96 (dd, *J* = 3.6, 1.6 Hz, 1H), 2.88 (t, *J* = 16.3 Hz, 2H), 2.35 – 2.00 (m, 4H), 1.95 – 1.76 (m, 1H), 1.70 – 1.39 (m, 7H), 1.22 – 1.05 (m, 1H).

$^{13}$C NMR (101 MHz, $CDCl_3$) δ 135.65, 131.92, 125.00, 123.77, 117.50, 114.61, 114.18, 113.23, 110.07, 103.47, 70.95, 57.35, 56.91, 55.46, 55.38, 38.39, 25.84, 24.45, 20.72.

HRMS (ESI+) m/z found 294.1975 [M+H]+, $C_{19}N_{24}N_3$ calculated 294.1970 (Δ = 1.7 ppm).

**(4R*,9a'R*)-8-methyl-3',4',7',8',9',9a'-hexahydro-2'H,5H,6'H-spiro[pyrrolo[1,2-a]quinoxaline-4,1'-quinolizine] 5.25**

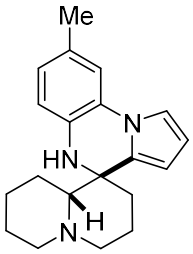

Light yellow solid (49.2 mg, 32 %).

$^1$H NMR (400 MHz, DMSO-$d_6$) δ 7.31 (dd, *J* = 2.9, 1.5 Hz, 1H), 7.26 (d, *J* = 8.0 Hz, 1H), 6.82 (d, *J* = 1.8 Hz, 1H), 6.38 (dd, *J* = 8.0, 1.8 Hz, 1H), 6.17 (t, *J* = 3.2 Hz, 1H), 5.94 (dd, *J* = 3.5, 1.6 Hz, 1H), 5.71 (s, 1H), 2.94 – 2.65 (m, 2H), 2.22– 2.10 (1H), 2.16 (s, 3H), 2.04 – 1.90 (m, 2H), 1.86 (d, *J* = 14.0 Hz, 1H), 1.69 – 1.59 (m, 1H), 1.57 – 1.19 (m, 7H), 1.14 – 0.99 (m, 1H). $^{13}$C NMR (101 MHz, DMSO-$d_6$) δ 136.27, 134.03, 131.53, 121.14, 117.45, 115.23, 114.28, 113.76, 110.13, 103.60, 71.10, 69.68, 56.92, 56.64, 38.73, 25.81, 25.64, 24.33, 21.32, 20.14.HRMS (ESI+) m/z found 308.2120 [M+H]+, $C_{20}H_{26}N_3$ calculated 308.2126 (Δ = -1.95 ppm).

**(4R*,9a'R*)-7-chloro-3',4',7',8',9',9a'-hexahydro-2'H,5H,6'H-spiro[pyrrolo[1,2-a]quinoxaline-4,1'-quinolizine] 5.26**

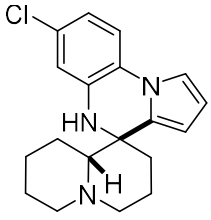

Pale white solid (64.7 mg, 40%).

$^1$H NMR (400 MHz, $CDCl_3$) δ 7.12 (d, *J* = 8.4 Hz, 1H), 7.08 (dd, *J* = 3.0, 1.5 Hz, 1H), 6.75 (d, *J* = 2.3 Hz, 1H), 6.63 (dd, *J* = 8.4, 2.2 Hz, 1H), 6.29 (t, *J* = 3.2 Hz, 1H), 5.96 (dd, *J* = 3.5, 1.6 Hz, 1H), 5.01 (s, 1H), 2.87 (dd, *J* = 19.5, 11.8 Hz, 2H), 2.23 (d, *J* = 10.6 Hz, 1H), 2.19 – 2.01 (m, 3H), 1.85 (q, *J* = 13.8, 13.4 Hz, 1H), 1.68 – 1.53 (m, 4H), 1.52 – 1.36 (m, 3H), 1.22 – 1.05 (m, 1H).$^{13}$C NMR (101 MHz, $CDCl_3$) δ 136.72, 131.39, 129.87, 122.35, 117.05, 115.03, 114.15, 113.23, 110.45, 103.86, 70.94, 57.20, 56.79, 55.60, 38.59, 25.74, 24.33, 20.64.

HRMS (ESI+) m/z found 328.1578 [M+H]+, $C_{19}H_{23}ClN_3$ calculated 328.1580 (Δ = -0.61 ppm).

# 7 References


(1) Guillier, F.; Orain, D.; Bradley, M. Linkers and Cleavage Strategies in Solid-Phase Organic Synthesis and Combinatorial Chemistry. **2000**. https://doi.org/10.1021/cr980040.

(2) K, P. Paclitaxel Against Cancer: A Short Review. *Med Chem (Los Angeles)* **2012**, *02* (07). https://doi.org/10.4172/2161-0444.1000130.

(3) Tu, Y. Artemisinin: Ein Geschenk Der Traditionellen Chinesischen Medizin an Die Welt (Nobel-Aufsatz). *Angewandte Chemie* **2016**, *128* (35), 10366–10382. https://doi.org/10.1002/ange.201601967.

(4) Pye, C. R.; Bertin, M. J.; Lokey, R. S.; Gerwick, W. H.; Linington, R. G. Retrospective Analysis of Natural Products Provides Insights for Future Discovery Trends. *Proc Natl Acad Sci U S A* **2017**, *114* (22), 5601–5606. https://doi.org/10.1073/pnas.1614680114.

(5) Wang, S.; Dong, G.; Sheng, C. Structural Simplification of Natural Products. *Chemical Reviews*. American Chemical Society March 27, 2019, pp 4180–4220. https://doi.org/10.1021/acs.chemrev.8b00504.

(6) Eder, J.; Sedrani, R.; Wiesmann, C. The Discovery of First-in-Class Drugs: Origins and Evolution. *Nat Rev Drug Discov* **2014**, *13* (8), 577–587. https://doi.org/10.1038/nrd4336.

(7) Koch, M. A.; Schuffenhauer, A.; Scheck, M.; Wetzel, S.; Casaulta, M.; Odermatt, A.; Ertl, P.; Waldmann, H.; Lerner, R. A. *Charting Biologically Relevant Chemical Space: A Structural Classification of Natural Products (SCONP)*; 2005. www.thomsonderwent.com.

(8) Nö Ren-Mü, A.; Reis-Corrê, I.; Prinz, H.; Rosenbaum, C.; Saxena, K.; Schwalbe, H. J.; Vestweber, D.; Cagna, G.; Schunk, S.; Schwarz, O.; Schiewe, H.; Waldmann, H. *Discovery of Protein Phosphatase Inhibitor Classes by Biology-Oriented Synthesis*; 2006. www.pnas.orgcgidoi10.1073pnas.0601490103.

(9) Wetzel, S.; Bon, R. S.; Kumar, K.; Waldmann, H. Biology-Oriented Synthesis. *Angewandte Chemie - International Edition*. November 11, 2011, pp 10800–10826. https://doi.org/10.1002/anie.201007004.

(10) Newman, D. J.; Cragg, G. M. Natural Products as Sources of New Drugs from 1981 to 2014. *Journal of Natural Products*. American Chemical Society March 25, 2016, pp 629–661. https://doi.org/10.1021/acs.jnatprod.5b01055.

(11) Huigens, R. W.; Morrison, K. C.; Hicklin, R. W.; Timothy, T. A.; Richter, M. F.; Hergenrother, P. J. A Ring-Distortion Strategy to Construct Stereochemically Complex and Structurally Diverse Compounds from Natural Products. *Nat Chem* **2013**, *5* (3), 195–202. https://doi.org/10.1038/nchem.1549.

(12) Tasker, S. Z.; Cowfer, A. E.; Hergenrother, P. J. Preparation of Structurally Diverse Compounds from the Natural Product Lycorine. *Org Lett* **2018**, *20* (18), 5894–5898. https://doi.org/10.1021/acs.orglett.8b02562.

(13) Rafferty, R. J.; Hicklin, R. W.; Maloof, K. A.; Hergenrother, P. J. Synthesis of Complex and Diverse Compounds through Ring Distortion of Abietic Acid. *Angewandte Chemie - International Edition* **2014**, *53* (1), 220–224. https://doi.org/10.1002/anie.201308743.

(14) Garcia, A.; Drown, B. S.; Hergenrother, P. J. Access to a Structurally Complex Compound Collection via Ring Distortion of the Alkaloid Sinomenine. *Org Lett* **2016**, *18* (19), 4852–4855. https://doi.org/10.1021/acs.orglett.6b02333.

(15) Llabani, E.; Hicklin, R. W.; Lee, H. Y.; Motika, S. E.; Crawford, L. A.; Weerapana, E.; Hergenrother, P. J. Diverse Compounds from Pleuromutilin Lead to a Thioredoxin Inhibitor and Inducer of Ferroptosis. *Nat Chem* **2019**, *11* (6), 521–532. https://doi.org/10.1038/s41557-019-0261-6.
(16) O' Connor, C. J.; Beckmann, H. S. G.; Spring, D. R. Diversity-Oriented Synthesis: Producing Chemical Tools for Dissecting Biology. *Chem Soc Rev* **2012**, *41* (12), 4444–4456. https://doi.org/10.1039/c2cs35023h.
(17) Galloway, W. R. J. D.; Isidro-Llobet, A.; Spring, D. R. Diversity-Oriented Synthesis as a Tool for the Discovery of Novel Biologically Active Small Molecules. *Nature Communications*. Nature Publishing Group 2010. https://doi.org/10.1038/ncomms1081.
(18) Nielsen, T. E.; Schreiber, S. L. Towards the Optimal Screening Collection: A Synthesis Strategy. *Angewandte Chemie - International Edition*. 2008, pp 48–56. https://doi.org/10.1002/anie.200703073.
(19) Zhang, J.; Wu, J.; Hong, B.; Ai, W.; Wang, X.; Li, H.; Lei, X. Diversity-Oriented Synthesis of Lycopodium Alkaloids Inspired by the Hidden Functional Group Pairing Pattern. *Nat Commun* **2014**, *5*. https://doi.org/10.1038/ncomms5614.
(20) Karageorgis, G.; Foley, D. J.; Laraia, L.; Waldmann, H. Principle and Design of Pseudo-Natural Products. *Nat Chem* **2020**, *12* (3), 227–235. https://doi.org/10.1038/s41557-019-0411-x.
(21) Karageorgis, G.; Reckzeh, E. S.; Ceballos, J.; Schwalfenberg, M.; Sievers, S.; Ostermann, C.; Pahl, A.; Ziegler, S.; Waldmann, H. Chromopynones Are Pseudo Natural Product Glucose Uptake Inhibitors Targeting Glucose Transporters GLUT-1 and -3. *Nat Chem* **2018**, *10* (11), 1103–1111. https://doi.org/10.1038/s41557-018-0132-6.
(22) Foley, D. J.; Zinken, S.; Corkery, D.; Laraia, L.; Pahl, A.; Wu, Y. W.; Waldmann, H. Phenotyping Reveals Targets of a Pseudo-Natural-Product Autophagy Inhibitor. *Angewandte Chemie - International Edition* **2020**, *59* (30), 12470–12476. https://doi.org/10.1002/anie.202000364.
(23) Burhop, A.; Bag, S.; Grigalunas, M.; Woitalla, S.; Bodenbinder, P.; Brieger, L.; Strohmann, C.; Pahl, A.; Sievers, S.; Waldmann, H. Synthesis of Indofulvin Pseudo-Natural Products Yields a New Autophagy Inhibitor Chemotype. *Advanced Science* **2021**, *8* (19). https://doi.org/10.1002/advs.202102042.
(24) Sandhu, J.; Li, S.; Fairall, L.; Pfisterer, S. G.; Gurnett, J. E.; Xiao, X.; Weston, T. A.; Vashi, D.; Ferrari, A.; Orozco, J. L.; Hartman, C. L.; Strugatsky, D.; Lee, S. D.; He, C.; Hong, C.; Jiang, H.; Bentolila, L. A.; Gatta, A. T.; Levine, T. P.; Ferng, A.; Lee, R.; Ford, D. A.; Young, S. G.; Ikonen, E.; Schwabe, J. W. R.; Tontonoz, P. Aster Proteins Facilitate Nonvesicular Plasma Membrane to ER Cholesterol Transport in Mammalian Cells. *Cell* **2018**, *175* (2), 514-529.e20. https://doi.org/10.1016/j.cell.2018.08.033.
(25) Xiao, X.; Kim, Y.; Romartinez-Alonso, B.; Sirvydis, K.; Ory, D. S.; R Schwabe, J. W.; Jung, M. E.; Tontonoz, P.; Kliewer, S. A.; Yang, H. Selective Aster Inhibitors Distinguish Vesicular and Nonvesicular Sterol Transport Mechanisms. https://doi.org/10.1073/pnas.2024149118/-/DCSupplemental.
(26) Whitmarsh-Everiss, T.; Olsen, A. H.; Laraia, L. Identification of Inhibitors of Cholesterol Transport Proteins Through the Synthesis of a Diverse, Sterol-Inspired Compound Collection. *Angewandte Chemie - International Edition* **2021**, *60* (51), 26755–26761. https://doi.org/10.1002/anie.202111639.

(27) *Structure and Health Effects of Natural Products on Diabetes Mellitus*; Springer Singapore, 2021. https://doi.org/10.1007/978-981-15-8791-7.
(28) Ba, G. R. H.; Baskett, T. F.; Frcsc, M. B. *History of Anesthesia In the Arms of Morpheus: The Development of Mor-Phine for Postoperative Pain Relief*; 2000; Vol. 47.
(29) Paulke, A.; Kremer, C.; Wunder, C.; Achenbach, J.; Djahanschiri, B.; Elias, A.; Stefan Schwed, J.; Hübner, H.; Gmeiner, P.; Proschak, E.; Toennes, S. W.; Stark, H. Argyreia Nervosa (Burm. f.): Receptor Profiling of Lysergic Acid Amide and Other Potential Psychedelic LSD-like Compounds by Computational and Binding Assay Approaches. *J Ethnopharmacol* **2013**, *148* (2), 492–497. https://doi.org/10.1016/j.jep.2013.04.044.
(30) Ribaric, S. The Pharmacological Properties and Therapeutic Use of Apomorphine. *Molecules*. May 2012, pp 5289–5309. https://doi.org/10.3390/molecules17055289.
(31) Millan, M. J.; Maiofiss, L.; Cussac, D.; Audinot, V.; Boutin, J. A.; Newman-Tancredi, A. Differential Actions of Antiparkinson Agents at Multiple Classes of Monoaminergic Receptor. I. A Multivariate Analysis of the Binding Profiles of 14 Drugs at 21 Native and Cloned Human Receptor Subtypes. *Journal of Pharmacology and Experimental Therapeutics* **2002**, *303* (2), 791–804. https://doi.org/10.1124/jpet.102.039867.
(32) Cameron, L. P.; Tombari, R. J.; Lu, J.; Pell, A. J.; Hurley, Z. Q.; Ehinger, Y.; Vargas, M. v.; McCarroll, M. N.; Taylor, J. C.; Myers-Turnbull, D.; Liu, T.; Yaghoobi, B.; Laskowski, L. J.; Anderson, E. I.; Zhang, G.; Viswanathan, J.; Brown, B. M.; Tjia, M.; Dunlap, L. E.; Rabow, Z. T.; Fiehn, O.; Wulff, H.; McCorvy, J. D.; Lein, P. J.; Kokel, D.; Ron, D.; Peters, J.; Zuo, Y.; Olson, D. E. A Non-Hallucinogenic Psychedelic Analogue with Therapeutic Potential. *Nature* **2021**, *589* (7842), 474–479. https://doi.org/10.1038/s41586-020-3008-z.
(33) Kaplan, A. L.; Confair, D. N.; Kim, K.; Barros-Álvarez, X.; Rodriguiz, R. M.; Yang, Y.; Kweon, O. S.; Che, T.; McCorvy, J. D.; Kamber, D. N.; Phelan, J. P.; Martins, L. C.; Pogorelov, V. M.; DiBerto, J. F.; Slocum, S. T.; Huang, X.-P.; Kumar, J. M.; Robertson, M. J.; Panova, O.; Seven, A. B.; Wetsel, A. Q.; Wetsel, W. C.; Irwin, J. J.; Skiniotis, G.; Shoichet, B. K.; Roth, B. L.; Ellman, J. A. Bespoke Library Docking for 5-HT2A Receptor Agonists with Antidepressant Activity. *Nature* **2022**. https://doi.org/10.1038/s41586-022-05258-z.
(34) Martin, S. F. Bridging Known and Unknown Unknowns: From Natural Products and Their Mimics to Unmet Needs in Neuroscience. *Acc Chem Res* **2022**, *55* (17), 2397–2408. https://doi.org/10.1021/acs.accounts.1c00773.
(35) Sahn, J. J.; Granger, B. A.; Martin, S. F. Evolution of a Strategy for Preparing Bioactive Small Molecules by Sequential Multicomponent Assembly Processes, Cyclizations, and Diversification. *Org Biomol Chem* **2014**, *12* (39), 7659–7672. https://doi.org/10.1039/c4ob00835a.
(36) Klein, J.; Heal, J. R.; Hamilton, W. D. O.; Boussemghoune, T.; Tange, T. Ø.; Delegrange, F.; Jaeschke, G.; Hatsch, A.; Heim, J. Yeast Synthetic Biology Platform Generates Novel Chemical Structures as Scaffolds for Drug Discovery. *ACS Synth Biol* **2014**, *3* (5), 314–323. https://doi.org/10.1021/sb400177x.
(37) Frankowski, K. J.; Setola, V.; Evans, J. M.; Neuenswander, B.; Roth, B. L.; Aubéa, J. Synthesis and Receptor Profiling of Stemona Alkaloid Analogues Reveal a Potent Class of Sigma Ligands. *Proc Natl Acad Sci U S A* **2011**, *108* (17), 6727–6732. https://doi.org/10.1073/pnas.1016558108.

(38) McLeod, M. C.; Singh, G.; Plampin, J. N.; Rane, D.; Wang, J. L.; Day, V. W.; Aubé, J. Probing Chemical Space with Alkaloid-Inspired Libraries. *Nat Chem* **2014**, *6* (2), 133–140. https://doi.org/10.1038/nchem.1844.

(39) Foley, D. J.; Waldmann, H. Ketones as Strategic Building Blocks for the Synthesis of Natural Product-Inspired Compounds. *Chemical Society Reviews*. Royal Society of Chemistry May 4, 2022, pp 4094–4120. https://doi.org/10.1039/d2cs00101b.

(40) Houghton, P. J. *CHEMISTRY AND BIOLOGICAL ACTIVITY OF NATURAL AND SEMI-SYNTHETIC CHROMONE ALKALOIDS*; 2000; Vol. 21.

(41) van der Horst, E.; Okuno, Y.; Bender, A.; IJzerman, A. P. Substructure Mining of GPCR Ligands Reveals Activity-Class Specific Functional Groups in an Unbiased Manner. *J Chem Inf Model* **2009**, *49* (2), 348–360. https://doi.org/10.1021/ci8003896.

(42) Bajaj, S.; Ong, S. T.; Chandy, K. G. Contributions of Natural Products to Ion Channel Pharmacology. *Natural Product Reports*. Royal Society of Chemistry May 1, 2020, pp 703–716. https://doi.org/10.1039/c9np00056a.

(43) Grynkiewicz, G.; Gadzikowska, M. Tropane Alkaloids as Medicinally Useful Natural Products and Their Synthetic Derivatives as New Drugs*. *Pharmacological Reports* **2008**, *60*, 439–463.

(44) Lakstygal, A. M.; Kolesnikova, T. O.; Khatsko, S. L.; Zabegalov, K. N.; Volgin, A. D.; Demin, K. A.; Shevyrin, V. A.; Wappler-Guzzetta, E. A.; Kalueff, A. v. DARK Classics in Chemical Neuroscience: Atropine, Scopolamine, and Other Anticholinergic Deliriant Hallucinogens. *ACS Chemical Neuroscience*. American Chemical Society May 15, 2019, pp 2144–2159. https://doi.org/10.1021/acschemneuro.8b00615.

(45) Narayan, R.; Bauer, J. O.; Strohmann, C.; Antonchick, A. P.; Waldmann, H. Catalytic Enantioselective Synthesis of Functionalized Tropanes Reveals Novel Inhibitors of Hedgehog Signaling. *Angewandte Chemie - International Edition* **2013**, *52* (49), 12892–12896. https://doi.org/10.1002/anie.201307392.

(46) Lowe, R. A.; Taylor, D.; Chibale, K.; Nelson, A.; Marsden, S. P. Synthesis and Evaluation of the Performance of a Small Molecule Library Based on Diverse Tropane-Related Scaffolds. *Bioorg Med Chem* **2020**, *28* (9). https://doi.org/10.1016/j.bmc.2020.115442.

(47) Ouach, A.; Pin, F.; Bertrand, E.; Vercouillie, J.; Gulhan, Z.; Mothes, C.; Deloye, J. B.; Guilloteau, D.; Suzenet, F.; Chalon, S.; Routier, S. Design of A7 Nicotinic Acetylcholine Receptor Ligands Using the (Het)Aryl-1,2,3-Triazole Core: Synthesis, in Vitro Evaluation and SAR Studies. *Eur J Med Chem* **2016**, *107*, 153–164. https://doi.org/10.1016/j.ejmech.2015.11.001.

(48) Karnik, S. S.; Gogonea, C.; Patil, S.; Saad, Y.; Takezako, T. Activation of G-Protein-Coupled Receptors: A Common Molecular Mechanism. *Trends in Endocrinology and Metabolism*. Elsevier Inc. 2003, pp 431–437. https://doi.org/10.1016/j.tem.2003.09.007.

(49) Hauser, A. S.; Attwood, M. M.; Rask-Andersen, M.; Schiöth, H. B.; Gloriam, D. E. Trends in GPCR Drug Discovery: New Agents, Targets and Indications. *Nat Rev Drug Discov* **2017**, *16* (12), 829–842. https://doi.org/10.1038/nrd.2017.178.

(50) Tan, Y.; Xu, P.; Huang, S.; Yang, G.; Zhou, F.; He, X.; Ma, H.; Xu, H. E.; Jiang, Y. Structural Insights into the Ligand Binding and Gi Coupling of Serotonin Receptor 5-HT5A. *Cell Discov* **2022**, *8* (1). https://doi.org/10.1038/s41421-022-00412-3.

(51) Hoyer, D. Serotonin Receptors Nomenclature. In *The Serotonin System: History, Neuropharmacology, and Pathology*; Elsevier, 2019; pp 63–93. https://doi.org/10.1016/B978-0-12-813323-1.00004-9.

(52) Barnes, N. M.; Ahern, G. P.; Becamel, C.; Bockaert, J.; Camilleri, M.; Chaumont-Dubel, S.; Claeysen, S.; Cunningham, K. A.; Fone, K. C.; Gershon, M.; di Giovanni, G.; Goodfellow, N. M.; Halberstadt, A. L.; Hartley, R. M.; Hassaine, G.; Herrick-Davis, K.; Hovius, R.; Lacivita, E.; Lambe, E. K.; Leopoldo, M.; Levy, F. O.; Lummis, S. C. R.; Marin, P.; Maroteaux, L.; McCreary, A. C.; Nelson, D. L.; Neumaier, J. F.; Newman-Tancredi, A.; Nury, H.; Roberts, A.; Roth, B. L.; Roumier, A.; Sanger, G. J.; Teitler, M.; Sharp, T.; Villalón, C. M.; Vogel, H.; Watts, S. W.; Hoyer, D. International Union of Basic and Clinical Pharmacology. Cx. Classification of Receptors for 5-Hydroxytryptamine; Pharmacology and Function. *Pharmacol Rev* **2021**, *73* (1), 310–520. https://doi.org/10.1124/PR.118.015552.

(53) Kimura, K. T.; Asada, H.; Inoue, A.; Kadji, F. M. N.; Im, D.; Mori, C.; Arakawa, T.; Hirata, K.; Nomura, Y.; Nomura, N.; Aoki, J.; Iwata, S.; Shimamura, T. Structures of the 5-HT 2A Receptor in Complex with the Antipsychotics Risperidone and Zotepine. *Nat Struct Mol Biol* **2019**, *26* (2), 121–128. https://doi.org/10.1038/s41594-018-0180-z.

(54) Kwan, A. C.; Olson, D. E.; Preller, K. H.; Roth, B. L. The Neural Basis of Psychedelic Action. *Nature Neuroscience*. Nature Research November 1, 2022, pp 1407–1419. https://doi.org/10.1038/s41593-022-01177-4.

(55) McClure-Begley, T. D.; Roth, B. L. The Promises and Perils of Psychedelic Pharmacology for Psychiatry. *Nat Rev Drug Discov* **2022**, *21* (6), 463–473. https://doi.org/10.1038/s41573-022-00421-7.

(56) di Giovanni, G.; de Deurwaerdère, P. New Therapeutic Opportunities for 5-HT2C Receptor Ligands in Neuropsychiatric Disorders. *Pharmacology and Therapeutics*. Elsevier Inc. January 1, 2016, pp 125–162. https://doi.org/10.1016/j.pharmthera.2015.11.009.

(57) Gore, S.; Baskaran, S.; König, B. Fischer Indole Synthesis in Low Melting Mixtures. *Org Lett* **2012**, *14* (17), 4568–4571. https://doi.org/10.1021/ol302034r.

(58) Xu, J.; Liang, L.; Zheng, H.; Chi, Y. R.; Tong, R. Green Oxidation of Indoles Using Halide Catalysis. *Nat Commun* **2019**, *10* (1). https://doi.org/10.1038/s41467-019-12768-4.

(59) Zeng, H.; Wang, Z.; Li, C. Two-in-One Strategy for Palladium-Catalyzed C−H Functionalization in Water. *Angewandte Chemie* **2019**, *131* (9), 2885–2889. https://doi.org/10.1002/ange.201813391.

(60) Ryabukhin, S. v.; Panov, D. M.; Plaskon, A. S.; Tolmachev, A. A.; Smaliy, R. v. Application of Chlorotrimethylsilane in Pictet-Spengler Reaction. *Monatsh Chem* **2012**, *143* (11), 1507–1517. https://doi.org/10.1007/s00706-012-0804-7.

(61) Wünsch, B.; Zott, M. Chirale 2-Benzopyran-3-carbonsäure-Derivate Durch Oxa-Pictet-Spengler-Reaktion von (S)-3-Phenylmilchsäure-Derivaten. *Liebigs Ann Chem* **1992**, *1992* (1), 39–45. https://doi.org/10.1002/jlac.199219920109.

(62) Maier, C. A.; Wünsch, B. Novel Spiropiperidines as Highly Potent and Subtype Selective σ-Receptor Ligands. Part 1. *J Med Chem* **2002**, *45* (2), 438–448. https://doi.org/10.1021/jm010992z.

(63) Miklós, F.; Fülöp, F. “Dry” and “Wet” Green Synthesis of 2,2′ -Disubstituted Quinazolinones. *European J Org Chem* **2010**, No. 5, 959–965. https://doi.org/10.1002/ejoc.200901052.

(64) Stotani, S.; Lorenz, C.; Winkler, M.; Medda, F.; Picazo, E.; Ortega Martinez, R.; Karawajczyk, A.; Sanchez-Quesada, J.; Giordanetto, F. Design and Synthesis of

Fsp3-Rich, Bis-Spirocyclic-Based Compound Libraries for Biological Screening. *ACS Comb Sci* **2016**, *18* (6), 330–336. https://doi.org/10.1021/acscombsci.6b00005.

(65) Mullen, G.; Napier, J.; Balestra, M.; Decory, T.; Hale, G.; Macor, J.; Mack, R.; Loch, J.; Wu, E.; Kover, A.; Verhoest, P.; Sampognaro, A.; Phillips, E.; Zhu, Y.; Murray, R.; Griffith, R.; Blosser, J.; Gurley, D.; Machulskis, A.; Zongrone, J.; Rosen, A.; Gordon, J. (-)-Spiro[1-Azabicyclo[2.2.2]Octane-3,5'-Oxazolidin-2-One], a Conformationally Restricted Analogue of Acetylcholine, Is a Highly Selective Full Agonist at the A7 Nicotinic Acetylcholine Receptor. *J Med Chem* **2000**, *43* (22), 4045–4050. https://doi.org/10.1021/jm000249r.

(66) Tatsumi, R.; Fujio, M.; Satoh, H.; Katayama, J.; Takanashi, S. I.; Hashimoto, K.; Tanaka, H. Discovery of the A7 Nicotinic Acetylcholine Receptor Agonists. (R)-3′-(5-Chlorothiophen-2-Yl)Spiro-1-Azabicyclo[2.2.2]Octane-3, 5′-[1′,3′]-Oxazolidin-2′-One as a Novel, Potent, Selective, and Orally Bioavailable Ligand. *J Med Chem* **2005**, *48* (7), 2678–2686. https://doi.org/10.1021/jm049188d.

(67) Colomer, I.; Empson, C. J.; Craven, P.; Owen, Z.; Doveston, R. G.; Churcher, I.; Marsden, S. P.; Nelson, A. A Divergent Synthetic Approach to Diverse Molecular Scaffolds: Assessment of Lead-Likeness Using LLAMA, an Open-Access Computational Tool. *Chemical Communications* **2016**, *52* (45), 7209–7212. https://doi.org/10.1039/c6cc03244c.

(68) Gadgaard, C.; Jensen, A. A. Functional Characterization of 5-HT1A and 5-HT1B Serotonin Receptor Signaling through G-Protein-Activated Inwardly Rectifying K+ Channels in a Fluorescence-Based Membrane Potential Assay. *Biochem Pharmacol* **2020**, *175*. https://doi.org/10.1016/j.bcp.2020.113870.

(69) Jensen, A. A.; McCorvy, J. D.; Leth-Petersen, S.; Bundgaard, C.; Liebscher, G.; Kenakin, T. P.; Bräuner-Osborne, H.; Kehler, J.; Kristensen, J. L. Detailed Characterization of the In Vitro Pharmacological and Pharmacokinetic Properties of N-(2-Hydroxybenzyl)-2, 5-Dimethoxy-4-Cyanophenylethylamine (25CN-NBOH), a Highly Selective and Brain-Penetrant 5-HT2A Receptor Agonist. *Journal of Pharmacology and Experimental Therapeutics* **2017**, *361* (3), 441–453. https://doi.org/10.1124/jpet.117.239905.

(70) Vass, M.; Kooistra, A. J.; Yang, D.; Stevens, R. C.; Wang, M. W.; de Graaf, C. Chemical Diversity in the G Protein-Coupled Receptor Superfamily. *Trends in Pharmacological Sciences*. Elsevier Ltd May 1, 2018, pp 494–512. https://doi.org/10.1016/j.tips.2018.02.004.

(71) Hauser, A. S.; Attwood, M. M.; Rask-Andersen, M.; Schiöth, H. B.; Gloriam, D. E. Trends in GPCR Drug Discovery: New Agents, Targets and Indications. *Nat Rev Drug Discov* **2017**, *16* (12), 829–842. https://doi.org/10.1038/nrd.2017.178.

(72) Mewshaw, R. E.; Silverman, L. S.; Mathew, R. M.; Kaiser, C.; Sherrill, R. G.; Cheng, M.; Tiffany, C. W.; Karbon, E. W.; Bailey, M. A.; Borosky, S. A.; Ferkany, J. W.; Abreu, M. E. *Bridged 7-Carbolines and Derivatives Possessing Selective and Combined Affinity for 5-HT2 and D2 Receptors*; 1993; Vol. 36. https://pubs.acs.org/sharingguidelines.

(73) Bodnar, A. L.; Cortes-Burgos, L. A.; Cook, K. K.; Dinh, D. M.; Groppi, V. E.; Hajos, M.; Higdon, N. R.; Hoffmann, W. E.; Hurst, R. S.; Myers, J. K.; Rogers, B. N.; Wall, T. M.; Wolfe, M. L.; Wong, E. Discovery and Structure-Activity Relationship of Quinuclidine Benzamides as Agonists of A7 Nicotinic Acetylcholine Receptors. *J Med Chem* **2005**, *48* (4), 905–908. https://doi.org/10.1021/jm049363q.

(74) Elmore, C. S.; Landvatter, S.; Dorff, P. N.; Powell, M. E.; Killick, D.; Blake, T.; Hall, J.; Heys, J. R.; Harding, J.; Urbanek, R.; Ernst, G. Synthesis of Three Alpha 7 Agonists in Labeled Form. *J Labelled Comp Radiopharm* **2014**, *57* (5), 342–349. https://doi.org/10.1002/jlcr.3186.

(75) Zhang, J.; Liu, Y. Q.; Fang, J. The Biological Activities of Quinolizidine Alkaloids. In *Alkaloids: Chemistry and Biology*; Academic Press Inc., 2022. https://doi.org/10.1016/bs.alkal.2022.06.001.

(76) Toyooka, N.; Kobayashi, S.; Zhou, D.; Tsuneki, H.; Wada, T.; Sakai, H.; Nemoto, H.; Sasaoka, T.; Garraffo, H. M.; Spande, T. F.; Daly, J. W. Synthesis of Poison-Frog Alkaloids 233A, 235U, and 251AA and Their Inhibitory Effects on Neuronal Nicotinic Acetylcholine Receptors. *Bioorg Med Chem Lett* **2007**, *17* (21), 5872–5875. https://doi.org/10.1016/j.bmcl.2007.08.045.

(77) Vacca, J. P.; Timmermans, P. B. M. W. M.; van Zwieten, P. J.; Latimer, N.; Mcadams, R. P.; Rhodes, K. F.; Sharma, S.; Turner, S. J.; Waterfall, J. F.; Ferry, N.; Goodhardt, M.; Hanoune, J.; Sevenet, T.; Kunieda, T.; Koga, K.; Yamada, S. *Structure-Affinity Relationships of Arylquinolizines at a-Adrenoceptors*; 1988; Vol. 31. https://pubs.acs.org/sharingguidelines.

(78) Sallinen, J.; Holappa, J.; Koivisto, A.; Kuokkanen, K.; Chapman, H.; Lehtimäki, J.; Piepponen, P.; Mijatovic, J.; Tanila, H.; Virtanen, R.; Sirviö, J.; Haapalinna, A. Pharmacological Characterisation of a Structurally Novel A2C -Adrenoceptor Antagonist ORM-10921 and Its Effects in Neuropsychiatric Models. *Basic Clin Pharmacol Toxicol* **2013**, *113* (4), 239–249. https://doi.org/10.1111/bcpt.12090.

(79) Ellis, J. M.; Fell, M. J. Current Approaches to the Treatment of Parkinson's Disease. *Bioorganic and Medicinal Chemistry Letters*. Elsevier Ltd 2017, pp 4247–4255. https://doi.org/10.1016/j.bmcl.2017.07.075.

(80) Wang, S.; Che, T.; Levit, A.; Shoichet, B. K.; Wacker, D.; Roth, B. L. Structure of the D2 Dopamine Receptor Bound to the Atypical Antipsychotic Drug Risperidone. *Nature* **2018**, *555* (7695), 269–273. https://doi.org/10.1038/nature25758.

(81) Zhuang, Y.; Xu, P.; Mao, C.; Wang, L.; Krumm, B.; Zhou, X. E.; Huang, S.; Liu, H.; Cheng, X.; Huang, X. P.; Shen, D. D.; Xu, T.; Liu, Y. F.; Wang, Y.; Guo, J.; Jiang, Y.; Jiang, H.; Melcher, K.; Roth, B. L.; Zhang, Y.; Zhang, C.; Xu, H. E. Structural Insights into the Human D1 and D2 Dopamine Receptor Signaling Complexes. *Cell* **2021**, *184* (4), 931-942.e18. https://doi.org/10.1016/j.cell.2021.01.027.

(82) Roth, B. L.; Irwin, J. J.; Shoichet, B. K. Discovery of New GPCR Ligands to Illuminate New Biology. *Nature Chemical Biology*. Nature Publishing Group November 1, 2017, pp 1143–1151. https://doi.org/10.1038/nchembio.2490.

(83) Allen, J. A.; Yost, J. M.; Setola, V.; Chen, X.; Sassano, M. F.; Chen, M.; Peterson, S.; Yadav, P. N.; Huang, X. P.; Feng, B.; Jensen, N. H.; Che, X.; Bai, X.; Frye, S. v.; Wetsel, W. C.; Caron, M. G.; Javitch, J. A.; Roth, B. L.; Jin, J. Discovery of β-Arrestin-Biased Dopamine D 2 Ligands for Probing Signal Transduction Pathways Essential for Antipsychotic Efficacy. *Proc Natl Acad Sci U S A* **2011**, *108* (45), 18488–18493. https://doi.org/10.1073/pnas.1104807108.

(84) Michael, J. P. Indolizidine and Quinolizidine Alkaloids. *Natural Product Reports*. 2008, pp 139–165. https://doi.org/10.1039/b612166g.

(85) Zhou, H.; Li, J.; Sun, F.; Wang, F.; Li, M.; Dong, Y.; Fan, H.; Hu, D. A Review on Recent Advances in Aloperine Research: Pharmacological Activities and Underlying Biological Mechanisms. *Frontiers in Pharmacology*. Frontiers Media S.A. October 29, 2020. https://doi.org/10.3389/fphar.2020.538137.

(86) Dang, Z.; Zhu, L.; Lai, W.; Bogerd, H.; Lee, K. H.; Huang, L.; Chen, C. H. Aloperine and Its Derivatives as a New Class of HIV-1 Entry Inhibitors. *ACS Med Chem Lett* **2016**, *7* (3), 240–244. https://doi.org/10.1021/acsmedchemlett.5b00339.

(87) Zhang, X.; Lv, X. Q.; Tang, S.; Mei, L.; Li, Y. H.; Zhang, J. P.; Jiang, J. D.; Peng, Z. G.; Song, D. Q. Discovery and Evolution of Aloperine Derivatives as a New Family of HCV Inhibitors with Novel Mechanism. *Eur J Med Chem* **2018**, *143*, 1053–1065. https://doi.org/10.1016/j.ejmech.2017.12.002.

(88) Li, Y. H.; Wu, Z. Y.; Tang, S.; Zhang, X.; Wang, Y. X.; Jiang, J. D.; Peng, Z. G.; Song, D. Q. Evolution of Matrinic Ethanol Derivatives as Anti-HCV Agents from Matrine Skeleton. *Bioorg Med Chem Lett* **2017**, *27* (9), 1962–1966. https://doi.org/10.1016/j.bmcl.2017.03.025.

(89) Basilico, N.; Parapini, S.; Sparatore, A.; Romeo, S.; Misiano, P.; Vivas, L.; Yardley, V.; Croft, S. L.; Habluetzel, A.; Lucantoni, L.; Renia, L.; Russell, B.; Suwanarusk, R.; Nosten, F.; Dondio, G.; Bigogno, C.; Jabes, D.; Taramelli, D. In Vivo and in Vitro Activities and ADME-Tox Profile of a Quinolizidine-Modified 4-Aminoquinoline: A Potent Anti-P. Falciparum and Anti-P. Vivax Blood-Stage Antimalarial. *Molecules* **2017**, *22* (12). https://doi.org/10.3390/molecules22122102.

(90) Luo, Y.; Liu, Y.; Luo, D.; Gao, X.; Li, B.; Zhang, G.; Zhang´chengdu, G.; Zhang´chengdu, Z. *Cytotoxic Alkaloids from Boehmeria Siamensis*.

(91) Romanelli, M. N.; Gratteri, P.; Guandalini, L.; Martini, E.; Bonaccini, C.; Gualtieri, F. Central Nicotinic Receptors: Structure, Function, Ligands, and Therapeutic Potential. *ChemMedChem*. June 11, 2007, pp 746–767. https://doi.org/10.1002/cmdc.200600207.

(92) Tong, S. T. (Amy); Barker, D. A Concise Synthesis of (±) and a Total Synthesis of (+)-Epiquinamide. *Tetrahedron Lett* **2006**, *47* (29), 5017–5020. https://doi.org/10.1016/j.tetlet.2006.05.092.

(93) Zhang, J.; Wang, Y. Q.; Wang, X. W.; Li, W. D. Z. Transannular Reductive Rearrangement of α-Amino Ketones: Construction of Aza-Tricyclic Frameworks of Several Alkaloids. *Journal of Organic Chemistry* **2013**, *78* (12), 6154–6162. https://doi.org/10.1021/jo4007943.

(94) Boddy, A. J.; Bull, J. A. Stereoselective Synthesis and Applications of Spirocyclic Oxindoles. *Organic Chemistry Frontiers*. Royal Society of Chemistry March 7, 2021, pp 1026–1084. https://doi.org/10.1039/d0qo01085e.

(95) Pellegrini, C.; Sthissler, C.; Weber, M.; Borschberg, H.-J. *Synthesis of the Oxindole Alkaloid (-)-Horsfiline*; 1994; Vol. 5.

(96) Hussain, H.; Green, I. R.; Ahmed, I. Journey Describing Applications of Oxone in Synthetic Chemistry. *Chemical Reviews*. American Chemical Society May 8, 2013, pp 3329–3371. https://doi.org/10.1021/cr3004373.

(97) Wang, J.; Gong, F.; Liang, T.; Xie, Z.; Yang, Y.; Cao, C.; Gao, J.; Lu, T.; Chen, X. A Review of Synthetic Bioactive Tetrahydro-β-Carbolines: A Medicinal Chemistry Perspective. *European Journal of Medicinal Chemistry*. Elsevier Masson s.r.l. December 5, 2021. https://doi.org/10.1016/j.ejmech.2021.113815.

(98) Abuhamdah, S.; Habash, M.; Taha, M. O. Elaborate Ligand-Based Modeling Coupled with QSAR Analysis and in Silico Screening Reveal New Potent Acetylcholinesterase Inhibitors. *J Comput Aided Mol Des* **2013**, *27* (12), 1075–1092. https://doi.org/10.1007/s10822-013-9699-6.

(99) Mokrosz, M. J.; Duszynska, B.; Bojarski, A. J.; Mokrosz, J. L. *Structure-Activity Relationship Studies of CNS Agents XVH. Spiro[Piperidine-4',l-(1,2,3,4-Tetrahydro-[-*

*Carbofine)] as a Probe Defining the Extended Topographic Model of 5-HT1A Receptors*; 1995; Vol. 3.

(100) Campiani, G.; Cappelli, A.; Nacci, V.; Anzini, M.; Vomero, S.; Hamon, M.; Cagnotto, A.; Fracasso, C.; Uboldi, C.; Caccia, S.; Consolo, S.; Mennini, T. *Novel and Highly Potent 5-HT 3 Receptor Agonists Based on a Pyrroloquinoxaline Structure †*; 1997. https://pubs.acs.org/sharingguidelines.

(101) Liu, S.; Scotti, J. S.; Kozmin, S. A. Emulating the Logic of Monoterpenoid Alkaloid Biogenesis to Access a Skeletally Diverse Chemical Library. *Journal of Organic Chemistry* **2013**, *78* (17), 8645–8654. https://doi.org/10.1021/jo401262v.

(102) Jensen, A. A.; McCorvy, J. D.; Leth-Petersen, S.; Bundgaard, C.; Liebscher, G.; Kenakin, T. P.; Bräuner-Osborne, H.; Kehler, J.; Kristensen, J. L. Detailed Characterization of the In Vitro Pharmacological and Pharmacokinetic Properties of N-(2-Hydroxybenzyl)-2, 5-Dimethoxy-4-Cyanophenylethylamine (25CN-NBOH), a Highly Selective and Brain-Penetrant 5-HT2A Receptor Agonist. *Journal of Pharmacology and Experimental Therapeutics* **2017**, *361* (3), 441–453. https://doi.org/10.1124/jpet.117.239905.

(103) Gadgaard, C.; Jensen, A. A. Functional Characterization of 5-HT1A and 5-HT1B Serotonin Receptor Signaling through G-Protein-Activated Inwardly Rectifying K+ Channels in a Fluorescence-Based Membrane Potential Assay. *Biochem Pharmacol* **2020**, *175*. https://doi.org/10.1016/j.bcp.2020.113870.

(104) Jensen, A. A.; Plath, N.; Pedersen, M. H. F.; Isberg, V.; Krall, J.; Wellendorph, P.; Stensbøl, T. B.; Gloriam, D. E.; Krogsgaard-Larsen, P.; Frølund, B. Design, Synthesis, and Pharmacological Characterization of N - And O-Substituted 5,6,7,8-Tetrahydro-4H-Isoxazolo[4,5-d]Azepin-3-Ol Analogues: Novel 5-HT2A/5-HT2C Receptor Agonists with pro-Cognitive Properties. *J Med Chem* **2013**, *56* (3), 1211–1227. https://doi.org/10.1021/jm301656h.

(105) Sandager-Nielsen, K.; Ahring, P. K.; Klein, J.; van Hout, M.; Thaneshwaran, S.; dos Santos, A. B.; Jacobsen, T. A.; Amrutkar, D. v.; Peters, D.; Jensen, A. A.; Kohlmeier, K. A.; Christophersen, P.; Dyhring, T. Characterization of AN317, a Novel Selective Agonist of A6β2-Containing Nicotinic Acetylcholine Receptors. *Biochem Pharmacol* **2020**, *174*. https://doi.org/10.1016/j.bcp.2019.113786.

(106) Timmermann, D. B.; Sandager-Nielsen, K.; Dyhring, T.; Smith, M.; Jacobsen, A. M.; Nielsen, E.; Grunnet, M.; Christensen, J. K.; Peters, D.; Kohlhaas, K.; Olsen, G. M.; Ahring, P. K. Augmentation of Cognitive Function by NS9283, a Stoichiometry-Dependent Positive Allosteric Modulator of A2- and A4-Containing Nicotinic Acetylcholine Receptors. *Br J Pharmacol* **2012**, *167* (1), 164–182. https://doi.org/10.1111/j.1476-5381.2012.01989.x.